Targeted siRNA carrier systems for the treatment of acute myeloid leukaemia (AML)

Von der Fakultät Energie-, Verfahrens- und Biotechnik der Universität Stuttgart zur Erlangung der Würde eines Doktors der Naturwissenschaften (Dr. rer. nat.) genehmigte Abhandlung

Vorgelegt von
Miriam Rothdiener
aus Landstuhl

Hauptberichter:	Prof. Dr. Roland Kontermann
Mitberichter:	Dr. Olaf Heidenreich, Senior Lecturer (Newcastle University)

Tag der mündlichen Prüfung: 25. August 2009

Institut für Zellbiologie und Immunologie
Universität Stuttgart
2009

Table of contents

Abbreviations

ADCC	antibody dependent cellular cytotoxicity
AMD	age-related macular degeneration
AML	acute myeloid leukaemia
ara-C	cytarabine
BBB	blood-brain-barrier
BCR	B cell receptor
CBF	core binding factor
CD	cluster of differentiation
CDC	complement dependent cytotoxicity
CDK	cyclin dependent kinase
CDR	complementarity determining region
CEA	carcinoembryonal antigen
CPD	phosphate-dextrose solution
DLS	dynamic light scattering
EC_{50}	mean effective concentration
EGFR	endothelial growth factor receptor
EPC	egg-phosphatidylcholine
EPR	enhanced permeability and retention
FAB	French-American-British classification
Fab’	antibody fragment containing the variable and the first constant domains
FAP	fibroblast activation protein
FPLC	fast protein liquid chromatography
GM-CSF	granulocyte macrophage colony-stimulating factor
GO	Gemtuzumab-Ozogamicin
HBV	Hepatitis B virus
HIV	Human immunodeficiency virus
HPLC	high pressure liquid chromatography
HSPC	hydrogenated soy-phosphatidylcholine
IFN	interferon
Ig	immunoglobulin
IL	immunoliposome
ILP	immunolipoplex
IMAC	immobilized metal ion affinity chromatography
IPP	immunopolyplex
ITIM	immunoreceptor tyrosin-based inhibition motif

mAb	monoclonal antibody
mal	maleimide
MFI	mean fluorescence intensity
miRNA	micro RNA
NFκB	nuclear transcription factor kappa B
NK cell	natural killer cell
ODN	oligodeoxynucleotide
ORF	open reading frame
PCR	polymerase chain reaction
PEG	polyethylene glycol
PEI	polyethylenimine
PKR	protein kinase R
PLA	poly(lactic acid)
RES	reticuloendothelial system
RISC	RNA induced silencing complex
RNAi	RNA interference
RSV	respiratory syncytial virus
scFv	single chain Fv antibody fragment
SDR	specificity determining residues
SEC	size exclusion chromatography
SH2	Src homology-2 domain
shRNA	short hairpin RNA
Siglec	silaic acid binding Ig like lectin
siRNA	small interfering RNA
SNALP	stable nucleic acid-lipid particle
TfR	transferrin receptor
TGF	transforming growth factor
TLR	Toll-like receptor
TNF	tumour necrosis factor
TRBP	trans-activation-responsive RNA-binding protein
UTR	untranslated region
VEGF	vascular endothelial growth factor
V_H	variable heavy chain
V_L	variable light chain
ZFP	zinc finger protein

Summary

Active targeting is an important prerequisite for selective administration of therapeutic agents into tumour cells. In acute myeloid leukaemia (AML) a targeted drug delivery via antibody fragments directed against CD33 can be reached. CD33 is an internalizing receptor expressed on the surface of myeloid blasts. Several variants of recombinant anti-CD33 single chain Fv (scFv) fragments differing in the order of their variable domains (V_HV_L or V_LV_H) were expressed. Immunoliposomes (ILs) were generated by conventional coupling to malPEG$_{2000}$-functionalized liposomes and by postinsertion of scFv-coupled micelles into preformed PEGylated liposomes, respectively. The exclusively high binding activity of anti-CD33 ILs with scFv molecules in the V_HV_L configuration is remarkable and provides evidence of a possible influence of domain order on binding activity. ILs containing 0.3 mol% of scFv-coupled lipid showed the highest binding and uptake activity on target cells. Binding activity remained constant for several days and required only a few scFv molecules per liposome. SiRNA was encapsulated passively, either as naked siRNA, or complexed with polyethylenimine (PEI) or protamine with loading efficiencies between 24 and 100 %. ILs had a diameter of approximately 130 to 140 nm after encapsulation of siRNA. In addition, immunopolyplexes (IPPs) were generated by coupling of scFv CD33 V_HV_L to the synthetic polymer PEI, forming complexes with siRNA. Size of IPPs was very heterogenous and ranged from 180 to 450 nm, with a slightly negative surface charge. Target cell specific binding and uptake of both carrier systems could be shown by flow cytometry and fluorescence microscopy studies. Transfection of the carrier systems and silencing of the target leukaemic fusion gene AML1/MTG8 by encapsulation of a specific siRNA showed a selective, quantitative silencing of AML1/MTG8 on protein level. Knockdown of AML1/MTG8 expression led to a decreased cell clonogenicity, demonstrated in colony formation assays. However, observed target gene knockdown effects were not very pronounced and, depending on the concentration of the carrier system, knockdown could also be insufficient or unspecific caused by a narrow window between inefficient and unspecific or even cytotoxic concentrations. Furthermore, a stimulating effect of ILs on the clonogenicity of the target cells was observed.

In the present study, basic procedures for the targeted delivery of siRNA via ILs and IPPs were established, which should be improved by further approaches. As a first step towards therapeutic applications, humanization of the murine scFv V_HV_L molecule via CDR-grafting was performed, resulting in a humanized scFv with identical binding properties and improved stability.

Zusammenfassung

Aktives Targeting ist eine wichtige Voraussetzung für die selektive Verabreichung therapeutischer Agenzien in Tumorzellen. In der akuten myeloischen Leukämie (AML) kann eine zielgerichtete Wirkstoffverabreichung über Antikörperfragmente, die gegen CD33 gerichtet sind, erreicht werden. CD33 ist ein internalisierender Rezeptor, der auf der Zelloberfläche myeloischer Blasten exprimiert wird. Mehrere verschiedene Varianten rekombinanter anti-CD33 single chain Fv (scFv) Fragmente, die sich in der Anordnung ihrer variablen Domänen unterscheiden (V_HV_L bzw. V_LV_H), wurden produziert. Immunliposomen (IL) wurden mit Hilfe der konventionellen Kopplung an malPEG_{2000}-funktionalisierte Liposomen oder durch die Postinsertion von scFv-gekoppelten Micellen in vorgeformte PEGylierte Liposomen hergestellt. Bemerkenswert ist die ausschließliche, starke Bindungsaktivität der anti-CD33 IL, die mit scFv Molekülen in der V_HV_L Konfiguration gekoppelt wurden. Dies weist auf einen möglichen Einfluss der Anordnung der Domänen auf die Bindungsaktivität der IL hin. IL mit 0,3 mol% scFv-gekoppelten Lipids zeigten die höchste Bindungsaktivität und Aufnahme in Zielzellen. Die Bindungsaktivität blieb über mehrere Tage stabil und erforderte nur wenige scFv Moleküle pro Liposom. Liposomen wurden passiv mit siRNA beladen, entweder in freier Form oder als Komplex mit Polyethylenimin (PEI) oder Protamin. Die Beladungseffizienz variierte zwischen 24 und 100 %. Die IL wiesen eine Größe von 130 bis 140 nm nach siRNA Beladung auf. Zusätzlich zu IL wurden Immunopolyplexe (IPP), durch Kopplung von scFv CD33 V_HV_L an das synthetische Polymer PEI und siRNA-Komplexierung, hergestellt. Die Größen der IPP waren sehr heterogen und reichten von 180 bis 450 nm bei leicht negativer Oberflächenladung. Zielzellspezifische Bindung und Aufnahme konnte für beide Trägersysteme in der Durchflusszytometrie und Fluoreszenzmikroskopie gezeigt werden. Transfektion der Trägersysteme und Silencing des leukämischen Fusionsgens AML1/MTG8 durch die Verpackung spezifischer siRNA zeigten ein selektives, quantitatives Silencing von AML1/MTG8 auf Proteinebene. AML1/MTG8 Knockdown führte zu einem verminderten Proliferationspotential, das im Colony Formation Assay gezeigt werden konnte. Die beobachteten Knockdown-Effekte waren jedoch nicht sehr ausgeprägt und konnten, je nach Konzentration des Trägersystems, unzureichend oder unspezifisch sein, verursacht durch ein schmales Fenster zwischen Insuffizienz und Unspezifität oder gar Toxizität. Ein stimulierender Effekt der IL auf die Proliferation der Zielzellen wurde gezeigt.

In dieser Arbeit wurden die Grundlagen für eine zielgerichtete Verabreichung von siRNA über IL und IPP geschaffen, die in weiteren Ansätzen verbessert werden sollten.

Ein erster Schritt in Richtung therapeutischer Anwendung, wurde durch die Humanisierung des murinen scFv V_HV_L Moleküls mittels CDR-grafting gemacht, was zu einem humansierten scFv mit identischen Bindungseigenschaften und verbesserter Stabilität führte.

1 Introduction

1.1 Acute myeloid leukaemia (AML)

Leukaemia in general characterizes unregulated proliferation of leukocytes derived from abnormal hematopoietic precursor cells which lose the ability to differentiate into functional blood cells, but rest in an active proliferation state. This leads to the elimination of healthy hematopoietic tissue in the bone marrow first, followed by spreading of the leukaemic cells into the peripheral blood. As a consequence, the leukaemic blasts may infiltrate multiple organs like the liver, spleen and lymph nodes. According to their progression, leukaemias are divided into the acute and chronic form. Acute leukaemia is characterized by a sudden occurrence and fast mortality when left untreated. Chronic leukaemias show a slow development and a long asymptomatic phase before they also enter an acute phase, the blast crisis. Besides progression, leukaemia can also be classified by the nature of the malignant cells, whether they are myeloid or lymphoid (McKenzie, 1996). Acute myeloid leukaemia (AML) is the most frequent form of leukaemia in adults (Appelbaum et al., 2001) and develops by unregulated proliferation of immature myeloid cells.

1.1.1 Classification and clinical findings

The French-American-British (FAB) classification divides AML into several subtypes, distinguished by cytochemical and cytomorphological findings. The subtype M2, which represents the differentiation status of acute myeloblastic leukaemia with maturation, is very often concerned by a t(8;21) translocation (Parisi et al., 2002). In acute leukaemia, functional leukocytes as well as other blood cells are displaced by the proliferating tumour cells. Patients suffer from enhanced bleeding tendency, bruising and petechial haemorrhages because of decreased thrombocyte numbers, susceptibility to infections due to diminished functional leukocytes and low erythrocyte numbers lead to the occurrence of anaemic symptoms like pallor, fatigue and weakness. Other clinical findings like hepato- and splenomegaly and bone tenderness are possible (McKenzie, 1996).
AML treatment is mostly divided into two chemotherapeutical phases, the remission induction and the post-remission therapy. The first part of treatment is aimed to reduce the leukaemic bulk. It usually involves treatment with two chemotherapy drugs, cytarabine (ara-C) and an anthracycline drug such as daunorubicin or idarubicin. If induction is successful, no leukaemia cells will be found in the blood, and the number of blast cells in the bone marrow will be less than 5 % within a week or two. Remission rates of 60 to 70 % in adults are reached, depending on specific prognosis factors. Normal bone marrow cells will return in a

couple of weeks and start making new blood cells. Further treatment may be given to try to destroy any remaining leukaemia cells and help prevent a relapse. The options for AML consolidation therapy are several courses of high-dose ara-C chemotherapy and allogeneic or autologous stem cell transplantation to restore blood cell production. Ara-C chemotherapy leads to a four-year remission of 40 % in young patients and around 15 % in older patients above 60 years (American Cancer Society, 2009). A new approach in AML treatment is a targeted chemotherapy with the anti-CD33-calicheamicin construct gemtuzumab ozogamicin (GO) (Hamann et al., 2002). It consist of an AML-targeting monoclonal antibody (mAb) fused to a chemotherapeutic agent, calicheamicin. Within the acidic environment of lysosomes after internalization, calicheamicin dissociates from the mAb and migrates to the nucleus where it binds within the minor groove of DNA and causes dsDNA breaks (Zein et al., 1988). Adverse effects of GO therapy are hepatotoxicity and delayed recovery of the haematopoietic system (Kell et al., 2003). However, in clinical studies, it showed promising results when used in combination with standard therapy (Feldman, 2005).

1.1.2 Leukaemic fusion genes: AML1/MTG8

In contrast to most types of solid tumours, many leukaemias are associated with distinct chromosomal changes like translocations or inversions and show a high genetic stability. RAS is the most common oncogene in AML. It encodes a 2nd messenger G-protein, which mediates GTP hydrolyzation, involved in signalling cascades of growth factor receptors. The RAS oncogene produces more active G-proteins and thus increases signal transduction for cell proliferation or differentiation (McKenzie, 1996). The t(8;21) translocation is associated with approximately 15 % of AML and 40 % of AML-M2 subtype (Mitelman et al., 1992). It rearranges the AML1 gene on chromosome 21q22 and the MTG8 gene on chromosome 8q22, generating the AML1/MTG8 fusion gene (Miyoshi et al., 1991). AML1/MTG8 represents a chimeric transcription factor which impairs differentiation by histone deacetylation: The DNA binding domain of AML1 fuses to the almost complete open reading frame (ORF) of MTG8 (Downing., 1999). AML1 is an essential transcription factor for definite haematopoiesis, its direct interaction partners in transcriptional regulation are for example interleukin (IL)-3 (Shoemaker et al., 1990) and granulocyte macrophage colony-stimulating factor GM-CSF (Takahashi et al., 1995), both haematopoiesis-specific genes. MTG8 is a part of histone deacetylase-containing complexes. Although MTG8 contains a zinc finger motif, it does not directly interact with DNA (Erickson et al., 1996). It binds the corepressors N-Cor and mSin3 and thus recruits histone deacetylase activity (Lutterbach et al., 1998; Gelmetti et al., 1998; Wang et al., 1998). Lower levels of histone acetylation lead to less accessible chromatin. The translocation converts the transcriptional modulator to a constitutive

repressor of gene expression. The resulting fusion protein AML1/MTG8 inhibits myelopoiesis by directly binding to and sequestering transcription factors, such as SMAD3, vitamin D receptor and C/EBPα and supports clonal expansion of hematopoietic stem cells. C/EBPα is an essential transcription factor for granulocytic development. Thus, AML1/MTG8 interferes with signal transduction pathways controlling differentiation and proliferation (Westendorff et al., 1998; Pabst et al., 2001). Another one of AML1/MTG8 target pathways is the transforming growth factor β (TGFβ) pathway, which is inhibited by binding of AML1/MTG8 to the TGFβ activated transcription factor SMAD3 (Jakubowiak et al., 2000). This may lead to a block in TGFβ /vitamin D_3-mediated myeloid differentiation. AML1 contains the α subunit of the core binding factor (CBF), a heterodimeric complex that binds to core enhancer elements. The CBFα subunit directly binds DNA whereas the β subunit enhances binding of CFBα. AML1 forms a complex with CBFβ (Wang et al., 1993) via the region which is also responsible for DNA binding, the RHD region. It is homologous to the *Drosophila runt* gene (Kagoshima et al., 1993). T(8;21) occurs in leukaemic stem cells as it has been shown by the ability of leukaemic cells from patients with AML-M2 engrafting in SCID mice (Lapidot et al., 1994). But AML1/MTG8 alone may not be sufficient to induce leukaemia (Rhoades et al., 2000). Transgenic mice expressing AML1/MTG8 under the control of a myeloid specific promoter did not develop leukaemia unless further treatment. However, a high percentage of the AML1/MTG8 transgenic mice developed AML after treatment with high doses of ENU, a strong carcinogenic mutagen (Yuan et al., 2001). In fact, activating mutations in the c-KIT receptor tyrosine kinase, frequently associated with CBF-related leukaemias, suggest that activated growth factor signals, which increase cell proliferation and enhance cell survival may cooperate with AML1/MTG8 to induce transformation (Beghini et al., 2000). C-KIT mutations have been shown to increase the risk of relapse in AML patients (Paschka et al., 2006). In contrast, the proto-oncogene c-myc is often down regulated after t(8;21) translocation.

1.1.3 Immunoglobulin receptor superfamily: CD33

Sialic acid binding Ig like lectins (Siglecs) are type I membrane proteins and belong to the immunoglobulin (Ig) receptor superfamily, characterized by an N-terminal variable V-set Ig domain that mediates sialic acid binding, followed by various numbers of constant C2-set Ig domains, one domain in the case of CD33 (Crocker et al., 1999) (Fig. 1-1). Siglecs were found to mediate cell-cell interactions *in vitro* via recognition of sialylated glycoconjugates (Crocker et al., 1991). The Siglec family consists of ten members. Siglec 3 is also known as CD33. Members five to ten belong to the CD33-related Siglecs, which are collectively expressed on human peripheral blood leukocytes.

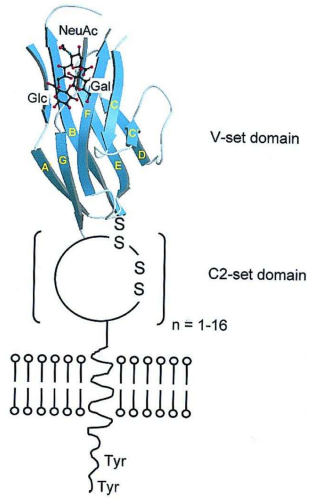

Fig.1-1: Sialic acid binding lectin (Siglec) (Crocker and Varki, 2001)
N-terminal V-set Ig domian, C2-set domains, single transmembrane domain, C-terminal intracellular domain with two tyrosin-based inhibitory motives

All the members contain two conserved intracellular inhibitory motives, the immunoreceptor tyrosin-based inhibition motives (ITIMs). They are suggested to be involved in the regulation of cellular activation of the immune system. An emerging theme is that these inhibitory receptors can interact with broadly expressed self ligands and thus regulate myeloid cell activation. This could be an important mechanism for preventing inappropriate auto reactivity during immune response (Ravetch and Lanier, 2000). Sialic acid is a generic term for a large family of 9-carbon sugars that are all derivatives of neuraminic acid or ketodeoxynonulosonic acid. They are typically found at the exposed, non-reducing ends of oligosaccharide chains attached to a wide variety of proteins and lipids (Schauer, 1982). Many different types of sialic acids exist in mammalians and each can occur in a variety of glycosidic linkages. Thus, in addition to their well known roles in preventing cell-cell interactions through charge-repulsion effects and in masking subterminal sugars, sialic acids are also well suited to act as ligands for mediating selective cell-cell interactions. Almost all known Siglecs recognize forms and linkages of sialic acids, mostly only a terminal sialic acid in conjunction with its next sugar, that are commonly found at cell surfaces and in the extracellular environment. One consequence is that the Siglec binding site can be masked by *cis* interactions with sialic acids on the same cell surface, thereby preventing them from mediating cell-cell-interactions. Unmasking may occur during cellular activation (Crocker and Varki; 2001). Unlike other commonly found sugars, sialic acids are thought to have appeared relatively late in evolution and therefore should be absent from the majority of potential pathogens (Angata and Varki, 2000). These observations lead to the following hypothesis: A Siglec on an effector cell that becomes unmasked upon activation might become re-engaged if there is an adjacent normal host cell with cell surface sialic acids, but not if there is a potential pathogen (Crocker and Varki, 2001). Interestingly, many known pathogens, like for example *Neisseria* and *Haemophilus* have independently evolved the capacity to express sialic acids (Kelm and

Schauer, 1997). This also leads to re-engagement of the inhibitory function of Siglec although a pathogen is present and an appropriate immune response would be essential. Recent investigations demonstrate an inhibitory effect of CD33 on cell signal transduction. The cytoplasmic domain contains two ITIMs, which bind to SHP-1 and SHP-2 phosphatases after phosphorylation by ligand binding of CD33, at a specific tyrosine residue 324. Another potential ITIM sequence containing the tyrosine residue 342 plays a minor role. Tyrosine phosphorylation of ITIM results in the recruitment and activation of at least one of the Src homology-2 domain (SH2) containing SHP-1 and SHP-2 (Taylor et al., 1999). SHP-1 may associate with the CD33 phosphorylated ITIM in *trans*, binding the same ITIM from two different CD33 tails of an oligomer. SHP-1 acts by modulating the functions of growth promoting receptors like c-KIT, CSF-1, EGFR, IL-3-receptor and erythropoietin receptor (summarized by Vitale et al., 2001). An inhibitory effect on FcγRI signalling has also been observed (Paul et al., 2000), presumably due to co-ligation of CD33 and competition with FcγRI signalling. FcγRI activation by tyrosine phosphorylation and the resulting calcium influx is probably competed by the inhibitory function of CD33. Furthermore, it has been shown that crosslinking of CD33 inhibited cell growth and induced apoptosis, observed by binding of Annexin V and DNA fragmentation in CD33 expressing cells, indicating a regulatory function of CD33 in myeloid cells (Vitale et al., 1999, 2001). CD33 is expressed as a monomer or homodimer on myeloid precursors, monocytes, macrophages and to a weaker extend on granulocytes and dendritic cells. More than 80 % of AML patients carry CD33 on their tumour cells (Dinndorf et al., 1986) and even on AML stem cells (Taussig et al., 2005). The nature of the tyrosine kinase phopsphorylating CD33 ITIM is still unknown. Ulyanowa et al. (1999) speculated that it might be a Src family kinase and/or Syk as they are widely expressed in AML. ITIMs also control internalization of CD33-ligand-complexes (Walter et al., 2005). Endocytosis via clathrin-coated pits is by far the predominant mechanism for internalization of cell surface receptors and their cargo. Indeed, the ITIMs of CD33 resemble motives of a major tyrosine-based signal involved in clathrin-mediated endocytosis of the transferrin- and asialoglycoprotein receptor (Bonifacino and Traub, 2003; Mukherjee et al., 1997).

1.2 RNA interference

In 1998, RNA interference (RNAi) was discovered by Fire and Mello (Fire et al., 1998) in C*aenorhabditis elegans*. RNAi is a fundamental pathway in eukaryotic cells, by which small RNA molecules are able to target and degrade complementary mRNA and thus regulate gene expression. Fire and Mello gained the Nobel Prize for their findings in 2006. The first study to demonstrate that exogenous siRNA is capable of sequence-specific knockdown in mammalian cells was published three years after the discovery of RNAi (Elbashir et al.,

2001). Studies describing sequence specific gene silencing using siRNA in mice (McCaffrey et al., 2002) and in non-human primates (Zimmermann et al., 2006) followed.
RNAi pathways are guided by small RNAs that include small interfering RNAs (siRNAs) and micro-RNAs (miRNAs). Physiologically, RNAi within mammalian cells occurs via miRNAs, deriving from imperfectly paired non-coding hairpin structures that are naturally transcribed by the genome. MiRNAs mediate translational repression and transcript degradation for imperfectly complementary mRNA targets whereas gene silencing by siRNA is induced through sequence-specific cleavage of perfectly complementary target mRNA. Extensive investigations on RNAi, with leading studies in *Drosophila* and *C. elegans*, offered convergences of observations from diverse experimental systems suggesting a conserved biochemical mechanism of homology dependent gene silencing responses (Fougerolle et al., 2007).

1.2.1 Mechanism of RNAi

In figure 1-2, the silencing mechanism of exogenous RNA is shown. Silencing triggers in form of double stranded RNA (dsRNA) may be presented in the cell as synthetic siRNAs, replicating viruses or may be transcribed from nuclear genes. In mammalians, dsRNA is recruited to Dicer by TRBP, a dsRNA binding protein (Castanotto et al., 2007). DsRNAs are recognized by Dicer and converted into siRNAs of approximately 22 nucleotides with 5' phosphorylation and 3' overhangs of two nucleotides. This format is essential for entering the silencing pathway. Dicer, a 220 kDa protein, belongs to the family of RNase III enzymes containing dual catalytic domains, additional helicase and PAZ motives and a zinc finger protein ZFP1, forming the RNA binding site. Members of this family have been found to initiate RNAi (Bernstein et al., 2001). The conversion of dsRNA into siRNA by Dicer can be explained by the following model (Fig. 1-3): Based upon the known mechanisms for the RNase III family of enzymes, Dicer is thought to work as a dimeric enzyme. DsRNA cleavage into precisely sized fragments is determined by the fact that one of the two active sites in each Dicer subunit is defective due to mutations in the consensus sequence of the catalytic centres. Antiparallel alignment of the two Dicer subunits on the dsRNA substrate results in the formation of the two inactive sites in the middle. As a consequence, the periodicity of cleavage is shifted from nine to eleven nucleotides for bacterial RNase III to approximately 22 nucleotides for Dicer family members (Blaszczyk et al., 2001).

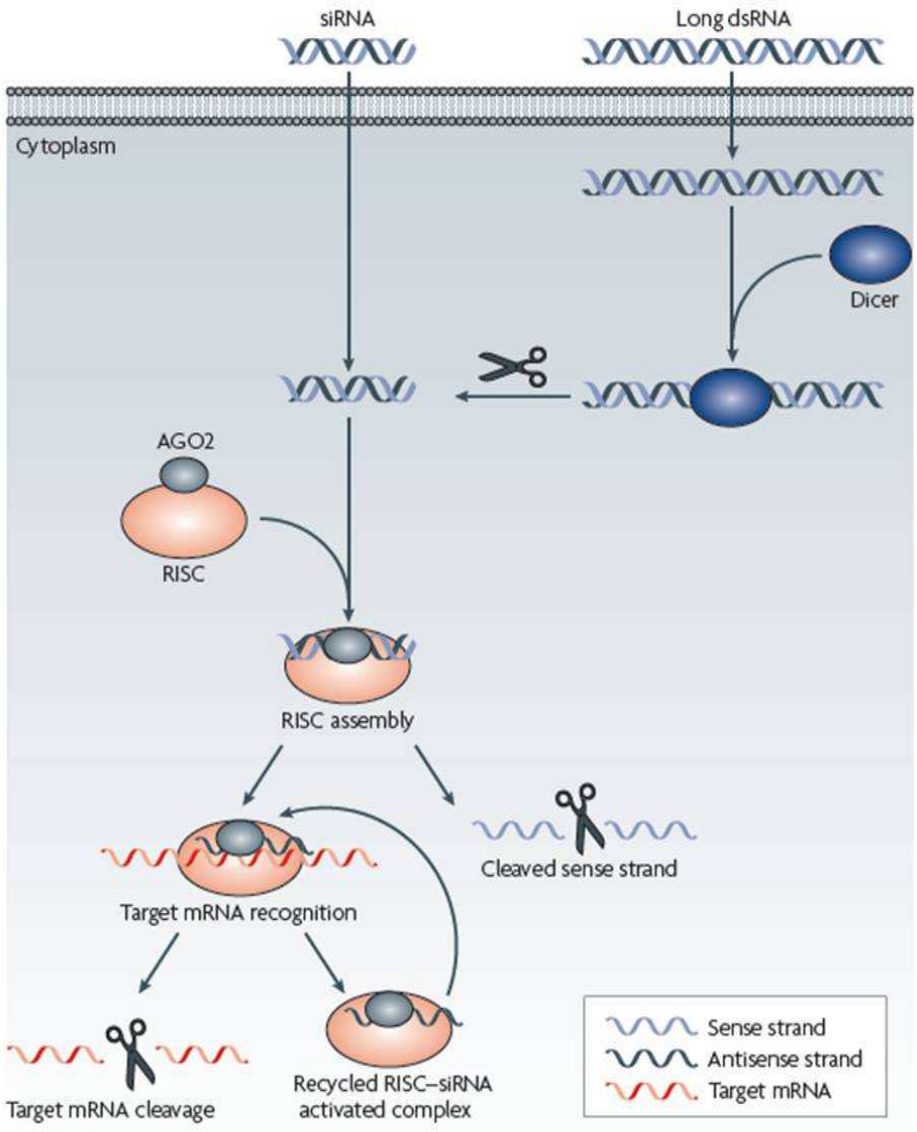

Fig.1-2: Mechanism of RNA interference (Whitehead et al., 2009)
DsRNA is processed by Dicer into 22 nucleotide siRNA which is then incorporated into RISC. Activated RISC unwinds siRNA and binds target mRNA by the siRNA antisense strand. MRNA is cleaved by the Ago2 subunit of RISC.

The duplex siRNAs are passed to RISC (RNA induced silencing complex) and the complex becomes activated by ATP-dependent unwinding of the duplex. Several helicases have been identified as candidates for RISC activation (Cogoni et al., 1999; Wu-Scharf et al., 2000; Tijstermann et al., 2002). Which RNA strand is incorporated into RISC depends on the stability of the strand ends. Activated RISC can regulate gene expression at many levels. Almost certainly, such complexes act in a post-transcriptional mode by promoting mRNA degradation and translational inhibition. The core complex of RISC is responsible for

receiving the 22 nucleotide dsRNA from Dicer and using it as a guide to identify its homologues mRNA.

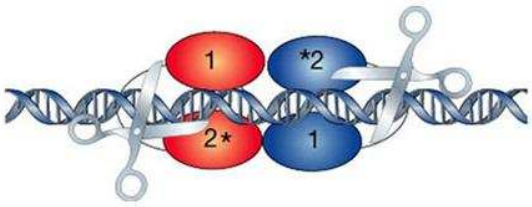

Fig.1-3: Mechanism of Dicer mRNA cleavage (Hannon et al., 2002)
Diagrammed representation of Dicer, not all Dicer domains are shown. Mutations in one of two RNase III sites in each Dicer domain (indicated by an asterisk) result in cleavage at 22 nucleotide intervals.

Depending upon the structure of the dsRNA and its complementarity to the mRNA, different effector functions could join the core. In the case of siRNA, nucleases would be incorporated into RISC, whereas upon miRNA incorporation translational repressors would join in the complex. The nuclease, incorporated into RISC in case of siRNA incorporation, is Ago2, a 100 kDa member of the Argonaute gene family, an evolutionary conserved gene family with representatives in most eukaryotic genomes. It consists of two homology regions, an N-terminal 130 amino acids PAZ domain and a C-terminal PIWI domain. SiRNA is transferred to RISC by an assembly with Dicer over the PAZ domains, contained in both molecules. Transient interactions between Dicer and Ago2 have been reported as well as between RISC and the ribosome (Hammond et al., 2001). The PIWI domain is responsible for the cleavage of target mRNA, which occurs near the middle of the duplex, the PIWI domain folds into a structure analogous to the catalytic domain of RNase H (Liu et al., 2004).

1.2.2 RNAi as a therapeutic tool

Sequencing of the human genome opens the gates for the development of nucleic acid based drugs as an increasing number of genes involved in human diseases are identified. Oncogenes, such as leukaemic fusion proteins, which arise from chromosomal translocations, are promising targets for gene silencing approaches as they are exclusively expressed by cancerous tissue. Additionally, they are frequently indispensable for maintaining malignancy. A prominent example, besides BCR-ABL in chronic myeloid leukaemia or MLL-AF4 in acute lymphatic leukaemia, is AML1/MTG8 involved in AML. Three different approaches for mRNA silencing have been presented in a comprehensive review comparing antisense oligodeoxynucleotides (ODNs), ribozymes and siRNAs (Scherer and Rossi, 2003). ODNs hybridize mRNA to produce a substrate for RNase H (Kurreck, 2003), whereas ribozymes bind and degrade RNA by catalyzing hydrolysis of the mRNA

phosphodiester backbone (Doudna et al., 2002). Knockdown effects of ODNs and siRNAs have been compared (Bertrand et al., 2002; Kong et al., 2007) and concluded that siRNA is more efficient *in vitro* and *in vivo*. There are important differences in the subcellular location between ODNs and siRNA. ODNs primarily induce the cleavage of target mRNA in the nucleus, whereas siRNA functions primarily in the cytosol. Moreover, siRNA enters an endogenous cellular pathway, which could explain the high efficiency of siRNA to inhibit the expression of a target gene. It can be 1000-fold higher than ODN efficiency targeting the same molecule (Kurreck, 2009). The RNAi machinery can be exploited for silencing any gene in the body. It is possible to harness this endogenous pathway in two ways: either by using a viral vector to express short hairpin RNA (shRNA) that resembles miRNA-precursors, or by introducing synthetic siRNA molecules mimicking processed dsRNAs. This shortcut reduces the potential for innate immune response and to interfere with endogenous gene regulation. Additionally, viral vectors can induce systemic toxicity by the activation of immune response. A further disadvantage of shRNA is a possible influence on the regulatory cellular miRNAs as they compete for nuclear export via Exportin 5 (Castanotto et al., 2007). Synthetic siRNAs harness the natural RNAi pathway in a predictable and consistent manner making them attractive as therapeutics. Therapeutic siRNA is designed and selected with regard to potency, specificity and nuclease stability. Algorithms can be used to predict their effectivity. Immunogenicity and off-target effects can be prevented, for example by avoiding targeting the mRNA 3’ or 5’ untranslated regions (UTRs), seed regions or regions with high G-C contents (Jackson et al., 2006a). Usually, siRNA is designed *in silico*, tested *in vitro*, and, if necessary, stabilized by appropriate chemical modifications like 2’-O-methylation (Jackson et al., 2006b). Modifications should not interfere with the recognition of the siRNA by RISC. Another important point is the choice of the guide (antisense) strand by RISC. Therefor, its 5’ terminus must be less stable than the 5’ terminus of the sense strand. Furthermore, an adenosine residue at position 11 of the antisense strand (the complementary position of cleavage site) can be of advantage because RISC prefers to cleave RNA to the 3’ side of uridine (Thomas et al., 2006). But a compromise has to be found if the siRNA target is the fusion site of a fusion transcript and the wild-type transcript must not be concerned. Then, perfect siRNA sequence complementarity is superior to optimal design. Scanning of the fusion site with overlapping siRNAs can help to identify an active and target specific siRNA. This has been described for the MLL-AF4 fusion site (Thomas et al., 2005). Subsequently, an appropriate delivery mode is chosen and the formulation is tested *in vivo.* Selected examples of siRNA delivery *in vivo* in animal models are listed in table 1-1.

Table 1-1: Modes of siRNA delivery

	mode	**formulation**	**target**	**disease**
naked	topical		eye	AMD
	local		lung	RSV
	systemic		liver	hypercholesterolaemia
conjugated	systemic	cholesterol	liver	dyslipidaemia
	systemic	fatty acids and bile salts	liver	dyslipidaemia
	local	protamine	tumour xenograft	cancer
	systemic	ligands (e.g. peptides)	tumour xenograft	cancer
complexed	systemic	cationic lipids	knee joints	arthritis
	systemic	lipidoids	liver	dyslipidaemia
	systemic	SNALP	liver	HBV
	local	cationic polymers (e.g. PEI)	tumour xenograft	cancer

from Whitehead et al., 2009; Fougerolle et al., 2007
AMD, age-related macular degeneration; RSV, respiratory syncytial virus; SNALP, stable nucleic acid-lipid particles; HBV, Hepatitis B virus; PEI, polyethylenimine

Many tissues in the body require a siRNA delivery system to facilitate transfection because naked siRNA is subjected to degradation by endogenous enzymes and is too large (approximately 13 kDa) and too negatively charged to cross cellular membranes. The reason why some tissue types are able to take up naked siRNA (e.g. lung, brain) while others are not, is still unclear. Local administration offers the advantage of high bioavailability and reduced adverse effects. Several tissues, like the eye, skin, mucus surfaces and local tumours are amenable to localized therapy. But naked siRNAs are degraded in human plasma with a half-life of seconds to minutes (Dykxhoorn and Lieberman, 2005). Synthetic materials have demonstrated potential as effective non-viral siRNA delivery systems which facilitate cellular siRNA uptake. Systemic delivery requires particles which have the ability to avoid uptake and clearance by non-target tissues. Renal clearance can be circumvented by a particle size above 6 nm. Still, several physiological barriers and hurdles have to be overcome: After injection into the blood circulation, the siRNA complex must avoid opsonisation and uptake by phagocytes, unintended aggregation with serum proteins and enzymatic degradation by endogenous nucleases. Most RNases are inactive against dsRNA,

but some serum nucleases can degrade siRNA (Dykxhoorn and Lieberman, 2005). The polymer polyethylene glycol (PEG) can prevent charged complexes from binding to serum proteins without making them ineffective. Additionally, PEG conjugation can control particle size, prevent particle aggregation (Auguste et al., 2008) and evade the immune system and associated phagocytes. Crossing the vascular endothelial barrier represents a significant challenge, falling away in the case of leukaemia therapy. Entry of larger molecules (~200 nm) into organs of the reticuloendothelial system (RES) and to some tumours is possible because of a more permeable endothelium, leading to the enhanced permeability and retention effect (EPR) of drug delivery (Whitehead et al., 2009). Especially the structure of the discontinuous endothelium of the liver brings circulating macromolecules into free contact with parenchymal cells (Nishida et al., 1991). Humans have evolved host-defence mechanisms against RNA molecules as it is a feature of certain viral infections. Typical siRNAs of 22 nucleotides do not evoke severe immune response due to their small size below the critical number of 30 nucleotides. Still, unmodified siRNAs can induce nonspecific activation of the immune system through Toll-like receptor 7 (TLR7) signalling, inducing an IFNα response (Hornung et al., 2005). This hurdle, as well as possible off-target effects, can be overcome by chemical modification of siRNA, e.g. by 2'-O-methyl modification.

In the last years many efforts were made in the field of siRNA-based therapeutics. Liposomes developed for therapeutic delivery of siRNA consist of several components, each playing an important role in fusogenicity and pharmacokinetic properties of the liposome. They are typically composed of multiple lipids, often containing cationic and/or fusogenic lipids, cholesterol and a polyethylene-glycosylated lipid. Successful approaches with liposomal siRNA delivery systems have been described by Zimmermann et al. in 2006, Morrisey et al. in 2005 and Geisbert et al. in 2006. In all three cases a stable nucleic acid lipid particle (SNALP) delivery system has been applied. Intravenous injection of siRNA-encapsulated SNALPs dramatically silenced ApoB in the liver of both mice and non-human primates. Treatment was well tolerated in these experiments. The same SNALP formulation also effectively delivered siRNA to the liver in animal models of hepatitis B and Ebola virus infection. Whether these SNALPs can be used for siRNA delivery to other organs than the liver has not been described. However, systemic delivery of cationic lipoplexes resulted in specific caveolin-1 and TNF gene silencing in the lung and knee joints of mice (Miyawaki-Shimizu et al., 2006; Khoury et al., 2006). Formulations of lipid-like materials with siRNA were capable of achieving potent and persistent silencing of various lung and liver targets in mice, rats and cynomolgus monkeys (Akinc et al., 2008). SiRNA can also be complexed with cationic peptides and polymers by ionic interactions with their negatively charged phosphate backbones to form stable nanoparticles. Often, PEG is incorporated to prevent aggregation and control particle size. One of the most intensively studied polymers for the delivery of

nucleic acid is polyethylenimine (PEI). PEI polymers are synthetic, linear or branched structures with high cationic charge densities. The cationic polyplexes formed with siRNA interact electrostatically with the cell surface and are internalized by unspecific endocytosis. PEI-siRNA complexes have been reported to show therapeutic benefit in a number of disease models like Her2 dependent anti tumour activity (Urban-Klein et al., 2005). A significant concern about using PEI is the extreme toxicity seen in higher doses. Furthermore, there are siRNA-cholesterol conjugates under investigation (Soutschek et al., 2004, DiFiglia et al., 2007) and conjugates of siRNA and fatty acids in combination with bile salts (Wolfrum et al., 2007). Protamine, a histone-like cationic polypeptide, condensing DNA during spermatogenesis, can also be taken for siRNA complexation and delivery. Moreover, siRNA delivery can even be improved and specified by fusion proteins with antibodies. For example, a protamine-antibody fusion protein was used to deliver non covalently bound siRNA to HIV envelope expressing tumour cells and HIV infected CD4 T cells *in vitro* (Song et al., 2005). Besides, transferrin-protamine fusion proteins (Wagner et al., 1990) and anti-ErbB2 scFv-protamine fusion proteins (Li et al., 2001) have also been used for the delivery of plasmid DNA.

Some of the therapeutic approaches shown in table 1.1 are already in clinical trials: The most advanced trials rely on forms of localized siRNA delivery, although several ongoing clinical trials involve the use of delivery agents. Several of the most advanced clinical studies focus on the treatment of age-related macular degeneration (AMD). Naked siRNA targeted to genes for vascular endothelial growth factor (VEGF) and its receptor has shown therapeutic potential in its inhibition of excessive neovascularisation of the eye (Fattal et al., 2006). The first pulmonary studies are directed at treating respiratory syncitial virus (RSV) and have been found to be effective, safe and well tolerated (Alnylam, 2008). Delivery to the lung by inhalation is noninvasive and directly targets the tissue epithelium avoiding high drug doses and systemic side effects. Clinical studies on systemically delivered siRNA targeting the liver and kidney are also in progress (Whitehead, 2009).

1.2.2.1 Endosomal release: The proton sponge effect

Having been taken up into the target cell, particles must escape the endosome to reach the cytoplasm. If the particle is unable to exit the endosome it is trafficked through decreasing pH to degradative conditions in the lysosome. Finally, the siRNA must be released from the carrier to the RNAi machinery. Cationic polymers with a linear or branched structure can serve as efficient transfection agents because of their ability to bind and condense siRNA into stabilized nanoparticles. Such materials have also been shown to stimulate nonspecific endocytosis and endosomal escape (Behr, 1996; Akhtar et al., 2007). A proposed mechanism for the endosomal escape of PEI is the ‘proton-sponge’ effect, whereby buffering

of the endosome during acidification leads to an accumulation of ions (protons and chloride ions) and water within this compartment and an osmotic pressure that eventually bursts the endosome (Akinc et al., 2005) (Fig. 1-4). Every third atom of PEI is a protonable amino nitrogen atom, which makes the polymeric network an effective proton sponge. Under physiological conditions, about 15 % of nitrogen atoms are protonated, increasing to 45 % in the late endosome (Boussif et al., 1995). The influx of ions is mediated by the vacoular type H^+-ATPase, which can be inhibited by bafilomycin A1, providing evidence for the hypothesis (Merdan et al., 2002). Several pH triggered polymers, e.g. polyarginine that facilitate endosomal escape and that could be incorporated into nanoparticles have been identified (Torchilin et al., 2005).

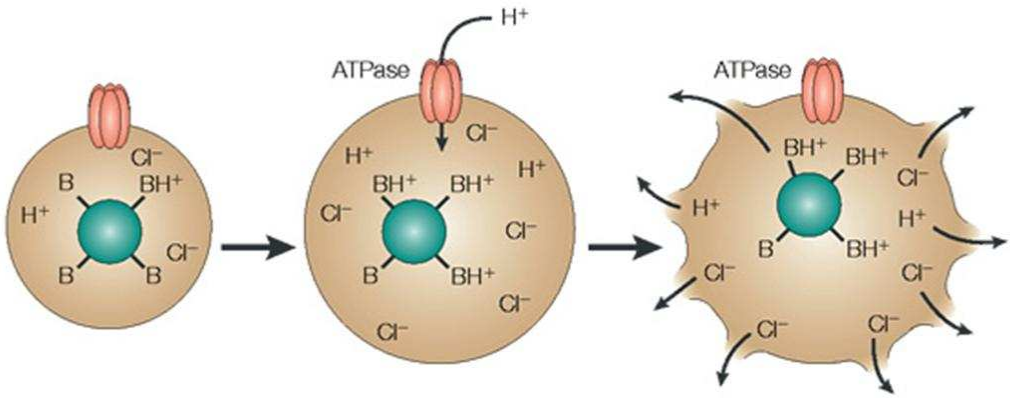

Fig. 1-4: The proton sponge effect (Nature Publishing Group, 2005)
Buffering of a base (B) in the endosome enhances active proton (H^+) transport during acidification and leads to swelling and rupture of the endosome.

Merdan et al. (2002) could show in living cell microscopy that ensdosomal release occurs in a sudden event, very likely due to bursting of the endosome. The finding represented the first experimental evidence for the endosomal escape of PEI. The polyplex should be sufficiently stable during endocytosis, but thereafter, siRNA should be released into the cytosol. Extension of the polymer network during acidification or interactions of PEI and lysosomal or cytoplasmic constituents might be responsible for the destabilization of the complex. Dissociation of the polymer and nucleic acid compound in the cytosol is essential for silencing activity. If the release takes place from the late endosome or lysosome, lysosomal contents, like hydrolytic enzymes can harm the cell (Brunk et al., 1997) and might be a limiting factor for that kind of delivery.

1.3 Targeted drug delivery

A promising alternative or supplementation to conventional tumour therapy is the targeted drug delivery. A systemic administration of cytostatic drugs or local tumour treatment, for example by radiation, can be supported by the targeted delivery of anti tumour agents or simply monoclonal antibodies (mAb) mediating immune response. A famous example is the combination therapy of non-Hodgkin's lymphoma with chemotherapy and anti CD20 monoclonal antibody Rituximab. The requirements of systemic drug delivery are tumour targeted delivery, passage of cell membrane and targeting specifically oncogenes. Systemically administered, tumour specific immunoliposomes (IL) with high transfection efficiency represent a promising approach. Wang et al. (2008) hypothesized a treatment of AML by directly targeting both leukaemia stem cells and oncogenic molecules with specific scFv-ILs as a deliverer of siRNA. Some of the first targeted liposomal approaches were carried out by Hashida et al. (2001) with galactosylated liposomes for liver targeting via internalization of specific liver receptors or with cationic ILs covalently conjugation to anti-transferrin receptor (TfR)-scFv over a cysteine at the 3' end of the protein and a maleimide on the liposome (Xu et al., 2002). Besides ILs, immunopolyplexes represent suitable carriers, especially for siRNA. Schiffelers et al. (2004) targeted integrin on activated endothelial cells in tumour vasculature with ligand-conjugated siRNA-PEGPEI polyplexes. The integrin ligand they used was RGD peptide, a fibronectin motif. However, it must be considered that natural, non antibody ligands compete for binding with endogenous ligands *in vivo*. Internalization of the carrier is an important prerequisite. This was shown in a study comparing doxorubicin-loaded anti CD19 and anti CD20 ILs. CD19, in contrast to CD20, is an internalizing receptor and therefore, CD19 ILs show a significanltly higher therapeutic outcome in mice (Sapra and Ellen, 2002). Bartlett et al., 2007 showed in a PET experiment that the primary advantage of the targeting molecule is cellular uptake rather than tumour localization.

1.3.1 General aspects of targeted drug delivery

Tumour therapy involving antibodies or antibody derived molecules offers the possibility for a targeted offence by directly reaching the tumour cells via surface antigen binding. Ideally, to avoid side effects, a tumour specific antigen is targeted. In case of the delivery of chemotherapeutics it is therefore important not to target antigens on haematopoietic stem cells. Another important prerequisite to provide specificity is a constant expression and preferably overexpression of the antigen on target cells. Moreover, with regard to the uptake of the therapeutic agent into the target cell, the antigen must be internalized after binding of the ligand. This is not the case if the therapeutic effect of the antibody is due to antibody dependent cellular cytotoxicity (ADCC) or complement dependent cytotoxicity (CDC).

Jin et al., (2006) described leukaemic stem cells, which do not yet express differentiation markers, are responsible for the development and maintenance of leukaemia. Targeting antigens on leukaemic stem cells allows for reduction of the tumour as well as affecting the cell population responsible for relapse. The principle has been shown for CD44 on AML stem cells. Various techniques of targeting have been described, including covalent and noncovalent approaches. First approaches in this direction were accomplished using mAbs coupled with active compounds, such as anti-tumour drugs (Weiner and Carter, 2003). Pharmacological and immunological activities of the drug-antibody-conjugates have to be preserved. Covalent reactions seem to be an effective way to irreversibly fix ligands to colloidal carriers. However, it has to be considered that the coupling reaction must not interfere with the biological activity of the ligand. Therefore, the use of antibody fragments having available thiol functions, is preferable compared to conjugation through primary amines, which often affect antigen binding site. Gautier et al. (2001) used a covalent binding method for the preparation of poly(lactic acid) (PLA) nanoparticles. A conjugate of biotin and poly(methyl methacrylate-*co*-methacrylic acid) was synthesized and coprecipitated with PLA into stable nanoparticles. For active targeting, such nanoparticles could be used for a multistep approach using the avidin-biotin interaction. Noncovalent methods have the great advantage of being easy to be carried out without the need of aggressive reagents and the disadvantage of relatively low ligand binding to the carrier (Nobs et al., 2004).

1.3.2 Antibody molecules in targeted delivery systems

Leukaemia is ideally suited to treatment with mAb because of the accessibility of malignant cells in the blood, bone marrow, spleen and lymph nodes. Moreover, the well defined immunophenotypes of the various lineages and stages of haematopoietic differentiation have permitted the identification of antigen targets (Sabbath et al., 1985). MAbs mediate ADCC and CDC via their Fc part binding to Fc receptors on monocytes and natural killer (NK) cells and activating the complement cascade, respectively (Adams and Weiner, 2005; Wright et al., 1997; Niwa et al., 2004). This leads to lysis of the target cell. IgGs need to be produced in mammalian cells. Immunoliposomes with mAbs against Her2 have already been investigated (Park et al., 2002; Li et al., 2001). Fab' fragments, either resulting from pepsin digestion of IgG molecules (Fig. 1-5) and subsequent mild reduction or from recombinant expression, posses a molecular mass of about 50 kDa and at least one free sulfhydryl group. There have been detailed investigations for delivery with sterically stabilized ILs. Fab' fragments lead to a reduced immugenicity compared to IgG molecules (Gagné et al., 2002) and the ILs show a three-fold increasing half-life (Pastorino et al., 2003). Sapra et al. (2004) could show a better therapeutic outcome of Fab' liposomes compared to mAb liposomes. ScFv fragments are

generated by connecting the variable domains of the light and heavy chains with a peptide linker and posses a molecular mass of about 25 kDa. ScFv molecules can be obtained by phage display (Hoogenboom, 2005), from hybridoma or recombinant by antibody engineering. In order to achieve binding to functionalized lipids, one or more additional cysteine residues are attached to the C-terminus of scFv, leading to site directed coupling to liposomes (Völkel et al., 2004). This formulation has been denoted as scFv'. Several scFv ILs have already shown efficient drug delivery *in vitro* and *in vivo* (Xu et al., 2002; Nielsen et al., 2002). ScFv can be bacterially produced, show better tissue penetration because of their small size and lack the immunogenic Fc part. One disadvantage, compared to IgG and Fab' fragments, is their monovalency, leading to a rapid dissociation from their target antigens (Tomlinson and Holliger, 2000).

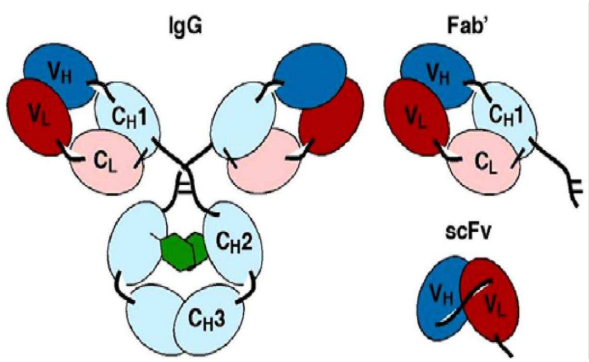

Fig. 1-5: Antibodies and antibody fragments (Kontermann, 2006) IgG, immunoglobulin G; V_H, variable heavy domain; V_L, variable light domain; C, constant domain; Fab', Fragment containing the variable and the first constant domains; scFv, single chain Fv fragment

To further reduce immunogenicity of antibody molecules *in vivo*, mouse constructs can be replaced by human constructs, or, as mouse constructs require easier production methods, mouse antibodies can be adapted to human antibodies. Genetic engineering techniques allow for the generation of human mouse chimeric antibodies that combine mouse variable regions with human constant regions or more fully humanized mAbs that have human framework and constant regions. These humanized mAbs have been CDR grafted so that only the original mouse antigen binding sites are retained (Caron et al., 1992). Therapeutic application can be improved due to several advantages. Immunogenicity by human anti-mouse antibody response has been shown to be reduced for 4D5, a humanized anti-Her2 antibody (Carter et al., 1992). Humanized antibodies are more specific and thus effective in recruiting human effector functions (Caron et al., 1992). Moreover, binding can be improved by molecular modelling, e.g. substitution of single amino acids. Elevated production yields and higher purity have been described for anti-EGFR huC225' (Nusser, 2009).

Humanization by CDR-grafting of mouse monoclonal anti-CD33 IgG M195 resulted in the humanized version, HuM195 or Lintuzumab. It possesses an eightfold higher binding activity compared to M195, rapid internalization and enhanced ADCC and CDC activity (Caron et al., 1992). Genetically engineered chimeric and humanized antibodies have demonstrated activity against a variety of tumours. While humanized anti-CD33 mAb Lintuzumab has only modest single-agent activity against AML, targeted chemotherapy with anti-CD33-calicheamicin construct gemtuzumab ozogamicin (Hamann et al., 2002) appears promising when used in combination with standard therapy (Jurcic, 2007). Enhancement of cytotoxicity through similarities in their signalling pathways has been suggested (Balaian et al., 2005).
A clinical study from Feldman et al. (2005) provided first clinical evidence with the administration of an anti-CD33 antibody in combination with induction chemotherapy and the conclusion that addition of Lintuzumab was save, but did not result in a statistically significant improvement in response or survival rates in AML patients.

1.3.2.1 Tumour surface antigens as targets for drug delivery systems

A tumour surface antigen, suitable as a target for drug delivery systems, must fulfil several properties. It must be expressed permanently and to a sufficient extent on tumour cells and, if possible, exclusively on the target cells. Another important prerequisite is the rapid internalization of the ligand-antigen complex. Recent studies in AML have focused primarily on CD33, a cell-surface glycoprotein found in most myeloid leukaemias as well as on committed myelomonocytic precursor cells, but not on mature granulocytes or non-haematopoietic tissues (Andrews et al., 1989). The high internalization rate of CD33 (van Der Velden et al., 2001), its restriction to the myeloid lineage and its expression on AML cells and leukaemic stem cells make it a suitable antigen for targeted drug delivery. CD33 is down regulated in mature granulocytes but retained in monocytes. CD33 has already been used for clinical approaches of targeted drug delivery systems (Caron et al., 1994, Jurcic et al., 2002). Experience with Gemtuzumab-Ozogamycin (GO, Mylotarg) has shown clinical relevance (Sievers et al., 1999). Latest investigations gave evidence for the expression of CD33 on hematopoietic stem cells (Taussig et al., 2005), which would provide a disadvantage for the clinical application of CD33 derived drugs. However, recovery of the haematopoietic system after GO treatment is ensured (Sievers, 2004). This may be due to CD33 expression on a minority of haematopoietic stem cells.
Taking other leukaemic diseases into consideration, CD19 represents a suitable target for B-cell lymphoma. As well as CD33, CD19 also belongs to the Ig superfamily. The surface protein CD19 is a glycoprotein of a molecular mass of 95 kDa, contains two Ig like extracellular domains (Tedder and Isaacs, 1989) and a cytoplasmic region essential for CD19 dependent signal transduction. On mature B-cells, CD19 forms a complex with other

membrane bound proteins like CD21, CD81 and Leu 13. Moreover, CD19 is associated with members of the B-cell receptor (BCR) complex and serves as a regulator of transmembrane signalling in activation, proliferation and differentiation of B-lymphoid cells (Fearon and Carroll, 2000; Fujimoto et al., 2000). CD19 is expressed from the proB-cell stadium up to mature B-cells over all maturation stages and is only downregulated in plasma cells. It is restricted to the B-lympoid lineage and it remains expressed in B-lymphoid leukaemias (Nadler et al., 1983). In contrast to CD20 and CD21, which also serve as target antigens in drug delivery, CD19 is already expressed in early B-cell progenitors. Additionally, CD19 is internalized after antigen binding (Press et al., 1989). This attribute predestines CD19 for an antibody based treatment of lymphatic leukaemia and lymphoma, although no CD19 targeting antibody-therapeutic has gained clinical accreditation yet. However, besides therapeutic mAbs being investigated, immunotoxins against CD19 and CD33 are in development (Schwemmlein et al., 2007a; Schwemmlein et al., 2006). They represent monovalent immunotoxins consisting of scFv CD19 or CD33 fused to a derivative of *Pseudomonas* exotoxin A. A truncated version lacking domain I, the binding domain for CD91, which is expressed on most mammalian cells, was applied (Wels et al, 1995). Induction of efficient antigen restricted apoptosis of several human leukaemia- and lymphoma-derived cell lines and of primary malignant cells could be shown.
CD13, a type II transmembrane ectopeptidase, belongs to the integrin superfamily and is also called aminopeptidase N. It is a multifunctional cell surface aminopeptidase, which forms a noncovalently bound homodimer on the cell membrane. Aminopeptidases catalyze the cleavage of amino acids from the amino terminus of protein or peptide substrates. As zinc is involved in substrate liganding CD13 belongs to the metalloproteinases. Aminopeptidases are responsible for protein maturation, degradation and possibly determination of protein stability (Bachmair et al., 1986). Although CD13 was originally described as a marker for haematopoietic cells of the myeloid lineage, it is also expressed on endothelium cells, where it is upregulated during angiogenesis and specifically interacts with galectin-3, a proangiogenetic protein, in a carbohydrate recognition-dependent manner. Additionally, it is expressed on fibroblasts, brain cells, liver, kidney and intestine. CD13 is also implicated in tumour growth (Mechtersheimer and Moller, 1990; Alliot et al., 1999; Dixon et al., 1994). It plays a role as a regulator of various hormones and cytokines, protein degradation, antigen presentation, cell proliferation and migration (Pasqualini et al., 2000; Luan and Xu, 2007; Curnis et al., 2002). CD13 is suggested to be involved in the degradation of neuropeptides, cytokines and immunomodulatory peptides, as well as angiotensins (Lendeckel et al., 1999; Chang et al., 2005). Aminopeptidase N is synthesized as an intracellular precursor of 967 residues and posttranslationally modified in the Golgi to produce a 150 kDa mature cell surface molecule comprising a short cytoplasmic N-terminal

domain, a single transmembrane part and an extracellular domain containing the active site (Razak and Newland, 1992; Look et al., 1989). Within the mature, glycosylated protein almost 1/3 of the molecular mass is composed of carbohydrates. Differential utilization of O-glycosylation sites results in at least five isoforms (O'Connell et al., 1991). Binding of CD13 to natural peptide substrates or to antibodies may induce conformational changes and exposure of cryptic epitopes (Xu et al., 1997).
Recent studies have suggested an important role in tumour progression in several human malignancies (Ishii et al., 2001; Hashida et al., 2002; Tokuhara et al., 2006). It was demonstrated that CD13 is directly involved in signal transduction pathways, including the phosphorylation of mitogen-activated protein kinases in monocytes (Santos et al., 2000).

1.3.3 Immunoliposomes

Liposomes are used as carriers for drugs, acting as a slow release reservoir, and for nucleotides. They protect the patient against unwanted side effects. Size, lamellarity, bilayer rigidity, charge and bilayer modifications are parameters which determine the fate of liposomes. Unsaturated phosphatidylcholins from natural sources like egg or soybean give more permeable and less stable bilayers than saturated phosphilipids with long acyl chains. Circulation time is dramatically increased upon attachment of PEG chains by reducing the rate of uptake by macrophages. The goals of liposomes are drug solubilisation, protection and internalization, duration of action and directing potential (Crommelin and Storm, 2003). Doxil is a prominent example for a liposome formulation containing the chemotherapeutic doxorubicin, which has already gained clinical accreditation (Gabizon and Martin, 1997).
ILs, generated by coupling of antibodies to a liposomal surface allow for an active tissue targeting, e.g. through binding to tumour cell-specific receptors, and thus presenting a promising approach for targeted drug delivery. In 1980, the concept of targeting liposomes to cells by antibodies (Leserman et al., 1980) or antibody fragments (Heath et al., 1980) has been introduced 15 years after the discovery of liposomes by Bangham et al. in 1965. Generally, ligands are bound to the surface of liposomes through hydrophobic anchors, commonly long fatty acids, having functional groups. Among the hydrophobic anchors, phosphatidyletanolamine (PE) is frequently used (Weissig et al., 1986). The reaction between thiol functions of the antibody fragment and functional maleimide groups of the anchor lipid is a highly efficient reaction that gives stable thioether bonds (Park et al., 1997). Taylor et al. (2001) observed that chemical cross-linking to thiol groups in cysteine with maleimide groups (Fig. 1-6) is stable in reducing cellular environment. Other possibilities of attaching ligands to liposomes are via a disulfide linkage (Martin et al., 1981), via hydrazine bonds (Koning et al., 1999), via crosslinking between carboxylic acid functions or primary

amines on the surface of liposomes and primary amines of the ligand (Torchilin et al., 1978) or in a multistep attachment using the avidin-biotin interaction (Hansen et al., 1995). A simple noncovalent coupling method is to add the ligand to the mixture of phospholipids during liposome preparation (Huang et al., 1979).

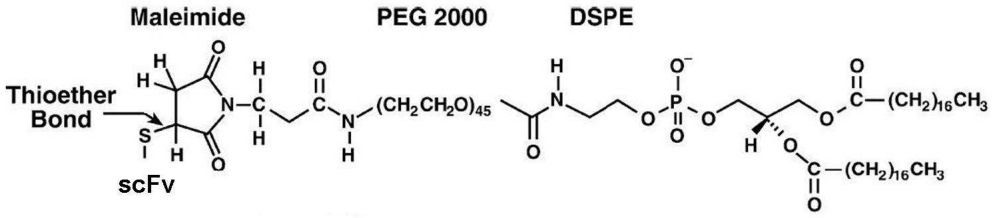

Fig. 1-6: Hydrophobic lipid anchor malPEG$_{2000}$-DSPE for the covalent coupling of scFv' via the functional maleimide group.
modified from Nellis et al., 2005

Coupling of antibodies or antibody fragments directly to the lipid surface results in the formation of type I ILs, coupling to the distal ends of functionalized PEG chains to type II ILs (Kontermann, 2006), restoring IL antigen binding that may be sterically disturbed by the PEG-chains in type I ILs (Hansen et al., 1995). This could lead to a reduced interaction and uptake into tumour cells (Park et al., 2002; Kirpotin et al., 1997). Whole antibodies coupled to liposomes were highly immunogenic and rapidly removed by Fc-mediated phagocytosis by macrophages (Harding et al., 1997; Bendas et al., 2003; Koning et al., 2003). These disadvantages can be circumvented using Fab' or scFv molecules as ligands. They can be easily modified through genetic engineering, for instance, by insertion of an additional cysteine residue (scFv'). This permits a very defined and site-directed coupling to reactive groups of liposomes. Most of the work on liposome targeting has been done with antibodies or antibody fragments attached to the liposome surface (Mastrobattista et al., 1999). Two approaches to generate scFv' ILs have been described in the literature. On the one hand the conventional method, by which antibody molecules are directly coupled to the liposome surface (Kontermann, 2006) (Fig. 1-7a), and on the other hand the postinsertion method, where the ligands are coupled to micelles prepared from functionalized lipids and subsequently inserted into preformed liposomes (Iden and Allen, 2001) (Fig. 1-7b).

1.3.3.1 Conventional immunoliposomes

Immunoliposomes generated by coupling of antibodies to the liposomal surface allow for an active tissue targeting, for example through binding to tumour cell-specific receptors. Instead of whole antibodies, scFv fragments, which represent the smallest part of an antibody containing the entire antigen-binding site, find increasing usage as targeting moieties.

Genetically modified scFv' molecules form a thioether bond with maleimide functionalized lipids, which are incorporated into the lipid bilayer.

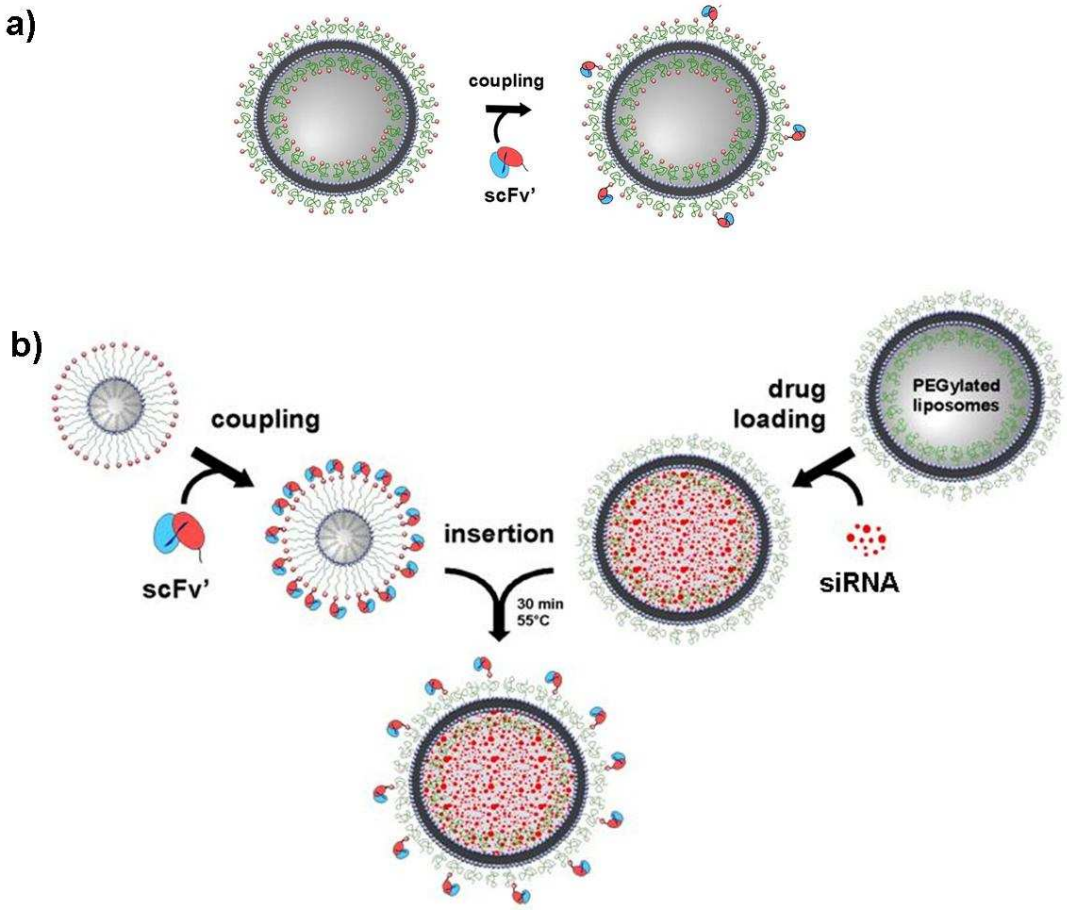

Fig. 1-7: Immunoliposome techniques (modified from Messerschmidt et al., 2009)
a) conventional coupling method
b) postinsertion method in combination with encapsulation of siRNA

ScFv' ILs can be generated by the conventional method of direct coupling of scFv' molecules to preformed liposomes. For the conventional method the maleimide-PEG-lipid (malPEG$_{2000}$-DSPE) is incorporated into the lipsomal bilayer already during generation of the liposomes. ScFv' molecules are then directly coupled to the liposomal surface by the formation of a thioether bond with the maleimide group. A lipid composition of phosphatidylcholine, cholesterol and malPEG$_{2000}$-DSPE anchor lipid is used for the preparation of conventional ILs. A thin lipid film is formed in a round bottom flask by dissolving the lipids in chloroform and removing the solvent in a rotary evaporator. Subsequently the lipid film is dried completely and rehydrated until all components are

dissolved. Extrusion through a membrane of constant pore size obtains small unilamellar vesicles. Other methods for the preparation of liposomes are, for example, detergent dialysis (reviewed by Connor et al., 1985) or reverse phase evaporation (Szoka and Papahadjopoulus, 1980). Rüger et al. (2005) presented a noncovalent coupling of scFv via His-Tag to nickel-nitrilotriacetic acid functionalized liposomes.

1.3.3.2 Postinsertion immunoliposomes

The postinsertion technique was first described by Iden and Allen in 2001: The reduced scFv' molecules are first coupled to malPEG$_{2000}$-DSPE micelles and then the micellar lipid is inserted into the outer liposomal layer. The preformed liposomes contain non-functionalized PEG chains. The post-insertion technique has several advantages compared to the conventional method, if it comes to the generation of drug- or siRNA loaded ILs for therapy. With this method, coupling and drug loading are independent processes and can be optimized separately. Thus, it is hoped that scFv molecules directed against various target molecules can be easily combined with various liposomal drug formulations to create ILs tailored to the properties of the target cell (Allen et al., 2002). If the coupling reaction is achieved on preformed carriers, there is some risk of altering the structure of the particle and in some cases, the encapsulated compound. Therefore, it is important to choose nonaggressive reagents and to work under mild, controlled conditions (Nobs et al., 2004). For passive encapsulation, siRNA is added to a dry lipid film and, during resolving the lipid, the siRNA in the aqueous phase is passively loaded into the liposomes. SiRNA-loaded liposomes can subsequently be adapted to the optimal conditions for postinsertion of scFv' coupled micelles. To enhance the encapsulation efficiency, siRNA was complexed to polycationic moieties. These could be the synthetic polymer PEI or protamine, a polycationic, histone like protein. The first approach with shRNA encapsulated, stabilized, EGFR targeted liposomes was performed by Zhang et al. in 2004. Boado (2005) described dual targeted PEGylated liposomes obtaining anti-TfR IgG for crossing the blood-brain-barrier (BBB) via transcytosis and anti-insuline IgG for targeting insuline receptors on brain cancer cells. The liposomes were encapsulated with a therapeutic shRNA against EGFR. Dan Peer showed in two publications the selective gene silencing in activated leukocytes, firstly by targeting siRNAs with antibody-protamine fusion proteins (Peer et al., 2007), and secondly by siRNA-protamine encapsulated ILs (Peer et al., 2008).

1.3.4 Immunopolyplexes

Polyplexes between siRNA and PEI derivatives are promising nonviral carriers. Boussif et al. (1995) tested PEI for intracerebral delivery of luciferase genes and found out that it is one of

the most efficient synthetic polynucleotide delivery systems. Its positive charge allows for efficient, unspecific endocytosis on negatively charged cell membranes. Moreover, due to its 'proton sponge' effect, PEI polyplexes have no need of additional endosomolytic reagents like chloroquine. Grzelinski et al. (2006) could show that unconjugated PEI-siRNA polyplexes deliver siRNA into tissues, hardly any siRNA molecules could be detected in peripheral blood. Furthermore, PEI could be detected in tumour xenografts. However, *in vivo* the formation of aggregates was described, confirming observations by Goula et al. in 1998. Surface modifications of nanoparticles lead to enhanced biocompatibility (Kidane et al., 1999), increased systemic circulation (Monfardini et al., 1998) and alteration of biodistribution (Dams et al., 2000). Polyplexes have been PEGylated with the result of reduced complement activation and increased complex stabilities based on the stealth effect. PEGylation shows strong effects on shape and surface charge of polyplexes (Petersen et al., 2002). Conjugation of antibodies or other target specific ligands has been described (Buschle et al., 1995; Kircheis et al., 1997), leading to high target specificity and subsequent uptake by receptor mediated endocytosis. The most common approach for labelling polymeric nanoparticles with ligands is adsorption, for example of monoclonal antibodies, to their surface (Couvreur, 1988). To optimize the coupling of antibodies to nanoparticles, especially with respect to the orientation of the antibodies, spacer molecules are used. *Staphylococcus aureus* Protein A on the surface of nanoparticles interacts specifically with the Fc fragment of IgG. The competitive displacement of the adsorbed antibodies in presence of serum proteins has been discussed controversially (Davis and Illum, 1983; Manil and Couvreur, 1986). *In vivo*, the particles accumulate in liver and spleen. PEGPEIs with targeting ligands as carrier systems for siRNA have been described by Kim et al. in 2006 and by Schiffelers et al. (2004), who targeted PEGylated PEI with integrin binding RGD-peptide for the delivery of siRNA with high tissue specificity in neuroblastoma xenografts. Much effort has been done on the optimization of immunopolyplexes (IPPs): Mao et al. showed in 2006 that stability and siRNA condensation of polyplexes are severely influenced by PEGPEI structure, PEG chain length and degree of substitution. The best PEGPEI molecule for the antibody-targeted delivery of siRNA was identified as PEI-$PEG_{2000(10)}$ (Germershaus et al., 2006). Increasing N/P ratio (the ratio of nitrogen atoms of PEI to phosphor atoms in siRNA) leads to higher transfection efficiency, but loss of specificity due to nonspecific interaction of cationic PEI with the cell surface, and targeting effects disappear. Coupling of antibodies to PEGPEI via bifunctional linker molecules does not significantly influence the physicochemical properties of the complexes, i.e. complexation efficiency, zeta potential and size (Germershaus et al., 2006). In the current study, NHS-PEG_{2000}-OPSS is used (Fig. 1-8), which covalently binds PEI via its functional succinimidyl group, and covalently binds scFv' via its functional (ortho-pyridyl)disulfide (OPSS) residue.

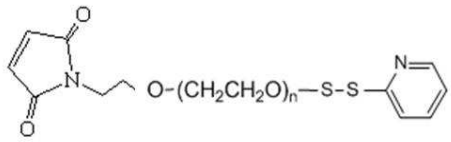

Fig. 1-8: Heterobifunctional PEG linker NHS-PEG_{2000}-OPSS
(modified from Nanocs and Creative PEGWorks)

1.4 Aim of the work

The goal of this work was to combine targeted drug delivery via scFv' ILs targeting leukaemic cell lines via the receptor CD33 with encapsulation and delivery of a therapeutic siRNA directed against the leukaemic fusion gene AML1/MTG8. Different variants of recombinant scFv' CD33 had to be generated and compared, concerning their binding activity to target cells and their coupling efficiency to carrier systems. An optimal scFv' molecule should then be chosen for the preparation of ILs by two different techniques, conventional coupling of scFv' to preformed, functionalized liposomes, and postinsertion of scFv'-coupled, functionalized micelles, into preformed liposomes. Both formulations should be investigated concerning binding and uptake into target cells, stability in human plasma and size. Moreover, the ideal ratio of scFv' to lipid had to be determined as well as the specificity of IL binding. Liposomal encapsulation of siRNA should be established and optimized, specific binding and uptake of siRNA-loaded ILs and immunolipoplexes (ILPs), ILs loaded with complexed siRNA, into target cells should be provided as well as their endosomal escape. Therefor, different polycations for the complexation of siRNA were tested and compared to free siRNA with regard to an improved encapsulation efficiency and endosomal release. Finally, a suitable transfection procedure for the carriers into target cells should be established and silencing of the leukaemic fusion gene AML1/MTG8 should be detected on mRNA level, protein level and in a functional assay representing the clonogenicity of the transfected leukaemic cells. Besides ILs and ILPs, immunopolyplexes (IPPs), consisting of PEI cores, as another possible siRNA carrier system should be prepared and investigated in a comparative manner to ILs and ILPs. Furthermore, humanization of the murine scFv' CD33 should be performed by CDR-grafting.
Thus, this work represents a new approach of supporting conventional leukaemia therapy.

2 Materials and methods

2.1 Materials

2.1.1 Instruments and implements

balances: 440-49N, 440-33N and ALJ 120-4 [Kern, Balingen, Germany]

blotter: Trans-Blot SD Semy-dry transfer cell [BioRad, Krefeld, Germany]

centrifuges: Eppendorf 5415 C [Eppendorf, Wesseling, G]; J2-MC, AvantiJ-30I with rotors JA10, JA14 and JA20 [Beckman Coulter, Munich, Germany] and GR 412 [Jouan, Rennes, France]

chromatography columns: PolyPrep [Bio-Rad, Hercules, USA]

cover slips: 15 mm round cover slips [Roth, Karlsruhe, Germany]

cryobox: Nalgene, Rochester, USA

dialyser: D-Tube Dialyzer Mini (cut-off 6 – 8 kDa [Calbiochem, Merck, Darmstadt, Germany])

dialysis tubes: cellulose tubular membranes 40 mm (cut-off 8 – 10 kDa [Roth, Karlsruhe, Germany]) and 23 mm (cut-off 12,4 kDa [Sigma-Aldrich, St. Louis, USA])

electrophoresis systems: Sub-Cell GT Agarose Gel Electrophoresis System, Mini-PROTEAN 3 Electrophoresis System and Power Pac Basic [BioRad, Krefeld, Germany]

electroporation cuvette: 4 mm [PEQLAB, Erlangen, Germany]

electroporator: EPI 2500 [Fischer, Heidelberg, Germany]

extruder: Liposofast [Avestin, Ottawa, Canada]

fermenter: KLF 2000 [Bioengineering, Wald, Switzerland]

film developing machine: X-OMAT 1000 Processor [Kodak, Stuttgart, Germany] and Curix 60 [AGFA, Mortsel, Belgium]

flow cytometer: EPICS XL-MCL and Cytomics FC 500 [Beckman Coulter, Munich, Germany]

FPLC: ÄKTA FPLC system with SP Sepharose HP cation exchange column [ÄKTA Prime, Amersham, Freiburg, Germany]

heating block: HBT-1-131 HLC [Thermostat, Bovenden, Germany]

HPLC: Phenomenex with sepharose column SEC 2000 [Phenomenex, Aschaffenburg, Germany]

IMAC affinity matrix: His-Select Nickel Affinity Gel [Qiagen, Hilden, Germany]

incubators: Binder BD-53 [Tuttlingen, Germany], Multitron [INFORS, Bottmingen, Germany], Innova 2100 Platform Shaker [New Brunswick Scientific, Edison, USA] and CO_2 Inkubator 2424-2 [Zapf, Sarstedt, Germany]

magnetic stirrer: MR 3001K 800W [Heidolph, Heidelberg, Germany]

microplate reader: TECAN infinite M200 [TECAN, Männedorf, Switzerland]

microscopes: Cell Observer [Zeiss, Jena, Germany], CK2 [Olympus, Hamburg, Germany], DM IRB [Leitz, Wetzlar, Germany] with camera AxioCam MRC [Zeiss, Jena, Germany] and Leica confocal microscope TCS SL [Leica, Wetzlar, Germany]

microscopy slides [Roth, Karlsruhe, Germany]

NanoDrop Spectrophotometer ND-1000 [PEQLAB, Erlangen, Germany]

nitrocellulose membrane: BioTrace NT Membrane [Pall, Ann Arbor, USA]

orbital shaker: GFL 3013 [GFL, Burgwedel, Germany]

PCR machines: RoboCycler 96 [Stratagene, La Jolla, USA] and ABI Prism 7900 HT Sequence Detection System [AB Applied Biosystems, Foster City, USA] with software SDS 2.0.

pH meter: PH 522 [Schütt, Göttingen, Germany]

photometers: GeneQuant [Pharmacia Biotech, Uppsala, Sweden] and BioPhotometer plus [Eppendorf, Hamburg, Germany]

polycarbonate filter membrane: Liposofast (pore diameter: 100 nm, 50 nm; diameter: 19 mm) [Avestin, Ottawa, Canada]

power supply: PowerPac Basic [BioRad, Krefeld, Germany]

pump: Ismatec mp13 GJ-10 [Ismatec, Wertheim-Mondfeld, Germany]

PVDF membrane: ROTI-PVDF [Roth, Karlsruhe, Germany]

rotor evaporator: LABORATA 4000, VAC control automatic, ROTAVAC valve control [Heidolph, Schwalbach, Germany]

Sepharose CL4B: Amersham [Uppsala, Sweden]

sonicator: Sonopuls HD200 [Bandelin, Berlin, Germany]

sterile bench: Variolab Mobilien W90 [Waldner, Wangen, Germany]

syringe filters: Acrodisc Syringe Filters (cut-off 0.2 µm) [Pall, Ann Arbor, USA]

transilluminator: biostep transilluminator [Biostep, Jahnsdorf, Germany]

ultrafiltration spin columns: Centricon YM-10, MWCO 10 kDa [Millipore, Schwalbach, Germany]

vacuum drying oven: Binder [Tuttlingen, Germany]

vortexer: Sky Line [Elmi, Riga, Latvia]

waterbath: MA6 [Lauda, Lauda-Königshofen, Germany] and Haake DC10 [Thermo Haake, Karlsruhe, Germany]

whatman paper: 3 mm [Schleicher & Schuell, Brentford, UK]

x-ray films: Medical X-Ray film 100 NIF [Fuji, Düsseldorf, Germany] and RP NEW Medical Xray screen film blue sensitive [CEA, Hamburg, Germany]

zeta cell: DTS1060C clear disposable zeta cell [Malvern, Herrenberg, Germany]

ZetaSizer NanoZS ZEN 3600 [Malvern, Herrenberg, Germany]

2.1.2 Plastic and glass implements

All cell culture plastic implements were purchased from Greiner [Kremsmünster, Austria]. Glass implements were purchased from Schott [Mainz, Germany].

2.1.3 Chemicals

All lipids were purchased from Avanti Polar Lipids [USA], dissolved in chloroform and stored at -20℃. Egg phosphatidylcholine (EPC) was purchas ed from Lipoid [Ludwigshafen, Germany], cholesterol was purchased from Calbiochem [Merck, Darmstadt, Germany]. The lipid stock solutions had the following concentrations:

Egg phosphatidylcholine: 300 g/l

Cholesterol: 100 g/l

1,2-distearoyl-sn-glycero-3-phosphoethanolamine-N-[maleimide(polyethylene glycol)-2000] (ammonium salt) (malPEG$_{2000}$-DSPE): 30 g/l

1,2-distearoyl-sn-glycero-3-phosphoethanolamine-N-[methoxy(polyethylene glycol)-2000] (ammonium salt) (mPEG$_{2000}$-DSPE): 51 g/l

1,1'-dioctadecyl-3,3,3',3'-tetramethylindocarbocyanine perchlorate (DiI): 3.44 g/l

Hydrogenated soy phosphatidylcholine (HSPC): 35 g/l

All other chemicals were purchased from Roth [Karlsruhe, Germany], Sigma-Aldrich [St. Louis, USA], Merck [Darmstadt, Germany], Roche [Basel, Switzerland] and Invitrogen [San Diego, USA] unless otherwise stated and had a purity of ≥99%.

2.1.4 Solutions and media

Buffers and solutions

Bradford reagent: BioRad Protein Assay [BioRad, Krefeld, Germany]

Cell tracker green-CMFDA [Invitrogen, San Diego, USA]

Coomassie staining solution: 0.25 % (w/v) Coomassie Brilliant Blue R250 in destaining solution: 45 % methanol, 10 % acetic acid

1,1'-dioctadecyl-3,3,3',3'-tetramethylindocarbocyanine perchlorate (DiI) [Sigma-Aldrich, St. Louis, USA]

3,3'-dioctadecyloxacarbocyanine perchlorate (DiO), 1 mM [Invitrogen, San Diego, USA]

DNA loading buffer (5x): 10 % 50 x TAE buffer, 25 % glycerine, 0.02 % (w/v) bromophenole blue

DTT: dithiothreitol [Sigma-Aldrich, St.Louis, USA]

ECL solution A for western blot: 1.25 mM Luminol, 0.1 M Tris/HCl pH 8.6

ECL solution B for western blot: 0.011 % para-hydroxycoumaric acid in dimethylsulfoxide (DMSO), mix 10 % solution B in solution A and 0.001 % H_2O_2 and SuperSignal West Dura Extended Duration Substrate [Pierce, Rockford, USA]

FITC: Fluorescein isothiocyanate [Molecular Probes, Karlsruhe, Germany]

IMAC elution buffer: 50 mM Na-phosphate pH 7.5, 250 mM NaCl, 250 mM imidazole

IMAC loading buffer: 50 mM Na-phosphate pH 7.5, 250 mM NaCl, 20 mM imidazole

IMAC wash buffer: 50 mM Na-phosphate pH 7.5, 250 mM NaCl, 35 and 40 mM imidazole

L-cysteine stock solution: 100 mM with 2 mM EDTA in H_2O

Mounting medium: Mowiol [Polysciences, Warrington, USA] and Vectashield Hard Set Mounting Medium with DAPI [Vector, Burlingame, USA]

Nellis buffer: 10 mM Na_2HPO_4/NaH_2PO_4 buffer, 0.2 mM EDTA, 30 mM NaCl, pH 6.7

PBS: 0.15% $Na_2HPO_4*2H_2O$, 0.02% KH_2PO_4, 0.8% NaCl, 0.02 % KCl

PEG linker: Orthopyridly-disulfide poly (ethylene glycol)- succinimidyl propionic acid (NHS-PEG_{2kDa}-OPSS) [Nektar Therapeutics, San Carlos, USA]

Polyethylenimine: PEI 25 [BASF, Ludwigshafen, Germany]

PPB (periplasmic preparation buffer): 30 mM Tris-HCl, pH 8.1 mM EDTA, 20 % sucrose

Protamine sulphate salt from salmon P 4020 [Sigma-Aldrich, St. Louis, USA]

SDS electrophoresis buffer: 1.4 % glycine, 0.3 % TrisHCl, 0.1 % SDS, pH 8.3

SDS loading buffer (5x): 30 % glycerine, 3 % SDS, 0.0001% bromophenole blue; for reducing buffer: + 5 % β-mercaptoethanol

TAE buffer: 0.5 % Tris, 0.1 % acetic acid, 1 mM EDTA, pH 8

TCEP Bond Breaker Solution [Pierce, Rockford, USA]

urea buffer: 9M urea, 4 % CHAPS, 1 % DTT

western blot blocking solution: 5 % (w/v) milk powder and 0.1 % (v/v) TWEEN20 in PBS

western blot buffer: 20 % methanol, 192 mM glycine, 25 mM Tris, pH 8.3

Media and supplements

Bacterial culture

Ampicillin stock solution: 100 mg/ml in H_2O

Batch-medium: 0.1 % $(NH_4)_2H$-citrate, 0.2 % Na_2SO_4, 0.27 % $(NH_4)_2SO_4$, 0.05 % NH_4Cl, 1.46 % K_2HPO_4 * 3 H_2O, 0.4 % NaH_2PO_4 * H_2O, 2.75 % glucose * H_2O, 0.2 % $MgSO_4$, 0.3 % SEL, 0.1 % thiamine

Feed-medium I: 26.4 % glucose * H_2O, 0.78 % $MgSO_4$* 7 H_2O, 0.004 % SEL, 0.02 % thiamine, 1.25 % rhamnose

Feed-medium II: 18.8 % $(NH_4)_2HPO_4$

Isopropyl-β,D-thiogalactopyranoside (IPTG) [GERBU, Geilberg, Germany]

1x LB medium: 1 % peptone, 0.5 % yeast extract, 0.5 % NaCl

LB agar plates: LB medium as indicated above + 1.5 % agar, 0.01 % ampicillin, and 1 % glucose

Minimal-medium: 0.1 % $(NH_4)_2$H-citrate, 0.2 % Na_2SO_4, 0.27 % $(NH_4)_2SO_4$, 0.05 % NH_4Cl, 1.46 % K_2HPO_4 * 3 H_2O, 0.4 % NaH_2PO_4 * H_2O, 1.1 % glucose * H_2O, 0.2 % $MgSO_4$, 0.3 % SEL, 0.1 % thiamine, pH 7

2x TY/amp medium: 1.6 % peptone, 1 % yeast extract, 0.5 % NaCl, 0.01 % ampicillin

Cell culture

DMSO: Roth, Karlsruhe, Germany

Fetal calf serum (FCS): [Invitrogen, San Diego, USA], [PAA, Pasching, Austria] and HyClone [Thermo Fisher Scientific, Fremont, USA], heat inactivated for 1h at 56℃

Growth factor: rh GM-CSF, 100 µg/ml in H_2O [Immuno Tools, Friesoythe, Germany]

Lipofectamine: Lipofectamine 2000 [Invitrogen, San Diego, USA]

Methylcellulose: Methocell MC [Fluka, Buchs, Switzerland]

Opti-MEM: Opti-MEM + glutamine [Invitrogen, San Diego, USA]

Penicillin/streptomycin (100x): 10,000 U/ml Penicillin, 10,000 µg/ml Streptomycin [Gibco/Invitrogen, San Diego, USA]

RPMI 1640 Glutamin [Gibco/Invitrogen, San Diego, USA]

Trypsin/EDTA solution (10x) (0.5% Trypsin, 5.3 mM EDTA) [Invitrogen, San Diego, USA]

Zeocin: 100 mg/ml in H_2O [Invitrogen, San Diego, USA]

2.1.5 Kits, antibodies, enzymes, etc.

Kits

NucleoBond Xtra plasmid purification [Macherey-Nagel, Düren, Germany]

NucleoSpin Extract II Kit [Macherey-Nagel, Düren, Germany]

Platinum(R) SybR(R)Green qPCR Super Mix-UDG [Invitrogen, San Diego, USA]

PureLink HiPure Plasmid MidiPrep Kit [Invitrogen, San Diego, USA]

QIAshredder [QIAGEN, Hilden, Germany]

REDTaq ReadyMix [Sigma-Aldrich, St. Louis, USA]

Revert Aid H first strand cDNA synthesis kit [Fermentas, St. Leon-Rot, Germany]

RNeasy Mini Kit [QIAGEN, Hilden, Germany]

XTT assay: *in vitro* toxicology assay kit XTT based [Sigma-Aldrich, St. Louis, USA]

Antibodies

anti-AML1/RHD Domain (Ab-2) (50-177) Rabbit pAb, PC285 [Calbiochem, Merck, Darmstadt, Germany]

anti CD13 (Cat. No. 21330133S), CD19 (Cat. No. 21330193S), CD33 (Cat. No. 21330333S) mAb: anti-human FITC-conjugated [Immuno Tools, Friesoythe, Germany]

anti His-Tag unconjugated mAb IgG1 mouse, Ref. DIA 900 [Dianova, Hamburg, Germany]

goat anti-mouse IgG-R-Phycoerythrin (PE), P9287 [Sigma-Aldrich, St. Louis, USA]

goat anti-rabbit IgG peroxidase conjugate, A0545 [Sigma-Aldrich, St. Louis, USA]

His-probe (H-3) Horseradish Peroxidase (HRP)-conjugated mouse monoclonal antibody, sc-8036 [Santa Cruz Biotechnology, Santa Cruz, USA]

rabbit anti-mouse IgG-FITC, F9137 [Sigma-Aldrich, St. Louis, USA]

scFv CD13-1, scFv CD19 4G7 and scFv CD33 K132 [G.H. Fey, University or Nuremberg-Erlangen, Germany]

Enzymes

alkalic phosphatase (1 U/µl) [Promega, Madison, USA]

restriction enzymes (10 U/µl) and 10x buffers: ApaLI, EcoRI, HindIII, NcoI, NdeI, NotI, SfiI, XhoI [Fermentas, St.Leon-Rot, Germany]

TAQ polymerase (1 U/µl) [Fermentas, St. Leon-Rot, Germany]

T4 DNA Ligase (5 U/µl) [Fermentas, St. Leon-Roth, Germany]

Markers

Gene Ruler DNA Ladder Mix ready-to-use #SM0333 [Fermentas, St. Leon-Rot, Germany]

Page Ruler Prestained Protein Ladder #SM0671 [Fermentas, St. Leon-Rot, Germany]

siRNA

siAGF1 [Alnylam, Cambridge, USA]: 5'- `ccu cga aau cgu acu gag aag` -3'

siAGF6 [Alnylam, Cambridge, USA]: 5'- `ccu cga auu cgu ucu gag aag` -3'

siAMX AML1/MTG8 [Eurofins MWG Operon, Ebersberg, Germany]: 5'- `ccu cga aau cgu acu gag a(dTdT)` -3'

siMAX Cy3-AML1/MTG8 [Eurofins MWG Operon, Ebersberg, Germany]: 5'- (Cy3) `ccu cga aau cgu acu gag a(dTdT)` -3'

2.1.6 Primers and vectors

Primers for screening and sequencing

All primers were purchased from Metabion, Martinsried, Germany

pAB1/pABC4: LMB2: 5'- `gta aaa cga cgg cca gt` -3'

LMB3: 5'- `cag gaa aca gct atg acc a` -3'

pSecTagA: pET-Seq1: 5'- `taa tac gac tca cta tag g` -3'

pSEC-Seq2: 5'- `tag aag gca cag tcg agg` -3'

Primers for cloning of pWA21 scFv' CD33 V_HV_L HC4

Primers were purchased from Sigma-Aldrich, St. Louis, USA

NdeI-pelB-back: 5'-`gga att cca tat gaa ata cct att gcc tac ggc`-3'

stop-pAB-HindIII-for: 5'-`tta ccc aag ctt acg gcc agt gaa ttc tta`-3'

Primers for qRT-PCR

All primers were purchased from Sigma-Aldrich, St. Louis, USA

AML1/MTG8 forward: 5'- aat cac agt gga tgg gcc c -3'

AML1/TMG8 reverse: 5'- tgc gtc ttc aca tcc aca gg -3'

GAPDH forward: 5'- gaa ggt gaa ggt cgg agt c -3'

GAPDH reverse: 5'- gaa gat ggt gat ggg att tc -3'

Vectors

Following vectors were used for bacterial and mammalian expression and cloning of scFv' variants (Fig.2-1):

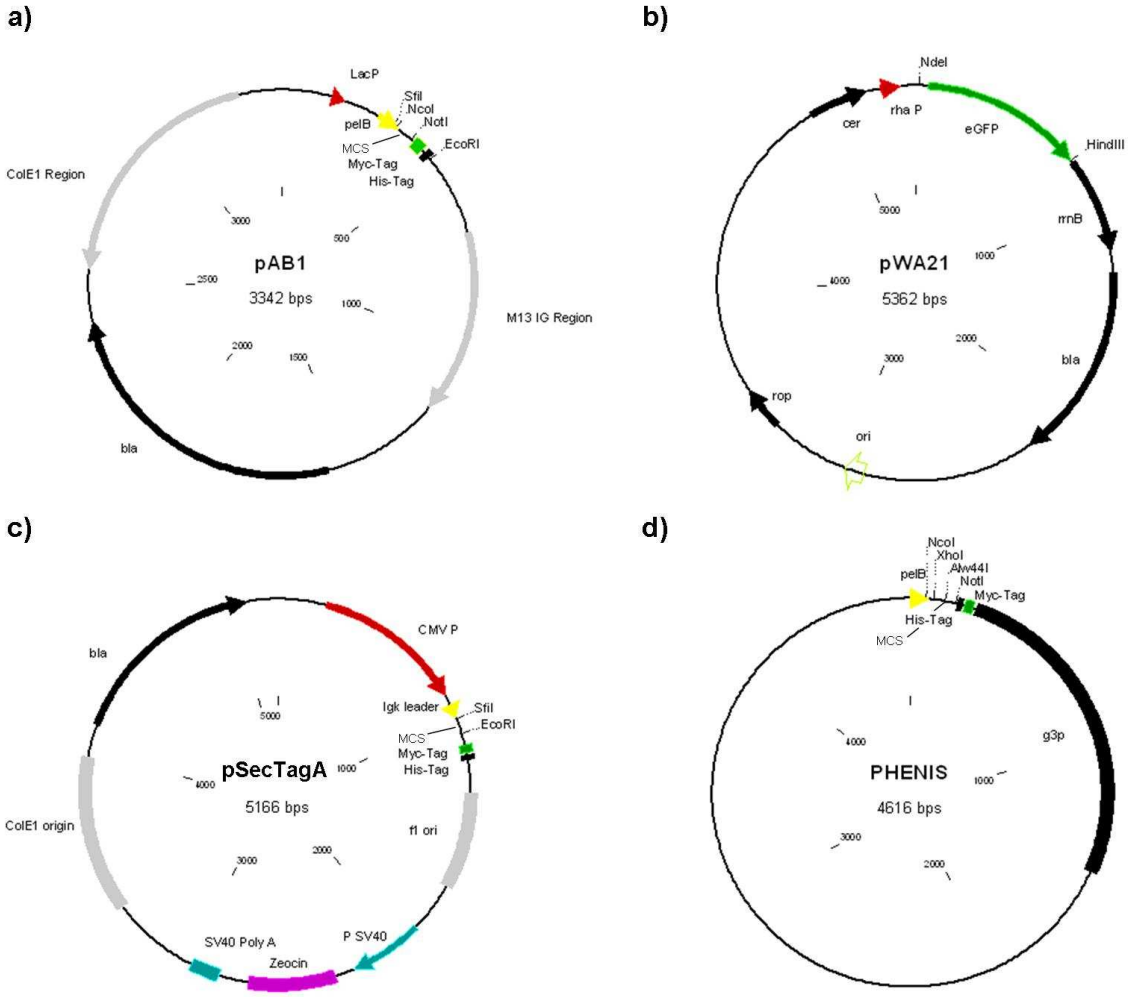

Fig. 2-1: Cloning and expression vectors

a) pAB1 bacterial expression vector: Lac P, lacI repressor and lacZ IPTG inducible promoter; pelB, signalling sequence for periplasmic secretion; MCS, multiple cloning site with restriction sites SfiI, NcoI, NotI, EcoRI; Myc-Tag, c-myc tag; His-Tag, hexahistidine tag; M13 IG region, intergenic region; bla, β-lactamase (ampicillin resistance); ColE1, origin of replication. pABC4 differs in an additional cysteine downstream of His-Tag and lack of Myc-Tag.

b) pWA21 bacterial expression vector: rha P, rhamnose inducible promoter; eGFP, sequence for recombinant eGFP; rrnB, rRNA operon; bla; ori, origin of replication; rop, encoding Rop protein; cer: constrained execution region.
c) pSecTagA mammalian expression vector: CMV P, human cytomegalie-virus promoter; Igκ leader, signalling sequence for protein secretion; MCS with restriction sites SfiI, EcoRI; f1 ori/PSV40/Zeocin/SV40 Poly A, transcription cassette for zeocin resistance; ColE1; bla
d) pHENIS scFv cloning vector: pelB; MCS with restriction sites NcoI, XhoI, ApaLI (Alw44I), NotI and G-S linker between positions 82 and 132; Myc-Tag; His-Tag; g3p, Gene III product

2.1.7 Mammalian cell lines and bacterial strains

mammalian cell lines

Table 2-1: Mammalian cell lines and DSMZ numbers

cell line	origin	culture	media
Daudi ACC 78	human Burkitt lymphoma	suspension	RPMI 1640 + 10 % FCS
HEK293 ACC 305	human embryonic kidney	adherent	RPMI 1640 + 5 % FCS
Jurkat ACC 282	human T-cell leukaemia	suspension	RPMI 1640 + 10 %
Kasumi1 ACC 220	human acute myeloid leukaemia	suspension	RPMI 1640 + 10 % FCS
SEM ACC 546	human acute lymphoblastic leukaemia	suspension	RPMI 1640 + 10 % FCS
SKNO1 (received from O. Heidenreich)	human acute myeloblastic leukaemia	suspension	RPMI 1640 + 20 % FCS + 7 ng/ml GM-CSF

Bacteria strains

***E.coli* TG1**

Genotype: *F´ traD36 lacI^q Δ(lacZ)M15 proA$^+$B$^+$/supE Δ(hsdM-mcrB)5 ($r_k^-m_k^+$McrB$^-$) thi Δ (lac-proAB)*

TG1 is a suppressor strain where the codon TAG is translated to glutamine. It can be used for production of proteins under control of the lac promoter.

***E.coli* BL21 rha$^-$**

Genotype: *F´ompT hsdS_B (r_B^- m_B^-) gal dcm rha*

BL21 rha$^-$ is derived from B834 with inactivation ofthe *rhaB* gene encoding for L-rhamnulose kinase. It can be used for production of proteins under control of the rhamnose promoter (Wilms et al., 2001).

2.2 Cloning of single chain Fv' molecules

For cloning of the scFv' format, containing a C-terminal cysteine, scFv genes were cut from the vector pAB1 (Fig. 2-1) by restriction digestion with the enzymes SfiI and EcoRI and inserted into the vector pABC4.

2.2.1 Restriction digestion

10 µg of pAB1 scFv DNA and 5 µg of pABC4 DNA were mixed with 1 µl NcoI, 5 µl 10x buffer Tango and H_2O to a total volume of 50 µl and incubated over night (o/n) at 37 °C. For buffer exchange the NucleoSpin Extract II Kit was used. Total DNA was mixed with 2 µl NotI and 5 µl 10x buffer O and incubated for 4h at 37 °C. 1 µl of alkaline phosphatase was added to the vector mix and incubated for additional 1 h at 37 °C.

2.2.2 Agarose gel electrophoresis

Digested DNA was mixed with 5x DNA loading buffer and separated in a 1 % agarose gel in TAE buffer containing 1 µg/ml ethidium bromide. DNA samples and a DNA size standard were run at 85 V for 60 min. The DNA fragments were identified by size under UV light, cut out, purified with the NucleoSpin Extract II Kit according to the manufacturer's protocol and dissolved in 30 µl H_2O. Preparations were held on ice or stored at -20 °C until further use.

2.2.3 Ligation

For ligation with T4 DNA ligase various ratios of vector to insert were used and prepared as shown in Table 2-2:

Table 2-2: Ligation of digested DNA fragments

	I	**II**	**III**
vector (pABC4), cut NcoI/NotI	1 µl	1 µl	1 µl
inserts (pAB1 scFv CD13, CD19, CD33), cut NcoI/NotI	10 µl	5 µl	-

ligase buffer (10 x)	2 µl	2 µl	2 µl
T4 DNA ligase (5 U/µl)	1 µl	1 µl	1 µl
H_2O	6 µl	11 µl	16 µl
total	20 µl	20 µl	20 µl

Ligation was carried out at room temperature (RT) for 1 h. Preparations were held on ice or stored at -20 °C until further use.

2.2.4 Transformation

For transformation, $CaCl_2$ competent *E. coli* TG1 cells were thawed on ice and 100 µl were mixed with 10 µl of ligated DNA, incubated for 15 min on ice and then for 90 sec at 42 °C in a waterbath. After incubation for 1 min on ice, 1 ml of LB medium was added to each sample and incubated for 1 h at 37 °C whilst shaking.

2.2.5 Screening of clones

For screening, cells were pelleted by centrifugation for 1 min at 13.000 rpm. After having discarded the supernatant, cells were resuspended in the retained liquid, plated on agar plates ($LB_{amp, glc}$) and incubated o/n at 37 °C. For screening of positive clones, single clones were picked from the agar plates and used as templates in PCR with 50 % REDTaq ReadyMix and 1 pmol/µl of the primers LMB2 and LMB3 in the case of pABC4 and the primers pSec-Seq1 and pET-Sec2 in the case of pSecTagA. In parallel, these clones were plated on a masterplate and incubated o/n at 37 °C. PCR was performed for 30 cycles with 1 min at 94 °C, 1 min at 50 °C and 1 min at 72 °C, a pre-cycle of 5 min at 94 °C and a post-cycle of 5 min at 72 °C.

2.2.6 Plasmid-DNA isolation (Midi)

A positive clone was picked from the masterplate and grown in 100 ml LB/amp/glc medium o/n at 37 °C whilst shaking. 700 µl of o/n culture were transferred to a cryovial, mixed with 300 µl of sterile glycerine preparation (85 % glycerine in H_2O) and stored at -80 °C. The culture was centrifuged at 5000 rpm at 4 °C for 15 min. For DNA preparation from the bacterial pellet PureLink HiPure Plasmid MidiPrep Kit or NucleoBond Xtra plasmid purification kit were used according to the manufacturer's protocols. Purified DNA was resolved in 100 µl H_2O for 1 h on ice and stored at -20 °C until further use. To determine DNA concentration NanoDrop at a wavelength of 230 nm was used.

2.2.7 Sequence analysis of scFv' inserts

Approximately 1 µg of Midi-DNA was sequenced by Eurofin MWG Operon, Martinsried, Germany or GATC, Konstanz, Germany with primer LMB3, corresponding to MWG primer M13-rev and GATC primer M13-rp in case of the vector pABC4 and pSecSeq2 in case of the vector pSecTagA. This primer corresponds to MWG primer pCR3.1-BGH rev and GATC primer BGH reverse. Analysis of the resulting sequence was performed using the BLAST search tool in comparison to the sequence in CloneManager, version 7.04 software.

2.3 Expression and purification of scFv' molecules

2.3.1 Periplasmic protein expression in *E. coli* TG1

ScFv' molecules were produced in *E.coli* TG1 transformed with the plasmid pABC4 scFv' CD13, CD19 and CD33. 1 l 2x TY medium containing 100 µg/ml ampicillin and 0.1% glucose was inoculated with 10 ml of an o/n culture (2x TY/amp with 1% glucose) of TG1 pABC4 scFv' in a 2 l baffled shaking flask on a rotary shaker at 180 rpm. The culture was incubated at 37 °C until it reached OD_{600} values of 0.8 to 1. IPTG was added to a final concentration of 1 mM and cells were incubated for additional 3 h at RT whilst shaking at 180 rpm. Cells were centrifuged for 10 min at 5000 rpm and resuspended in 50 ml of PPB. Freshly prepared 1 % lysozyme solution (10 mg/ml in H_2O) was added to a final concentration of 50 µg/ml and the suspension was incubated on ice for 25 min. After adding $MgSO_4$ (1 M stock solution in H_2O) to a final concentration of 10 mM to inhibit further lysozyme activity, cells were centrifuged for 10 min at 8000 rpm. The supernatant was dialyzed in a dialyzing tube with a cut-off of 8 – 10 kDa against PBS o/n at 4 °C.

2.3.2 Mammalian cell expression in HEK 293

For the mammalian cell expression of scFv' CD13 the insert was cloned into the pSecTagA vector (Fig. 2-1) containing an Igκ leader. The cloning procedure was performed according to chapter 2.2 with a SfiI/EcoRI digestion of pSecTagA and pAB1 scFv CD13. For transfection of the plasmid into mammalian HEK293 cells the cells were seeded in a 6-well plate at $1x\ 10^6$ cells/well in 2 ml culture medium and incubated o/n. The next day, the medium was replaced by 1.33 ml serum-free medium (Opti-MEM). 166 µl Opti-MEM were incubated with 6.66 µl lipofectamine for 5 min at RT and another 166 µl Opti-MEM were mixed with 2.66 µg plasmid DNA. Both solutions were mixed together and incubated for 20 min at RT. Afterwards, this solution was drop wise added to the cells and incubated for 6 h at 37 °C. Opti-MEM was removed and fresh cell culture medium was added. After 3 days supernatants were analysed for transient protein expression by western blot analysis (2.4.2). For stable transfection the

cells were transfected as described above. One day after transfection cells were transferred to a 10 cm Petri dish and cultured in 8 ml of RPMI 5 % FCS for one other day. Transfected HEK293 cells were then selected for their ability to grow in the presence of zeocin. Therefor, zeocin was added to the 10 cm Petri dish to a final concentration of 300 µg/ml. Selection medium was replaced by fresh medium, supplemented with zeocin, twice a week until zeocin-resistant colonies appeared between two and three weeks after transfection. The zeocin concentration was decreased to 50 µg/ml and secreted products were assayed by taking samples of the supernatant and performing western blot analysis. Positive transfectants were expanded to a 75 cm² tissue culture flask and stocks of cells were cryopreserved at -80 ℃. For large scale production cells were grown in 175 cm^2 culture flasks until a confluence of approximately 80 % was reached. The medium was changed to 25 ml Opti-MEM per flask and replaced every 3 or 4 days for 2 weeks. Supernatants containing the protein were pooled and stored at 4 ℃. 390 g/l of $(NH_4)_2SO_4$ (corresponding to 60 % saturation) was slowly added to the pooled supernatants at 4 ℃ whilst stirring. After 30 min of continuous stirring the precipitated protein was centrifuged for 15 min at 8000 rpm and resuspended in 30 ml of PBS.

2.3.3 Purification by immobilized metal ion affinity chromatography (IMAC)

Dialysed bacterial supernatant, centrifuged for 15 min at 8000 rpm, and resuspended protein from the mammalian expression were loaded onto a Ni-NTA column previously washed with 10 ml of PBS and equilibrated with 10 ml of IMAC loading buffer (20 mM imidazole in IMAC buffer) to minimize unspecific binding of proteins. The column was then washed with IMAC wash buffer (35 mM imidazole in IMAC buffer). The column was washed until no more protein was detected by qualitative Bradford assay in aliquots of the wash buffer. Therefor, 10 µl of the test solution were mixed with 90 µl of Bradford reagent. Samples containing protein were detected by a change of the reagent colour from brown to blue. After washing, the bound proteins were eluted with IMAC elution buffer (250 mM imidazole in IMAC buffer) and collected in 500 µl fractions. Protein containing fractions were determined by SDS-PAGE analysis, pooled, and dialyzed in dialyzing tubes with a molecular mass cut-off of 12.4 kDa against PBS o/n at 4 ℃ to remove imidazole.

2.4 Characterization of scFv' molecules

The purified scFv' molecules were characterized concerning their size, integrity, purity and potential dimerization by SDS-PAGE and western blot analysis.

2.4.1 Determination of protein concentration

Protein concentrations were determined in NanoDrop under indication of their molecular mass and absorption factor at 280 nm, both determined in CloneManager 7.04.

2.4.2 SDS-PAGE and western blot analysis

30 µl of bacterial protein samples and 10 µl of mammalian samples were mixed with 5x reducing or non-reducing SDS loading buffer and boiled for 5 min at 95 ℃. A prestained protein marker was used for determination of protein size. 15 % polyacrylamid gels (Table 2-3) were run at 50 mA per gel for approximately 1 h. Afterwards gels were stained with Coomassie staining solution for 1 h whilst shaking and destained in destain solution o/n.

Table 2-3: Acrylamid gel compositions

	stacking gel	**separation gel**	
	3%	**10%**	**15%**
TRIS buffer (1.5 M, pH 8.8)	-	1.9 ml	1.9 ml
TRIS buffer (0.5 M, pH 6.8)	0.34 ml	-	-
H_2O	1.7 ml	2.9 ml	1.7 ml
30% bis-acrylamide	0.4 ml	2.5 ml	3.75 ml
10% SDS	0.025 ml	0.075 ml	0.075 ml
10% APS	0.025 ml	0.075 ml	0.075 ml
TEMED	0.003 ml	0.006 ml	0.006 ml

Identity of protein samples was confirmed by western blot analysis. After separation by 15 % SDS-PAGE, proteins were blotted for 30 min per gel at 10 V onto a nitrocellulose membrane. The nitrocellulose membrane was incubated in western blot blocking solution for 1 h at RT whilst shaking in order to block free binding sites. For detection of recombinant proteins the membrane was then incubated with a HRP-conjugated mouse anti-his_6-tag antibody diluted 1: 1000 in blocking solution for 1 h at RT or o/n at 4 ℃. After washing the membrane three times with PBS, 0.05 % Tween and one time with PBS for 5 min the blot was developed with ECL substrate solution for 1 min. The blot was exposed to a film for 10 sec to 1 min, which was then automatically developed in a film developing machine.

2.5 Binding of scFv' molecules to target tumour cell lines

The recombinant scFv' molecules were tested for their specific binding ability to human leukaemic cell lines expressing the corresponding antigens. The cell lines Kasumi1, SKNO1, SEM, Jurkat and Daudi (Table 2-1) were cultured and analysed in flow cytometry.

2.5.1 Cell culture

Cells were maintained in 75 cm^2 culture flasks with 20 ml of the appropriate medium (Table 2-1) at 37 °C in a humidified CO_2 incubator. Cells were split every 2 to 3 days. Adherent HEK 293 cells were detached using Trypsin-EDTA. In order to store cells approximately 5 x 10^6 cells were resuspended in 1 ml FCS, 40 % RPMI, 10 % DMSO and gradually frozen to -80 °C in a special cryobox containing isopropanol. Cells were stored at – 80 °C or in liquid nitrogen. To thaw cells, they were quickly defrosted in a water bath at 37 °C and mixed with 1 ml of culture medium. Cells were then centrifuged at 1500 rpm for 5 min, resuspended in culture medium and transferred to a culture flask.

2.5.2 Flow cytometry

To determine binding of the scFv' to cells, 250000 cells per well were seeded into a V-shape 96-well cell culture plate in 100 µl of PBA. 10 µg/ml (354 nM) of scFv' were added to the cells and incubated for 2 h at 4 °C. Cells were washed three times with 150 µl PBA per well and centrifuged for 5 min at 1500 rpm. Cells were then incubated with a secondary mouse anti His-Tag unconjugated mAb in a dilution of 1: 400 for 1 h at 4 °C and again washed thrice. As a detection antibody a goat anti-mouse IgG-PE or a rabbit anti-mouse IgG-FITC, diluted 1: 400 was incubated with cells for 30 min at 4 °C in the dark. As a negative control, only the secondary and the detection antibodies were incubated on the cells. Finally, the cells were resuspended in 500 µl PBA and transferred to FACS tubes held on ice. Fluorescence analysis was performed using the flow cytometer. As a positive control, 5 µl FITC-conjugated anti-CD13, anti-CD19 and anti-CD33 monoclonal antibodies (final dilution 1: 20) were incubated on the cells for 1 h at 4 °C, washed thrice with PBA and analysed by flow cytometry. Both fluorescent dyes were excited at a wavelength of 488 nm, FITC emission was detected at 525 nm (FL1), PE emission at 575 nm (FL2). Data were analysed with the software WinMDI, version 2.8.

2.6 Cloning of scFv' CD33 variants

With regard to an improved scFv' coupling efficiency and IL binding ability, different variants of scFv' CD33 were cloned. Therefor, the order of the light and heavy variable chain was changed with the help of the cloning vector pHENIS (Fig. 2-1). Additionally, the length of the

peptide spacer between the His-Tag and the C-terminal cysteine was altered (see Fig. 3-3). The primers were synthesised by Metabion [Martinsried, Germany].

2.6.1 Cloning strategy and primer design

1. PCR (chapter 2.6.2) on pABC4 CD33 V_LV_H (scFv' CD33) for the amplification of V_H with inserted restriction sites NcoI and XhoI with primers:
- NcoI-V_H CD33 back: 5'-cat gcc atg gcg gag gtg cag ctg aag gag tca gga-3'
- V_H CD33-XhoI forward: 5'-gcg act cga gac ggt gac tga ggt tcc ttg acc-3'
Restriction digestion of the PCR product and the vector pHENIS with the enzymes NcoI and XhoI followed by ligation, transformation in *E. coli* TG1 and Midi preparation of the plasmid pHENIS CD33 V_H as described in chapters 2.2.3 to 2.2.6.

2. PCR on pABC4 CD33 V_LV_H (scFv' CD33) for the amplification of V_L with inserted restriction sites ApaLI and NotI with primers:
- ApaLI-V_L CD33 back: 5'-tta agt gca cag gac att gtg atg acc cag tct cac-3'
- V_L CD33-NotI forward: 5'-a tag ttt agc ggc cgc acg ttt tat ttc cag ctt ggt ccc ag-3'
Generation of the plasmid pHENIS CD33 V_HV_L.

3. Restriction digestion of pHENIS CD33 V_HV_L and pABC4 CD33 V_LV_H with the enzymes NcoI and NotI.
Ligation of the plasmid pABC4 CD33 V_HV_L.

All scFv' CD33 fragments were now available as HC1 variants.

4. PCR on pABC4 CD33 V_L-V_H (scFv' CD33) for the amplification of CD33 V_LV_H with prolonged spacer HC2 and inserted restriction sites NcoI and EcoRI with primers:
- NcoI CD13 back: 5'-cat gcc atg gcg gac tac aaa gac -3'
- His HC2-EcoRI forward: 5'-ccg gaa ttc tta gca tcc gga gcc gct gga tcc gcc gtg gtg atg gtg atg atg-3'
Generation of the plasmid pABC4 CD33 V_L-V_H HC2.

5. PCR on pABC4 CD33 V_LV_H (scFv' CD33) for the amplification of CD33 V_LV_H with prolonged spacer HC4 and inserted restriction sites NcoI and EcoRI with primers:
- NcoI CD13 back

- His HC4-EcoRI forward: 5'-ccg gaa ttc tta gca tcc gga gcc gct gga tcc gcc gct gga tcc gcc gtg gtg atg gtg atg atg-3'
Generation of the plasmid pABC4 CD33 V_LV_H HC4.

6. PCR on pABC4 CD33 V_HV_L for the amplification of CD33 V_HV_L with prolonged spacer HC2 and inserted restriction sites NcoI and EcoRI with primers:
- NcoI-V_H CD33 back
- His HC2-EcoRI forward
Generation of the plasmid pABC4 CD33 V_HV_L HC2.

7. PCR on pABC4 CD33 V_H-V_L for the amplification of CD33 V_HV_L with prolonged spacer HC4 and inserted restriction sites NcoI and EcoRI with primers:
- NcoI-V_H CD33 back
- His HC4-EcoRI forward
Generation of the plasmid pABC4 CD33 V_HV_L HC4.

The plasmids pABC4 scFv' CD33 V_HV_L, V_LV_H HC2, V_LV_H HC4, V_HV_L HC2 and V_HV_L HC4 were sequenced with the primer LMB3 by Eurofin MWG Operon [Ebersberg, Germany].

2.6.2 Polymerase chain reaction (PCR)

For the amplification of scFv' DNA sequences PCR with primers containing specific restriction sites and spacer sequences (2.6.1) was performed. The original scFv' CD33 was used as an initial template for PCR. The following reaction mix was prepared (Table 2-4).

Table 2-4: PCR reaction mix

template (1 ng/µl)	10 µl
10x buffer (with $(NH_4)_2$ SO_4	5 µl
$MgCl_2$ (25 mM)	4 µl
Primer-back (10 pmol/µl)	1 µl
Primer-for (10 pmol/µl)	1 µl
dNTPs (20 mM)	2.5 µl
Taq polymerase (1 U/µl)	1.25 µl
H_2O	25.25 µl
Total	50 µl

PCR was performed for 30 cycles with 1 min at 94 ℃ , 1 min at 50 ℃ and 1 min at 72 ℃, a pre-cycle of 5 min at 94 ℃ and a post-cycle of 5 m in at 72 ℃. 5x DNA loading buffer was

added to the PCR mix. DNA was separated in a 1% agarose gel in TAE buffer containing 1 µg/ml ethidium bromide, running the gel for 60 min at 85 V. For later digestion, the PCR product was identified by size under UV light, cut out from the gel, purified using the NucleoSpin Extract II Kit, according to the manufacturer's protocol, and dissolved in 30 µl H_2O. Preparations were held on ice or stored at -20 °C until further use.

2.7 Expression and purification of scFv' CD33 variants

All the scFv' CD33 variants were expressed in *E. coli* TG1 and purified as described in 2.3.1 and 2.3.3.

2.7.1 Fermentation of scFv' CD33 V_HV_L HC4

In order to increase the production yield of scFv' CD33 V_HV_L HC4, its sequence was cloned into the vector pWA21 and transformed into *E. coli* BL21 rha^- cells as described in chapter 2.2.4. This strain could be used for the rhamnose induced cytoplasmic expression of scFv' in a fermentation process. The scFv' CD33 V_HV_L HC4 gene was therefor amplified using 10 ng of the vector pABC4 scFv' CD33 V_HV_L HC4 as template and 10 pmol of the primers NdeI-pelB-back and stop-pAB-HindIII-for [Metabion, Martinsried, Germany]. PCR was performed as described in chapter 2.6.2, extension time was prolonged to 2 min at 72 °C. The PCR product was extracted from the agarose gel and inserted into the vector pWA21 with the help of the restriction enzymes NdeI and HindIII. Transformed *E. coli* TG1 cells were screened on ampicillin-containing LB agar plates for positive clones. Midi DNA preparation was performed without PCR screening for six clones. Control digestion was performed with XhoI, confirming the insertion of the scFv' sequence into the vector pWA21, correct sequence of scFv' CD33 V_HV_L HC4 was confirmed by sequencing with pET-Seq1. The plasmid was then transformed into *E. coli* BL21.

For the fed-batch fermentation process an o/n culture of *E. coli* BL21 pWA21 scFv' CD33 V_HV_L HC4 in LB-medium containing 0.01 % ampicillin was prepared and incubated at 25 °C whilst shaking. 100 µl of the o/n culture were inoculated in minimal-medium 0.01 % ampicillin and grown for approximately 8 h at 37 °C whilst shaking. A second o/n culture in mi nimal-medium 0.01 % ampicillin was inoculated with 1 ml from this culture and incubated at 30 °C whilst shaking. Batch-medium was then inoculated with the complete o/n culture and transferred into a sterile fermenter. pH value and O_2 concentration were registered and regulated permanently during the process. OD_{500} and glucose concentration were measured once per hour. At the time point when glucose was completely exhausted, feed-media I and II were continuously added. At the time point when an OD_{500} of 50 was exceeded, expression of scFv' was induced by adding 0.2 % rhamnose to the culture. Approximately 6 h after

induction feed-media were exhausted and the process was terminated by centrifugation of the bacterial culture at 5000 rpm for 15 min at 4 °C. Pellets were then used for cytoplasmic purification of scFv'.

2.7.2 Cytoplasmic purification of scFv' CD33 V_HV_L HC4

The bacterial pellets were resuspended in PBS containing 1 % triton X 100. For cell lysis the bacterial suspension was sonicated on ice and centrifuged at 8000 rpm for 30 min at 4 °C. The protein was purified from the supernatant by IMAC as described in chapter 2.3.3. A wash buffer containing 40 mM imidazole was used.

2.8 Characterization of scFv' CD33 variants

The purified scFv' variants were characterized concerning their size, integrity, purity and potential dimerization by 15 % SDS-PAGE and western blot analysis with a special regard on scFv' CD33 V_HV_L HC4. For this variant, periplasmic and cytoplasmic expression yields were compared and as additional investigations size exclusion chromatography and a melting point analysis were performed.

2.8.1 Size exclusion chromatography (SEC) of scFv' CD33 V_HV_L HC4

SEC was performed with a HPLC-SEC 2000 sepharose column. Approximately 10 µg of purified scFv' CD33 V_HV_L HC4 was injected in a volume of 20 µl PBS. The column was permanently flowed by PBS as a fluxing agent with a rate of 0.5 ml/min under a pressure of 200-300 psi. Eluting protein fractions were quantified by a UV detector at 280 nm. Retention time of the scFv' depended on its molecular mass. Analysis was performed with the help of Clartiy Lite software. The molecular mass was plotted against its retention time in comparison to standard proteins of known sizes (Table 2-5).

Table 2-5: Standard proteins for SEC

protein	**size [kDa]**
Aprotinine	6.5
Cytochrom C	12.4
Carbonic anhydrase	29
Bovine serum albumin	66
ß-Amylase	200
Apoferritin	443
Thyreoglobuline	669

2.8.2 Melting point determination of scFv' CD33 V_HV_L HC4

The melting point of the scFv' fragment was determined with the ZetaSizer Nano ZS. Therfor, 150 µg of purified scFv' CD33 V_HV_L HC4 were diluted in PBS to a total volume of 1 ml and sterile filtered into a quarz cuvette. Dynamic laser light scattering intensity was measured while the temperature was increased stepwise from 35 to 75 °C. The melting point was determined as the temperature, at which the light scattering intensity dramatically increased.

2.9 Binding of scFv' CD33 variants to target tumour cell lines

The scFv' variants were tested for their specific binding ability to human leukaemic cell lines Kasumi1, SKNO1 and Jurkat cells. Therefor, flow cytometry was performed as described in chapter 2.5.2. 10 µg/ml scFv' were incubated on 250000 cells for 1 h at 4 °C. For detection, a fluorescence-labelled secondary antibody was used.

2.10 Liposome preparation methods

Two different IL preparation methods, the conventional coupling method and the postinsertion method, were performed and compared. Therefor, the scFv' CD33 variants were used.

2.10.1 Conventional coupling method

In the conventional coupling method, liposomes containing maleimide-functionalized PEG-chains were directly coupled to reduced scFv' CD33.

2.10.1.1 Preparation of liposomes

A lipid composition of EPC: cholesterol: mal-PEG_{2000}-DSPE at a molar ratio of 65: 30: 5 (16.3 µl EPC, 11.6 µl cholesterol, 46.8 µl Mal-PEG_{2000}-DSPE stocks for 1 ml liposomes) was used for the preparation of liposomes. The lipid formulation contained DiI as a fluorescent lipid marker at a molar concentration of 0.3 mol% (8.1 µl DiI stock for 1 ml liposomes). A thin lipid film was formed in a round bottom flask by dissolving the lipids in chloroform and removing the solvent in a rotary evaporator for 10 min at 42 °C. Subsequently the lipid film was dried completely in a vacuum drying oven for at least 1 h at RT. The lipid film was hydrated in 10 mM HEPES buffer, pH 6.7 and vortexed until all components were dissolved. The final lipid concentration was 10 mM. The lipid solution was then extruded 21 times through a 50 nm pore size polycarbonate filter membrane using a LiposoFast extruder to obtain small unilamellar vesicles.

2.10.1.2 Coupling of scFv' molecules to liposomes

100 µg scFv' molecules were reduced by adding 5 µl TCEP (625 nmol TCEP per 1 nmol scFv') and incubated under nitrogen atmosphere for 2 h at RT. TCEP was then removed by dialysis against deoxygenated Nellis buffer pH 6.7 o/n at 4 °C. Dialysis buffer was refreshed after at least 4 h. Freshly prepared liposomes were incubated with reduced scFv' at any adequate molar ratio (e.g. 100 µg scFv' per 1 µmol lipid: 0.36 mol%). Liposomes incubated with the corresponding volume of PBS served as a negative control. The mixed solution was overlayed with nitrogen and incubated on an orbital shaker for at least 1 h at RT. 1 mM L-cysteine was added to the scFv'-coupled as well as to the control liposomes to saturate the unconjugated maleimide groups and was incubated for at least 10 min at RT.

2.10.2 Postinsertion method

In the postinsertion method, scFv' were coupled to malPEG$_{2000}$-DSPE micelles, which were inserted into preformed mPEG$_{2000}$-DSPE liposomes in a second step. For the postinsertion method the following lipid composition was used: EPC: cholesterol: mPEG$_{2000}$-DSPE in a molar ratio of 65: 30: 5 (16.3 µl EPC, 11.6 µl cholesterol, 27.5 µl m-PEG$_{2000}$-DSPE stocks for 1 ml liposomes). For detection purpose the lipid formulation contained DiI as a fluorescent lipid marker in a molar ratio of 0.3 mol%. Liposomes were prepared as described in 2.10.1.1. 50 µg (17 nmol) of mal-PEG$_{2000}$-DSPE stock solution were transferred into a 1.5 ml test tube for preparation of maleimide-functionalized micelles. The solvent was evaporated in the open tube at RT until a lipid film became visible. The lipid film was dissolved in H_2O to a final concentration of 4.2 mM for the formation of micelles and incubated for 5 min at 65 °C in a water bath by shaking from time to time. Micellar lipid and reduced scFv' were mixed at a molar ratio of 4.76: 1 by adding 100 µg (3.57 nmol) scFv' to the micellar lipid, overlaid with nitrogen and incubated for 30 min at RT. As a negative control, liposomes were mixed with the corresponding volume of PBS. To saturate the unconjugated coupling groups, L-cysteine was added to a final concentration of 1 mM to the scFv'-coupled micelles as well as to the control micelles and incubated for at least 10 min at RT. The scFv′-coupled micelles were then inserted into preformed PEGylated liposomes at any adequate molar ratio (between 0.1 and 10 mol% mal-PEG-DSPE of total lipid) by incubation for 30 min at 55 °C in a water bath.

2.10.3 Immunoliposome purification

Uncoupled scFv' molecules were removed from the IL preparation by gel filtration using a Sepharose CL4B column equilibrated with 10 mM HEPES buffer pH 7.4. Liposome containing fractions visible through incorporated fluorescent dye were pooled. The lipid concentration was estimated by dividing the initial amount of lipid by the final volume. Alternatively, uncoupled scFv' can be separated by ultra-centrifugation at 300000 g for 1 h at

4 ℃. To achieve an adequate lipid concentration (e .g. 10 mM) the liposomal pellet was dissolved in a defined volume of 10 mM HEPES pH 7.4.

2.10.4 Determination of liposome size

To determine liposome size liposomal formulations were diluted 1: 100 in PBS in a low volume disposable cuvette and size was measured by dynamic light scattering using a ZetaSizer Nano ZS.

2.10.5 Determination of scFv' coupling efficiency

For the determination of coupling efficiency western blots were performed as described in chapter 2.4.2. 2 µg of untreated scFv' were prepared as a control to compare with coupled samples. Accordingly, samples of scFv'-coupled micelles and ILs containing 2 µg of scFv' were prepared. ScFv' was detected with an HRP-conjugated mouse anti-His-Tag antibody diluted 1: 1000 in 5% MPBST. Intensities of protein bands of untreated scFv', micellar scFv' and liposomal scFv' were determined in Image Quant software. Coupling and insertion efficiencies were calculated by comparison of the intensities of lipid coupled scFv' protein bands to the untreated scFv' protein band and by comparison with the amount of scFv' which were introduced into the coupling reaction. Coupling efficiencies were determined for 0.3 mol% of micellar malPEG$_{2000}$-DSPE from the total lipid.

Calculation of the number of scFv' molecules per liposome:

Each sample contained 100 µg scFv' (3.57 nmol) and 17 nmol malPEG$_{2000}$-DSPE, resulting in a ratio of 1: 4.76. Consequently, 21 % of malPEG$_{2000}$-DSPE could be coupled to scFv' molecules. For a molar ratio of 0.3 mol% malPEG$_{2000}$-DSPE to total lipid, the molar ratio of scFv' resulted in 0.06 mol% of total lipid. To obtain a molar ratio of 0.3 mol% malPEG$_{2000}$-DSPE, 5.61 µmol preformed liposomes were added to scFv' coupled micelles. The measured diameter of ILs was 79 nm (see Table 3-3), resulting in a surface area of 19.61 * 10^6 Å^2 as calculated by the formula $A= 4\pi r^2$. According to Yuan et al. (2007) the thickness of a lipid layer is approximately 27 Á, resulting in 54 Á for the lipid bilayer of the IL. This would lead to a diameter of 73.6 nm for the inner lipid layer and a corresponding surface area of 17.08 * 10^6 Å^2. Forge et al., 1978 described the area of one molecule of phosphytidylcholine, tightly packed in cholesterol, with 38 Å^2. Consequently, the outer lipid layer contained 51.6 * 10^3 phosphatidylcholine lipid molecules and the inner layer contained 44.9 * 10^3 lipids. Taken together, one liposome contained 96.5 * 10^3 lipids. As described above, a molar ratio of 0.3 mol% malPEG$_{2000}$-DSPE resulted in 0.06 mol% scFv' to total lipid. Consequently, one liposome contained 58 scFv' molecules. For the determination of the actual coupling efficiencies, amounts of scFv' molecules were calculated from the intensities of protein bands after coupling and insertion into liposomes in comparison to the untreated scFv' bands.

2.11 Binding of immunoliposomes to target tumour cell lines

ScFv' CD33 ILs prepared by the conventional coupling method and by the postinsertion method with the different scFv' CD33 variants were tested for their specific binding ability to human leukaemic cell lines Kasumi1, SKNO1 and Jurkat. ILs attached to cells could be detected due to the incorporation of DiI into the liposomal membrane. 25 nmol (250 µM) of liposomes were used for FACS analysis as described in chapter 2.5.2. Liposomes were incubated with 250000 cells in cell culture medium for 1 h at 4 °C in the dark. As a reference to all the samples untreated cells were included along the whole procedure as well as unconjugated $mPEG_{2000}$-DSPE liposomes in the same concentration. DiI fluorescence could be excited at a wavelength of 488 nm and detected at 575 nm. To further confirm the antigen specificity of IL binding, ILs coupled with an anti-endoglin scFv' were tested in the same concentration as the scFv' CD33 IL on 250000 SKNO1 cells. Additionally, a blocking experiment was performed. Therefor, scFv' against CD33 or against carcinoembryonal antigen (CEA) in a concentration of 3 µM were preincubated on SKNO1 cells 30 min before IL were added.

2.11.1 Optimization of immunoliposome binding

For the optimization of IL binding, different percentages of scFv' CD33 V_HV_L HC4 coupled micelles were inserted into preformed $mPEG_{2000}$-DSPE liposomes by the postinsertion method. The range was 10 to 0.1 mol% $malPEG_{2000}$-DSPE and the ILs were prepared as described in chapter 2.10.5. 25 nmol (250 µM) of ILs were tested for their binding activity on 250000 SKNO1 cells in flow cytometry. Mean fluorescence intensities (MFI) were determined with the help of WinMDI, version 2.8 software dividing the MFI of unconjugated liposomes on SKNO1 cells.

2.11.2 Plasma stability of immunoliposomes

For the investigation of plasma stability, 25 nmol scFv' CD33 V_HV_L HC4 ILs with 0.3 mol% micellar lipid, prepared by the postinertion method, were incubated in 50 % human plasma, stabilized with citrate-phosphate-dextrose solution (CPD), and in PBS as negative control at 37 °C for up to ten days. Flow cytometry of 250 µM ILs was performed in comparison to fresh ILs on 250000 SKNO1 cells. MFIs of ILs were divided by the MFI of untreated SKNO1 cells. MFIs as a percentage of day 0 MFI of plasma incubated or PBS incubated liposomes on SKNO1 cells were shown. Unconjugated liposomes were carried along as a negative control.

2.12 Internalization of immunoliposomes into target tumour cell lines

For internalization studies 250000 SKNO1 cells were incubated with 2 µM DiO to stain the cell membrane for 2 min at 37 °C. Kasumi1 cells and Jurkat cells were incubated with 2.6 nM cell tracker green for 30 min at 37 °C to stain the cytosol of living cells. After a washing step with cell culture medium 40 nmol (400 µM) of scFv' CD33 V_HV_L HC4 ILs with 0.3 mol% malPEG_{2000}-DSPE, prepared by the postinsertion method, were incubated with the stained cells in a total volume of 100 µl for 1, 4 or 8 h at 37 °C. Cells were then washed with PBS and fixed in 2 % paraformaldehyde for 10 min at RT. The cells were taken up in mowiol, dropped on cover slips and inverted onto microscopy slides. The slides were viewed under a fluorescent microscope or a confocal microscope. DiO as well as cell tracker green were excited at a wavelength of 488 nm and detected at 525 nm. ILs incubated on CD33-negative Jurkat cells as well as unconjugated liposomes on Kasumi1 cells served as negative controls. Images were prepared with Leica and Zeiss Axiovision software.

2.13 SiRNA encapsulation into liposomes

As a therapeutic approach, targeted liposomes could be loaded with siRNA. For this purpose a less leaky liposome formulation was chosen. It contained the more rigid hydrogenated soy-phosphatidylcholine (HSPC) instead of egg-phosphatidylcholine (EPC) and the lipid concentration was increased to 100 mM. Two therapeutic siRNAs (siAGF1 and siAML1/MTG8) were used, possessing the same nucleotide sequence, from two different manufacturers. For convenience reasons, they were later denoted as siAGF1. SiAGF6 was used as a mismatch siRNA. Further, a fluorescence labelled Cy3-siAML1/MTG8 was used. SiRNA encapsulation into liposomes was performed passively during liposome formation. Encapsulation of naked siRNA resulted in siRNA-loaded liposomes, encapsulation of PEI- or protamine-complexed siRNA resulted in the formation of lipoplexes. In a further step, liposomes were coupled to scFv' molecules by the postinsertion method, resulting in the formation of siRNA-loaded ILs or immunolipoplexes (ILPs).

2.13.1 Passive encapsulation of free siRNA

20 µM of Cy3 labelled siRNA AML1/MTG8 and 50 µM siRNA siAGF1 and siAGF6 in 10 mM HEPES pH 6.7 were added to a dry lipid film in a round bottom flask. During resolving the lipid film by vortexing, the siRNA in the aqueous phase was passively encapsulated into the liposomes (Fig 2-2). Unencapsulated siRNA was then separated from the liposomes by

ultracentrifugation at 85000 rpm for 1 h at 4 ℃. T he liposomal pellet was taken up in 10 mM HEPES pH 6.7 at a concentration of 100 mM for postinsertion of scFv' coupled micelles.

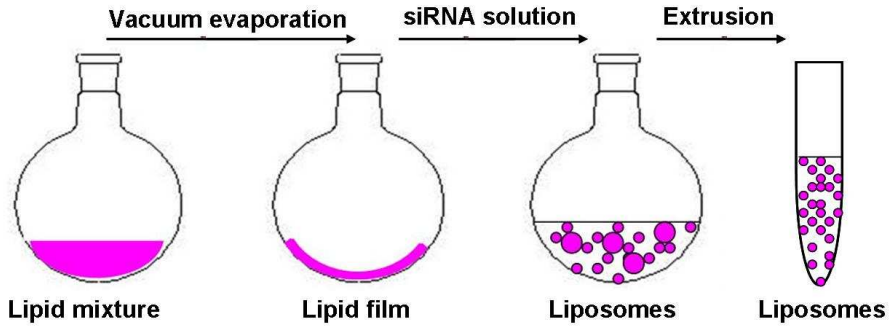

Fig. 2-2: Passive liposomal encapsulation of free and complexed siRNA
A lipid film was generated by vacuum evaporation of a soluble lipid mixture. Free siRNA or siRNA complexed to PEI or protamine was added in an aqueous solution to the dry lipid film. The lipid film was then dissolved in the siRNA solution by vortexing and sonication. During this step liposomes were formed and siRNA was encapsulated passively. During extrusion through membranes of constant pore size uniform liposomes were generated.

2.13.2 Passive encapsulation of complexed siRNA

To enhance encapsulation efficiency and endosomal escape, siRNA was complexed to polycationic moieties. These could be the synthetic polymer polyethylenimine (PEI) or protamine, a polycationic, histone like protein.

2.13.2.1 SiRNA-polyethylenimine (PEI) complexation

For an optimal complexation by electrostatic interactions a 25 kDa branched PEI was chosen and complexed to 20 µM respectively 50 µM siRNA in an N/P ratio of 5, representing the ratio of PEI nitrogen to siRNA phosphate ions. The amount of PEI corresponding to 10 pmol siRNA was calculated as follows:
10 pmol siRNA* 42P* 43 g/mol* 5= 90.3 ng PEI,
P represents the number of phosphate residues of the siRNA, 43 g/mol the molecular mass of one protonable nitrogen unit of PEI (NC_2H_5) and 5 the N/P ratio. In the process PEI was added to siRNA whilst both components were diluted in the same buffer volume. Complexation took place in 10 mM HEPES pH 7.4, where PEI was protonated. The mixture was pipetted up and down ten times, vortexed and incubated for 20 min at RT. The resulting molar ratio of PEI to siRNA was 1: 2.8.

2.13.2.2 SiRNA-protamine complexation

As a less cytotoxic alternative to PEI, siRNA was complexed to protamine. A molar ratio of siRNA: protamine of 1: 3 was taken. The complexation was performed as described for siRNA-PEI complexes in 2.13.2.1, whilst protamine in the same buffer volume was added to the siRNA. After complexation, the siRNA-PEI and siRNA-protamine complexes were encapsulated passively into liposomes as described for the free siRNA in chapter 2.13.1.

2.13.3 Determination of size

To determine the size of siRNA-loaded liposomes and ILs, lipoplexes and ILPs, the formulations were diluted 1: 100 in PBS in a low volume disposable cuvette and size was measured by dynamic light scattering using a ZetaSizer Nano ZS.

2.13.4 Determination of encapsulation efficiency

For the determination of encapsulation efficiency, 20 µM Cy3-labelled siRNA was used. Cy3 fluorescence could be excited at a wavelength of 488 nm and its emission was detected at 570 nm in a TECAN microplate reader. Cy3 signal intensity of the supernatant after seperation of the liposomes was determined and compared to the signal intensity of the siRNA solution before encapsulation. For the creation of a standard curve and a resulting formula for calculating siRNA concentrations, a serial dilution of Cy3-siRNA was analysed. Encapsulation efficiency was calculated indirectly from the unencapsulated siRNA in the supernatant of liposome samples for free siRNA, PEI- and protamine-complexed siRNA.

2.14 Binding and internalization of siRNA-loaded immunoliposomes to leukaemic cell lines

Free Cy3-siRNA was used for the preparation of siRNA-loaded liposomes and ILs in order to investigate their binding and uptake into SKNO1 and Kasumi1 cells. Jurkat cells incubated with ILs were taken as a negative control besides unconjugated liposomes incubated on SKNO1 and Kasumi1 cells. Binding and uptake were investigated by fluorescence microscopy. 250000 cells were therefor stained with cell tracker green as described in chapter 2.12 and incubated with 400 nmol liposomes and ILs for 1 to 8 h at 37 ℃ in a total volume of 100 µl. Cells were fixed in 2 % paraformaldehyde, mounted in mowiol and viewed on glass slides in a fluorescence microscope. Images were prepared in Zeiss Axiovision software.

2.15 Preparation of immunopolyplexes

2.15.1 Chemical synthesis

For the first synthesis approach (conjugate I, Fig. 2-3), polyethylenimine of a molecular mass of 25 kDa was fluorescently labelled with FITC (Merdan et al., 2002). Briefly, 20 mg PEI 25 were dissolved in 2 ml 0.1 M sodium bicarbonate buffer, pH 9.0 and mixed with 1 mg fluoresceine isothiocyanate in 200 ml DMSO, stirred in the dark for 3 h at RT and purified by ultrafiltration. The concentration of the purified sample was determined at 405 nm in a trinitrobenzenesulfonic acid (TNBS) assay. The absorbance of the fluorescent dye was found not to interfere with the results from the TNBS assay. For coupling of scFv', a heterobifunctional PEG-linker was coupled to PEI. For this step, 25 mg PEI 25 (1 µmol) were dissolved in HEPES buffered saline, pH 7.5, and reacted for 24 h with 27.6 mg (12 µmol) PEG linker, which had been dissolved in 200 µl absolute ethanol. Purification of the conjugates was achieved by modified ion exchange chromatography on an FPLC system equipped with cation exchange columns (Germershaus et al., 2006). The intermediate product, namely the FITC-labelled PEGylated PEI precursor was loaded to the exchange column with 150 mM NaCl, 20 mM HEPES buffer and eluted with a high ionic strength buffer containing 3 M NaCl, 20 mM HEPES. It was desalted using centricon YM-10 spin columns as recommended by the manufacturer. Aliquots of the products were characterized concerning their PEI concentration by TNBS assay and concerning their coupling degree by a pyridon-2-thion release assay. For this assay, an aliquot of PEGPEI was treated with a ten-fold molar excess of DTT for 4 h at RT for activation of the PEG-linker. Pyridon-2-thion release was measured spectrophotometrically at 343 nm and the activated PEGPEIs were purified using centricon YM-10 spin columns in presence of 10 mM EDTA to avoid metal catalyzed sulfhydryl oxidation (Hermanson et al., 1996). The second synthetic approach (conjugate II, Fig.2-3) did not involve FITC labelling. The PEPEI precursor was produced as described above, purified by FPLC, desalted and PEGylation degree was determined.

2.15.2 Conjugation of scFv' molecules

For scFv' coupling of the first conjugate, an aliquot of 300 µg PEI (540 µg PEGPEI, 12 nmol), of activated, purified and characterized precursor, was mixed with a three-fold molar excess of scFv'. ScFv' and activated PEI were coupled by formation of disulfide bonds after acidification to pH 6.5. After 24 h of incubation and another FPLC and ultrafiltration step, the concentration of PEI was determined in a TNBS assay, and the coupling degree of the conjugate was determined spectrophotometrically at 280 nm with background correction using a solution of activated PEGPEI of equal concentration. For coupling of the second conjugate, 40 nmol of scFv were activated by reduction in presence of a ten-fold excess of

DTT and dialyzed for 24 hours against N_2-degassed PBS buffer in a dialysis tube. The activated scFv' was mixed with 13 nmol PEGPEI and the reaction mixture was slightly acidified (pH 6.5) for disulfide bond formation. After 24 h of incubation, the reaction mixture was purified by FPLC and desalted by ultrafiltration before the concentration of PEI was determined in a copper complexation assay (Ungaro et al., 2003) and coupling degree of the conjugate was determined spectrophotometrically. Besides conjugation of scFv' CD33, immunoconjugates coupled with anti-EGFR scFv' were prepared for use as a negative control in cell culture studies.

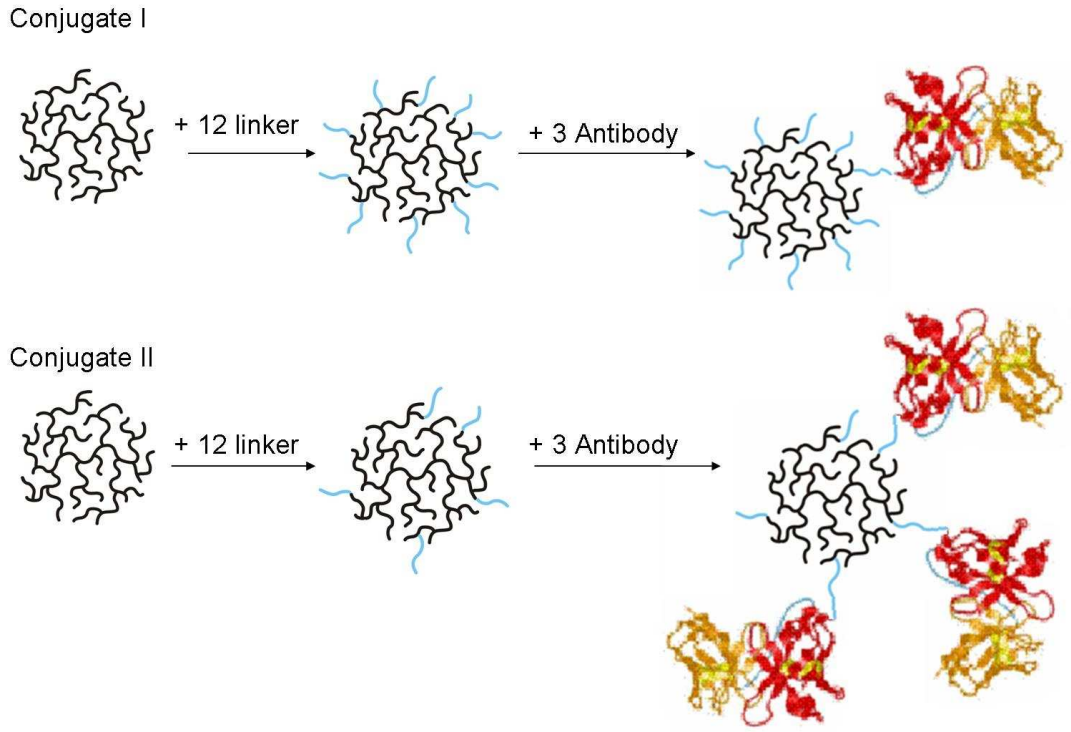

Fig. 2-3: Chemical synthesis of PEGylated PEI and conjugation of scFv'
PEI was conjugated to scFv' via a bifunctional PEG-linker.
Conjugate I contained 1 molecule scFv' per molecule PEI and was labelled with FITC.
Conjugate II contained 3 molecules scFv' per molecule PEI.

2.15.3 Determination of size and zeta potential

Size and zeta potential of polyplexes and immunoconjugates were determined by DLS analysis. The PEGPEIs and immunoconjugates were also investigated after siRNA complexation, as polyplexes or immunopolyplexes (IPPs), respectively. Therefor, siRNA siAGF1 was complexed with an N/P ratio of 5 as described for the siRNA-PEI complexes in chapter 2.13.2.1. The formulations were diluted 1: 100 in PBS in a low volume disposable

cuvette and size was measured by dynamic light scattering using a ZetaSizer Nano ZS. After size measurement, the content was transferred to a zeta cell and the zeta potential was determined in ZetaSizer Nano ZS.

2.16 Binding and internalization of immunopolyplexes to leukaemic cell lines

For binding and internalization studies, the FITC labelled conjugates were used and tested on SKNO1 and Jurkat cells. 500000 cells were incubated with 2, 1 or 0.5 µM polyplexes and anti-CD33 IPPs for 1 to 8 hours at 37 ℃. Anti CD33 IPPs were also investigated after complexation to Cy3-labelled siRNA AML1/MTG8 with an N/P ratio of 5. Cells were fixed with 2 % paraformaldehyde and mounted in Vectashield containing DAPI to stain the cell nuclei. DAPI fluorescence was excited at a wavelength of 346 nm and detected at 460 nm. The cells were viewed on glass slides with a fluorescent microscope and images were edited in Zeiss Axiovision software.

2.17 Transfection of target tumour cell lines

For the delivery of siRNA into leukaemic cell lines by ILs, ILPs and IPPs, transfection protocols had to be established.

2.17.1 SiRNA transfection by electroporation

In order to test the specific silencing activity of siAGF1 in general, siRNA was transfected into SKNO1 cells by electroporation. Therefor, 250000 cells in 100 µl cell culture medium were incubated with 200 nM siRNA siAGF1 or siAGF6 in a 4 mm electroporation cuvette for a few seconds whilst shaking. The cells were then electroporated for 10 ms with 350 V and incubated at RT for 15 min. Next, they were transferred in a 6-well tissue culture plate in 2 ml cell culture medium and incubated for 3 days at 37 ℃.

2.17.2 Transfection with siRNA-loaded immunoliposomes

For the transfection of ILs and ILPs, lipid concentrations of 1, 2 and 5 mM were tested in qRT-PCR and compared for their ability to silence the target fusion gene AML1/MTG8. 500 nmol liposomes for 500000 cells in 100 µl cell culture medium (5 mM lipid) turned out to be the optimal liposome concentration. Liposomes, lipoplexes, ILs and ILPs were added to the diluted cells in a 96-well tissue culture plate and incubated for 8 h at 37 ℃. Afterwards, the wells were completely filled with medium to a total volume of 400 µl and incubated for 3 days

at 37 ℃. For qRT-PCR and immunoblot the following formulations were transfected (Table 2-6).

2.17.3 Transfection with immunopolyplexes

For IPPs, like ILs and ILPs, several transfection concentrations were tested and the optimal concentration for the transfection of 500000 cells was found at 620 nM (62 pmol in 100 µl cell culture medium).
Transfections were performed as described for ILs and ILPs in chapter 2.17.2. For qRT-PCR and immunoblot the following formulations were transfected:

Table 2-6: Transfection of siRNA with different carrier systems

Carrier system	**scFv'**	**siRNA**	**complexation**
liposomes	-	siAGF1	-
liposomes	-	siAGF1	PEI
liposomes	-	siAGF1	protamine
liposomes	CD33	siAGF1	-
liposomes	CD33	siAGF1	PEI
liposomes	CD33	siAGF1	protamine
liposomes	CD33	siAGF6	-
liposomes	CD33	siAGF6	PEI
liposomes	CD33	siAGF6	protamine
PEGPEIs	-	siAGF1	-
PEGPEIs	CD33	siAGF1	-
PEGPEIs	CD33	siAGF6	-
PEGPEIs	EGFR	siAGF1	-

2.18 Preparation of transfected cells

After three days of incubation with the carrier system, cells were harvested and prepared for qRT-PCR and immunoblot analysis.

2.18.1 Preparation of cell lysates for quantitative real-time PCR (qRT-PCR)

Cells were counted and centrifuged for 5 min at 300x g and pellets were resuspended in RNeasy RLT buffer containing 1 % β-mercaptoethanol. For the separation of DNA

QiaShredder columns were used and mRNA was isolated with the RNeasy Mini Kit according to the manufacturer's instructions. MRNA concentrations were determined by NanoDrop at a wavelength of 230 nm.

2.18.2 Preparation of cell lysates for immunoblot

Total protein was isolated from the flow-through of the RNeasy column by precipitation with 2 volumes of acetone on ice. Samples were centrifuged for 15 min at 13000 rpm and 4 ℃ and pellets were dissolved in 9 M urea buffer with a concentration of 25000 cells/µl.

2.19 Quantitative real-time PCR (qRT-PCR)

For qRT-PCR, isolated mRNA was first transcribed reversely into cDNA with the help of a cDNA synthesis kit. Therefor, 1 µl random hexamers were added to 0.25 µg of mRNA in a total volume of 12 µl DPCE treated water. 8 µl of a master mix (Table 2-7) were added to each sample.

Table 2-7: Master mix for cDNA synthesis

5x buffer	4 µl
dNTPs (10 mM)	2 µl
Reverse transcriptase	1 µl
Ribolock RNase inhibitor	1 µl
total	8 µl

A PCR program with 10 min at 25 ℃, 60 min at 42 ℃ and 10 min at 70 ℃ was run for the synthesis of cDNA. 30 µl of DPCE treated water were added to each sample and qRT-PCR was performed in triplicates in a 384 well plate. Specific primers for AML1-MTG8 and for GAPDH as an internal quantification control were used for the preparation of a SYBR Green master mix (Table 2-8). 8 µl of master mix were used for each sample.

Table 2-8: SYBR Green master mix

2x SYBR Green	5 µl
Forward primer (10 µM)	0.3 µl
Reverse primer (10 µM)	0.3 µl
dH_2O	2.4 µl
total	8 µl

The following PCR program was run in a quantitative RT-PCR machine (Table 2-9) and AML1/MTG8 levels were quantified with the help of SDS 2.0 software and normalized to GAPDH.

Table 2-9: qRT-PCR program

2 min	50℃
10 min	95℃
40x 15 sec	95℃
40x 1 min	60℃
15 min	95℃
15 min	60℃
15 min	95℃

Evaluation of data was performed with GraphPad Prism 4 software. For each experiment, data sets were normalized to GAPDH and to untreated cells, either, or each group of liposomes, lipoplexes (siRNA, siRNA-PEI and siRNA-protamine) and polyplexes was normalized to siAGF6 control samples. The results represented mean values of three independent experiments.

2.19.1 Statistics

For statistical analysis, a nonparametric paired t-test was performed with the help of Graph Pad Prism 4 software. In a paired test, values in each population represent paired observations. Two tailed P-values and confidence intervals of 95 % were chosen.

2.20 Immunoblot

8 µl of total protein in 9 M urea buffer corresponding to 200000 cells were diluted in the same volume of 2x reducing SDS loading buffer without boiling. Proteins were separated by SDS-PAGE with a 10 % polyacrylamid separation gel (Table 2-3) with a voltage of 50 V applied in the stacking gel and of 150 V in the separation gel and were then transferred to a PVDF membrane, rinsed in 100 % methanol. The transfer was performed at 12 V for 90 min in a semidry western blot. The PVDF membrane was incubated in western blot blocking solution for 1 h at RT whilst shaking in order to block free binding sites. For detection of the AML1/MTG8 fusion protein the membrane was then incubated with a rabbit anti AML1/RHD antibody diluted 1: 40 in blocking solution o/n at 4 ℃. After washing the membrane three times with PBS, 0.05 % Tween and one time with PBS for 5 min the blot was incubated with a goat anti rabbit peroxidase labelled antibody diluted 1: 5000 in blocking solution for 1 h at

RT. After washing the blot was developed with SuperSignal ECL substrate for 5 min and was then exposed to an x-ray film for 10 sec to 1 min. The film was automatically developed in a film developing machine.

2.21 Colony formation assay

For colony formation assays SKNO1 and Kasumi1 cells were transfected as described in chapter 2.17.3. 20000 cells in 100 µl cell culture medium were transfected with 25 nmol (250 µM) siRNA-loaded ILs or ILPs and 3.1 pmol (31 nM) IPPs, respectively. After 8 h of incubation at 37 °C, cells were seeded in 2 ml semi solid cell culture medium containing 0.5 % methylcellulose and split into four wells of a 24-well tissue culture plate. Colony formation took place during seven days of incubation in case of Kasumi1 and ten days of incubation in case of SKNO1 cells at 37 °C. For each sample within one experiment, colonies from 4 wells were counted. Evaluation of data was performed with GraphPad Prism 4 software. The results represented mean values of three independent experiments. Colony numbers of untreated cells were taken as 100 %.

2.21.1 Evaluation of colony size

Besides the determination of colony numbers, colony sizes were evaluated with the help of Image J software. These were allocated together with colony numbers to total colony areas from representative photographs of three independent experiments for Kasumi1 cells.

2.22 XTT assay

To investigate optional effects of the ILs themselves on the target cells, XTT assay as a cell clonogenicity assay was performed. 20000 Kasumi1 and SKNO1 cells were seeded in 96-well plates in 100 µl cell culture medium and incubated with different concentrations of scFv' (3.9, 15.6, 62.5, 250 and 1000 nM). Therfor, 1 µM scFv' CD33 V_HV_L HC4 and anti-FAP scFv' 36 as a negative control, were diluted in 1: 4 steps in cell culture medium. Empty anti-CD33 ILs, corresponding to the same scFv' concentrations, were also tested. Thereby, complete coupling and insertion were postulated, leading to a lower scFv' concentration compared to the samples containing free scFv'. Incubation took two days for Kasumi1 and three days for SKNO1 cells. 20 µl of XTT substrate were added to the samples and incubated for 4 h at 37 °C. The enzymatic processing of the substrate correlated with cell viability and was quantified in a microplate reader at 450 nm. Fluorescence intensity of untreated cells was taken as 100 % cell viability.

2.23 Humanization of scFv' molecules

Humanization of scFv' was performed by CDR-grafting in a knowledge-based approach and supported by gene database research.

2.23.1 scFv' CD33 V_HV_L HC4

The first step in the humanization approach was a BLAST database supported search for the most homologous germline genes, separately for the heavy and light variable chain of the murine scFv' CD33. The identified murine germline genes were next checked for their humanness in SHAB database, calculating a z-score for humanness between -2 and +2. As scaffold structures the germline genes VH3-53 and VK1-39 with a z-score of 1.875 and 1.204 respectively, were chosen. The canonical CDR structures of both genes were determined in VBASE database using auto generated specificity determining residues (SDR)-templates and assigned to a CDR class. In the next step, CDR-grafting was performed. The canonical structures of the humanized scFv' were then compared to the murine scFv' again using VBASE database. The murine as well as the humanized scFv' showed the following CDR classes: CDR L1 Class 2/11A, CDR L2 Class 1/7A, CDR L3 Class 1/9A, CDR H1 Class 1/10A, CDR H2 Class 1/9A. With the help of EXPASY database the amino acid sequence was reversely translated to a DNA sequence. With the help of Clone Manager, version 7.04, restriction sites for SfiI, XhoI, BamHI, NotI, EcoRI and NcoI, a His-Tag, a C-terminal cysteine as well as peptide linkers and spacers according to the murine scFv' were inserted into the sequence. The construct was then codon optimized for CHO cells and synthesized by GeneArt. Afterwards, the sequence was cloned into the pAB1 expression vector by restriction digestion with NcoI/EcoRI as described above.

2.23.2 scFv' CD19

ScFv' CD19 was humanized as described for scFv' CD33 V_HV_L HC4 in chapter 2.23.1. The identified murine germline genes for V_H and V_L were CD19-3 and CD19-A29 with a z-score of -0.301 and -1.819 respectively. The CDR classes of the murine as well as the humanized scFv' were: CDR L2 Class 1/7A and CDR H1 Class 1/10A. The CDR classes of CDR L1 and CDR H2 could not be assigned in both cases, the murine and the humanized scFv'.

2.24 Comparative analysis of humanized versus murine scFv'

The humanized scFv's were compared to their murine precursors with regard to their production yield in *E. coli* TG1, their melting points and their binding activity on leukaemic cell lines. In case of the humanized scFv' CD33 V_HV_L HC4, ILs were prepared by the

postinsertion method and compared to ILs of the murine scFv' in flow cytometry. All the experiments were performed as described above.

2.24.1 Binding of scFv CD33 to leukaemic cell lines

For a closer investigation of the binding activity of the humanized scFv CD33 including the determination of its mean effective concentration EC_{50}, the sequence was cloned in pAB1 in a SfiI/NotI restriction digestion to get rid of the C-terminal cysteine. The humanized as well as the murine scFv CD33 were produced in *E. coli* TG1 and investigated in flow cytometry. To compare the binding activities of the murine and the humanized scFv CD33, CD33 positive Kasumi1 cells were incubated with decreasing concentrations of the scFv reaching from 3 µM to 17 pM in 1: 3 dilution steps for 3 h at 4 ℃. For the detection of scFv binding strength a secondary mouse anti His-Tag unconjugated mAb and a PE-conjugated goat anti-mouse IgG were applied as described in chapter 2.5.2. Evaluation of concentration dependent MFIs in Graph Pad Prism 4 software resulted in a saturation kinetic and EC_{50} was calculated by the Michaelis-Menden equation $y= [B_{max}*x] / [K_D+x]$. Analysis were repeated for two times. MFIs represented the MFIs of scFv bound cells, divided by the MFI of the detection antibodies and the MFI of the highest scFv concentration of 3 µM was set to 100 %. Nonlinear curve fits of the constructs were created with Graph Pad Prism 4 software and P-values were determined by GraphPad Software.

3 Results

3.1 ScFv' molecules for the generation of targeted carrier systems

For the generation of targeted carrier systems scFv' antibody fragments targeting surface antigens of leukaemic cells were chosen. Three different scFv' molecules were produced and purified: scFv' CD13 targeting myelocytes and monocytes at different stages of differentiation, scFv' CD19 against B-lymphocytes at different differentiation stages and scFv' CD33 recognizing immature myeloid blasts.

3.1.1 Production of scFv' CD13, CD19 and CD33

The scFv molecules CD13, CD19 and CD33 were cloned into the vector pABC4 to introduce a C-terminal cysteine. They were expressed in *E.coli* TG1 using an IPTG inducible system. Additionally, scFv' CD13 was produced in mammalian HEK 293 cells. Therefor, the sequence was cloned into the vector pSecTagA by SfiI/EcoRI restriction digestion. The proteins were purified by IMAC. Production yields varied between 0.4 and 1.8 mg/l for the different constructs (Table 3-1).

Table 3-1: scFv' production yields

construct	expression system	yield [mg/l]
scFv' CD 13	*E. coli* TG1	1.1
	HEK 293	1.8
scFv' CD19	*E. coli* TG1	0.4
scFv' CD33	*E. coli* TG1	0.8

The highest production yields were reached with scFv' CD13, especially in HEK 293 with 1.8 mg scFv'/l supernatant and in bacteria with 1.1 mg/l bacterial culture, while scFv' CD33 reached a production yield of 0.8 mg/l and scFv' CD19 of only 0.4 mg scFv'/l bacterial culture.

3.1.2 Characterization of scFv' molecules

Integrity and purity of the purified scFv' molecules were confirmed by SDS-PAGE analysis (Fig. 3-1). Size of the scFv' molecules was predicted to be between 26.6 and 29 kDa based on the vector sequence. Under reducing conditions, single protein bands at nearly 28 kDa

were detected, which fit to the expected molecular mass for the monomeric scFv'. Under non-reducing conditions, a second band at about 55 kDa appeared, which corresponded to a dimer of two single chain fragments with an expected molecular mass of 53.2 to 58 kDa.

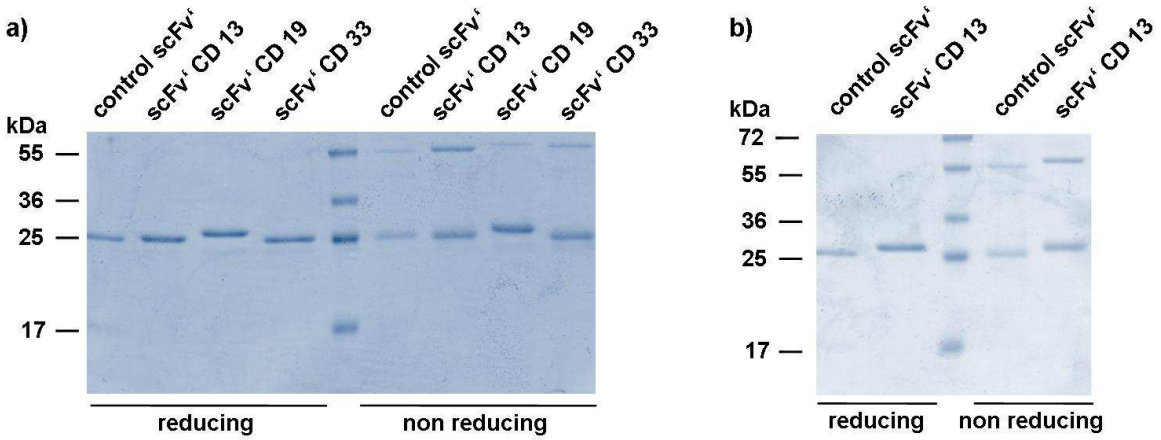

Fig. 3-1: Analysis of purified scFv' molecules by 15 % SDS-PAGE, Coomassie stained (2 µg scFv' per lane) under reducing and non-reducing conditions. An irrelevant scFv' served as a control construct. a) scFv' molecules produced in *E. coli* TG1, b) scFv' CD13 produced in HEK 293

3.1.3 Binding of scFv' molecules to leukaemic cell lines

10 µg/ml of scFv' molecules were analysed by flow cytometry for binding on 250000 antigen-positive and antigen-negative leukaemic cell lines (Fig. 3-2). Antigen expression was detected by anti-CD13, anti-CD19 and anti CD-33 monoclonal antibodies (mAbs) and compared to the scFv' binding activity. All scFv' molecules showed antigen specific binding.

3.2 Generation of scFv' CD33 variants

ScFv' CD33 was chosen as the preferred antibody fragment for the purpose of this work because it is expressed on leukaemic cells of the myeloid lineage and reached acceptable production yields. In contrast, CD13 is broadly expressed on different cell types and scFv' CD19 could only be produced in very low yields. Targeting of CD33 allows for an accumulation of carrier systems in the leukaemic tissue. For the optimization of scFv' CD33 as a targeting moiety for carrier systems, several variants of the molecule were produced and investigated.

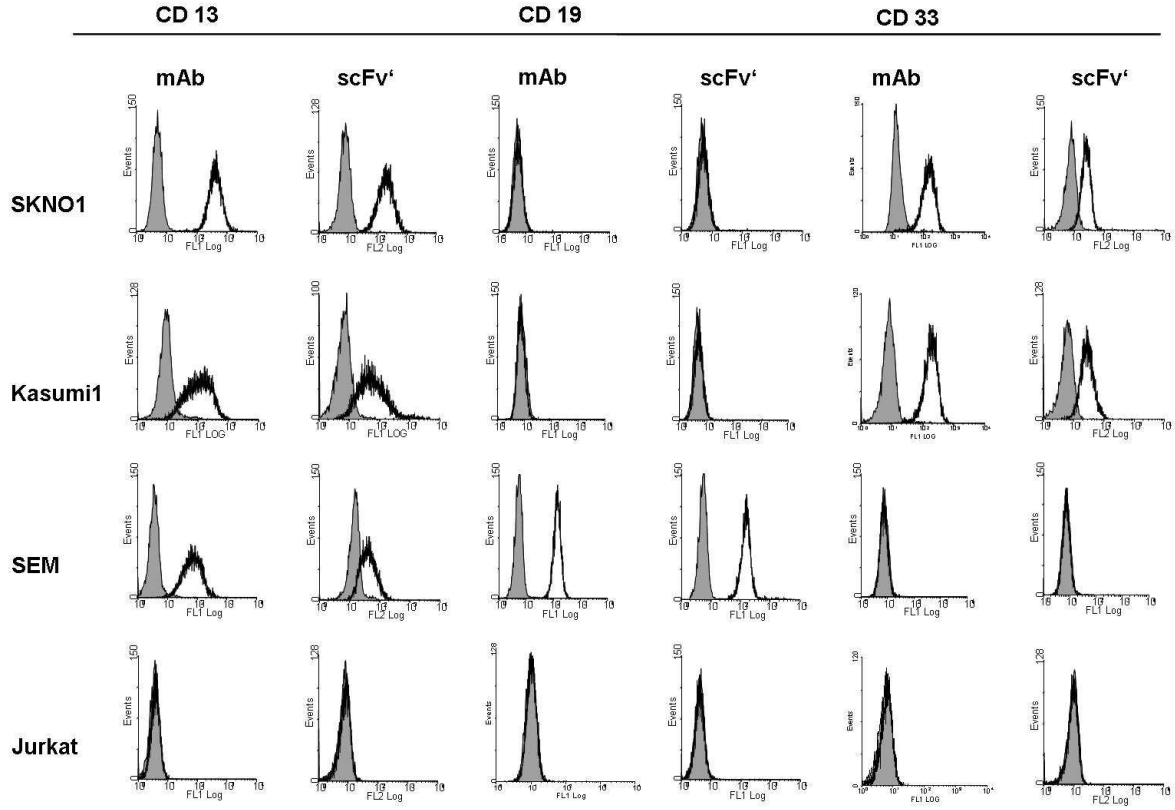

Fig. 3-2: Binding activity of monoclonal antibodies (1: 20) and 10 µg/ml (354 nM) scFv' on leukaemic cell lines SKNO1, Kasumi1, SEM and Jurkat (250000 cells in 100 µl) determined by flow cytometry. Gray, cells alone; black line, monoclonal antibody / scFv'.

3.2.1 Cloning and expression

Four variants of scFv' CD33, differing in the order of V_H and V_L and in the length of the peptide spacer between the His-Tag and the C-terminal cysteine (Fig. 3-3), were cloned according to the cloning strategy described in chapter 2.6.1. The proteins were expressed in E. coli TG1 and purified by IMAC. Production yields varied between 0.2 mg/l bacterial culture for the VHVL and VLVH HC4 constructs and 0.7 mg/l for the VLVH HC2 construct (Table 3-2). In comparison to the original scFv' CD33, a production yield decrease of 0.1 to 0.6 mg/l in the scFv' CD33 variants was observed.

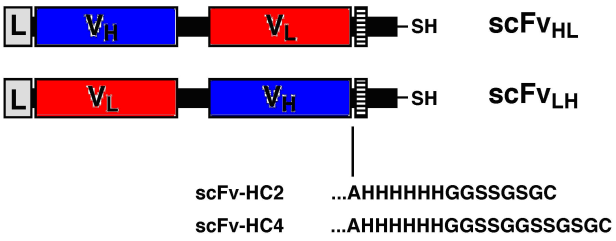

Figure 3-3: Schematic structure of scFv' CD33 variants
Two scFv' molecules differing in the order of V_H and V_L were each elongated in their peptide spacers by two different sequences (HC2 and HC4). L, leader peptide; V_H, variable heavy chain; V_L, variable light chain; SH, cysteine sulfydryl residue

Integrity and purity of the scFv' molecules were confirmed by SDS-PAGE and western blot analysis (Fig. 3-4). Size of the scFv' molecules was predicted to be between 28 and 28.5 kDa, based on the vector sequence. Under reducing conditions, single protein bands at nearly 28 kDa were detected, which fit to the expected molecular mass for the monomeric scFv' molecules. Under non-reducing conditions, a second band at about 55 kDa appeared, which corresponded to a dimer of two single chain fragments with an expected molecular mass of 56 to 57 kDa. In the V_HV_L constructs, the protein bands of the dimeric scFv' were more pronounced than in V_LV_H constructs. This would imply a stronger coupling ability of the V_HV_L constructs to liposomal and polymeric carrier systems compared to V_LV_H constructs.

Table 3-2: Production yields of scFv' CD33 variants

construct	**yield [mg/l]**
V_HV_L HC2	0.3
V_HV_L HC4	0.2
V_LV_H HC2	0.7
V_LV_H HC4	0.2

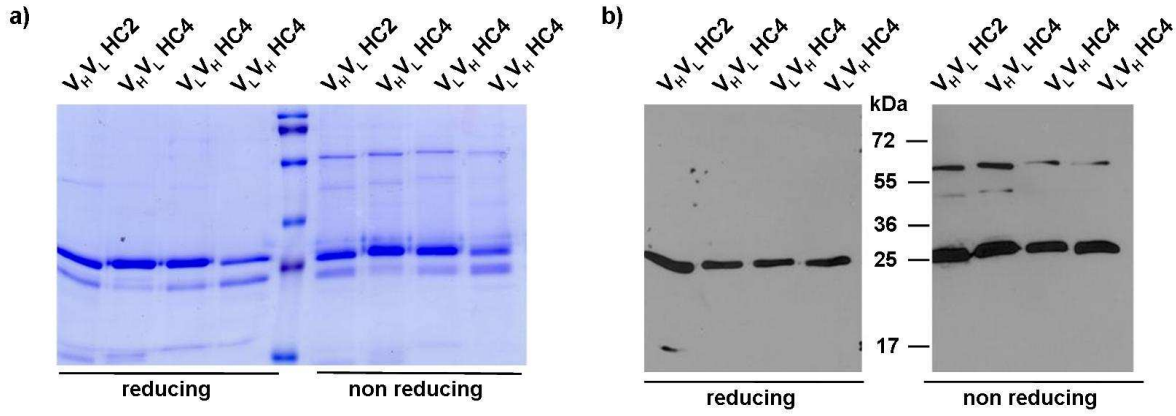

Fig. 3-4: Analysis of purified scFv' CD33 variants by
a) 15 % SDS-PAGE, Coomassie stained (2 µg scFv' per lane) and
b) western blot (1 µg scFv' per lane) under reducing and non-reducing conditions.
ScFv' molecules were separated by 15 % SDS PAGE and blotted on a nitrocellulose membrane. Bands were detected by a HRP-labelled anti His-Tag antibody.

3.2.2 Binding of scFv' variants to leukaemic cell lines

The scFv' variants were analysed by flow cytometry in a concentration of 10 µg/ml (354 nM) on 250000 antigen-positive and antigen-negative leukaemic cell lines (Fig. 3-5) as described in 3.1.3. The variants showed antigen-specific binding but differed in their binding strength. The scFv' CD33 V_HV_L constructs showed stronger binding on Kasumi1 and SKNO1 cells as compared to the V_LV_H constructs under the applied assay conditions, whereas the differences on Kasumi1 cells were more distinct. Mean fluorescence intensities (MFIs) on SKNO1 cells showed variations of approximately 30 % among the scFv' variants. In contrast, the V_LV_H variants on Kasumi1 cells only reached 15 to 25 % of the binding activity of V_HV_L constructs.

3.3 Immunoliposomes

ILs were generated by two different techniques, the conventional and the postinsertion method, and all scFv' CD33 variants were used as coupling moieties. Due to genetic modification with a C-terminal cysteine residue, scFv' molecules formed a thioether bond with maleimide-functionalized lipids, incorporated in the lipid bilayer.

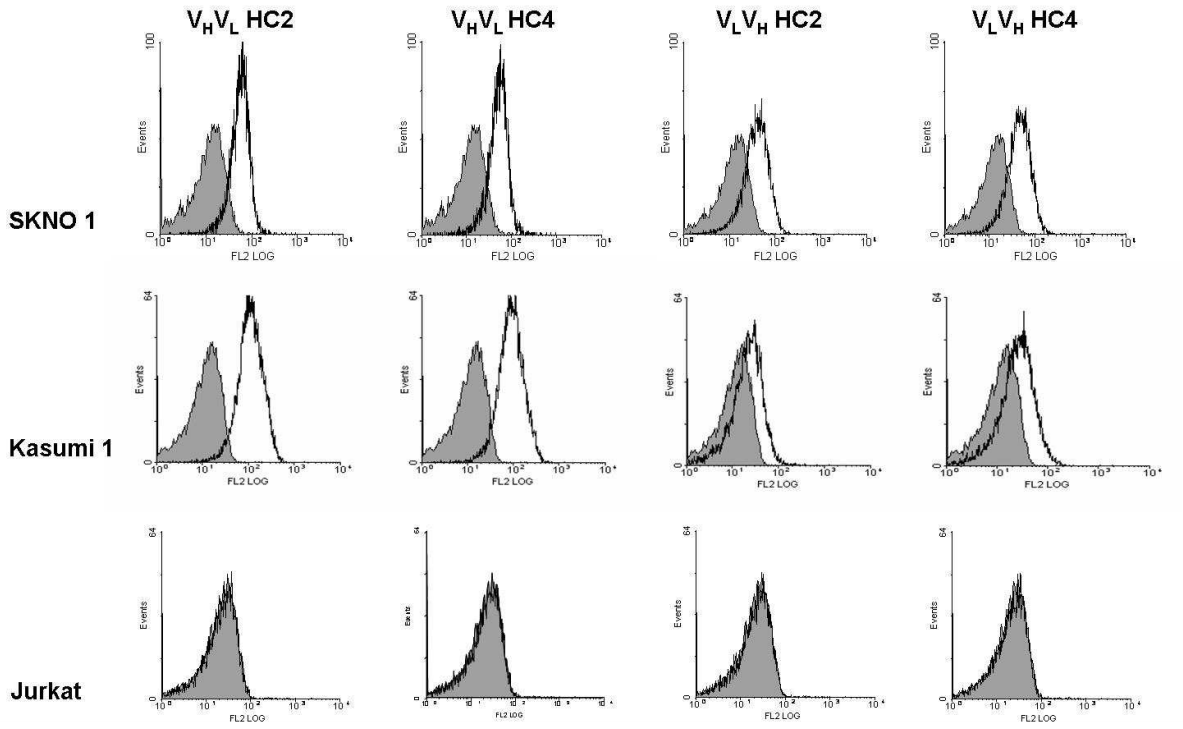

Fig. 3-5: Binding activity of 10 µg/ml (354 nM) scFv' CD33 variants on leukaemic cell lines (250000 cells in 100 µl) SKNO1, Kasumi1 and Jurkat determined by flow cytometry. Gray, cells alone; black line, scFv'.

The methods were compared with regard to coupling efficiency and IL binding on target cells. In both methods, lipid formulations of EPC: cholesterol: DSPE-PEG_{2000} at a molar ratio of 65: 30: 5 were used. In the conventional method, maleimide-functionalized DSPE-PEG_{2000} was used, whereas in the postinsertion method, non-functionalized $mPEG_{2000}$-DSPE was used.

3.3.1 The conventional coupling method

In the conventional coupling method, 5 mol% maleimide-functionalized PEG-chains were directly incorporated into the liposomal membrane and subsequently coupled to reduced scFv' CD33. Conventional ILs with a molar ratio of 0.36 mol% scFv'-coupled lipid compared to total lipid were prepared. To determine the coupling efficiency of scFv' molecules, western blots of free scFv' CD33 and corresponding micelles and ILs samples, according to the same amount of free scFv', were performed. Coupling of $malPEG_{2000}$-DSPE to scFv' was indicated by a shift in the protein band of about 2 kDa (Fig. 3-6). Besides the protein band at 28 kDa, which corresponded to free scFv', a second band at about 30 kDa was detected. This band most probably corresponded to the scFv' coupled to the anchor lipid. However, additional

bands with higher molecular masses appeared in the conventional coupling method. They probably resulted from coupling of more than one lipid to the scFv' molecule, e. g. through reactive amino groups. Free scFv' could hardly be detected, indicating a successful separation of scFv' molecules and ILs.

3.3.2 The postinsertion method

In the postinsertion method, scFv' molecules were coupled to malPEG$_{2000}$-DSPE micelles, which were inserted into preformed liposomes in a second step. The preformed liposomes contained non-functionalized PEG-chains. Micellar lipid and scFv' were introduced at a molar ratio of 4.76: 1. The scFv′-coupled micelles were then inserted into PEGylated liposomes in a molar ratio of 1 mol% micellar lipid to total lipid. Thus, postinsertion ILs with a molar ratio of 0.21 mol% scFv'-coupled lipid compared to total lipid were prepared. One distinct band of malPEG$_{2000}$-DSPE coupled scFv' was visible in the micelles samples besides a band of free scFv' (Fig. 3-6). Free scFv' could almost completely be separated from ILs in the postinsertion method, similar to conventional ILs. ScFv' CD33 V_HV_L HC4 showed the most specific coupling pattern in conventional ILs with almost no additional lipid coupling, shown by the absence of additional bands of higher molecular mass in the western blot. In contrast, all ILs in the postinsertion method showed similar coupling and insertion patterns.

3.3.3 Binding of immunoliposomes to leukaemic cell lines

Specific binding of ILs to their target cells was detected by flow cytometry due to excitation of the fluorescent dye DiI incorporated in the liposomal bilayer. For binding assays, 25 nmol of all variants of scFv' CD33 ILs were incubated with 250000 SKNO1, Kasumi1 and Jurkat cells at 4 ℃ for 1h in a volume of 100 µl. A comparison of conventional ILs (Fig. 3-7) and ILs prepared by the postinsertion method (Fig. 3-8) showed similar results. Conventional anti-CD33 ILs showed specific binding activity on SKNO1 cells and Kasumi1 cells. Binding to Kasumi1 cells was weaker in comparison to SKNO1 and the differences between the scFv' CD33 variants were dispensable. On SKNO1 cells, a clear advantage in binding activity for anti-CD33 V_HV_L HC4 ILs became obvious with a MFI, which was almost two-fold higher compared to all the other constructs. No binding of anti-CD33 ILs to antigen- negative Jurkat cells was observed.

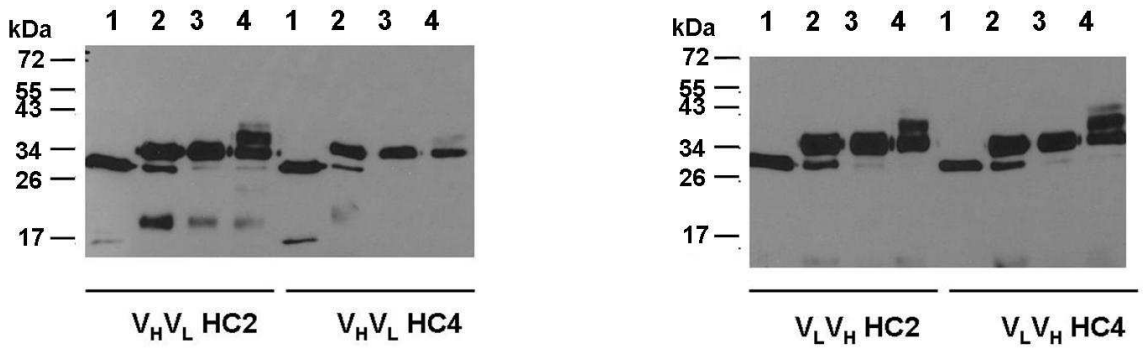

Fig. 3-6: Coupling of scFv' CD33 variants to malPEG$_{2000}$-DSPE micelles and insertion into preformed liposomes (postinsertion) or coupling to preformed malPEG$_{2000}$-DSPE liposomes (conventional). ScFv' molecules were separated by 15 % SDS PAGE and blotted on a nitrocellulose membrane. Bands were detected by a HRP-labelled anti-His-Tag antibody. 1= scFv' CD33 variant (2 µg), 2= scFv' coupled micelles, 3= ILs, postinsertion, 4= ILs, conventional

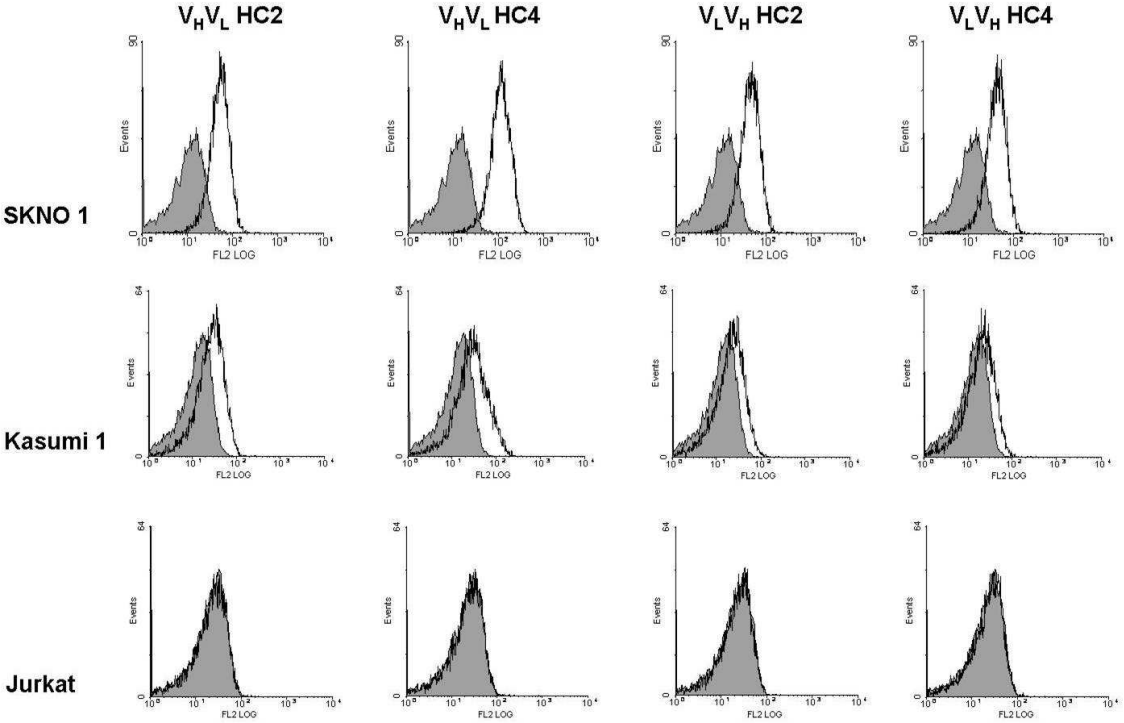

Fig. 3-7: Binding activity of 25 nmol (250 µM) conventional anti-CD33 ILs on leukaemic cell lines SKNO1, Kasumi1 and Jurkat (250000 cells) determined by flow cytometry.
Gray, cells alone; black line, anti-CD33 immunoliposomes.

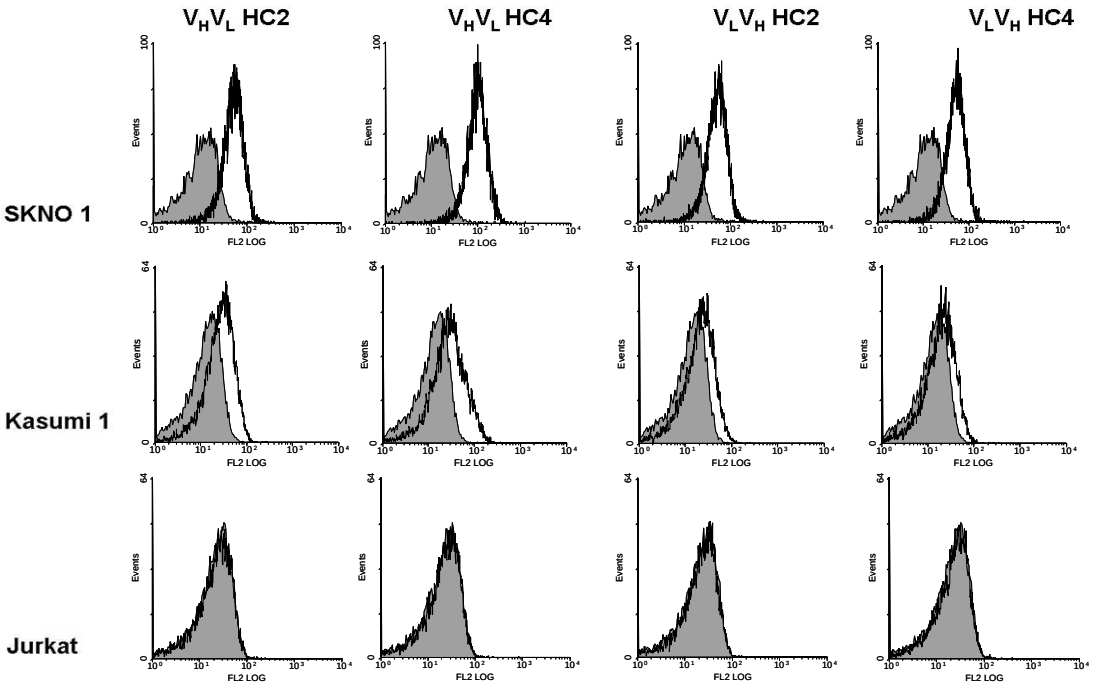

Fig. 3-8: Binding activity of 25 nmol (250 µM) postinsertion CD33 ILs on leukaemic cell lines SKNO1, Kasumi1 and Jurkat (250000 cells) determined by flow cytometry.
Gray, cells alone; black line, anti-CD33 immunoliposomes.

Binding activities of anti-CD 33 ILs, prepared by the postinsertion method, were comparable to those prepared by the conventional method. On SKNO1cells, the predominance of anti-CD33 V_HV_L HC4 ILs was even more distinct compared to conventional ILs. Here, the MFI of anti-CD33 V_HV_L HC4 ILs lay between 2.2 to 2.5-fold higher compared to all the other variants. For this reason, this format was chosen for all the following IL, immunolipoplex (ILP) and immunopolyplex (IPP) formulations.

3.4 scFv' CD33 V_HV_L HC4

For a more detailed investigation, scFv' CD33 V_HV_L HC4 was analysed by size exclusion chromatography (SEC) in an HPLC sepharose column (Fig. 3-9a). Additionally, its melting point was defined by dynamic light scattering (DLS) within a temperature range from 35 to 75 ℃ (Fig. 3-9b). The melting point was defined as th e temperature at which measured size dramatically increased due to aggregation of the protein.

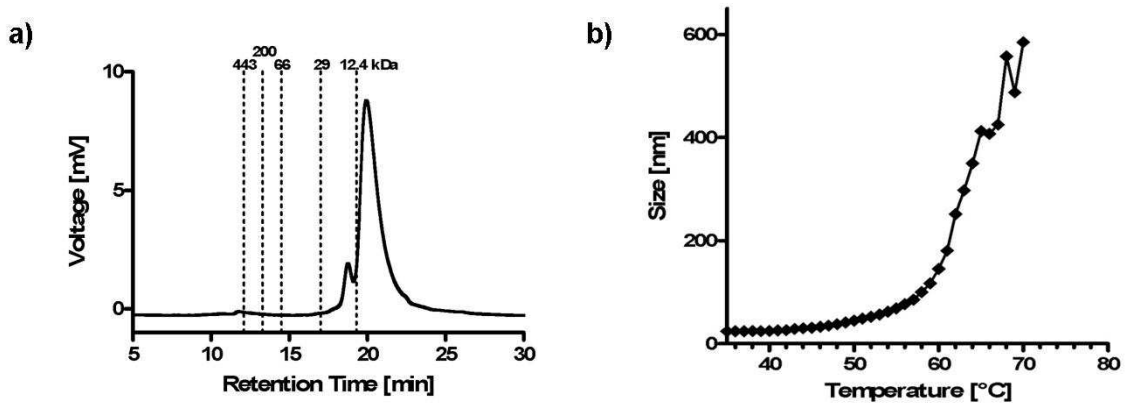

Fig. 3-9: Characterization of scFv' CD33 V_HV_L HC4

a) Size exclusion chromatography, dotted lines indicate sizes of standard proteins

b) Melting point analysis by dynamic light scattering

SEC analysis under non-reducing conditions showed a minor protein peak after 18.5 min retention time and a major peak after 20.5 min. The major peak represented the monomeric scFv' with a molecular mass of < 12.4 kDA. The minor peak represented the scFv' dimer of > 12.4 kDA and < 29 kDa. Molecular mass was plotted against retention time in comparison to standard proteins of known molecular mass. SEC data suggested a pure and stable protein. The molecular mass of the scFv' molecules in SEC appeared too low in comparison to SDS PAGE, which was a common observation for scFv' molecules in SEC. Melting point analysis by dynamic light scattering determined a melting point of approximately 60 ℃.

3.4.1 Cytoplasmic expression and purification

For the upscale production of scFv' CD33 V_HV_L HC4 in *E.coli* BL21 rha$^-$ cells using a rhamnose-inducible system, the DNA sequence of scFv' CD33 V_HV_L was cloned into the vector pWA21 under the control of a rhamnose promoter. Fermentation was performed by the fed-batch method, induced with rhamnose and purified by IMAC, as described in 2.7.1. Production yield was determined and compared to the periplasmically produced scFv'. In the fermentation system 4.0 mg scFv'/l bacterial culture were purified, representing a 20-fold increase of production yields compared to 0.2 mg/l in periplasmic expression. Integrity and purity of the scFv' molecules were compared to the periplasmically produced scFv' by SDS-PAGE analysis (Fig. 3-10). Integrity of scFv' molecules in both production methods was similar under reducing and non-reducing conditions while there was a distinct loss of purity in the cytoplasmically produced scFv'. For this reason, the periplasmic expression was used as a standard production method for scFv' in further experiments.

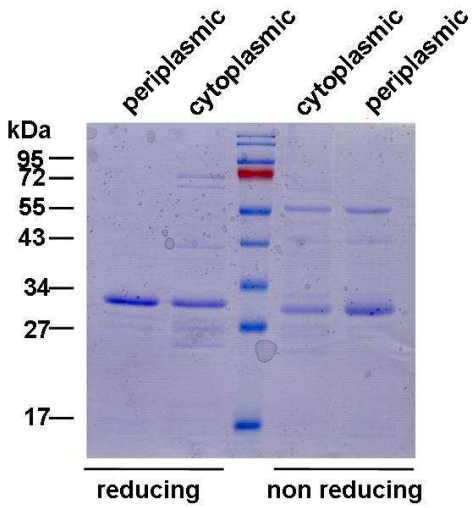

Fig. 3-10: Comparison of periplasmic and cytoplasmic production of scFv' CD33 V_HV_L HC4 15 % SDS-PAGE, Coomassie stained (2 µg scFv' per lane) under reducing and non-reducing conditions.

3.5 Immunoliposome characterization

For the determination of size of the liposomes and scFv' CD33 V_HV_L HC4 ILs their hydrodynamic diameter was measured by DLS (Table 3-3). The lipid formulations were EPC: cholesterol: DSPE-PEG_{2000} 65: 30: 5 with malPEG_{2000}-DSPE in conventional liposomes and mGEG_{2000}-DSPE in postinsertion liposomes. 0.36 mol% scFv' were coupled to conventional IL and 1 mol% micellar malPEG_{2000}-DSPE was inserted into the postinsertion liposomes. Lipid concentration during measurement was 100 nM in PBS.

Table 3-3: Hydrodynamic diameters of liposomes and immunoliposomes (mean values and standard deviations of n= 4 independent measurements)

	Liposome [nm]	**Immunoliposome [nm]**
Conventional (malPEG)	62 ± 2	65 ± 4
Postinsertion (mPEG)	75 ± 2	79 ± 1

Postinsertion (mPEG_{2000}-DSPE) liposomes and ILs showed 13 to 14 nm higher diameters than the conventional ones (malPEG_{2000}-DSPE). Size of ILs increased for 3 to 4 nm compared to unconjugated liposomes in both methods.

Antigen-specificity of anti-CD33 V_HV_L HC4 IL binding activity to target cells was further confirmed by flow cytometry. First, 25 nmol (250 µM) unconjugated mPEG_{2000}-DSPE liposomes and ILs containing 1 mol% micelles coupled to an anti-endoglin scFv' were incubated on 250000 CD33-positive SKNO1 cells in a volume of 100 µl. No binding was

detected in both cases (Fig. 3-11a). In a second experiment, preincubation of 3 µM free scFv' CD33 on SKNO1 cells resulted in a complete loss of binding for anti-CD33 V_HV_L HC4 ILs with 1 mol% micellar lipid. In contrast, preincubation of an anti-carcinoembryonic antigen (CEA)-specific scFv' in the same concentration did not affect the anti-CD33 IL binding activity (Fig. 3-11b). These results provided evidence for an antigen-specific binding of anti-CD33 ILs.

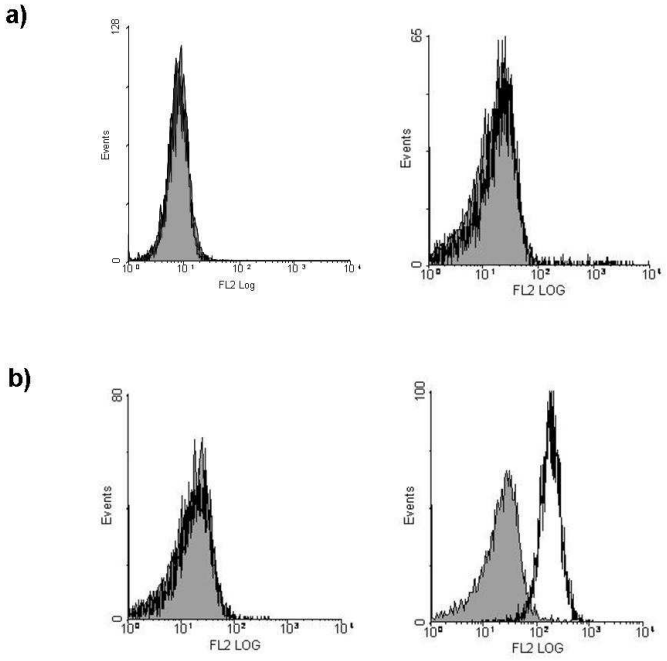

Fig. 3-11: Specificity of IL binding determined by flow cytometry.
a) 25 nmol (250 µM) unconjugated $mPEG_{2000}$-DSPE liposomes (left) and anti-endoglin ILs (right) on 250000 SKNO1 cells
b) 25 nmol CD33 ILs after preincubation with 3 µM scFv' CD33 (left) and scFv' CEA (right) on 250000 SKNO1 cells. Gray, cells alone; black line, anti-CD33 ILs

3.5.1 Optimization of immunoliposome binding

In order to determine the optimal ratio of scFv'-coupled micellar lipid to total liposomal lipid, anti-CD33 V_HV_L HC4 ILs with different molar ratios of $malPEG_{2000}$-DSPE were prepared by the postinsertion technique. Inserted micellar lipid ratios between 10 mol% and 0.01 mol% were investigated. The optimum with regard to binding activity was determined in flow cytometry by calculating the MFI of SKNO1 cells after IL binding and dividing the MFI after binding of unconjugated liposomes. FACS analysis was performed as described in chapter 3.3.3. Optimal binding activity was achieved at a ratio of 0.3 mol% micellar scFv'-coupled

malPEG with an MFI of 126 (Fig. 3-12). MalPEG$_{2000}$-DSPE concentrations above 1 mol% or below 0.04 mol% caused a remarkable decrease in IL binding activity.

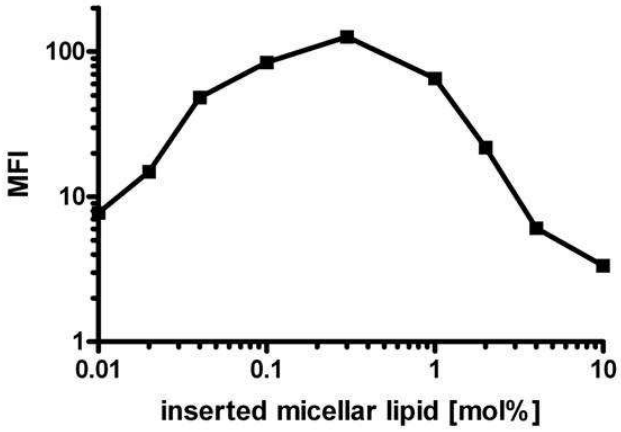

Fig. 3-12: Binding activity of 25 nmol (250 µM) anti-CD33 V_HV_L HC4 ILs with different ratios of inserted malPEG$_{2000}$-DSPE micelles on 250000 SKNO1 cells.
MFIs plotted against molar ratios of malPEG$_{2000}$-DSPE to total lipid. n= 1

The efficiency of coupling of scFv' to malPEG$_{2000}$-DSPE-micelles and insertion of the micelles into mPEG$_{2000}$-DSPE liposomes was determined for the scFv' CD33 V_HV_L HC4 construct with the optimal micellar lipid concentration of 0.3 mol%. Therefor, the intensities of protein bands of free scFv' and lipid-coupled scFv' in western blot were quantified. Calculation was done as described in chapter 2.10.5. The coupling and insertion efficiency for anti-CD33 V_HV_L HC4 ILs in the postinsertion method for 0.3 mol% micellar lipid was 49.7 %, compared to the amount of introduced scFv'. It resulted from the determined intensity of the lipid-coupled protein band of 142 units compared to the intensity of scFv', before it was introduced into the coupling reaction, of 286 units. Both samples represented aliquots from the IL preparation steps containing the theoretical amount of 2 µg scFv'. This resulted in an approximated number of 29 scFv' molecules per IL, compared to the calculated maximum of 58 scFv' molecules per liposome and a molar ratio of 0.03 mol% scFv' to total lipid (see chapter 2.10.5). However, experimental variations occurred in the coupling and insertion efficiency of scFv' molecules during IL formation. For further experiments, only scFv' CD33 V_HV_L HC4 coupled ILs, prepared with 0.3 mol% micellar lipid in the postinsertion method, were applied.

3.5.2 Plasma stability of immunoliposomes

With regard to their *in vivo* stability, 25 nmol of anti-CD33 ILs were incubated in 50% human plasma at 37 ℃ for one, three, five, seven and ten days. Binding activity on 250000 SKNO1 cells in a volume of 100 µl was checked in flow cytometry and compared to anti-CD33 ILs incubated in PBS under the same conditions (Fig. 3-13). As a comparison, ILs stored at 4 ℃ were tested (day 0). A fast decrease in binding activity to 63 % of day 0 MFI was observed after one day with marginal further loss of MFI up to day ten. Binding activity of PBS-incubated ILs showed only a very slow decrease to 74 % of day 0 MFI on day ten. Non-inserted mPEG liposomes served as a negative control. The results were shown as a percentage of MFI of day 0 plasma incubated ILs and PBS incubated ILs, respectively and indicated a sufficient plasma stability concerning *in vivo* application of ILs.

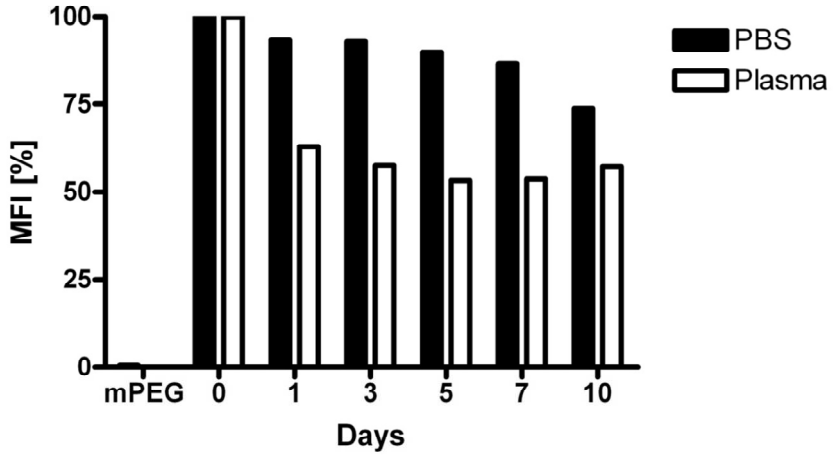

Fig. 3-13: Plasma stability of anti-CD33 ILs
Binding activity (MFI) of 25 nmol (250 µM) ILs, incubated in 50 % human plasma, on 250000 SKNO1 cells was detected in flow cytometry up to day 10 and compared to anti-CD33 ILs incubated in PBS. Non inserted mPEG liposomes served as negative control. MFIs in percentage of day 0 MFI were shown. n= 1

3.5.3 Internalization of immunoliposomes into leukaemic cell lines

IL internalization studies were performed at 37 ℃ to allow for receptor-mediated endocytosis. Uptake of 40 nmol (400 µM) fluorescently labelled ILs (DiI) into 250000 membrane labelled cells (DiO) or cytoplasm labelled cells (cell tracker) could then be visualized by fluorescence microscopy. Antigen-specific uptake into SKNO1 and Kasumi1 cells was observed. Images after 1 h (Fig. 3-14) and 4 h of incubation showed more IL binding and uptake than images after 8 h of incubation. Approximately 70 to 80 % of SKNO1 and Kasumi1 cells stained positive for DiI-incorporated ILs. CD33 negative Jurkat cells served as a negative control and

only showed weak binding of ILs. Additionally, only very weak binding of unconjugated liposomes to Kasumi1 cells was observed.

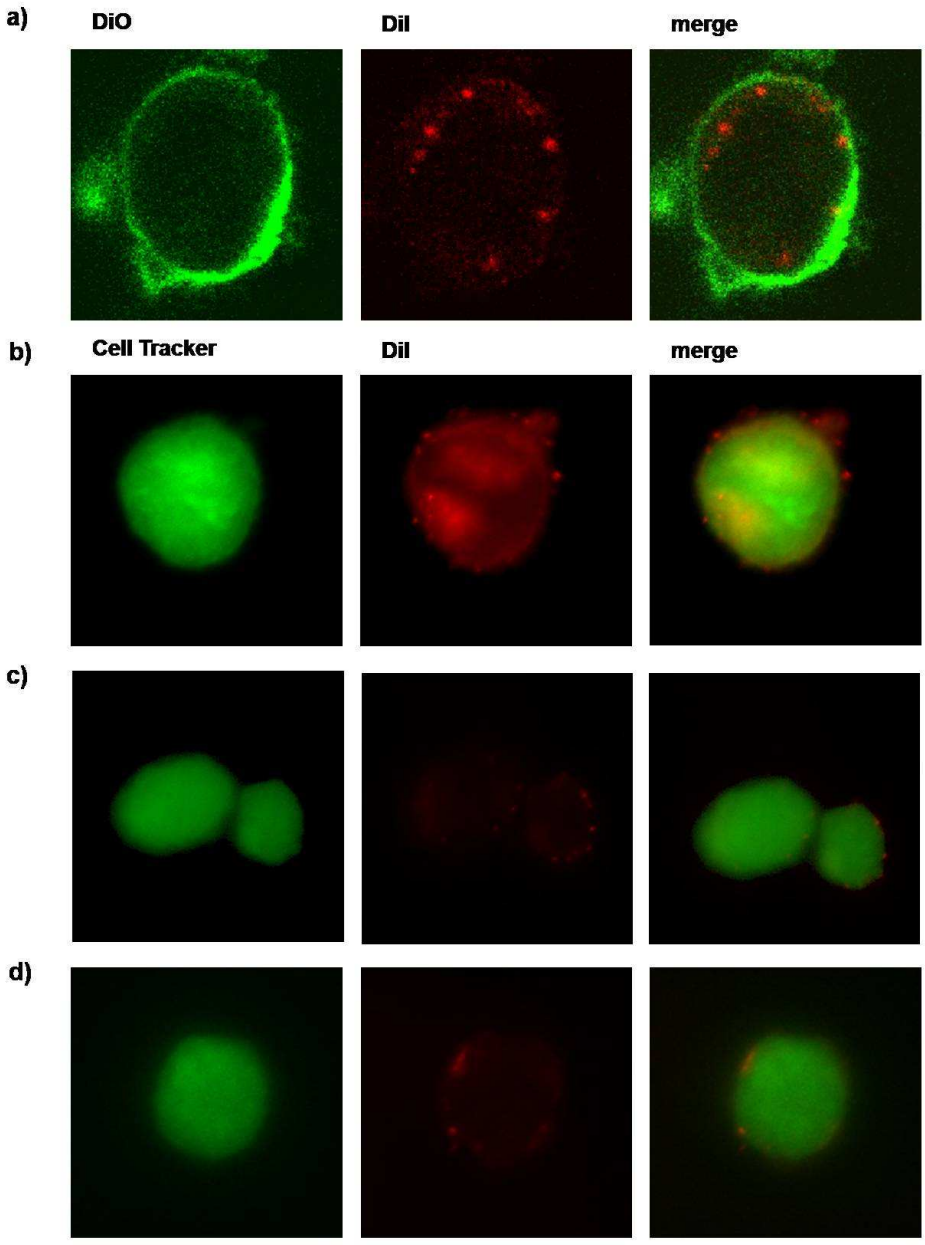

Fig. 3-14: Uptake of 40 nmol (400 µM) liposomes and anti-CD33 ILs into 250000 target cells after 1 h at 37 ℃. Cell membrane labelled with DiO, cyto plasm with cell tracker and ILs with DiI a) anti-CD33 ILs on CD33 positive SKNO1 cell, b) anti-CD33 ILs on CD33 positive Kasumi1 cell, c) non-targeted liposomes on CD33 positive Kasumi1 cells, d) anti-CD33 ILs on CD33 negative Jurkat cell.

3.6 SiRNA-loaded immunoliposomes

As a therapeutic approach targeted liposomes could be loaded with siRNA. For this purpose

a less leaky liposome formulation was chosen. It contained the more rigid hydrogenated soy-phosphatidylcholine (HSPC) instead of egg-phosphatidylcholine (EPC) and a higher lipid concentration of 100 mM. The following protocol was established: siRNA encapsulation into liposomes was performed by a passive loading method during liposome formation. In a further step, scFv'-coupled micelles were inserted into the siRNA-loaded liposomes by the postinsertion method. The protocol has been described in detail in chapter 2.13. Besides free siRNA, siRNA-polycation complexes with PEI and protamine were also applied.

3.6.1 Encapsulation of siRNA

Encapsulation of 20 µM Cy3-labelled siRNA was measured by fluorescence intensity in the aqueous siRNA solution before and after liposome formation. Therefor, after encapsulation, the liposomes were separated by ultracentrifugation at 300000x g and the supernatant was measured in a microplate reader at 535 nm. The fluorescence intensity was compared to an aliquot of the siRNA solution before encapsulation and the determination of siRNA concentrations was performed with the help of Cy3-siRNA calibration dilutions. SiRNA encapsulation efficiency depended on lipid concentration and increased with increasing lipid concentration (Table 3-4).

Table 3-4: Encapsulation efficiencies of 20 µM free Cy3-labelled siRNA with different lipid concentrations, n= 1

Lipid concentration [mM]	**Encapsulation efficiency [%]**
50	5
100	17
150	22

A lipid concentration of 150 mM, showing the highest encapsulation efficiency for free siRNA, could not be handled in a standard preparation method. Thus, encapsulation efficiencies of free siRNA, PEI- and protamine-complexed siRNA at a lipid concentration of 100 mM and a siRNA concentration of 20 µM from two independent experiments were compared (Table 3-5). SiRNA-PEI complexes were prepared in an N/P ratio of 5, siRNA-protamine complexes in a molar ratio of 1: 3 (compare Shim and Kwon, 2009; Peer et al., 2008).

Table 3-5: Encapsulation efficiencies of 20 µM free and complexed Cy3-labelled siRNA 1n 100 mM lipid (mean values and variation of n= 2 independent measurements)

	Encapsulation efficiency [%]
siRNA	24 ± 9
siRNA-PEI	nearly 100 ± 0
siRNA-protamine	67 ± 25

SiRNA encapsulation efficiency showed high experimental variations. Free siRNA had the lowest encapsulation efficiency of 24 ± 9 %, siRNA-protamine had an intermediate encapsulation efficiency of 67 ± 25 % and siRNA-PEI complexes were almost completely encapsulated. For ILs and ILPs loaded with 50 µM therapeutic siRNA, the results would lead to the following siRNA concentrations in 100 mM lipid: 50 µM for siRNA-PEI ILPs, 33.5 µM for siRNA-protamine ILPs and 12 µM for siRNA ILs.

3.6.2 Physicochemical characterization

For the determination of size of siRNA-loaded liposomes, lipoplexes, ILs and ILPs, their hydrodynamic diameter was measured by DLS (Table 3-6). Lipid concentration during the measurement was 100 nM in PBS. Liposomes as well as ILs with the therapeutic siRNA siAGF1 and a mismatch siRNA siAGF6 were measured in three independent experiments.

Table 3-6: Hydrodynamic diameters of siRNA-loaded liposomes and ILs (mean values and standard deviations of n= 3 measurements)

	Liposome [nm]	**Immunoliposome [nm]**
siAGF1	117 ± 27	143 ± 4
siAGF6	135 ± 2	131 ± 1
siAGF1-PEI	131 ± 1	135 ± 2
siAGF6-PEI	137 ± 3	129 ± 6
siAGF1-protamine	120 ± 5	114 ± 4
siAGF6-protamine	117 ± 2	131 ± 12

Liposome size varied within a small window from 117 nm for siAGF6-protamine lipoplexes to 137 nm for siAGF6-PEI lipoplexes. IL and ILP size varied between 114 nm for siAGF1-protamine and 143 nm for siAGF1 ILs. No reliable correlation of sizes between unconjugated and scFv' conjugated liposomes or between free and complexed siRNA could be seen.

3.6.3 Binding and internalization of siRNA-loaded immunoliposomes to leukaemic cell lines

Binding and internalization studies were performed with ILs loaded with uncomplexed Cy3-labelled siRNA at 37 ℃ to allow for receptor-media ted endocytosis. Binding and uptake of 400 nmol (4mM) ILs into 250000 cytoplasm labelled cells (cell tracker) could then be visualized due to the fluorescence-labelled siRNA (Cy3) within the ILs by fluorescence microscopy (Fig. 3-15). Antigen specific uptake into SKNO1 and, more attenuated, into Kasumi1 cells was observed. Images after 1 h and 4 h of incubation showed more IL binding and uptake than images after 8 h of incubation. Approximately 30 to 50 % of SKNO1 and Kasumi1 cells stained positive for Cy3siRNA-encapsulated ILs. CD33-negative Jurkat cells served as a negative control and only showed weak binding of ILs. Additionally, only very weak binding of unconjugated liposomes to SKNO1 and Kasumi1 cells was observed.

3.7 Immunopolyplexes

As an alternative delivery system besides ILs and ILPs, immunopolyplexes (IPPs) were generated and investigated. IPPs consisted of a 25 kDa PEI core chemically linked to NHS-PEG_{2000}-OPSS chains. Via this heterobifunctional linker, scFv' molecules were coupled to the polymer. Thus, the delivery systems showed comparable scFv' coupling chemistry targeting the engineered cysteine residue of scFv' molecules.

3.7.1 ScFv' coupling efficiency

The first approach (see chapter 2.15) yielded a fluorescently labelled conjugate which could be described by the following formula: FITC-PEI(25kDa)-$PEG(2kDa)_{10}$-$CD33_{0.9}$. Concentration after all purification and desalting steps was 1.68 mg/ml PEI, and the overall yield was 92 % of PEI but only 27.6 % of the antibody fragment. It was assumed that disulfide bonds might as well have formed between several PEGPEI molecules, resulting in PEI-PEG-S-S-PEG-PEI constructs, and that a great amount of the antibody fragment was eluted during purification.

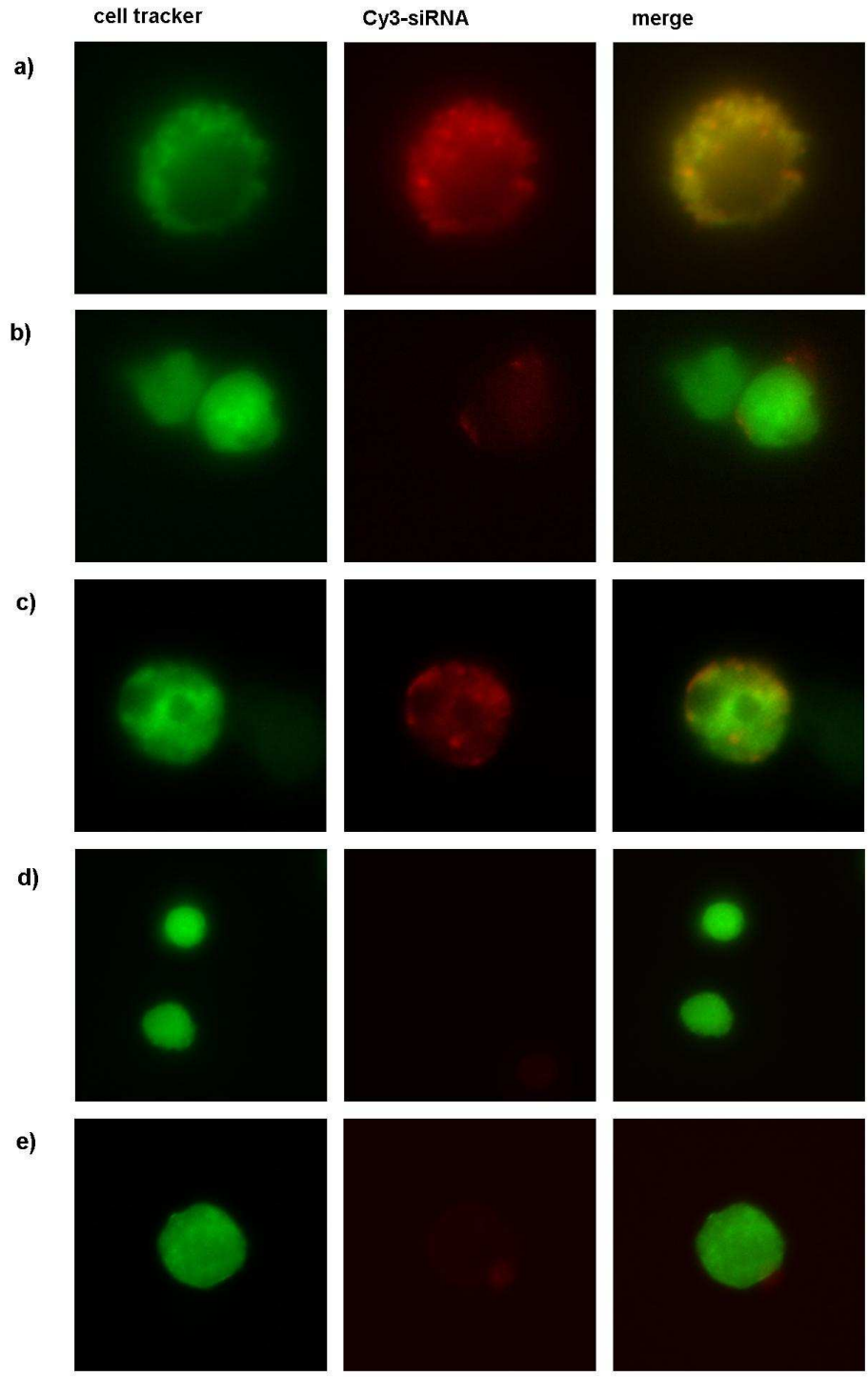

Fig. 3-15: Uptake of 400 nmol (4 mM) liposomes and anti-CD33 ILs into 250000 target cells after 1 h at 37 ℃. Cytoplasm labelled with cell tracker, s iRNA with Cy3
a) anti-CD33 ILs on CD33-positive SKNO1 cell, b) non-targeted liposomes on CD33-positive SKNO1 cells, c) anti-CD33 ILs on CD33-positive Kasumi1 cell, d) non-targeted liposomes on CD33-positive Kasumi1 cells, e) anti-CD33 ILs on CD33-negative Jurkat cell

Therefore, in the second approach (see chapter 2.15), the scFv' molecules were activated, not the PEGPEI intermediate, resulting in a higher coupling degree and higher yield of scFv' molecules. The conjugate could be described as PEI(25kDa)-PEG(2kDa)$_{10}$-CD33$_{3.3}$ with 0.3 mg/ml PEI and an overall yield of 46 % PEI and 50 % antibody fragment, while a later fraction containing only polymer was discarded. This led to a lower yield of PEI compared to the first approach.

3.7.2 Physicochemical characterization

As the PEI core of polyplexes was not surrounded, like liposomes and lipoplexes, by a neutral lipid film, zeta potentials were measured in addition to size. The zeta potential represented the surface charge of a particle in an aqueous solution. Size and zeta potential of PEGPEIs and scFv' coupled PEGPEIs, either with or without complexed siRNA in an N/P ratio of 5, were determined by DLS (Table 3-7). PEI concentration during the measurement was 360 nM in PBS. Polyplexes as well as IPPs with the therapeutic siRNA siAGF1 were measured. IPPs coupled to anti-endothelial growth factor receptor (EGFR)-scFv' molecules, prepared as a negative control, were also tested. Results of three independent experiments were shown.

Table 3-7: Hydrodynamic diameters and zeta potentials of polyplexes and IPPs (mean values and standard deviations of n= 3 measurements)

	Size [nm]	**Zeta potential [mV]**
PEGPEI	172 ± 51	0.7 ± 0.3
PEGPEI-EGFR	250 ± 18	0 ± 0.2
PEGPEI-CD33	363 ± 58	-0.1 ± 0.3
PEGPEI-siAGF1	181 ± 49	-1.9 ± 1.6
PEGPEI-EGFR-siAGF1	243 ± 15	-0.5 ± 0.6
PEGPEI-CD33-siAGF1	453 ± 34	-1.3 ± 1.5

A decrease in zeta potential of PEGPEIs from around 0.7 mV to around 0 mV was observed after coupling of scFv' and a further decrease to slightly negative charges between -0.5 mV and -1.9 mV after complexation of siRNA. In the same manner, the sizes of the polyplexes increased after scFv' conjugation from 172 nm to 250 nm for scFv'-EGFR and to 363 nm for scFv' CD33. SiRNA complexing had only little effects on the size of PEGPEI and PEGPEI-

EGFR. The large increase of size of PEGPEI-CD33 after scFv' coupling and again after siRNA complexation was remarkable.

3.7.3 Binding and internalization of immunopolyplexes to leukaemic cell lines

For binding and internalization studies, different concentrations of FITC-labelled PEG-PEIs and IPPs (2, 1 or 0.5 µM PEI) were used on 500000 SKNO1 cells in a volume of 100 µl. The studies were performed at 37 ℃ for 8 h to allow fo r extensive receptor-mediated endocytosis. The nuclei of the target cells were stained with DAPI. Binding and uptake of IPPs could be visualized by fluorescence microscopy. Due to Cy3 labelling, the uptake of complexed siRNA could be visualized independently. Antigen-specific binding and uptake of IPPs was shown, PEGPEI and siRNA were observed independently within the target cells and showed colocalization. Approximately 60 to 80 % of SKNO1 cells stained positive for FITC-labelled IPPs. However, unconjugated PEGPEIs showed binding to SKNO1 cells. Cells incubated with 2 µM IPPs (Fig. 3-16) showed higher binding and uptake efficiencies compared to 1 and 0.5 mM. CD33- negative Jurkat cells served as a negative control and showed no ati-CD33 IPP uptake.

3.8 Silencing of the target fusion gene

For the silencing of the target fusion gene AML1/MTG8, SKNO1 and Kasumi1 cells, both expressing the fusion gene, were transfected with the therapeutic siRNA siAGF1 and a mismatch siRNA siAGF6 either by electroporation or by incubation with ILs, ILPs and IPPs according to chapter 2.17. Specific gene silencing was investigated after harvesting and lysis of the cells three days after transfection on mRNA level in qRT-PCR and on protein level in immunoblot. A functional clonogenicity assay, the colony formation assay, was performed to investigate optional effects of the knockdown of AML1/MTG8 on the self-renewal capacity of the tumour cell. All methods were described in detail in chapter 2.19 to 2.21.

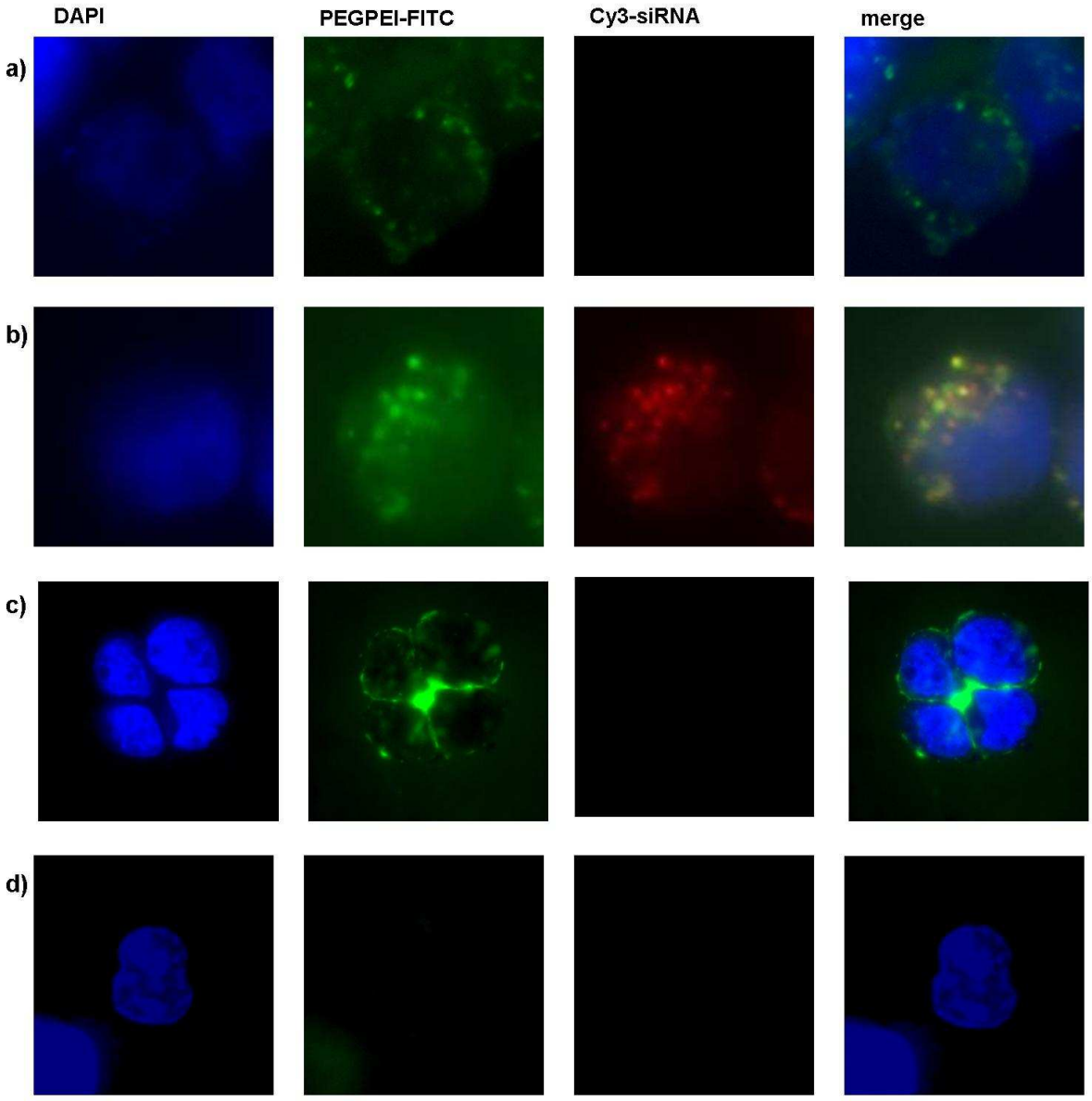

Fig. 3-16: Binding and uptake of 2 µM PEGPEI and anti-CD33-IPPs into 500000 SKNO1 cells after 8 h at 37 ℃. Cell nuclei labelled with DAPI, IPPs wi th FITC and siRNA with Cy3.
a) uncomplexed anti-CD33 PEGPEI on CD33-positive SKNO1 cell,
b) siRNA-complexed anti-CD33 IPP on CD33-positive SKNO1 cell,
c) unconjugated PEGPEI on CD33-positive SKNO1 cell,
d) uncomplexed anti-CD33 PEGPEI on CD33-negative Jurkat cell.

An anti-AML1 immunoblot of SKNO1 cells compared to Jurkat cells, not expressing the fusion protein, for different cell numbers was shown (Fig. 3-17). A strong expression of AML1 (55k Da) was detected in both cell lines, which showed a consistent increase with cell numbers and could therefore be used as a loading control.

In contrast, the fusion protein AML1/MTG8 (105 kDa) was only very weakly expressed in SKNO1 cells and only became visible after long x-ray film exposure times. As a consequence, also irrelevant bands appeared on the blot. After comparison to AML1/MTG8 negative Jurkat cells, it was getting obvious that the lower one of the double band around the 95 kDa marker band represented the fusion protein as it was not detected in AML1/MTG8 negative Jurkat cells. 250000 cells showed an adequate signal to noise ratio and were chosen as the cell number to insert into all the following immunoblots. However, due to experimental variations in cell numbers after transfection with ILs, ILPs and IPPs, only 200000 cells were inserted.

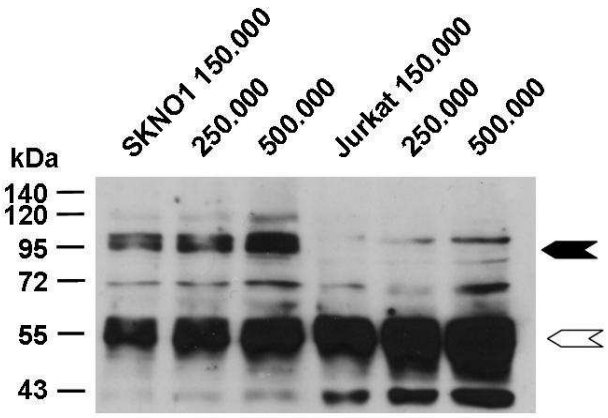

Fig. 3-17: Immunoblot AML1

Lysates of different cell numbers of SKNO1 and Jurkat cells were separated by 10 % SDS PAGE, blotted on PVDF membrane and incubated with anti AML1 antibody. Bands were detected by a secondary HRP labelled antibody. Black arrow, AML1/MTG8; white arrow, AML1

The activity and specificity of the siRNA siAGF1 was first tested in electroporation of 250000 SKNO1 cells in a concentration of 200 nM at 350 V for 10 ms and compared to the mismatch siRNA siAGF6. Lysates of the transfected Kasumi1 and SKNO1 cells were investigated in immunoblot three days after electroporation (Fig. 3-18). It could be shown that the fusion protein was specifically down regulated without affecting wild-type AML1.

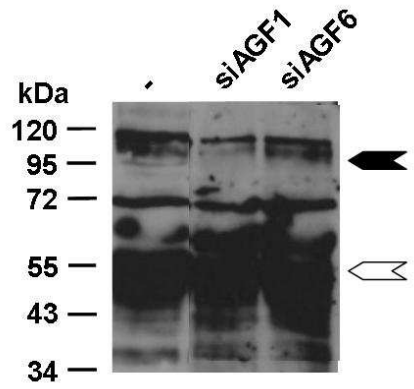

Fig. 3-18: Electroporation of 250000 SKNO1 cells with 200 nM siRNAs siAGF1 and siAGF6 for 10 ms at 350 V. After three days lysates were separated by 10 % SDS PAGE, blotted on PVDF membrane and incubated with anti AML1 antibody. Bands were detected by a secondary HRP labelled antibody. -, untreated cells; black arrow, AML1/MTG8; white arrow, AML1

3.8.1 SiRNA- and siRNA-PEI loaded immunoliposomes

For the investigation of silencing of the fusion gene by siRNA transfection with ILs and ILPs on mRNA level qRT-PCR was performed. In a preliminary experiment, three different lipid concentrations (1 mM, 2 mM and 5 mM) were tested for their silencing efficiency in qRT-PCR (Fig. 3-19). 500000 SKNO1 cells were transfected with 100, 200 and 500 nmol PEI complexed ILPs, corresponding to 0.5 µM, 1 µM and 2.5 µM siRNA, in a volume of 100 µl and investigated in qRT-PCR three days after transfection. 250 ng of isolated mRNA were used for qRT-PCR.

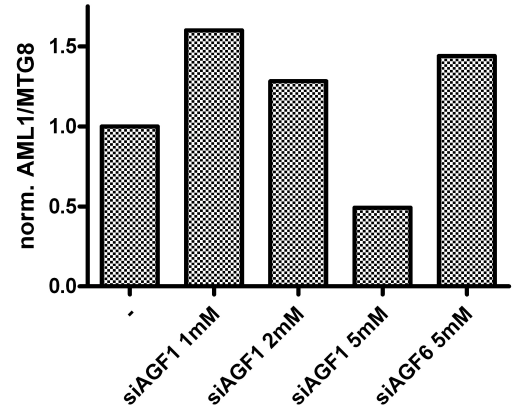

Fig. 3-19: qRT-PCR AML1/MTG8 of 250 ng mRNA of SKNO1 cells three days after transfection with 1 mM, 2 mM or 5 mM PEI-ILPs with siRNAs AGF1 and AGF6 (0.5, 1 and 2.5 µM). AML1/MTG8 mRNA levels were normalized to GAPDH and untreated cells. n =1

AML1/MTG8 mRNA knockdown depended on lipid concentration and increased with higher lipid concentrations. Comparison with mismatch siAGF6 ILPs under the same conditions at the highest lipid concentration of 5 mM proved a sequence-specific silencing effect. Therefore, a lipid concentration of 5 mM was used for further transfections. Interestingly, siAGF1 ILPs at low concentrations and siAGF6 ILPs showed increased AML1/MTG8 mRNA levels compared to untransfected cells.

500000 cells were transfected with 5 mM lipid, which corresponded to 2.5 µM siRNA in PEI containing ILPs where 100 % siRNA loading efficiency could be shown, and 600 nM siRNA in ILs containing free siRNA where only 24 % loading efficiency was reached (see Table 3-5). Cells were harvested after three days according to the description in chapter 2.18. Lysates of Kasumi1 and SKNO1 cells were split for qRT-PCR and immunoblot. The cellular total mRNA was isolated and 250 ng were reversely transcribed to cDNA. The amount of AML1/MTG8 cDNA was then determined by qRT-PCR and normalized against GAPDH and each group of liposomes (siRNA and siRNA-PEI loaded liposomes) was then normalized against the siAGF6 negative control (Fig.3-20).

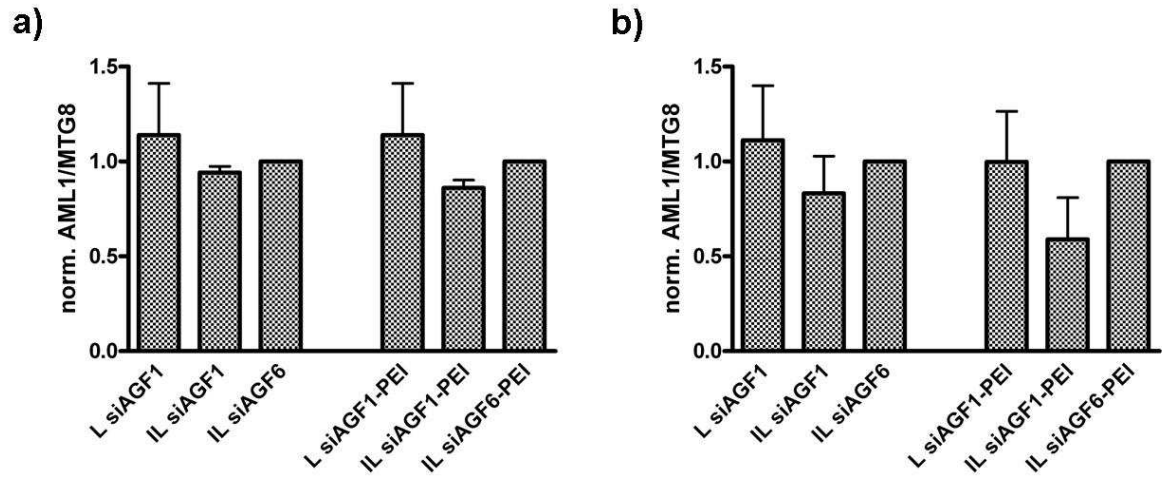

Fig. 3-20: qRT-PCR AML1/MTG8 of 250 ng mRNA of cell lines three days after transfection with 5 mM ILs and ILPs. SiRNA concentration in siRNA ILs was 600 nM, in siRNA-PEI ILPs 2.5 µM.
a) Kasumi1, b) SKNO1.
AML1/MTG8 mRNA levels were normalized to GAPDH and the siAGF6 negative control. Error bars represented standard deviations of n =3 independent experiments. For statistics t-test was performed.
-, untreated cells; L, liposomes; IL, immunoliposomes

It was shown that the expected silencing effects of siAGF1 ILs and ILPs on the AML1/MTG8 mRNA levels three days after transfection were very weak. AML1/MTG8 levels of siAGF1 ILs or siAGF1-PEI ILPs did not differ significantly from siAGF6 ILs and ILPs and nontargeted siAGF1 control liposomes and lipoplexes. Remarkably, the effects on SKNO1 cells were more distinct than on Kasumi1 cells. Here, the AML1/MTG8 mRNA level, after siAGF1-PEI ILP transfection, decreased to 59 % within standard deviation compared to the siAGF6-PEI ILP control. For the immunoblot, cell lysates corresponding to 200000 transfected cells were prepared. One representative from at least three immunoblots was chosen:

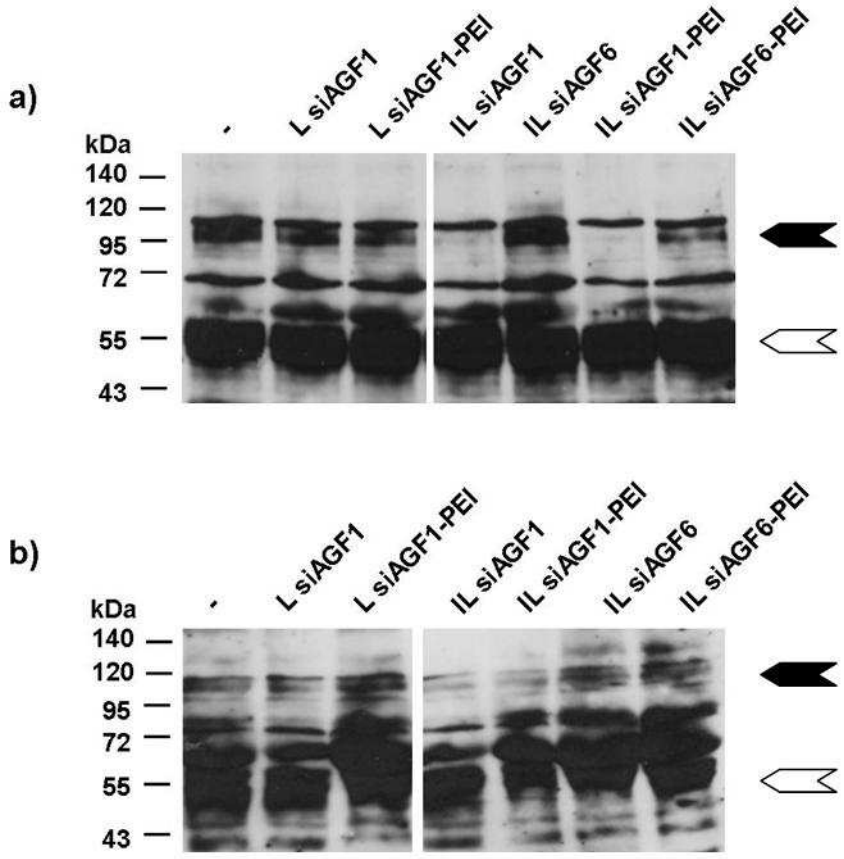

Fig. 3-21: Immunoblot AML1 of 200000 cells three days after transfection with 5 mM siRNA loaded (immuno-) liposomes. SiRNA concentration in siRNA ILs was 600 nM, in siRNA-PEI ILPs 2.5 µM. a) Kasumi1, b) SKNO1.
Lysates were separated by 10 % SDS PAGE, blotted on PVDF membrane and incubated with anti-AML1 antibody. Bands were detected by a secondary HRP labelled antibody. -, untreated cells; L, liposomes; IL, immunoliposomes; black arrow, AML1/MTG8; white arrow, AML1

Distinct silencing effects of siAGF1 ILs either with or without PEI compared to untreated cells, unconjugated liposomes and siAGF6 ILs and ILPs were detected for Kasumi1 cells. The same effects, but to a weaker extend, were observed for SKNO1 cells.

The silencing of AML1/MTG8 was supposed to arrest the self-renewal capacity of the concerned cells. For this reason colony formation assays were performed. Kasumi1 and SKNO1 cells were highly diluted (20000 cells/ml) and seeded out in semi-solid culture medium after transfection with 250 µM ILs or ILPs, representing 5 % of the lipid and siRNA concentration used for qRT-PCR and immunoblot. The transfection sample was split into four wells. Representative sections of Kasumi1 colony formation assays after seven days were shown (Fig. 3-22).

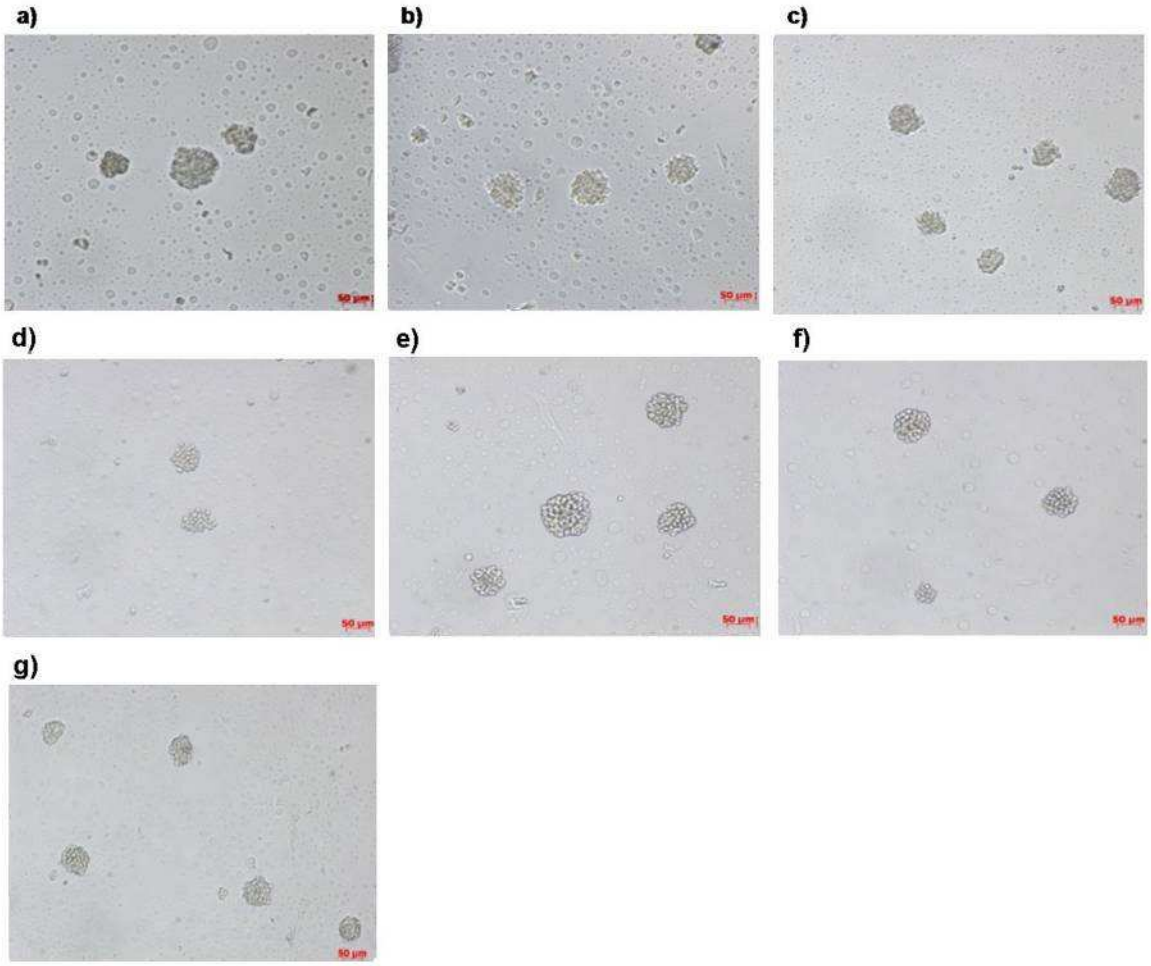

Fig. 3-22: Representative sections of colony formation assays of Kasumi1 cells seven days after transfection with 250 µM ILs or ILPs. 20000 cells were transfected and split for four colony formation samples.
a) untransfected cells, b) siAGF1 liposomes (30 nM siRNA), c) siAGF1-PEI lipoplexes (125 nM siRNA), d) siAGF1 ILs (30 nM siRNA), e) siAGF6 ILs (30 nM siRNA), f) siAGF1-PEI ILPs (125 nM siRNA), g) siAG6-PEI ILPs (125 nM siRNA).

Silencing effects of siAGF1 ILs and ILPs, namely a reduced colony number and colony size, became visible, especially in comparison with siAGF6 controls, but were not very pronounced. After seven (Kasumi1) or ten days (SKNO1) the colonies of four complete wells were counted (Fig. 3-23). The concentration of 250 µM lipid in the colony formation assay corresponded to 125 nM siRNA in siRNA-PEI ILPs and 30 nM in siRNA ILs. The results were shown as percentages of untreated cells:

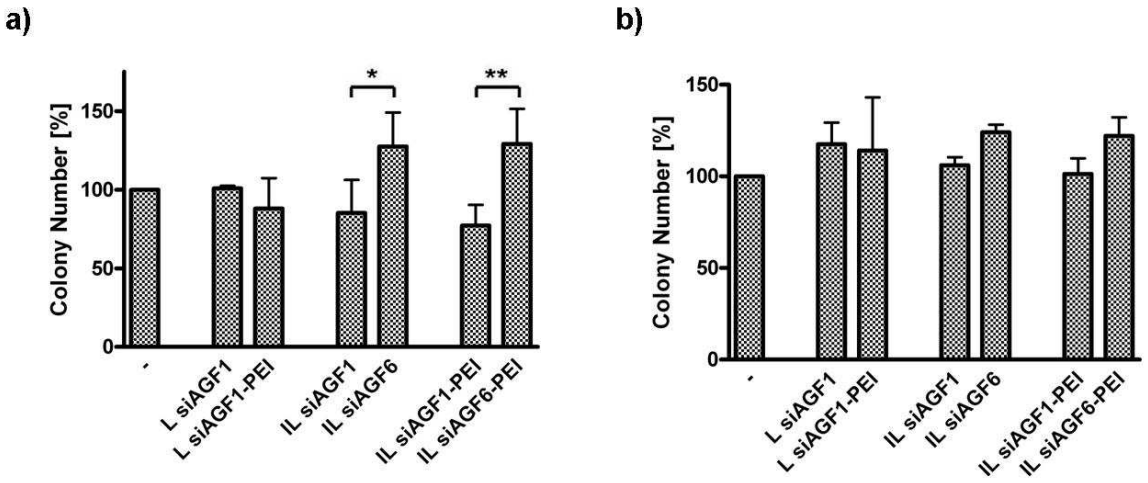

Fig. 3-23: Colony formation assay of leukaemic cell lines seven or ten days after transfection with ILs and ILPs in a concentration of 250 µM and a cell number of 20000. Error bars represented standard deviations of n= 3 independent experiments (four wells per experiment). For statistics t-test was performed. SiRNA concentration in siRNA-ILs was 30 nM, in siRNA-PEI ILPs 125 nM.
a) Kasumi1 cells, b) SKNO1 cells
-, untreated cells; L, liposomes; IL, immunoliposomes

Specific silencing effects of siAGF1 ILs and ILPs were observed, concerning colony number, in Kasumi1 cells and only very weakly in SKNO1 cells while siRNA-PEI ILPs showed stronger effects than ILs with free siRNA. T-test proved significant differences for both the siAGF1 ILs compared to siAGF6 ILs and the siAGF1-PEI ILPs compared to siAGF6-PEI ILPs with a decrease in colony number of 34 % in the case siAGF1 ILs and 40 % for siAGF1-PEI ILPs. P-values were 0.01 for the siRNA ILs and 0.004 in case of the siRNA-PEI ILPs. In addition to colony number, total colony area was determined for the case of Kasumi1 cells from representative sections of photographs in Image J software and illustrated as percentages from untreated cells (Fig. 3-24). A reduced total colony area in colony formation assay after transfection with siAGF ILs and ILPs compared to the negative controls, which was not significant according to t-test, was shown. Total colony area after siAGF1 IL transfection decreased to 72 %, siAGF1-PEI ILPs to 92% compared to untreated cells. Comparison to the siAGF1 liposomes and siAGF6 IL controls resulted in higher silencing effects in both cases. However, it had to be taken into consideration that only sections of one well out of four complete wells per experiment were investigated, which rather represented an exemplification than an additional experiment.

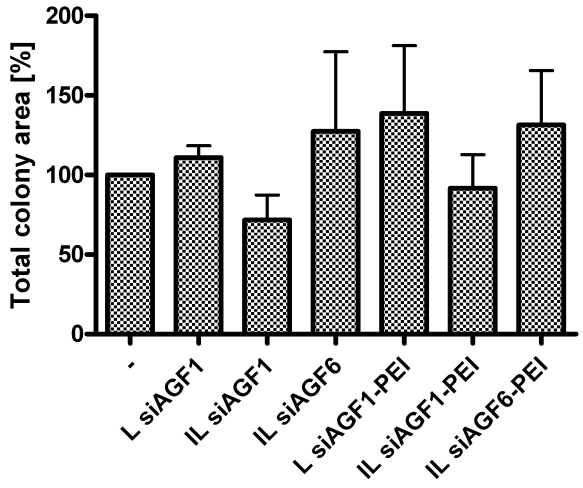

Fig. 3-24: Total colony area of Kasumi1 cells seven days after transfection with 250 µM siRNA loaded ILs and ILPs in colony formation assay. Representative sections of photographs were investigated. SiRNA concentration in siRNA-ILs was 30 nM, in siRNA-PEI ILPs 125 nM. Error bars represented standard deviations of n= 3 independent experiments. For statistics t-test was performed. -, untreated cells; L, liposomes; IL, immunoliposomes

The high colony numbers and total colony areas of samples transfected with siAGF6 ILs and ILPs, and in some cases siAGF1 liposomes and lipoplexes, were remarkable. For this reason, colony formation assays with 250 µM empty ILs (HSPC) as well as free scFv' in concentrations corresponding to scFv' molecules inserted in the siRNA-loaded ILs and ILPs, were performed. ScFv' concentration was calculated under the consideration of the molar ratio of 0.03 mol% scFv' to total lipid. It resulted in 75 nM scFv'. In parallel, cell viability assays with empty ILs and free scFv' molecules were performed for both cell lines. Here, different scFv' concentrations were used and ILs were introduced according to the concentration of scFv' coupled to their surface. ScFv' concentrations in ILs were calculated, postulating complete coupling and insertion, leading to lower scFv' concentrations in IL samples compared to the samples containing free scFv'.

Colony formation assay (Fig. 3-25) showed an enhanced colony number of 43 % and 48 % in Kasumi1 and SKNO1 cell lines, respectively, treated with empty ILs compared to untreated cells. Free scFv' had no significant effect on colony formation. These results could explain the high colony numbers of samples transfected with siAGF6 ILs and ILPs compared to untreated cells as a general IL effect. As a cell viability test, an XTT assay was chosen. 20000 Kasumi1 cells were incubated with different concentrations of scFv' (3.9, 15.6, 62.5, 250 and 1000 nM) and empty ILs corresponding to the same scFv' concentrations for two days, SKNO1 cells for three days.

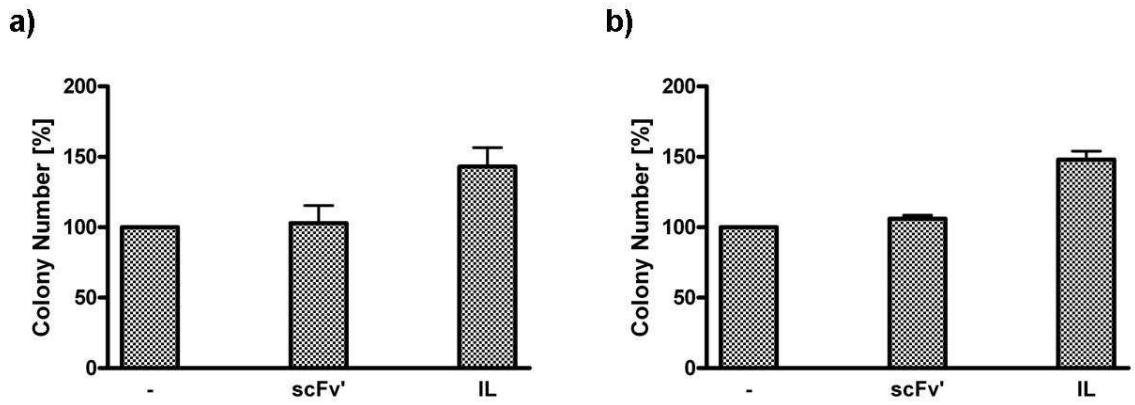

Fig. 3-25: Colony formation assay of 20000 leukaemic cell lines seven or ten days after transfection with 75 nM scFv' and 250 µM ILs (HSPC). Error bars represented standard deviations of n= 3 independet experiments (four wells per experiment). For statistics t-test was performed. -, untreated cells; IL, immunoliposomes

Besides scFv' CD33 and anti-CD33 ILs a control scFv' against fibroblast activating protein (FAP) in the same concentrations was carried along (scFv' 36). Kasumi1 and SKNO1 cell lines both were negative for FAP expression. Cell viability was determined by stoichiometrical enzymatic conversion of XTT to a quantifiable coloured product and measured at 450 nm in a microplate reader. Cell viability, as a percentage of untreated cells, was plotted against scFv' concentration. Both, scFv' CD33 and anti-CD33 ILs showed cytotoxic effects at higher concentrations on Kasumi1 as well as SKNO1 cells, reducing cell viability to approximately 50 % in SKNO1 cells at 1000 nM scFv'. In the case of Kasumi1 cells, the highest concentrations of scFv' CD33 led to a decrease of cell viability to approximately 70 %, ILs even to around 40 %. The control scFv' 36 had no effect on cell viability. The relevant, corresponding scFv' concentration of 75 nM, applied in colony formation assay, indicated by the dotted lines, had no toxic or stimulating effect in the case of Kasumi1 cells and only a weak cytotoxic effect on SKNO1 cells. However, scFv' concentrations of ILs were lower compared to free scFv' concentrations in this assay. This would argue for an actually stronger cytotoxic effect of ILs than it was shown in the assay. These results did not support the results from the colony formation assay with regard to the stimulating effect of empty ILs on the clonogenicity of the target cells (Fig.3-25).

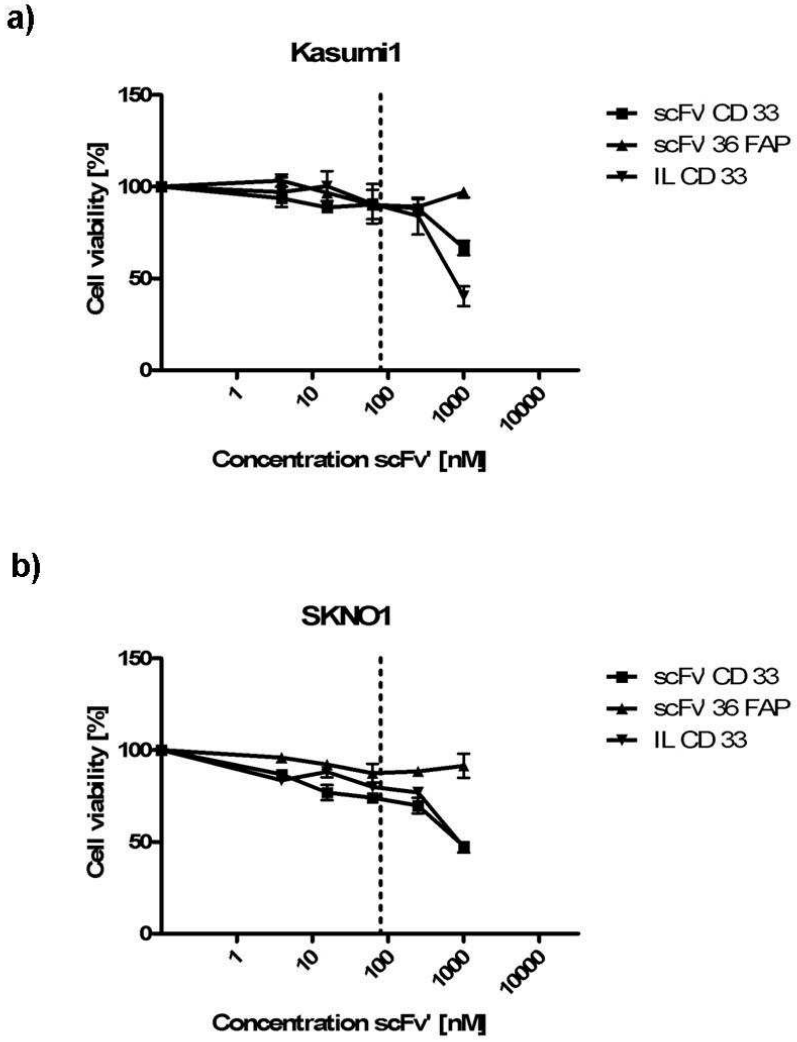

Fig. 3-26: XTT assay on 20000 cells with different concentrations of scFv' CD33, anti-FAP scFv' 36 and empty anti-CD33 ILs. Error bars represented standard deviations of n= 3 independent experiments.
a) Kasumi1 cells, b) SKNO1 cells
Dotted lines indicate the actual scFv' concentration of 75 nM used in colony formation assay.

3.8.2 SiRNA-protamine immunoliposomes

Investigations on protamine ILPs (Fig. 3-27 – 3-31) were performed exactly the same way as experiments on ILPs and ILs with PEI-complexed and free siRNA. Higher lipid concentrations of 8 mM were used for the protamine ILPs, corresponding to 2.7 µM siRNA as the encapsulation efficiency of siRNA-protamine complexes was 67 % (see Table 3-5). 400 µM ILPs were used in colony formation assay with 20000 cells in a volume of 100 µl with a corresponding siRNA concentration of 135 nM.

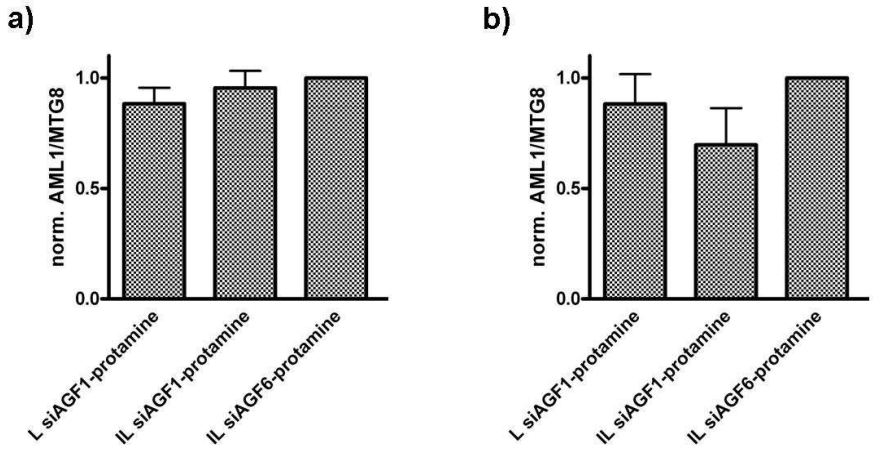

Fig. 3-27: qRT-PCR AML1/MTG8 of 250 ng mRNA of cells three days after transfection with 8 mM siRNA-protamine lLPs. SiRNA concentration was 2.7 µM.
a) Kasumi1, b) SKNO1.
AML1/MTG8 mRNA levels were normalized to GAPDH and the siAGF6 negative control. Error bars represented standard deviations of n= 3 independet experiments. For statistics t-test was performed. -, untreated cells; L, liposomes; IL, immunoliposomes

QRT-PCR demonstrated similar results for protamine ILP transfected Kasumi1 and SKNO1 cells as for the siRNA ILs and siRNA-PEI ILPs concerning the AML1/MTG8 mRNA levels. A nonsignificant reduction of AML1/MTG8 mRNA in the siAGF1 protamine ILP sample of 30 % compared to the siAGF6 control ILPs in SKNO1 cells could be shown. Kasumi1 cells showed no clear differences of protamine ILP treated samples and control samples.

In immunoblot (Fig. 3-28), like in qRT-PCR, no silencing effects of the siAGF1-protamine ILPs could be detected compared to untreated cells, unconjugated lipoplexes and siAGF6-protamine ILPs.
Protamine ILPs could not reach the silencing effects observed in siRNA ILs and siRNA-PEI ILPs. Representative sections of Kasumi1 colony formation assays after seven days were shown (Fig. 3-29) as well as total colony numbers of Kasumi1 and SKNO1 cells (Fig. 3-30).

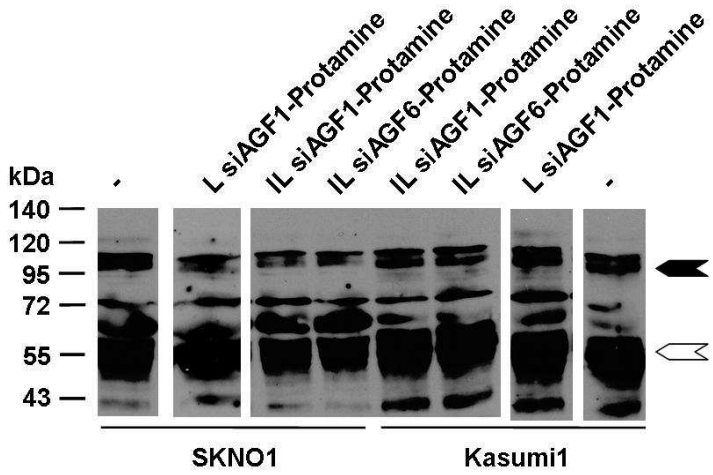

Fig. 3-28: Immunoblot AML1 of cell lines SKNO1 and Kasumi1 three days after transfection with 8 mM siRNA-protamine ILPs. SiRNA concentration was 2.7 µM.
Lysates of 200000 cells were separated by 10 % SDS PAGE, blotted on PVDF membrane and incubated with anti-AML1 antibody. Bands were detected by a secondary HRP labelled antibody. -, untreated cells; L, liposomes; IL, immunoliposomes; black arrow, AML1/MTG8; white arrow, AML1

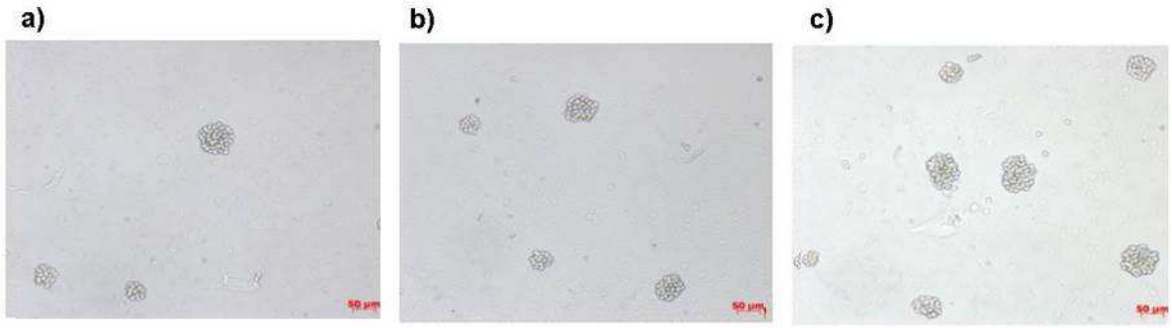

Fig. 3-29: Representative sections of colony formation assays of Kasumi1 cells seven days after transfection with protamine ILPs. 20000 cells were transfected and split for four colony formation samples.
a) siAGF1 LPs, b) siAGF1-protamine ILPs, c) siAGF6-protamine ILPs.
Lipid concentration 400 µM, siRNA concentration 135 nM.

In colony formation assay, only a very weak silencing effect was observed in Kasumi1 and SKNO1 cells transfected with siAGF1-protamine ILPs compared to siAGF6-protamine ILPs, but there was no significant difference. In comparison to untreated cells, there was almost no silencing effect in Kasumi1 cells. SKNO1 cells even showed increased colony numbers after transfection with siRNA-protamine ILPs compared to untreated cells.

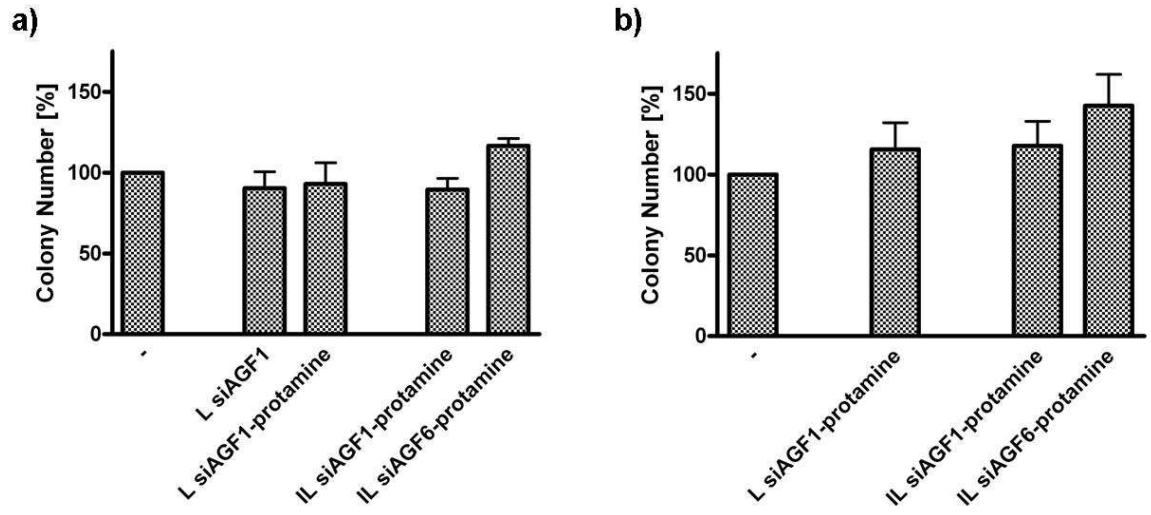

Fig. 3-30: Colony formation assay of leukaemic cell lines seven or ten days after transfection with siRNA-protamine ILPs in a concentration of 400 µM lipid, 135 nM siRNA and a cell number of 20000. Error bars represented standard deviations of n= 3 independent experiments (four wells per experiment). For statistics t-test was performed.
a) Kasumi1 cells, b) SKNO1 cells
-, untreated cells; L, liposomes; IL, immunoliposomes

In contrast, in total colony area (Fig.3-31) clear differences, but still not significant, could be observed. SiAGF1-protamine ILPs reached a decrease of 32 % compared to untreated cells, but unconjugated siAGF1-protamine lipoplexes also showed silencing effects of 25 % in this assay.

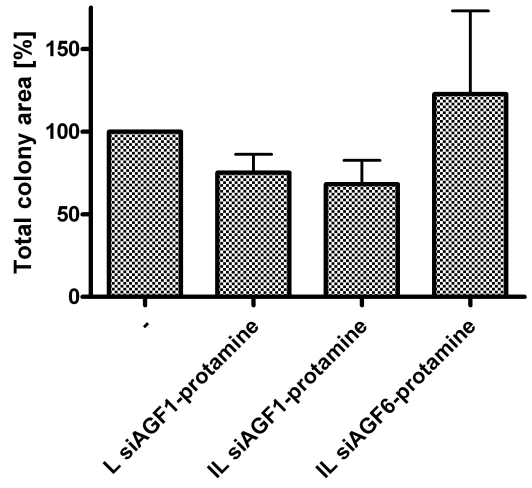

Fig. 3-31: Total colony area of Kasumi1 cells seven days after transfection with 400 µM siRNA-protamine ILPs in colony formation assay. SiRNA concentration was 135 nM. Error bars represented standard deviations of n= 3 independent experiments. For statistics t-test was performed. -, untreated cells; L, liposomes; IL, immunoliposomes

3.8.3 Immunopolyplexes

For IPP transfections, pretests led to an optimal concentration of 620 nM in qRT-PCR and immunblot and 31 nM in colony formation assay. These PEI concentrations resulted in siRNA concentrations of 1.74 µM in qRT-PCR and immunoblot and 86.8 nM in colony formation assay, due to a complete siRNA complexation to PEI and a molar ratio of PEI to siRNA of 1: 2.8. Higher concentrations showed cytotoxic effects. Transfection and assay procedures were the same as for ILs and ILPs. As a control IPP, besides the unconjugated polyplexes, which were expected to show silencing effects because of observed unspecific binding and uptake (see Fig. 3-16), an anti-EGFR scFv' was conjugated to PEGPEI. Both cell lines did not express EGFR on their surface, as attested by flow cytometry with a FITC-labelled monoclonal anti-EGFR antibody in a dilution of 1: 20 (Fig. 3-32).
In qRT-PCR of three independent transfections (Fig. 3.33) Kasumi1 cells again showed the expected silencing effect of PEGPEI-CD33-siAGF1 to a very weak extended. In contrast, SKNO1 showed a remarkable silencing effect of unconjugated PEGPEI-siAGF1 leading to a decrease of AML1/MTG8 mRNA levels to 54 % compared to untreated cells with a very high standard deviation. Anti-CD33 IPPs complexed with siAGF1 even showed enhanced mRNA levels on SKNO1 cells.

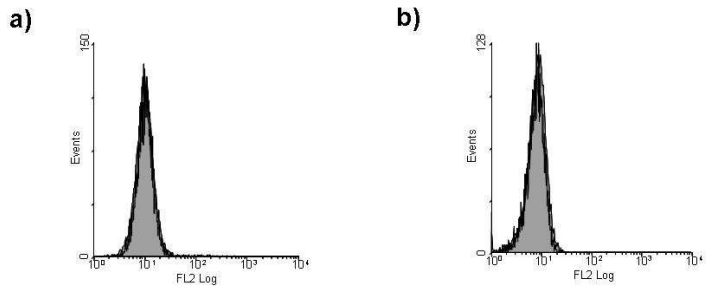

Fig. 3-32: EGFR expression of leukaemic cell lines
EGFR expression levels were detected by a FITC-labelled anti-EGFR monoclonal antibody in a dilution of 1: 20 in flow cytometry. Cell number 250000.
a) Kasumi1 cells, b) SKNO1 cells
Gray, cells alone; black lline, scFv'.

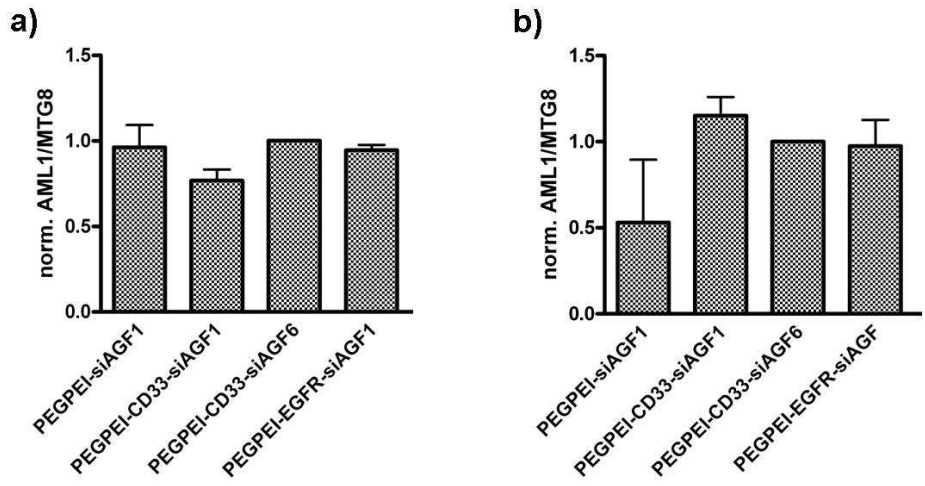

Fig. 3-33: qRT-PCR AML1/MTG8 of 250 ng mRNA of cell lines three days after transfection with 620 nM ILPs. SiRNA concentration was 1.74 µM.
a) Kasumi1, b) SKNO1
AML1/MTG8 mRNA levels were normalized to GAPDH and the siAGF6 negative control. Error bars represented standard deviations of n= 3 independent experiments. For statistics t-test was performed; -, untreated cells

For immunoblot (Fig 3-34), a representative example of three independent transfections was chosen:

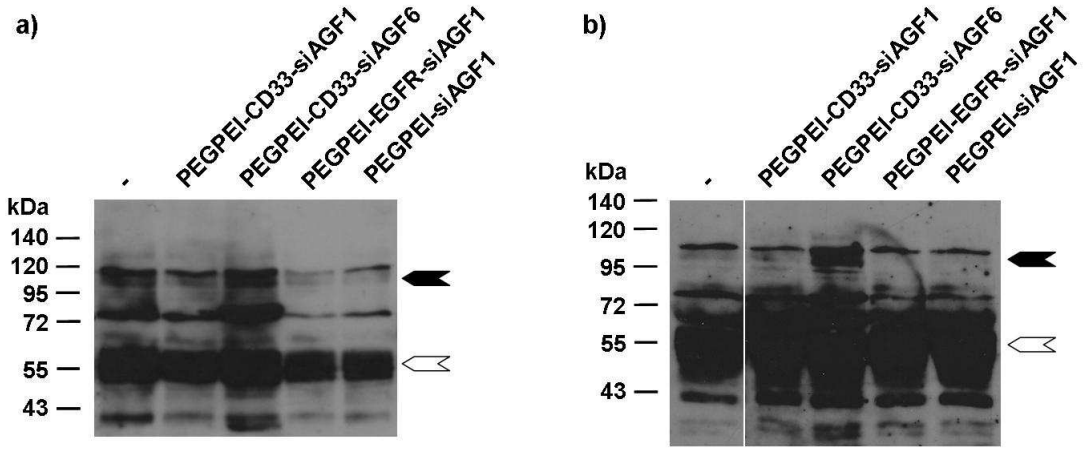

Fig. 3-34: Immunoblot AML1 of cell lines (200000 cells) three days after transfection with 620 nM IPPs on a) Kasumi1 cells and b) SKNO1 cells.
SiRNA concentration was 1.74 µM. Lysates were separated by 10 % SDS PAGE, blotted on PVDF membrane and incubated with anti-AML1 antibody. Bands were detected by a secondary HRP labelled antibody; -, untreated cells; black arrow, AML1/MTG8; white arrow, AML1

In both cell lines specific silencing effects of PEGPEI-CD33-siAGF1 IPPs were observed compared to PEGPEI-CD33-siAGF6. As expected, unconjugated PEGPEIs showed unspecific silencing effects. Even anti-EGFR conjugated IPPs complexed with siAGF1 showed the same effects. Representative sections of Kasumi1 colony formation assays after seven days were shown (Fig. 3-35) as well as total colony numbers of Kasumi1 and SKNO1 cells (Fig. 3-36).

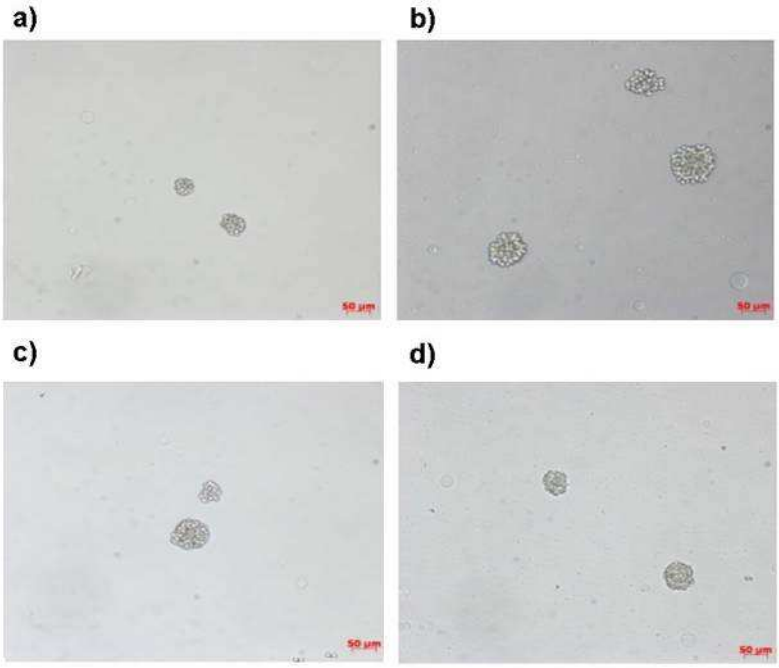

Fig. 3-35: Representative sections of colony formation assays of Kasumi1 cells seven days after transfection with IPPs. 20000 cells were transfected and split for four colony formation samples.
a) siAGF1 IPPs, b) siAGF6 IPPs, c) siAGF1 PPs, d) siAGF1-EGFR IPPs
PEI concentration 31 nM, siRNA concentration 86.8 nM.

Colony formation assay, where 20-fold lower concentrations of IPPs and siRNA were used, showed specific silencing for PEGPEI-CD33 complexed with siAGF1 compared to all the controls (Fig. 3-36). Colony numbers of Kasumi1 cells could be reduced to 68 % of untreated cells after transfection with CD33 IPPs complexed with siAGF1. SKNO1 cells showed the same silencing effects to a very weak extend. Determination of total colony area of Kasumi1 cells (Fig. 3-37) showed a weak reduction of total colony area in PEGPEI-CD33-siAGF1 transfected cells to 76 % of untreated cells with a very high standard deviation.

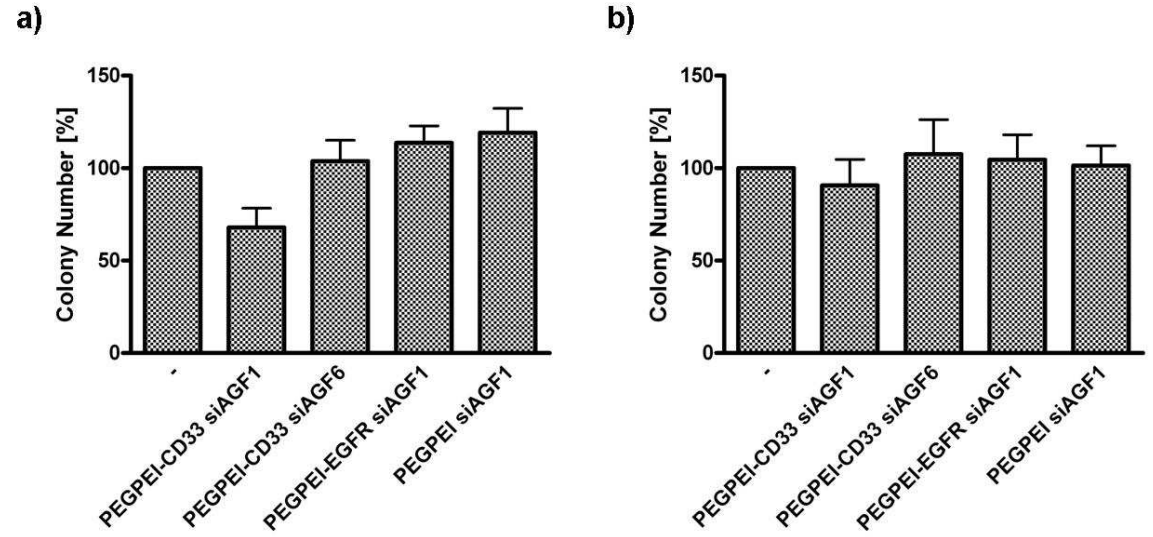

Fig. 3-36: Colony formation assay of 20000 cells seven or ten days after transfection with 31 nM IPPs. SiRNA concentration was 86.8 nM. Error bars represented standard deviations of n= 3 independent experiments (four wells per experiment). For statistics t-test was performed.
a) Kasumi1 cells, b) SKNO1 cells
-, untreated cells

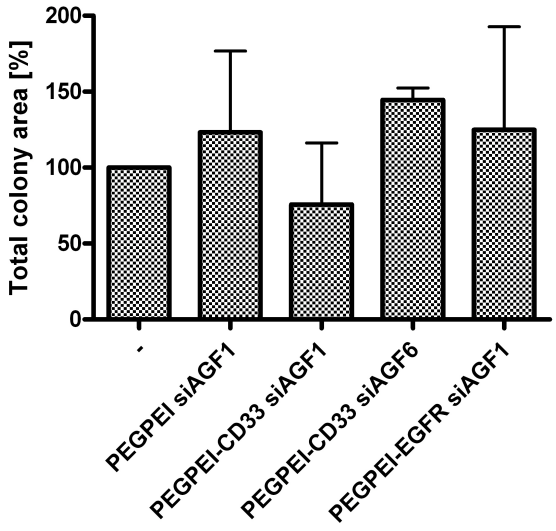

Fig. 3-37: Total colony area of Kasumi1 cells seven days after transfection with 31 nM IPPs. SiRNA concentration was 86.8 nM. Error bars represented standard deviations of n= 3 independent experiments. For statistics t-test was performed. -, untreated cells

Silencing of AML1/MTG8 by the delivery of therapeutic siRNA with different carrier systems could only be reached to a weak extend and specificity differed for the various carrier systems. The most reliable results could be shown with ILs of free or PEI-complexed siRNA. Protamine ILPs failed in silencing efficiency, IPPs in antigen specificity. The latter would possibly be a matter of concentration and further investigations would be advisable for all the carrier systems.

3.9 Humanization of scFv' molecules

Anti-CD33 scFv' V_HV_L HC4 and anti-CD19 scFv' were humanized in a knowledge-based approach by CDR-grafting and codon optimized for CHO cells as described in detail in chapter 2.23.

3.9.1 scFv' CD33 V_HV_L HC4

The humanized version of scFv' CD33 V_HV_L HC4 (scFv' IZI08.3) was expressed bacterially in the pAB1 vector by *E. coli* TG1. The expression yield of 0.42 mg/l bacterial culture was approximately two-fold of the murine construct with 0.2 mg/l. DiI labelled ILs were prepared with the humanized scFv' by the postinsertion method with 0.3 mol% micellar lipid and investigated for their binding activity on target cells (Fig. 3-38). They showed a similar binding pattern to the murine anti-CD33 ILs, i.e. strong binding to SKNO1 cells, weak binding to Kasumi1 cells and none to CD33-negative Jurkat cells.

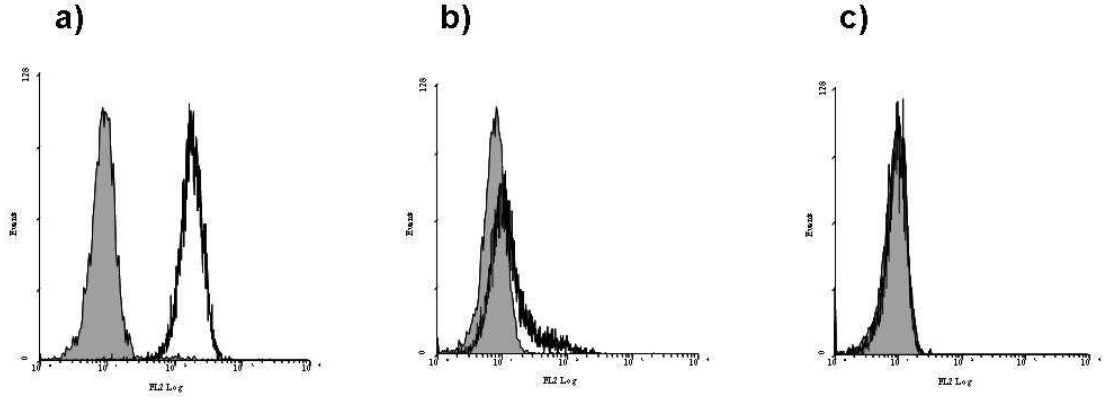

Fig. 3-38: Binding activity of 250 µM IZI08.3 ILs on leukaemic cell lines determined by flow cytometry.
a) SKNO1, b) Kasumi1 and c) Jurkat cells. Cell number 250000.
Gray, cells alone; black line, anti-CD33 immunoliposomes.

3.9.1.1 Comparative analysis of humanized versus murine scFv' molecules

Comparison of the melting points of the humanized (Fig. 3-39) and murine (Fig 3-9b) scFv' CD33 V_HV_L HC4 in a temperature gradient of 35 to 75 °C by DL S showed an enhanced stability of the humanized construct. Its melting point was increased from 60 °C in the murine to 65 °C in the humanized construct.

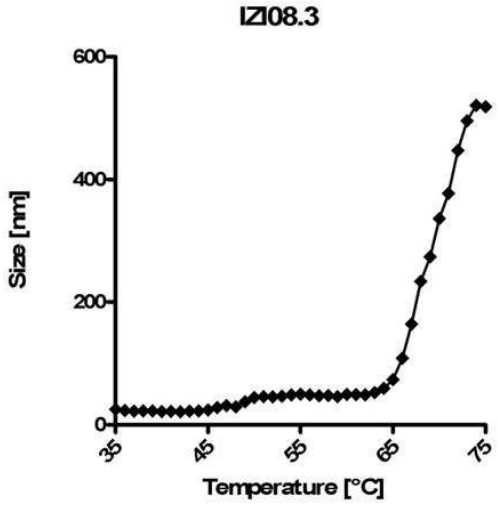

Fig. 3-39: Melting point analysis of scFv' IZI08.3. 100 µg scFv' were analysed by dynamic light scattering in a temperature gradient from 35 to 75 °C.

Binding activities of the murine and humanized scFv' CD33 V_HV_L HC4 were compared by flow cytometry on 250000 SKNO1 and Kasumi1 cells with increasing scFv' concentrations from 0.01 to 10 µg/ml (3.54 to 354 nM). MFIs were determined by dividing the MFI of cells incubated with the secondary, FITC-labelled antibody only (Fig. 3-40).

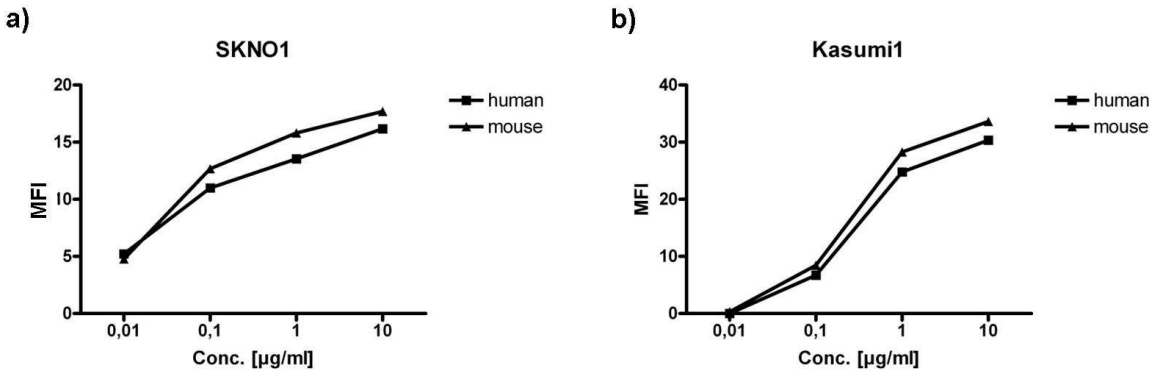

Fig. 3-40: Binding activity of murine and humanized scFv' on 250000 leukaemic cells determined by flow cytometry. n= 1

a) SKNO1, b) Kasumi1

MFIs plotted against scFv' concentrations.

Binding activities of murine and humanized scFv' molecules showed almost identical patterns on both cell lines with very slight advantages for the murine scFv'. Both constructs reached higher MFIs on Kasumi1 (30 for the humanized and 34 for the murine construct) compared to SKNO1 (16 for the humanized and 18 for the murine construct) cells referred to the applied concentrations. However, on SKNO1 cells a tendency towards saturation became visible, which was not the case for Kasumi1.

For the determination of EC_{50} values for the binding of the murine and humanized scFv constructs to Kasumi1 cells, both constructs were cloned into the pAB1 vector without a C-terminal cysteine. Binding activities of both scFv molecules to 250000 Kasumi1 cells were investigated in flow cytometry in concentrations reaching from 17 pM to 3 µM. Data from 17 pM to 111 nM were shown (Fig. 3-41). Nonlinear curve fits of the constructs showed almost identical courses for both scFv molecules.

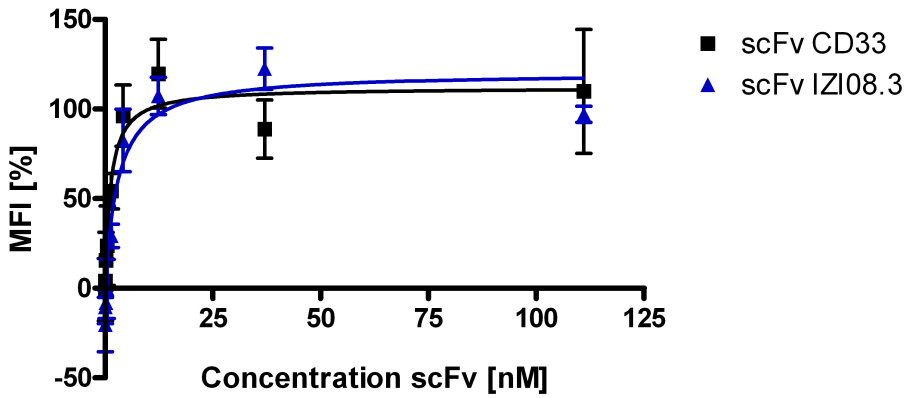

Fig. 3-41: Binding activity of murine and humanized scFv CD33 on 250,000 Kasumi1 cells determined by flow cytometry. Error bars represented standard deviations from n= 3 independent experiments. Nonlinear curve fits are shown.

Calculated EC_{50} values were 1.217 ± 0.57 nM for scFv CD33 V_HV_L with a saturation of 111.9 ± 11.12 % as determined by nonlinear regression, and 2.98 ± 1.136 nM for scFv IZI08.3 with a saturation of 120.5 ± 10.57 %. Negative MFIs resulted from a slight binding of the detection antibodies only.

Humanization of scFv' CD33 resulted in an advanced molecule concerning production yield and temperature stability. Binding activities of both constructs were not significantly different, proved by a P-value of 0.24.

3.9.2 scFv' CD19

The humanized version of scFv' CD19 (scFv' IZI08.4) was expressed bacterially in the pAB1 vector by *E. coli* TG1. The expression yield of 0.07 mg/l bacterial culture was approximately six fold lower than the yield of the murine construct of 0.4 mg/l.

3.9.2.1 Comparative analysis of humanized versus murine scFv' molecules

In contrast to CD33, comparison of the melting points of the humanized and murine scFv' CD19 (Fig. 3-42) showed a decreased stability of the humanized construct. Its melting point was lowered from 45 °C to 41 °C after humanization. Both, the murine and the humanized constructs were not suitable for the preparation of ILs in the postinsertion method requiring a temperature stability of at least 55 °C.

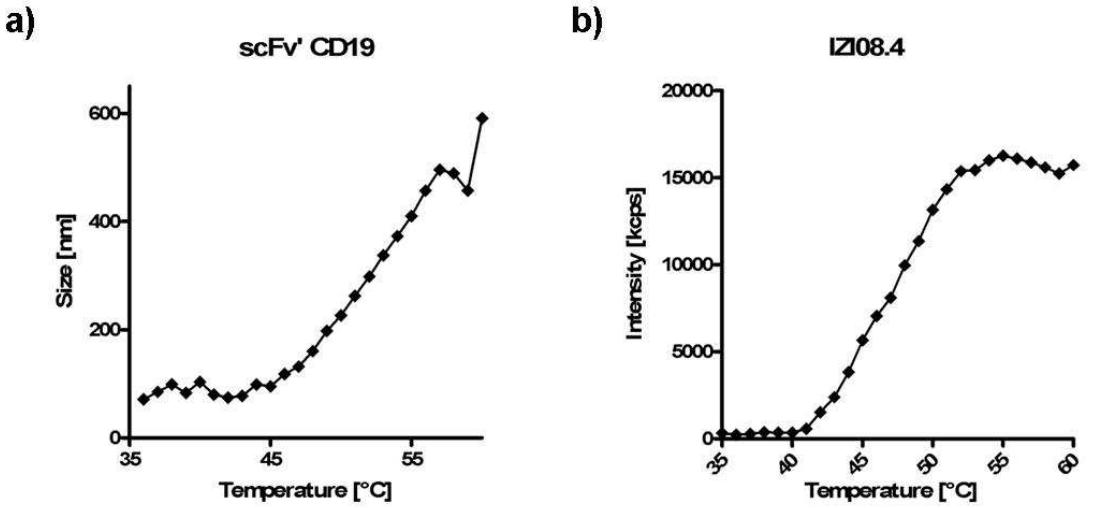

Fig. 3-42: Melting point analysis of scFv' CD19.
a) murine construct, b) humanized construct
100 µg scFv' were analysed by dynamic light scattering in a temperature gradient from 35 to 75 °C.

Binding activities of the murine and humanized scFv' CD19 were compared by FACS analysis on 250000 CD19 expressing SEM and Daudi cells with increasing scFv' concentrations from 0.01 to 10 µg/ml (3.54 to 354 nM). MFIs were determined by dividing the MFI of cells incubated with detection antibody only (Fig. 3-43).

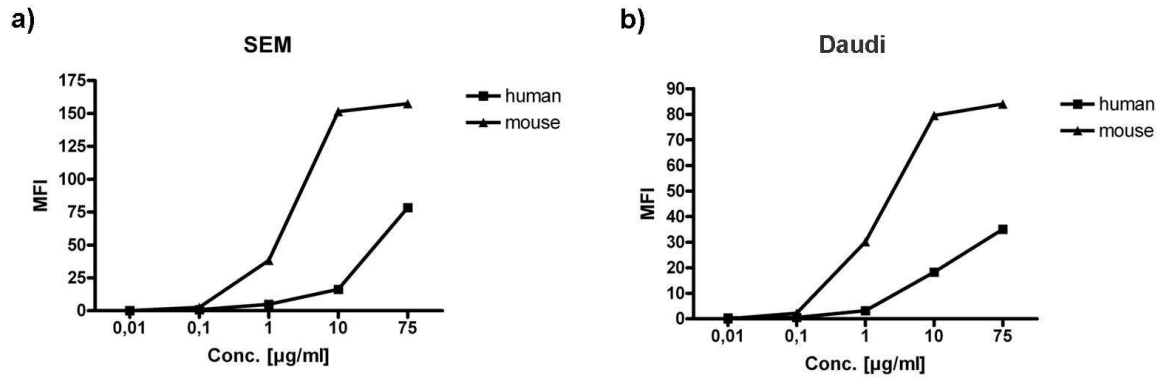

Fig. 3-43: Binding activity of murine and humanized scFv' on 250000 leukaemic cells determined by flow cytometry. n= 1
a) SEM, b) Daudi
MFIs plotted against scFv' concentrations.

Binding activity of the murine scFv' was clearly superior to the humanized scFv' and higher on SEM than on Daudi cells. On both cell lines, the murine scFv' CD19 showed a tendency towards saturation. The murine construct reached maximum MFIs of 157 on SEM and 84 on Daudi cells while the humanized construct only reached MFIs of 78 and 35 on SEM cells and on Daudi cells, respectively. The humanized scFv' did not reach maximum MFIs within the tested concentrations on both cell lines.
Humanization of scFv' CD19 resulted in a loss of production yield, temperature stability and binding activity.

4 Discussion

In this work, different carrier systems for the targeted delivery of therapeutic siRNA were generated and compared with regard to their target cell specific binding and uptake and their silencing efficiency *in vitro*. As a targeting moiety for the carrier systems, the scFv' antibody format was chosen. Different antibody formats such as whole antibodies (Park et al., 2002; Li et al., 2001), Fab' fragments (Sapra et al., 2004) and scFv fragments (Marty et al., 2001; Völkel et al., 2004; Park et al., 2002) have been used for the generation of carrier systems. However, whole antibodies have been shown to be immunogenic and are rapidly cleared from circulation through Fc-mediated uptake by macrophages, e.g. Kupffer cells of the liver (Koning et al., 2003). These disadvantages can be circumvented using Fab' or scFv molecules as ligands. They can be easily modified through genetic engineering, e. g., by insertion of an additional cysteine residue (scFv'). This permits a very defined and site-directed coupling to reactive groups of carriers.

4.1 Single chain Fv molecules

Three different scFv' molecules, representing the smallest antigen binding antibody fragments, were initially chosen as targeting moieties for different carrier systems in leukaemia therapy. These were anti-CD13 scFv' molecules targeting haematopoietic cells of the myeloid lineage, anti-CD19 scFv' molecules binding to all maturation stages of the B-lymphoid lineage except of plasma cells and anti-CD33 scFv' molecules targeting myelomonocytic precursor cells. All three antigens have been published as potential target antigens, using ligands or antibodies in therapeutic approaches of cancer and inflammation, some of them undergoing clinical trials, e. g. Gemtuzumab-ozogamicin, a CD33-targeting chemotherapeutic (Hamann et al., 2002) and Blinatumomab, an anti-CD19 and anti-CD3 bispecific antibody (Bargou et al., 2008). After comparison of production yields and scFv' characterization concerning purity, integrity, stability and binding activity, CD33 was finally chosen for the generation of ILs, ILPs and IPPs. Production yields of scFv' molecules were low compared to common in-house scFv production yields, probably due to the unpaired cysteine of the scFv' molecule. Schmiedl et al. (2000) reported that unpaired cysteine residues reduced binding activity, production yield and purity of antibody molecules. Eukaryotic expression of scFv' CD13 reached higher production yields, but represented a higher effort compared to bacterial expression. Fermentation of scFv' CD33 V_HV_L HC4 resulted in a 20-fold increase of production yield, but loss of purity. For these reasons, scFv' molecules were further produced in *E. coli* in a periplasmic expression. SDS PAGE revealed a small part of active scFv' molecules concerning coupling activity, represented by dimeric

scFv' molecules under non-reducing conditions. If scFv' molecules in the monomeric fraction remain inactive, is unclear. Flow cytometry proved target cell specific binding activity of the scFv' molecules. Binding affinities of scFv CD19 4G7 with 8.4 nM and scFv CD33 K132 with 11 nM were similar (Kügler et al., 2009; Schwemmlein, 2007b), whereas scFv CD13-1 showed a higher affinity of 0.73 nM (Peipp et al., 2001). After having selected CD33 as target antigen due to high scFv' production yields and an antigen expression restricted to immature myelocytes, the antibody fragment was modified with regard to an improved coupling efficiency and binding activity of ILs, ILPs and IPPs to target cells. Four different scFv' CD33 variants were created, differing in the order of their light and heavy variable chain and the length of the peptide spacer between the antibody domains and the C-terminal cysteine. The variants showed production yields, which were further decreased in comparison to the original scFv' CD33. This observation was not in accordance to observations from Messerschmidt et al. (2008), who reported similar production yields of anti-FAP scFv' and its variants. Western blot analysis showed a higher amount of scFv' dimerization of V_HV_L variants under non-reducing conditions compared to V_LV_H variants. These positive findings for the V_HV_L constructs continued in scFv' binding studies, where V_HV_L variants showed superior binding activity on SKNO1 and Kasumi1 cells. According to Kipriyanov et al. (1998), dimerized scFv' molecules probably achieved higher binding activities as a result of increased avidity. Moreover, an enhanced fluorescence signal can be achieved from a dimeric scFv' molecule in flow cytometry because of the detection of two His-Tags. Moreover, the results indicate a possible influence of domain order on binding activity of antibody fragments. Kim et al. (2008) reported a higher productivity of scFv molecules with the domain order V_HV_L compared to V_LV_H, but almost the same antigen-binding activity. In contrast, the enhanced productivity of V_HV_L constructs in E*. coli*, which has been described, could not be confirmed in the present study. Purity and integrity of scFv' CD33 V_HV_L HC4 were further confirmed by size exclusion chromatography. Additionally, a high thermostability of scFv' CD33 V_HV_L HC4 approved the choice of this scFv' variant for the generation of carrier systems.

4.2 Immunoliposomes

A protocol for IL preparation, firstly described by Ishida et al. (1999) was optimized by Kolbe (2007) for scFv' molecules as targeting moieties. The postinsertion of scFv´ fragments, coupled to micellar malPEG$_{2000}$-DSPE lipid, into a liposomal lipid bilayer depends on the transition temperature (T_m) (New et al., 1990). At RT, lipid bilayers are in a gel-like state. Above T_m, lipid bilayers change their conformation into the liquid-ordered or the liquid-crystalline state. Under these conditions micelles can insert into the outer layer of the

liposomal membrane. T_m depends, besides other factors, on the composition of the liposomal bilayer as phospholipids with saturated fatty acid chains have a higher T_m than those with unsaturated chains. EPC, e. g., is composed of mainly unsaturated fatty acid chains and T_m was determined to 36.6 °C. If cholesterol is added, liposomes show an enhanced stability (Moschetta et al 2001). For HSPC, a mixture of saturated phospholipids, a higher T_m of 54 °C was published (Park et al., 2002). In general, the higher the temperature, the more liquid is the liposomal membrane and therefore, the insertion efficiency will increase with temperature. But there are also certain limitations for temperature increase during the postinsertion process: High liquidity of the membrane might cause increased drug leakage in case of drug-loaded liposomes and, if the melting temperature of scFv molecules is exceeded, proteins will denaturate. It could be shown that for postinsertion of scFv' 36 into liposomes, a temperature of 55 °C is suitable. Melting temperature of scFv' CD33 V_HV_L HC4 was determined at approximately 60°C, and is therefore in a native state at 55°C.
Thus, the entire optimized postinsertion protocol could be adopted. ILs of all scFv' CD33 variants, prepared by the postinsertion method, were compared to ILs prepared by a conventional coupling. In this method, scFv' molecules were directly coupled to malPEG$_{2000}$-DSPE functionalized liposomes. Coupling efficiency of scFv' to malPEG$_{2000}$-DSPE was comparable for both methods and subsequent insertion of scFv' coupled micelles into preformed liposomes in the postinsertion method resulted in a similar efficiency as the direct scFv' coupling to liposomes, as shown by western blot. However, in the conventional coupling method, coupling of more than one malPEG$_{2000}$-DSPE chain to one scFv' molecule was detected in western blot, probably due to cross-reactivity of the maleimide group and amino groups of the scFv' molecule, although a specificity of maleimide reactions with sulfhydryl groups in the pH range 6.5 to 7.5 has been described (Hermanson, 1996). Although the coupling reaction was performed at a pH 6.7, additional coupling occurred. Interestingly, the coupling of scFv' molecules to micelles of the same lipid in the postinsertion method was also performed at pH 6.7. Here, no additional coupling of lipid chains was observed. This observation and a possible advantage for postinsertion ILs due the separation of drug loading and scFv' coupling, each performed under optimal conditions, has led to the establishment of the postinsertion technique for this study. However, both methods showed similar coupling efficiencies and adequate separation of non-conjugated scFv' molecules. Furthermore, all scFv' CD33 variants were equally suited for the generation of ILs by both techniques.

Binding studies of ILs on SKNO1 and Kasumi1 cells showed superior binding activity of scFv' CD33 V_HV_L HC4 ILs compared to all the other variants in both IL preparation methods, the postinsertion and conventional coupling method. The influence of the peptide spacer length

on antibody binding activity has been described by Nobs et al. (2004). They claimed that the use of an extended spacer arm can reduce the sterical hindrance, making the binding site better accessible. Advantages of the V_HV_L-format already became obvious in the binding activity of free scFv' CD33. Remarkably, ILs showed higher binding activity on SKNO1 cells compared to Kasumi1 cells. This observation could not be explained by a higher antigen expression of SKNO1 cells, as free scFv' molecules showed higher binding activities on Kasumi1 cells. Maybe, the access to the epitope on Kasumi1 cells was impeded for ILs due to sterical reasons. Dynamic light scattering revealed different sizes of $mPEG_{2000}$-DSPE and $malPEG_{2000}$-DSPE liposomes, probably due to specific properties of the lipids. The increase of size after scFv' coupling was similar for both methods, resulting in conventional ILs, which were smaller than postinsertion ILs. However, the differences were not relevant concerning cellular uptake of the ILs. Particles with a size below 200 nm are internalized by clathrin-mediated endocytosis (Rejman et al., 2004). Antigen binding of scFv' CD33 V_HV_L HC4 ILs was highly specific. Flow cytometry of non-targeted $mPEG_{2000}$-DSPE liposomes as well as anti-endoglin scFv' ILs showed no binding on SKNO1 cells. Additionally, a blocking experiment confirmed specificity. Introduction of a high excess of free scFv' molecules to block IL binding was adequate because of a high avidity of ILs, superior to free scFv', due to the insertion of several scFv' molecules in one liposome (Adams et al., 2006). IL binding activity was optimized with regard to the determination of the optimal ratio of scFv' coupled $malPEG_{2000}$-DSPE micelles to total lipid. Analysis of MFIs of ILs inserted with different percentages of $malPEG_{2000}$-DSPE micelles, from 0.01 to 10 mol%, on SKNO1 cells, revealed an optimum of 0.3 mol% $malPEG_{2000}$-DSPE. Lower $malPEG_{2000}$-DSPE ratios showed decreased MFIs due to an insufficient number of scFv' molecules per liposome. Higher $malPEG_{2000}$-DSPE ratios showed decreased MFIs, probably because of sterical hindrance between the scFv' molecules, leading to a reduction of binding activity. The optimal concentration of 0.3 mol% scFv' coupled micelles resulted in 29 scFv' molecules per liposome, representing a coupling and insertion efficiency of almost 50 %, which could be comprehended by western blot. These findings were in overall accordance with literature. Binding activity of ILs on cells depended on the number of coupled scFv molecules and required only a few scFv per liposome. Maximal binding for anti-Her2-scFv ILs was observed with 30 to 40 attached scFv per liposome (Nielsen et al., 2002). Kirpotin et al. (1997) reported appropriate IL binding with 35 to 70 scFv molecules per liposome. In-house experience shows optimal $malPEG_{2000}$-DSPE concentrations of, e. g., 0.3 mol% for scFv' huC225 ILs, 2 mol% for scFv' hu4D5 ILs (Nusser, 2009) and 0.6 mol% for scFv' 36 ILs (Kolbe, 2007). In contrast, Park et al. (2002) determined 7 mol% scFv' coupled lipid for maximum IL binding activity.

The investigation of IL plasma stability revealed an intermediate loss of binding activity after one day of incubation in human plasma at 37 °C. The effect was considerably weaker in PBS incubated ILs, indicating an interfering effect of plasma components rather than incubation temperature, as the PBS incubation also took place at 37 °C. Almost no further loss of binding activity could be observed up to ten days, which proved a sufficient plasma stability of ILs with regard to *in vivo* applications. However, it must be considered, that empty ILs were investigated and the results could not be projected on the stability of siRNA-loaded ILs. Fluorescence microscopy studies showed a highly antigen specific internalization of ILs into SKNO1 and Kasumi1 cells. Only weak binding, but no uptake could be detected in negative controls, ILs on CD33-negative Jurkat cells and non-targeted liposomes on Kasumi1 cells. These non-relevant interactions may be due to the adjacency of cells and ILs in a reaction tube and do not necessarily reflect the *in vivo* situation. IL uptake into SKNO1 cells showed an endosomal staining pattern. Conversely, a slight staining of the cytoplasm in Kasumi1 cells indicated endosomal release of ILs. However, ILs without further modifications were not expected to manage an enhanced endosomal escape.

4.2.1 Encapsulation of siRNA

Passive encapsulation of siRNA during liposome formation has not been expected to reach high loading efficiencies as neutral lipids were used, which have no ability to decoy negatively charged nucleic acids. Although phosphatidylcholine and ethanolamine, both contain one positively charged amino group, they also contain a negatively charged phosphate residue, resulting in a neutral net charge. Additionally, the lipids are shielded by PEG-chains. One effort to improve the efficiency is the application of very high lipid concentrations. It could be shown that siRNA loading efficiency was enhanced with increasing lipid concentrations because the high lipid density did hardly leave any volume outside of liposomes, which could contain non-encapsulated siRNA. Finally, a lipid concentration of 100 mM, which could barely be handled, was chosen. It resulted in an encapsulation efficiency of 24 % for free siRNA, 67 % for protamine-complexed siRNA and almost 100 % for PEI-complexed siRNA. It must be mentioned that only very weak Cy3 signals could be detected after siRNA complexation to PEI, before liposome formation as well as in the supernatant after separation of the liposomes. This observation argued for a possible quenching effect of PEI, complicating the determination of siRNA encapsulation efficiency. It raised the question, if siRNA-complexation and encapsulation of the complex into liposomes was really 100 %. Obviously, siRNA complexation could enhance loading efficiency, but was also performed to allow for endosomal release of siRNA-loaded ILs. Stuart and Allen (2000) confirmed a limitation to passive encapsulation of ODN within the aqueous phase of liposomes. A poor incorporation efficiency of approximately 20 % in

neutral liposomes has been described. They also claimed that entrapped ODN must be distinguished from those passively associated with the outside of the liposomal membrane. However, this was not the case in the present study and could probably falsify the results of siRNA encapsulation efficiency. Stuart and Allen (2000) further observed that the addition of 2 to 5 mol% PEG-DSPE into neutral liposomes doubles the incorporation efficiency. An ideal approach would be using a method that optimizes the charge interaction between the ODN and a cationic lipid, combined with a method that provides an outer coating of neutral lipid. For such a method, very high encapsulation efficiencies of 80 to 100 % were determined. Other statings have been made by Auguste et al. (2008) who encapsulated 19 % siRNA, however using another lipid formulation, and by Zheng et al. (2009) loading 3 % siRNA in a neutral lipid formulation. Complexation with PEI resulted in a two-fold siRNA loading efficiency compared to naked siRNA (Patil and Panyam, 2009). Compared to these data, we could reach rather high loading efficiencies. However, poor loading efficiencies could also be explained as a measurement artefact, resulting from lipid quenching of the Cy3 signal, hypothesized by t'Hoen et al. (2003). It would also be a possible explanation for the absence of a Cy3 signal from siRNA-loaded ILs in flow cytometry, which we observed even at very high lipid concentrations. SiRNA-encapsulated liposome and IL sizes were determined, but gave no reliable correlations for a siRNA-complexation dependent or a scFv' dependent change of size. Surprisingly, some of the liposomes show a decreased size after scFv' conjugation. This could be due to an increased hydrophilicity of targeted complexes and a decreased interaction between particles due to additional steric shielding (Germershaus et al., 2006). This would lead to a reduction of the hydrodynamic diameter of the particle. A decrease of size of siRNA-protamine-loaded liposomes in comparison to free siRNA-loaded liposomes was observed for siAGF6 and may be due to condensation effects between the nucleic acids and the polycations. Binding and internalization of siRNA-loaded ILs to leukaemic cell lines were investigated in fluorescence microscopy. For this purpose, liposomes encapsulated with free Cy3-labelled siRNA were used. Like in non-encapsulated liposomes, a highly antigen-specific uptake into CD33-positive SKNO1 and Kasumi1 cells could be shown. The reason, why Kasumi1 cells showed less distinct results compared to SKNO1 cells, remained unclear, but confirmed the observations from non-encapsulated ILs in flow cytometry. Both cell lines showed only weak binding and no uptake of non-targeted siRNA-loaded liposomes. The same result was seen for ILs on the CD33-negative Jurkat cell line.

4.2.2 Encapsulation of complexed siRNA

For the siRNA complexation to PEI, an N/P ratio of 5 was chosen, which has also been confirmed by Shim and Kwon (2009) as a suitable ratio. An important advantage of PEI

complexation, in comparison to protamine, is the ability of PEI to release siRNA from the complex in the cytosol. Brunk et al. (1997) gave possible explanations for this property of PEI: Extension of the polymer network during endosomal acidification or by PEI interactions with endosomal or cytoplasmic constituents could be responsible for siRNA release. Still, in some cases, intact PEI-plasmid particles were found in cell nuclei, indicating that complexes might be too stable to release plasmid into the cytosol. Consequently, no knockdown effects could be observed (Honore et al., 2005). Protamine has often been used for complexation in the delivery of plasmid DNA (Wagner et al., 1990; Li et al., 2001), where stable complexes in the cytosol represent an important prerequisite, necessary for subsequent nuclear transfection. Indeed, the strong cationic charge of protamine is described to limit the release of siRNA (Ikeda and Taira, 2006). For this reason, a relatively low molar ratio, compared to literature, of siRNA: protamine of 1: 3 was chosen for the present study. In contrast, Peer et al. (2008) applied siRNA-protamine complexes with a ratio of 1: 5.

4.3 Endosomal release

PEI was chosen for the complexation of siRNA in the present study because it has been shown to allow for endosomal escape of siRNA by the proton sponge effect (Akinc et al., 2005). Other siRNA complexing agents, like polypeptides, do not all reach this goal. Poly(L-lysine), e. g., shows no endosomal release (Merdan et al., 2002). If protamine is able to provide endosomal release has been discussed controversially in literature. Guy et al. (1995) and Behr et al. (1996) suggested additional procedures, e. g. the treatment with chloroquine, to provide endosomal release, while Maruyama et al. (2004) considered a proton sponge effect possible. Nevertheless, current studies manage endosomal release of protamine-complexes without further modification (Peer et al., 2008). In contrast, our data did not argue for a release of siRNA into the cytosol, either by inhibited endosomal escape or by insufficient release of siRNA from the complex.

In addition or as alternatives to PEI, many substances and modifications have been investigated during the last years to improve endosomal escape and thus silencing activity of nucleic acids. Popular lipid compositions contain DOPE, a pH-dependent and fusogenic lipid, which selectively destabilizes the liposomal membrane following acidification. DOPE undergoes lamellar to hexagonal phase transition at low pH values. Sasaki et al. (2008) showed enhanced endosomal escape of nanoparticles via synergistic action of pH-sensitive fusogenic peptide derivatives within the liposomal membrane and at the tips of PEG-chains. Recently, pH-sensitive ILs have been shown to trigger drug release by collapse of a terminally alkylated N-isopropylacrylamid homopolymer within the liposomal membrane due to pH-decrease during endosome acidification (Simard and Leroux, 2009). Another approach

is represented by the peptide diINF-7, a fusogen based on the N-terminal domain of influenza virus HA-2, which is activated upon pH drop (Crommelin et al., 2003). Recently, Shim and Kwon (2009) presented a modification of PEI, an acid degradable ketalized linear PEI, which reaches higher RNAi compared to non-modified PEI and exhibits biocompatibility. The PEI molecules, used in the present study, were not biodegradable and showed limitations in their application due to cytotoxic effects.

4.4 Immunopolyplexes

PEI(25kDa)-PEG(2kDa)$_{10}$, the polymer used in this study, has already been published as a conjugate with anti-Her2 mAb Trastuzumab (Germershaus et al., 2006). Charge neutral particles with a hydrodynamic diameter of 130-180 nm were generated. These particles, although coupled with whole mAbs, were smaller than our particles, coupled with scFv' antibody fragments. In our study, comparable sizes were only reached for unconjugated PEGPEIs with and without siRNA complexation. Conjugation to scFv' molecules led to an increase of size, which was very pronounced for scFv' CD33. In parallel, zeta potentials of PEGPEIs decreased after scFv' conjugation, due to an additional sterical shielding of the positive charge of the PEI core. Nevertheless, PEGylation of PEI obviously led to a sufficient shielding effect as the zeta potential of PEGPEI, of + 0.7 mV, was almost neutral. Complexation of siRNA resulted in a further increase of size in case of unconjugated PEGPEIs and a slight decrease of size in the case of PEGPEI-EGFR. This could be due to condensation effects between the nucleic acids and the polycations, as observed for the siRNA-PEI loaded ILs. In both cases, zeta potentials were further reduced after complexation with negatively charged siRNA. The dramatic increases of size after scFv' conjugation and siRNA complexation of PEGPEI-CD33 were remarkable and did not confirm the observations of Germershaus et al. (2006). In contrast to the present study, where size measurements were performed in PBS, Germershaus et al. (2006) performed the determination of particle size in 5 % glucose solution, which could lead to different results. Particle aggregation could also result in a dramatic increase of size. However, it was only observed for anti-CD33 IPPs, not for anti-EGFR IPPs and non-conjugated polyplexes. With a size of approximately 450 nm anti-CD33 IPPs exceeded the critical size for clathrin-mediated internalization of 200 nm by far (Rejman et al., 2004). Even the anti-EGFR IPPs with a size of 243 nm when complexed to siRNA, exceeded the critical size. It has been described that internalization of ligand-devoid microspheres with a diameter up to 200 nm involved clathrin-coated pits. With increasing size, a shift to a mechanism that relied on caveolae-mediated internalization became apparent, which became the predominant pathway of entry for particles of 500 nm in size. At these conditions, delivery to the lysosomes was no longer apparent. The data

indicate that the size itself of particles can determine their pathway of entry (Rejman et al., 2004). If this also holds true for targeted particles, remains to be investigated.

Nevertheless, IPP binding and uptake studies in fluorescence microscopy argued for an endosomal uptake, as the SKNO1 target cells showed a characteristic endosomal staining pattern. Binding and uptake were antigen-specific for IPPs and could be shown independently for PEGPEI-CD33 and complexed siRNA. Slight staining of the cytosol could also be detected, indicating an endosomal escape of polyplex and siRNA. On CD33-negative Jurkat cells, no binding or uptake could be observed. However, non-targeted PEGPEI showed binding and uptake into SKNO1 cells and Jurkat cells. This could result from an incomplete shielding of the transfecting PEI core by the PEG-chains. In contrast, Germershaus et al. (2006) reported negligible binding and uptake of non-targeted PEGPEIs. The optimal N/P ratio of PEGPEI-siRNA complexes is controversially discussed in literature and for this study, an N/P ratio of 5 has been chosen. Mao et al. (2006) applied an N/P ratio of 3 and reported unspecific effects at higher N/P ratios interfering with possible targeting effects. However, other published N/P ratios ranged from 6 to 8 (Grayson et al., 2006). At optimal N/P ratios, reporter gene expression using targeted complexes was up to sevenfold higher than that of unmodified PEGPEI complexes (Germershaus et al., 2006).
Coupling efficiencies of scFv' molecules to PEGPEI resulted in 27.6 % and 50 % in two different approaches. In the first approach, the free functional OPSS group of the NHS-PEG_{2000}-OPSS crosslinker was activated by reduction for the formation of disulfid bonds with scFv' molecules. This procedure probably resulted in the formation of PEGPEI aggregates reducing the coupling efficiency to scFv' molecules. Therfore, in the second approach the cysteine residues of scFv' molecules were activated instead of PEGPEI, improving the coupling efficiency to 50 % of inserted scFv'. Concluding these findings, we were able to control coupling degree and yield of scFv' by the synthesis route and provided two different conjugates for further *in vitro* characterization.
In flow cytometry of FITC labelled IPPs, all the tested samples (PEGPEI and PEGPEI-CD33 on CD33-positive SKNO1 cells and on CD33-negative Jurkat cells), even at very low concentrations showed binding activity. The high sensitivity of the method may be due to that finding, but contradicts to the absence of a signal from Cy3-siRNA encapsulated liposomes on target cells. In any case, the results argued against an antigen-specific binding activity of IPPs. Moreover, PEI is not degraded within the cell and shows cytotoxic effects in higher concentrations. This represents a general limitation for the carrier system. Delivery agents are rendered useless if they provoke unacceptable toxicity on either cellular or systemic level. Therefore, carefully formulated synthetic lipids and polymers have been developed alternatively. The use of biodegradable, high molecular mass polycations and

polymers containing linkages that can be cleaved inside the cells, can help reduce cytotoxicity (Whitehead et al., 2009).

4.5 Silencing of the target gene

Heidenreich et al. (2003) showed the specific suppression of the AML1/MTG8 fusion protein by electroporation with different siRNAs directed against the AML1/MTG8 fusion site. One of the siRNAs, siAGF1 was used within this study. To exclude off-target effects, different target specific and control siRNAs were tested by Heidenreich et al. (2003). Silencing was efficient and specific and did not affect wild-type AML1 expression. AML1/MTG8 depletion correlated with an increased susceptibility of Kasumi1 and SKNO1 cells to TGFβ_1/vitamin D_3 induced differentiation and reduction of clonogenicity. Moreover, an increased expression of CD11b, m-CSF receptor and C/EBPα were observed, all together indicating the onset of myelomonocytic differentiation via a TGFβ_1/vitamin D_3 activated pathway. Martinez et al. (2004) could confirm the inhibition of clonogenicity and proliferation and induction of differentiation after electroporation of Kasumi1 cells with two different siRNAs targeting AML1/MTG8. Furthermore, induction of a senescence-associated G1 cell cycle arrest and a diminished number of apoptotic cells were observed. Addition of haematopoietic growth factors could not rescue AML1/MTG8 knockdown cells from senescence and could only partially restore their clonogenicity. Martinez et al. (2004) claimed these results did not argue for general off target effects being responsible for the observed changes in cell proliferation and clonogenicity of siAGF1 treated Kasumi1 cells. Instead, the data suggested the siRNA-mediated depletion of the leukaemic fusion protein as the cause for the observed phenotypic changes. Dunne et al. (2006) found six genes with changed expression patterns after AML1/MTG8 depletion. Three of them were identified as direct AML1 interaction partners and three were indirect interaction partners. The genes were involved either in myeloid differentiation, antiproliferation or drug resistance.

The silencing activity of siAGF1 by electroporation was confirmed by AML1 immunoblot for SKNO1 cells in the current study. Only the fusion protein AML1/MTG8 was affected by the knockdown, not wild-type AML1. The first transfection experiments with carrier systems were performed with siRNA-PEI ILPs on SKNO1 cells to determine an appropriate lipid concentration. Possible silencing effects were investigated by qRT-PCR of total mRNA, isolated from the lysates of transfected cells. Surprisingly, lower lipid concentrations of 1 and 2 mM resulted in an increased AML1/MTG8 mRNA level compared to untreated cells. The same observation was made for control ILPs containing siAGF6 at the highest lipid concentration of 5 mM. However, distinct, sequence-specific silencing with 5 mM siAGF1

ILPs was reached. Unfortunately, qRT-PCR results were hardly reproducible for siRNA ILs and siRNA-PEI ILPs, resulting in insufficient silencing effects in Kasumi1 and SKNO1 cells throughout the whole study, whereas SKNO1 cells showed the clearer effects. This could maybe be due to a recovery of mRNA levels of Kasumi1 cells after three days. A few qRT-PCR and immunoblot experiments were performed one and two days after transfection, but showed no convincing results. Obviously, siRNA-PEI ILPs were more effective than siRNA ILs on mRNA level. In contrast, very distinct and specific silencing effects of siRNA ILs and siRNA-PEI ILPs could then be shown in immunoblot, with the same incubation times and lipid concentrations applied. The silencing effect in Kasumi1 cells was stronger compared to SKNO1, which represented a contradiction to binding and uptake studies, where stronger effects on SKNO1 cells compared to Kasumi cells were observed. Probably, a higher expression of the fusion protein in Kasumi1 cells compared to SKNO1 cells was responsible for that phenomenon. Superior effects of siRNA-PEI ILPs could not be confirmed in immunoblot, neither for Kasumi1 nor SKNO1 cells. Arguments for an enhanced endosomal escape due to PEI were therefore disproved. Moreover, the improved encapsulation efficiency of siRNA-PEI complexes into the liposomes resulted in a four-fold siRNA concentration in the siRNA-PEI ILPs compared to siRNA IPLs, assuming a correct determination of encapsulation efficiency. Still, siRNA-ILs showed comparable silencing effects to siRNA-PEI ILPs, while applied in equal lipid concentration. These results were not in accordance with our expectations. A possible explanation could be found in a retarded release of siRNA from the PEI complex into the cytosol. Compared to electroporation of siAGF1, very high siRNA concentrations were necessary in IL and ILP transfection, to reach similar results in immunoblot. Colony formation assays of Kasumi1 cells showed the expected effects, namely inhibition of the clonogenicity of the cell due to AML1/MTG8 depletion and therefore reduced colony formation. Here, a slight advantage for siRNA-PEI ILPs compared to siRNA ILs was observed again. Significantly reduced colony numbers of anti-CD33 siAGF1 ILs were determined with and without PEI complexation in comparison to siAGF6 controls, but only marginal differences to untreated cells could be shown. This was again representing a possible stimulating effect of the ILs and ILPs to the target cells. SKNO1 cells showed almost no silencing effects in colony formation assay. As SKNO1 cells were grown in a culture medium containing high concentrations of FCS and, additionally, the haematopoietic growth factor GM-CSF, which has been described to support clonogenicity and proliferation (Asou et al., 1991), this probably results in a neutralization of the silencing effects. In addition to colony numbers, total colony areas were determined, which did not show higher effects, but confirmed the results of the determination of colony number. However, they do not represent adequate, independent data because only sections of photographs from one out of four wells from each sample were analysed.

The fact that ILs, loaded with naked siRNA were able to induce knockdown of the target gene raised several questions. Fluorescence microscopy studies of siRNA-loaded ILs also revealed the presence of free siRNA in the cytosol, postulating endosomal release. No explanation for a spontaneous endosomal release of naked siRNA encapsulated in neutral liposomes could be found in literature. This would argue for an alternative cellular uptake, maybe of a portion of unecapsulated siRNA in the aqueous phase or passively associated with the outside of liposomal membranes. Therefor, the separation of free and lipid-encapsulated siRNA had to be incomplete. However, flow cytometry experiments, performed with free siRNA, showed no binding or uptake of free siRNA into SKNO1 and Kasumi1 cells.

The outstanding stimulation effects, observed upon target cells after the transfection with ILs and ILPs gave reason for further investigation of the carriers. Besides empty ILs, free scFv' molecules were tested for a possible influence on the target cells. They were inserted in colony formation assay in the same concentrations used for siRNA-loaded ILs and ILPs. Incubation with scFv' molecules had no effect on colony formation compared to untreated cells. In contrast, empty ILs, prepared with HSPC, showed enhanced colony formation in both cell lines, indicating a growth stimulating effect on target cells, probably resulting from liposomal properties, e. g. the lipid composition. Alternatively, ILs, in contrast to scFv' molecules, are able to crosslink cells, enhancing the probability of cell-cell interactions in a highly diluted cell suspension. Maybe, intercellular signals can then be responsible for enhanced clonogenicity. A cell viability assay, which was performed in parallel, showed a different result. Here, different scFv' concentrations were tested for possible effects on cell viability. Besides scFv' CD33, also an anti-FAP scFv' 36 for negative control was tested as well as empty anti-CD33 ILs. In this case, concentrations of scFv' in IL samples were lower compared to the free scFv' samples, because a complete coupling and insertion was assumed. However, due to the logarithmic illustration of scFv' concentrations, the difference in cell viability would be marginal. The control scFv' fragments showed no effect on cell viability, scFv' CD33 molecules and anti-CD33 ILs developed cytotoxic effects in high concentrations. However, such high concentrations were not used in colony formation assays. The relevant concentration for colony formation assays showed no signs of cytotoxicity in Kasumi1 cells and only slight cytotoxic effects on SKNO1 cells. These results disagree with the observations from the colony formation assay as they show no stimulating effects of ILs at any of the tested concentrations. The reason may be due to the short incubation time of two or three days for Kasumi1 cells and SKNO1 cells, respectively in XTT assay compared to seven and ten days for Kasumi1 and SKNO1 cells in colony formation assay. Therefore, further investigations on cell viability are necessary, which meet the conditions of the colony formation assay concerning incubation time and cellular

environment. In became obvious that lipid concentration and lipid composition were the crucial parameters responsible for stimulating effects in colony formation assay on the one hand and for a decrease of cell viability in XTT assay on the other hand. Although scFv' concentrations in IL samples were lower compared to the concentrations of free scFv' molecules in XTT assay, ILs showed equal or even lower effects in cell viability. A certain inhibitory effect on cell viability after scFv' binding could be expected because CD33 has been described as a receptor involved in the regulation of cellular activation.

SiRNA-protamine ILPs, in all assays, showed almost no silencing effects. Several parameters could be responsible for this observation. Possibly, the optimal incubation time of three days after transfection, determined for siRNA- and siRNA-PEI complexes, is not appropriate for siRNA-protamine ILPs. Lipid concentration has been increased compared to siRNA ILs and siRNA-PEI ILPs, still providing no knockdown results. However, there is only a small window in lipid concentration between ineffective and cytotoxic concentrations, of approximately 1 to 10 mM for qRT-PCR and western blot and 50 to 500 µM for colony formation assay. In literature, higher ratios of protamine: siRNA have been described and silencing effects after liposomal delivery were observed (Peer et al., 2008). Protamine has mostly been used for the delivery of plasmid DNA (Wagner et al., 1990; Li et al., 2001), which requires stable complexes within the cytosol. Stable complexes represent a disadvantage in the delivery of siRNA. Nevertheless, it would be profitable to test further molar ratios, especially the siRNA: protamine ratio of 1: 5, used by Peer et al. (2008). A higher percentage of protamine could benefit endosomal release. Maybe the applied molar ratio of 1: 3 was not sufficient to manage endosomal escape.
Obviously, lipid formulation seems to be an important parameter which can influence clogenicity of the target cells. Beyond that, it may also be important for the release of siRNA from the liposome or lipoplex and should be further investigated and optimized.

As expected, IPPs turned out to be very potent carrier systems. Because unconjugated PEGPEI was known to cause transfection, another negative control, anti-EGFR IPP, was introduced, after the confirmation by flow cytometry that both CD33 positive cells lines, Kasumi1 and SKNO1, do not express EGFR on their surface. In qRT-PCR, Kasumi1 cells showed a very weak, but specific response to IPPs. In contrast, SKNO1 cells, which showed a stronger response on mRNA level, represented the strong transfection and silencing activity of unconjugated PEGPEIs. Immunoblots confirmed this effect in both cell lines. Unconjugated PEGPEIs showed equal silencing effects to anti-CD33 IPPs. Only siAGF6 anti-CD33 IPPs did not silence the target gene, which further proved the sequence specificity of siAGF1. Surprisingly, even anti-EGFR IPPs showed AML1/MTG8 knockdown. These

results indicated an antigen-independent cellular uptake of IPPs. Receptor-mediated internalization was already questioned after the consideration of IPP particle sizes. The possibility of non-relevant cellular uptake of particles due to close proximity in the reaction tube could again be an explanation at this point. In colony formation assay, antigen-specific silencing effects of anti-CD33 siAGF1 IPPs were observed in Kasum1 cells concerning colony number and total colony area. SKNO1 cells again showed very weak response. In colony formation assays, only 5 % of the IPP concentration, compared to qRT-PCR and immunoblot, were used. This observation would argue for a concentration-dependent antigen-specificity of IPPs. However, in IPP transfection, the window between inefficient and unspecific transfection was even more narrow compared to ILs and ILPs. Strong cytotoxic effects allowed for little choice of IPP concentration.

A summary of the findings of transfection and knockdown experiments revealed several limitations of the investigated carrier systems and distinct differences concerning specificity and efficiency between them. The most convincing carrier systems tested in this study, were siRNA ILs and siRNA-PEI ILPs. SiRNA-protamine ILPs lack efficiency, IPPs fail in antigen specificity. Although ILs and ILPs showed stimulating effects on the clonogenicity of the leukaemic cells, their principle applicability is proven by comparison with siAGF6 control ILs and ILPs. The choice of an appropriate composition and concentration of the carrier systems seems to be an important parameter, which must be further improved for *in vitro* applications and adapted for *in vivo* applications. *In vivo*, the carrier systems might possess higher target cell specificity. Nevertheless, many successful applications of antisense nucleotide carrier systems have been described recently. IPPs targeted with Fab' fragments (Merdan et al., 2003) or mAbs (Germershaus et al., 2006) showed efficient silencing effects *in vitro*. SiRNA-protamine ILPs targeted with mAbs were shown to mediate specific gene silencing *in vitro* and *in vivo* (Peer et al., 2008). PEG stabilized ILs were described for the delivery of plasmid DNA via mAbs targeting the transferring receptor (Rivest et al., 2007) and for the transvascular delivery of shRNA (Boado, 2007).

4.6 Advanced and alternative delivery systems

Considerable effort has already been done in improving existing delivery systems and developing new delivery systems. In the case of ILs, lipid composition plays an important role. Altering acyl chain length or degree of saturation of the phophatidylcholine component leads to differences in therapeutic activity (Allen et al., 2005). Modifications of liposomes with thermosensitive lipids (Puri et al., 2008) and pH-dependent, fusogenic lipids (Simard and Leroux, 2009) have shown improved drug delivery. Cationic liposomes enhance the

encapsulation of nucleic acids on the one hand and improve transfection efficiency on the other hand. They have been applied for the delivery of siRNA in arthritis (Khoury et al., 2006) and HBV (Morrissey et al., 2005) models. However, this type of carrier has unfavourable pharmacokinetics for most *in vivo* applications (Stuart and Allen, 2000). In this context, approaches using cationic transfection reagents like i-FECT for intracranial plasmid DNA delivery (Felgner et al., 1987) and vitamin A-coupled Lipotrust liposomes for the delivery of anti gp 46 siRNA in a liver cirrhosis model (Sato et al., 2008) were presented and furthermore, oligofectamine liposomes for vaginal local application in HSV-2 treatment (Palliser et al., 2006). Akinc et al. (2008) introduced lipid-like materials, lipidoids, for the use in siRNA delivery. Lipidoids were synthesized through the conjugate addition of alkyl-acrylates and -amides to primary and secondary amines and then studied in cell culture. One leading candidate for *in vivo* gene knockdown was identified as $98N_{12}$-5(1), which comprises five 12-carbon alkyl-acrylamide chains attached to an amine core. Formulations of this material with siRNA were capable of achieving potent and persistent silencing of various lung and liver targets in mice, rats and cynomolgus monkeys. Importantly, lipidoid materials were shown to facilitate siRNA delivery without disrupting endogenous micro-RNA processing. Besides the improvement of the carrier systems themselves, production processes also need to be optimized, especially with regard to *in vivo* application. Hirsch et al. (2008) developed a preparation method for high amounts of sterile siRNA-liposomes with high entrapping efficiency. Targeting efficiency of delivery systems is often limited by antigen density on the target cell and can possibly be improved by targeting two different antigens expressed on the same cell, as it has been shown for CD19/CD20 ILs on B cells (Sapra and Allen, 2004). For an improved tumour cell selectivity, a pretreatment with free Ab fragments has been suggested to absorb shedded antigens and receptors (Sapra and Allen, 2003). As an alternative to antibodies and antibody fragments, novel binding proteins have been presented. They can be produced by phage display from randomized peptide libraries displayed on the phage surface (Ladner et al., 2004), even though the method is also possible for Fab' and scFv fragments (Hust and Dübel, 2005). Aptamers, nucleic acid targeting moieties, represent another interesting alternative.

As alternatives to PEI, dynamic polyconjugates were used for targeted *in vivo* delivery of siRNA to hepatocytes. They consist of a membrane active cationic polymer, which is masked until located in the endosome (Rozema et al., 2007). Chitosan is a natural, biodegradable polymer, able to complex siRNA. An effective *in vivo* intranasal delivery to lung epithelial cells and a systemic delivery to tumour xenografts could be shown (Howard et al., 2006; Pille et al., 2006). Other alternative polymers for complexation are, e. g., cyclodextrins, which showed silencing effects *in vivo* in metastatic Ewing sarcoma (Hu-Lieskovan et al., 2005).

Other possibilities are synthetic polycations consisting of histidine or polylysine residues (Read et al., 2005) or protamine conjugation. Besides approaches with either histidine or lysine, also histidine-lysine copolymers are used: Chen at al. (2002) and Aoki et al. (2001) presented linear and branched histidine-lysine polymers and showed that they could buffer and disrupt the endosome. Hatefi et al. (2006) applied recombinant techniques to generate a prototype vector comprised of tandem repeating units of lysine and histidine fused to a targeting moiety to mediate gene transfer in mammalian cell lines.

For an improved delivery of naked siRNA, avoiding the hydrodynamic delivery of naked siRNA (Lewis and Wolff, 2005), direct conjugation of the siRNA molecules with small molecules or peptides to the sense strand without affecting the activity of the antisense-stands is possible. SiRNA conjugation to cholesterol mediates binding serum albumin and thus results in an increased serum half-life. It also leads to biodistribution into the liver and was therefore applied for the silencing of ApoB and the Huntington gene (Soutschek et al., 2004; DiFiglia et al., 2007). Another possibility is siRNA conjugation to fatty acids and bile salt derivatives, leading to an interaction with HDL and targeting of the liver by HDL receptor (Wolfrum et al., 2007). Atelocollagen is a pepsin-treated type I collagen from calf dermis. Complexes with siRNA were applied systemically for the targeting of tumour xenografts and bone metastasis (Takei et al., 2004; Takeshita et al., 2005). One clinical trial with naked VEGFR-siRNA in AMD treatment has recently been questioned. It has been reported that anti-VEGF siRNA efficacy in the eye is not due to specific gene silencing , but is instead caused by nonspecific stimulation of the TLR3 pathway, which can reduce angiogenesis (Kleinman et al., 2008). However, the study does not explain the therapeutic effects observed in other applications of siRNA in which appropriate controls have been performed. Although the delivery of shRNA in viral vectors can induce systemic cytotoxicity by the activation of an immune response and can possibly influence endogenous RNAi, some successful approaches have been described in literature (Zhang et al., 2004; Boado et al., 2005; Shan et al., 2008).

Many suggestions from literature might help to improve our current carrier systems concerning antigen-specificity, silencing efficiency and biocompatibility.

4.7 Challenges in siRNA therapy

4.7.1 Off target effects

Heidenreich et al. (2003) applied several different siRNAs for the silencing of AML1/MTG8 and several controls to exclude off target effects. Chemical modifications, like 2'-O-methylation (Jackson et al., 2006b), introduction of phosphorothioate backbone linkages and incorporation of 2' sugar modifications (Bumcrot et al., 2006) can mediate nuclease resistance and avoid off target effects. Concerning a possible influence on knockdown effects, modifications are well tolerated in 5' but not in 3' ends (Amarzguioui et al., 2003). Czauderna et al. (2003) could confirm that 2'-O-methylation had no effect on siRNA activity. It was found out that siRNA sense strand modification has less effect than antisense modification (Prakash et al., 2005). Furthermore, the application of two or more different siRNAs for an enhanced target specificity has been suggested. Although combinatorial delivery of siRNAs reduces off target effects, it also reduces silencing efficacy by selective incorporation into RISC. Different siRNAs, and endogenous miRNAs, compete for the RNAi components of the cell. Thereby, TRBP contributes to preferential loading of different sequences into RISC (Castanotto et al., 2007).

4.7.2 Immunogenicity

Immune response to nucleic acids, after bacterial or viral infection or artificial transfection, is mediated by a class of innate pattern recognition receptors, the toll-like receptors (TLRs). In literature, the role of TLRs in immune response to siRNA, is discussed controversially. The strong response to bacterial DNA results from the recognition of unmethylated CpG dinucleotides in a particular base context – mammalian DNA has a lower frequency of CpG sequences and they are usually methylated (Hemmi et al., 2000). Of the ten known TLRs that have now been identified, TLR3 and TLR9 are responsible for the nucleic acid response and TLR7 appears to mediate the immune response to siRNA (Hornung et al., 2005). An immune response in gene silencing can lead to toxicity issues and off-target effects associated with inflammation. However, an immune response by siRNA or its carrier complex can be desirable for applications like vaccination or ADCC enhancing approaches with ODNs (Judge et al., 2005; Sioud et al., 2005) or in the treatment of cancer and viral infections. TLR7 and TLR3 are located in the endosomal membrane, the cell compartment by which siRNA delivery systems enter the cell. Due to the small size of the siRNA molecule, it cannot be recognized by TLR7 (Elbashir, 2001). In contrast, other publications claim for an immune response due to the cytosolic dsRNA-dependent protein kinase R (PKR) a key mediator of antiviral effects of interferon (IFN) and an active player in apoptosis: Lee et al. (2007) reported that TLR3 signalling does not play a role because of endosomal release, but siRNA

is then recognized by PKR. SsRNA molecules have been shown to evoke a stronger immune response than dsRNA molecules (Sioud, 2005). The same study showed that siRNA electroporation did not induce immune response, but lipid delivery did. This finding would transfer the problem of immunogenicity from siRNA to the delivery system. Judge et al. (2005) simplified siRNA dependent immune responses to a matter of concentration, Grzelinski et al. (2006) summarized that siRNA formulation seems to be of critical importance as well as its subcellular localization.
Some studies deal with an improvement of siRNA silencing efficiency: siHybrids, e. g., are RNA/DNA ds molecules containing a DNA sense strand and an RNA antisense strand, responsible for target mRNA hybridization. The DNA sense strand makes the molecule more potent and thus leads to longer lasting silencing effects (Hogrefe et al., 2006; Lamberton and Christian, 2003). Another approach deals with small molecules, which can enhance RNAi by intracellular modulation of the RNAi pathway via TRBP, associated with Ago2. Coadministration of shRNA and Penetrex (enoxacin), which belongs to the class of quinolones, showed promising results. Enhanced shRNA mediated gene silencing was not caused by enhanced expression of RNAi proteins, but improved interaction of shRNA and Ago2 via TRBP (Shan et al., 2008).

4.8 Targets in the delivery of siRNA

4.8.1 The myeloid receptor CD33

Recent data suggest AML has its origin in leukaemic stem cells, a small cell population with the ability of self renewal, the leukaemic bulk has lost the ability (Hope et al., 2003). It has been assumed that the leukaemic stem cells are responsible for relapse in AML patients (Ailles et al., 1999). Therefore, AML stem cells represent an attractive target for antibody-mediated drug delivery. Leukaemic stem cells were supposed to reside in the $CD34^+$, $CD38^-$ and $CD33^-$ population and were potentially distinguished from normal haematopoietic stem cells by the expression of CD123, IL3-R alpha (Jordan et al., 2000). This would reduce the efficiency of targeting CD33. However, latest data suggest the expression of CD33 in leukaemic stem cells (Taussig et al., 2005). Furthermore, it has been reported that CD33 expression on a patient's AML blasts correlates with the expression of CD33 on the patient's leukaemic stem cells (Hauswirth et al., 2007). It provides evidence for the existence of CD33-positive leukaemic stem cells, which are arrested in their proliferation state. The finding of CD33 on AML stem cells enhances its importance as a target antigen as it also affects the basic stem cell population regenerating AML blasts. Latest findings gave evidence for CD33 expression on haematopoietic stem cells (Taussig et al., 2005), which could explain adverse

effects in GO therapy, namely the delayed recovery of the haematopoietic system. This feature would question the importance of CD33 as a target antigen. However, GO is still successfully applied in the clinical treatment of AML. Moreover, it would only limit the targeted delivery of chemotherapeutic drugs, but not of specific, antisense nucleotides, if they were delivered in an untoxic system. The exclusive expression of CD123 on leukaemic stem cells could represent another, suitable target antigen for AML therapy, if it was sufficiently internalized, possibly in a cotargeting approach with CD33. Leukaemic stem cells can further be distinguished from normal haematopoietic stem cells by their permanent activation of NFkB (Jordan et al., 2000). Inhibitors of NFkB could possibly support treatment. Orr et al. (2007) showed that phosphorylated CD33 is proteasomally degraded by the 26S proteasom. Consequently, the antigen expression of CD33 on target cells could be decreased after internalization of antigen-antibody complexes and this would represent another limitation which had to be overcome.
In the context of the current approach, studies with primary, CD33-positive leukaemic blasts are intended to be performed, concerning binding and uptake of anti-CD33 ILs and ILPs and IPPs in a first step and silencing of the leukaemic fusion protein AML1/MTG8 by the targeted delivery of siRNA in second step.

4.8.2 The fusion gene AML1/MTG8

Many attempts of establishing an animal model for t(8;21) failed. Knocking in the AML1/MTG8 fusion gene into the *Aml1* locus has resulted in embryonic lethality, demonstrating that AML1/MTG8 is a dominant inhibitor of normal AML1/CBFß function during early haematopoietic lineage commitment (Yergeau et al., 1997; Okuda et al., 1998). These effects were strikingly similar to those seen in AML1-/- mice (Okuda et al., 1996). In contrast, transgenic mice with a tetracycline inducible AML1/MTG8 system did not develop leukaemia despite strong fusion gene expression (Rhoades et al., 2000). Another transgenic system, with a MRP8 inducible AML1/MTG8 expression using a myeloid specific promoter, did not develop leukaemia either (Yuan et al., 2001). These observations clearly proved that t(8;21) is not the only responsible event for the development of AML. Martinez et al. (2009) established a xenotransplantation model for t(8;21)-associated AML representing extramedullar tumours, as they may develop in AML. They showed that even transient, siRNA mediated depletion of AML1/MTG8 causes a significant increase in median survival. In a previous study, they could show that silencing AML1/MTG8 transiently with siRNA leads to cellular senescence (Martinez et al., 2004). Besides other molecules, p53, a regulator of cell cycle progression, is involved in the establishment of senescence (Pelicci, 2004). Cellular senescence limits the proliferative capacity of cells and is characterized by an irreversible G1 arrest (Ben-Porath et al., 2004). It has been shown that AML1/MTG8 also

interferes with p53-dependent cell cycle arrest and apoptosis by suppressing the p53-stabilizing protein $p14^{ARF}$ (Linggi et al., 2002). Other affected genes of AML1/MTG8 siRNA knockdown were discovered by gene array (Dunne et al., 2006). These were genes of myeloid differentiation, antiproliferation, drug resistance and genes related to poor prognosis. An expression pattern suggesting the onset of myeloid differentiation and inhibition of leukaemic proliferation was detected. AML1/MTG8 suppression may also enhance drug sensitivity. Expression of AML1/MTG8 in human CD34 cells produces differential effects, depending on the state of progenitor cell maturation. Expression of AML1/MTG8 in more mature progenitor cells resulted in growth arrest and abrogated colony formation in primary clonogenic assays. In contrast, AML1/MTG8 expression in stem cells resulted in the preferential expansion and/or self-renewal of stem cells. Furthermore, it could be shown that AML1/MTG8 does not result in a total block of differentiation, mature cells are detectable in flow cytometry and histochemistry. Only a second mutation, in which a strong proliferative signal is acquired, can transform a t(8;21) positive cell to AML (Mulloy et al., 2002). Burel et al., (2001) described a dichotomy of AML1/MTG8 function: AML1/MTG8 alone leads to a growth arrest via decreased expression of cyclin dependent kinase 4 (CDK4), c-myc and Bcl-2. This leads to enhanced apoptosis, whereby c-myc downregulation causes CDK4 downregulation, and a reduction of granulopoietic differentiation via decreased C/EBPα expression. Bcl2 is connected to apoptosis and works downstream of cell cycle, but AML1/MTG8 does not directly interact with Bcl2. Apoptosis may be a result of the inability to overcome senescence. This status must be overcome by additional mutations to cause leukaemia. Besides AML1/MTG8, NFkB and the tyrosine kinase FLT3 represent responsible oncogenic molecules in leukaemic stem cells to cause leukaemia. Moreover, c-KIT mutations frequently occur together with t(8;21) in AML (Wang et al., 2008).

4.9 Humanization of scFv' molecules

For therapeutic applications in humans, scFv antibody fragments need to have high thermodynamic stability and should be humanized to avoid a neutralizing antibody response (Mirick et al., 2004). Humanization of anti-CD33 mAbs has previously been described, e. g. the humanization of the murine IgG2a M195 (Caron et al., 1992), known as Lintuzumab, and the humanized IgG_4 hP67.7 (Giles et al., 2003) known as Gemtuzumab. In the present study, humanization of scFv' CD33 V_HV_L HC4 was performed with the help of a knowledge-based approach by CDR-grafting. The humanized construct fulfilled the demand concerning production yield, it reached a two-fold increase compared to the murine scFv' CD33 V_HV_L HC4 construct. Binding activity on target cells was equal to the binding activity of the murine construct. ILs, prepared by postinsertion of the humanized construct (scFv' IZI08.3), showed

specific binding activity to SKNO1 and Kasumi1 cells, which was comparable to ILs prepared with the murine construct. Furthermore, by reengineering of the scFv' during humanization, an improved construct concerning thermal stability has been generated. The melting temperature of scFv' IZI08.3 of 65 °C showed an inc rease of approximately 5 °C compared to the murine scFv'. A detailed investigation of binding activity of murine scFv CD33 V_HV_L and humanized scFv IZI08.3 on Kasumi1 cells by flow cytometry, resulted in very similar EC_{50} values of 1.22 nM for scFv CD33 V_HV_L and 2.98 nM for scFv IZI08.3. Schwemmlein (2007b), who also investigated the binding activity of scFv' CD33 K132 in the V_LV_H format, found a K_D value of 11 nM. Comparison indicates an enhanced binding activity of the V_HV_L format, although different CD33-positive cell lines were used, which may exhibit different CD33-expression. Taken together, the successful humanization of scFv' CD33 V_HV_L HC4 resulted in an equal, in some demands even superior, molecule. Caron et al. (1992) reported a similar binding activity of their chimeric anti-CD33 mAbs and an increased binding activity of their humanized anti-CD33 monoclonal antibodies in comparison to mouse antibodies. This goal could not be reached in the present study.

The humanized scFv' CD19 (scFv' IZI08.4) failed in demands of improved production yield, thermal stability and binding activity in comparison to the murine construct. The sequences of the humanized scFv molecules have been codon optimized relative to expression in CHO cells. This may be a reason for the decreased production yield of scFv' IZI08.4 in bacteria. In another study, scFv CD19 4G7 has been stabilized and humanized by designed point mutations and CDR-grafting in a knowledge-based approach (Kügler et al., 2009). Two different constructs, one mutant scFv CD19 4G7 and one humanized scFv CD19-4G7, were generated and showed greater thermodynamic stability and stability in human serum compared to the wild-type scFv. Binding affinities of the two constructs on CD19-positive leukaemic cell lines were decreased slightly compared to the wild-type scFv. Additionally, with regard to *in vivo* application, scFv' molecules must obtain another expression and purification procedure as His-Tag purification of bacterially produced antibody fragments may copurify bacterial proteins.

4.10 Summary and outlook

The ultimate goal for RNAi therapeutics in oncology is the selective elimination of tumour cells without damaging normal cells. SiRNAs may target genes that are exclusively expressed in cancer cells, and that are crucially involved in their growth and survival. The aim of the present study was to generate and compare different targeted carrier systems for the delivery of a therapeutic siRNA in AML treatment. As a target antigen, the myeloid receptor CD33 was chosen, which is expressed on immature myeloid cells, leukaemic blasts

and leukaemic stem cells. It was targeted by an anti-CD33 scFv' antibody fragment, covalently linked to the carrier system. As carrier systems ILs, ILPs and IPPs were tested. IPPs consist of PEGylated PEI, complexed to siRNA. For the generation of ILs, free siRNA was encapsulated, for ILPs PEI- or protamine-complexed siRNA was encapsulated passively into ILs.
Target cell specific binding and uptake of ILs and ILPs could be shown. SiRNA transfection of target cells with all carrier systems resulted in sequence specific silencing of the target leukaemic fusion gene AML1/MTG8 without affecting wild-type AML1. AML1/MTG8 depletion was detected on mRNA level and on protein level, postulating a successful escape of siRNA from the endosomal compartment. An inhibitory effect of AML1/MTG8 knockdown on the clonogenicity of the target cells could be demonstrated in colony formation assay.
The observed knockdown effects should be optimized concerning antigen-specificity of IPPs and silencing efficiency of ILs and ILPs, especially by avoiding stimulation of target cell clonogenicity.
The successful humanization of scFv' CD33 V_HV_L HC4 resulted in an equal, in some demands even superior molecule and represented a first step towards the development of a therapeutic application.

The proof of concept for targeted siRNA delivery with the help of ILs, ILPs and IPPs could be shown. Accumulation of the carrier systems in the leukaemic tissue due to targeting of CD33 and sequence specific silencing of the leukaemic fusion gene by RNAi were combined in this study. However, results show that further improvements of the carrier systems are necessary. Targeted delivery has yet to be optimized for most cell types and tissues. Solutions will probably need to be adapted for each target cell type and disease indication.

5 Reference list

Adams GP, Weiner LM. (2005) Monoclonal antibody therapy of cancer. Nat Biotechnol. 23:1147-57

Adams GP, Tai MS, McCartney JE, Marks JD, Stafford WF 3rd, Houston LL, Huston JS, Weiner LM. (2006) Avidity-mediated enhancement of in vivo tumor targeting by single-chain Fv dimers. Clin Cancer Res. 12(5)

Ailles LE, Gerhard B, Kawagoe H, Hogge DE. (1999) Growth characteristics of acute myelogenous leukemia progenitors that initiate malignant hematopoiesis in nonobese diabetic/severe combined immunodeficient mice. Blood. 1999 Sep 1;94(5):1761-72

Akhtar S, Benter IF. (2007) Nonviral delivery of synthetic siRNAs in vivo. J Clin Invest.117:3623-32

Akinc A, Thomas M, Klibanov AM, Langer R. (2005) Exploring polyethylenimine-mediated DNA transfection and the proton sponge hypothesis J Gene Med. 7:657-63

Akinc A, Zumbuehl A, Goldberg M, Leshchiner ES, Busini V, Hossain N, Bacallado SA, Nguyen DN, Fuller J, Alvarez R, Borodovsky A, Borland T, Constien R, de Fougerolles A, Dorkin JR, Narayanannair Jayaprakash K, Jayaraman M, John M, Koteliansky V, Manoharan M, Nechev L, Qin J, Racie T, Raitcheva D, Rajeev KG, Sah DW, Soutschek J, Toudjarska I, Vornlocher HP, Zimmermann TS, Langer R, Anderson DG. (2008) A combinatorial library of lipid-like materials for delivery of RNAi therapeutics. Nat Biotechnol. 26:561-9

Allen TM, Sapra P, Moase E, Moreira J, Iden D. (2002) Adventures in targeting. J Liposome Res. 12:5-12

Allen TM, Mumbengegwi DR, Charrois GJ. (2005) Anti-CD19-targeted liposomal doxorubicin improves the therapeutic efficacy in murine B-cell lymphoma and ameliorates the toxicity of liposomes with varying drug release rates. Clin Cancer Res. 11:3567-73

Alliot F, Rutin J, Leenen PJ, Pessac B. (1999) Pericytes and periendothelial cells of brain parenchyma vessels co-express aminopeptidase N, aminopeptidase A, and nestin. J Neurosci Res. 58:367-78

Amarzguioui M, Holen T, Babaie E, Prydz H. (2003) Tolerance for mutations and chemical modifications in a siRNA. Nucleic Acids Res. 31:589-95

Andrews RG, Singer JW, Bernstein ID. (1989) Precursors of colony-forming cells in humans can be distinguished from colony-forming cells by expression of the CD33 and CD34 antigens and light scatter properties. J Exp Med.169:1721-31

Angata T, Varki A. (2000) Cloning, characterization, and phylogenetic analysis of siglec-9, a new member of the CD33-related group of siglecs. Evidence for co-evolution with sialic acid synthesis pathways. J Biol Chem. 275:22127-35

Aoki Y, Hosaka S, Kawa S, Kiyosawa K (2001) Potential tumor-targeting peptide vector of histidylated oligolysine conjugated to a tumor-homing RGD motif. Cancer Gene Ther. 8:783-7

Appelbaum RF, Rowe JM, Radich J, Dick JE. (2001) Acute myeloid leukemia. Hematology Am Soc Hematol Educ Program. 62-86

Asou H, Tashiro S, Hamamoto K, Otsuji A, Kita K, Kamada N. (1991) Establishment of a human acute myeloid leukemia cell line (Kasumi-1) with 8;21 chromosome translocation. Blood. 77:2031-6

Auguste DT, Furman K, Wong A, Fuller J, Armes SP, Deming TJ, Langer R. (2008) Triggered release of siRNA from poly(ethylene glycol)-protected, pH-dependent liposomes. J Control Release, 130:266-74

Bachmair A, Finley D, Varshavsky A. (1986) In vivo half-life of a protein is a function of its amino-terminal residue. Science,234:179-86

Balaian L, Ball ED. (2005) Anti-CD33 monoclonal antibodies enhance the cytotoxic effects of cytosine arabinoside and idarubicin on acute myeloid leukemia cells through similarities in their signaling pathways. Exp Hematol. 33:199-211

Bangham AD, Standish MM, Miller N. (1965) Cation permeability of phospholipid model membranes: effect of narcotics. Nature, 208:1295-7

Bargou R, Leo E, Zugmaier G, Klinger M, Goebeler M, Knop S, Noppeney R, Viardot A, Hess G, Schuler M, Einsele H, Brandl C, Wolf A, Kirchinger P, Klappers P, Schmidt M, Riethmüller G, Reinhardt C, Baeuerle PA, Kufer P. (2008) Tumor regression in cancer patients by very low doses of a T cell-engaging antibody. Science.321:974-7

Bartlett DW, Su H, Hildebrandt IJ, Weber WA, Davis ME (2007) Impact of tumor-specific targeting on the biodistribution and efficacy of siRNA nanoparticles measured by multimodality in vivo imaging. Proc Natl Acad Sci U S A., 104:15549-54

Beghini A, Ripamonti CB, Castorina P, Pezzetti L, Doneda L, Cairoli R, Morra E, Larizza L. (2000) Trisomy 4 leading to duplication of a mutated KIT allele in acute myeloid leukemia with mast cell involvement. Cancer Genet Cytogenet. 119:26-31

Behr JP. (1996) Gene transfer with amino lipids and amino polymers C R Seances Soc Biol Fil.190:33-8

Bendas G, Rothe U, Scherphof GL, Kamps JA (2003) The influence of repeated injections on pharmacokinetics and biodistribution of different types of sterically stabilized immunoliposomes. Biochim Biophys Acta. 1609:63-70

Ben-Porath I, Weinberg RA. (2004) When cells get stressed: an integrative view of cellular senescence. J Clin Invest. 113(1):8-13

Bernstein E, Denli AM, Hannon GJ. (2001) The rest is silence. RNA, 7:1509-21

Bertrand JR, Pottier M, Vekris A, Opolon P, Maksimenko A, Malvy C. (2002) Comparison of antisense oligonucleotides and siRNAs in cell culture and in vivo. Biochem Biophys Res Commun. 296:1000-4

Blaszczyk J, Tropea JE, Bubunenko M, Routzahn KM, Waugh DS, Court DL, Ji X. (2001) Crystallographic and modeling studies of RNase III suggest a mechanism for double-stranded RNA cleavage. Structure, 9:1225-36

Boado RJ. (2005) RNA interference and nonviral targeted gene therapy of experimental brain cancer. NeuroRx. 2:139-50

Bonifacino JS, Traub LM (2003) Signals for sorting of transmembrane proteins to endosomes and lysosomes. Annu Rev Biochem. 72:395-447

Boussif O, Lezoualc'h F, Zanta MA, Mergny MD, Scherman D, Demeneix B, Behr JP. (1995) A versatile vector for gene and oligonucleotide transfer into cells in culture and in vivo: polyethylenimine. Proc Natl Acad Sci U S A. 92:7297-301

Brunk UT, Dalen H, Roberg K, Hellquist HB. (1997) Photo-oxidative disruption of lysosomal membranes causes apoptosis of cultured human fibroblasts. Free Radic Biol Med. 23:616-26

Bumcrot D, Manoharan M, Koteliansky V, Sah DW. (2006) RNAi therapeutics: a potential new class of pharmaceutical drugs. Nat Chem Biol. 2006 Dec;2(12):711-9

Burel SA, Harakawa N, Zhou L, Pabst T, Tenen DG, Zhang DE. (2001) Dichotomy of AML1-ETO functions: growth arrest versus block of differentiation. Mol Cell Biol. 21:5577-90

Buschle M, Cotten M, Kirlappos H, Mechtler K, Schaffner G, Zauner W, Birnstiel ML, Wagner E. (1995) Receptor-mediated gene transfer into human T lymphocytes via binding of DNA/CD3 antibody particles to the CD3 T cell receptor complex. Hum Gene Ther. 6:753-61

Caron PC, Co MS, Bull MK, Avdalovic NM, Queen C, Scheinberg DA. (1992) Biological and immunological features of humanized M195 (anti-CD33) monoclonal antibodies. Cancer Res. 52:6761-7

Caron PC, Schwartz MA, Co MS, Queen C, Finn RD, Graham MC, Divgi CR, Larson SM, Scheinberg DA. (1994) Murine and humanized constructs of monoclonal antibody M195 (anti-CD33) for the therapy of acute myelogenous leukemia. Cancer, 73:1049-56

Carter P, Presta L, Gorman CM, Ridgway JB, Henner D, Wong WL, Rowland AM, Kotts C, Carver ME, Shepard HM. (1992) Humanization of an anti-p185HER2 antibody for human cancer therapy. Proc Natl Acad Sci U S A. 89:4285-9

Castanotto D, Sakurai K, Lingeman R, Li H, Shively L, Aagaard L, Soifer H, Gatignol A, Riggs A, Rossi JJ. (2007) Combinatorial delivery of small interfering RNAs reduces RNAi efficacy by selective incorporation into RISC. Nucleic Acids Res. 35:5154-64

Chang YW, Chen SC, Cheng EC, Ko YP, Lin YC, Kao YR, Tsay YG, Yang PC, Wu CW, Roffler SR. (2005) CD13 (aminopeptidase N) can associate with tumor-associated antigen L6 and enhance the motility of human lung cancer cells. Int J Cancer. 116:243-52

Chen QR, Zhang L, Luther PW, Mixson AJ. (2002) Optimal transfection with the HK polymer depends on its degree of branching and the pH of endocytic vesicles. Nucleic Acids Res. 30:1338-45

Cogoni C, Macino G. (1999) Gene silencing in Neurospora crassa requires a protein homologous to RNA-dependent RNA polymerase. Nature, 399:166-9

Connor J, Sullivan S, Huang L. (1985) Monoclonal antibody and liposomes. Pharmacol Ther. 28:341-65

Couvreur P (1988) Polyalkylcyanoacrylates as colloidal drug carriers. Crit Rev Ther Drug Carrier Syst. 5:1-20

Crocker PR, Kelm S, Dubois C, Martin B, McWilliam AS, Shotton DM, Paulson JC, Gordon S. (1991) Purification and properties of sialoadhesin, a sialic acid-binding receptor of murine tissue macrophages. EMBO J. 10:1661-9

Crocker PR, Vinson M, Kelm S, Drickamer K. (1999) Molecular analysis of sialoside binding to sialoadhesin by NMR and site-directed mutagenesis. Biochem J.341:355-61

Crocker PR, Varki A. (2001) Siglecs in the immune system.Immunology.103:137-45

Crommelin DJ, Storm G. (2003) Liposomes: from the bench to the bed. J Liposome Res. 13:33-6

Curnis F, Arrigoni G, Sacchi A, Fischetti L, Arap W, Pasqualini R, Corti A (2002) Differential binding of drugs containing the NGR motif to CD13 isoforms in tumor vessels, epithelia, and myeloid cells. Cancer Res. 62:867-74

Czauderna F, Fechtner M, Dames S, Aygün H, Klippel A, Pronk GJ, Giese K, Kaufmann J. (2003) Structural variations and stabilising modifications of synthetic siRNAs in mammalian cells. Nucleic Acids Res. 31:2705-16

Dams ET, Laverman P, Oyen WJ, Storm G, Scherphof GL, van Der Meer JW, Corstens FH, Boerman OC. (2000) Accelerated blood clearance and altered biodistribution of repeated injections of sterically stabilized liposomes. J Pharmacol Exp Ther. 292:1071-9

Davis SS, Illum L. (1983) Drug delivery systems. Practitioner. 227:1537-43

van **Der Velden VH**, te Marvelde JG, Hoogeveen PG, Bernstein ID, Houtsmuller AB, Berger MS, van Dongen JJ. (2001) Targeting of the CD33-calicheamicin immunoconjugate Mylotarg (CMA-676) in acute myeloid leukemia: in vivo and in vitro saturation and internalization by leukemic and normal myeloid cells. Blood, 97:3197-204

DiFiglia M, Sena-Esteves M, Chase K, Sapp E, Pfister E, Sass M, Yoder J, Reeves P, Pandey RK, Rajeev KG, Manoharan M, Sah DW, Zamore PD, Aronin N. (2007) Therapeutic silencing of mutant huntingtin with siRNA attenuates striatal and cortical neuropathology and behavioral deficits. Proc Natl Acad Sci U S A. 2007 Oct 23;104(43):17204-9

Dinndorf PA, Andrews RG, Benjamin D, Ridgway D, Wolff L, Bernstein ID. (1986) Expression of normal myeloid-associated antigens by acute leukemia cells. Blood. 67:1048-53

Dixon J, Kaklamanis L, Turley H, Hickson ID, Leek RD, Harris AL, Gatter KC. (1994) Expression of aminopeptidase-n (CD 13) in normal tissues and malignant neoplasms of epithelial and lymphoid origin. J Clin Pathol. 47:43-7

Doudna JA, Cech TR. (2002) The chemical repertoire of natural ribozymes. Nature, 418:222-8

Downing JR. (1999) The AML1-ETO chimaeric transcription factor in acute myeloid leukaemia: biology and clinical significance. Br J Haematol. 106:296-308

Dunne J, Cullmann C, Ritter M, Soria NM, Drescher B, Debernardi S, Skoulakis S, Hartmann O, Krause M, Krauter J, Neubauer A, Young BD, Heidenreich O. (2006) siRNA-mediated AML1/MTG8 depletion affects differentiation and proliferation-associated gene expression in t(8;21)-positive cell lines and primary AML blasts. Oncogene. 25:6067-78

Dykxhoorn DM, Lieberman J. (2005) The silent revolution: RNA interference as basic biology, research tool, and therapeutic. Annu Rev Med.56:401-23

Elbashir SM, Martinez J, Patkaniowska A, Lendeckel W, Tuschl T. (2001) Functional anatomy of siRNAs for mediating efficient RNAi in Drosophila melanogaster embryo lysate. EMBO J. 20:6877

Erickson PF, Dessev G, Lasher RS, Philips G, Robinson M, Drabkin HA. (1996) ETO and AML1 phosphoproteins are expressed in CD34+ hematopoietic progenitors: implications for t(8;21) leukemogenesis and monitoring residual disease. Blood.88:1813-23

Fattal E, Bochot A. (2006) Ocular delivery of nucleic acids: antisense oligonucleotides, aptamers and siRNA. Adv Drug Deliv Rev. 58:1203-23

Fearon DT, Carroll MC. (2000) Regulation of B lymphocyte responses to foreign and self-antigens by the CD19/CD21 complex. Annu Rev Immunol. 18:393-422

Feldman EJ, Brandwein J, Stone R, Kalaycio M, Moore J, O'Connor J, Wedel N, Roboz GJ, Miller C, Chopra R, Jurcic JC, Brown R, Ehmann WC, Schulman P, Frankel SR, De Angelo D, Scheinberg D. (2005) Phase III randomized multicenter study of a humanized anti-CD33 monoclonal antibody, lintuzumab, in combination with chemotherapy, versus chemotherapy alone in patients with refractory or first-relapsed acute myeloid leukemia. J Clin Oncol. 23:4110-6

Felgner PL, Gadek TR, Holm M, Roman R, Chan HW, Wenz M, Northrop JP, Ringold GM, Danielsen M. (1987) Lipofection: a highly efficient, lipid-mediated DNA-transfection procedure. Proc Natl Acad Sci U S A. 84:7413-7

Fire A, Xu S, Montgomery MK, Kostas SA, Driver SE, Mello CC. (1998) Potent and specific genetic interference by double-stranded RNA in Caenorhabditis elegans. Nature 391:806-11

Forge A, Knowles PF, Marsh D. (1978) Morphology of egg phosphatidylcholine-cholesterole single-bilayer vesicles, studied by freeze-etch electron microscopy. J Membr Biol. 41:249-63

de **Fougerolles A**, Vornlocher HP, Maraganore J, Lieberman J. (2007) Interfering with disease: a progress report on siRNA-based therapeutics. Nat Rev Drug Discov. 6:443-53

Fujimoto M, Poe JC, Hasegawa M, Tedder TF. (2000) CD19 regulates intrinsic B lymphocyte signal transduction and activation through a novel mechanism of processive amplification. Immunol Res. 22:281-98

Gabizon A, Martin F. (1997) Polyethylene glycol-coated (pegylated) liposomal doxorubicin. Rationale for use in solid tumours. Drugs. 54:15-21

Gagné JF, Désormeaux A, Perron S, Tremblay MJ, Bergeron MG. (2002) Targeted delivery of indinavir to HIV-1 primary reservoirs with immunoliposomes. Biochim Biophys Acta. 1558:198-210

Gautier S, Grudzielski N, Goffinet G, de Hassonville SH, Delattre L, Jérĵme R. (2001) Preparation of poly(D,L-lactide) nanoparticles assisted by amphiphilic poly(methyl methacrylate-co-methacrylic acid) copolymers. J Biomater Sci Polym Ed. 12:429-50

Geisbert TW, Hensley LE, Kagan E, Yu EZ, Geisbert JB, Daddario-DiCaprio K, Fritz EA, Jahrling PB, McClintock K, Phelps JR, Lee AC, Judge A, Jeffs LB, MacLachlan I. (2006) Postexposure protection of guinea pigs against a lethal ebola virus challenge is conferred by RNA interference. J Infect Dis. 193:1650-7

Gelmetti V, Zhang J, Fanelli M, Minucci S, Pelicci PG, Lazar MA (1998) Aberrant recruitment of the nuclear receptor corepressor-histone deacetylase complex by the acute myeloid leukemia fusion partner ETO. Mol Cell Biol. 18:7185-91

Germershaus O, Merdan T, Bakowsky U, Behe M, Kissel T. (2006) Trastuzumab-polyethylenimine-polyethylene glycol conjugates for targeting Her2-expressing tumors. Bioconjug Chem.17:1190-9

Giles F, Estey E, O'Brien S. (2003) Gemtuzumab ozogamicin in the treatment of acute myeloid leukemia. Cancer. 98:2095-104

Goula D, Benoist C, Mantero S, Merlo G, Levi G, Demeneix BA. (1998) Polyethylenimine-based intravenous delivery of transgenes to mouse lung. Gene Ther. 5:1291-5

Grayson AC, Doody AM, Putnam D (2006) Biophysical and structural characterization of polyethylenimine-mediated siRNA delivery in vitro. Pharm Res. 23:1868-76

Grzelinski M, Urban-Klein B, Martens T, Lamszus K, Bakowsky U, Höbel S, Czubayko F, Aigner A. (2006) RNA interference-mediated gene silencing of pleiotrophin through polyethylenimine-complexed small interfering RNAs in vivo exerts antitumoral effects in glioblastoma xenografts. Hum Gene Ther. 17:751-66

Guy J, Drabek D, Antoniou M. (1995) Delivery of DNA into mammalian cells by receptor-mediated endocytosis and gene therapy. Mol Biotechnol. 3:237-48

Hamann PR, Hinman LM, Hollander I, Beyer CF, Lindh D, Holcomb R, Hallett W, Tsou HR, Upeslacis J, Shochat D, Mountain A, Flowers DA, Bernstein I. (2002) Gemtuzumab ozogamicin, a potent and selective anti-CD33 antibody-calicheamicin conjugate for treatment of acute myeloid leukemia. Bioconjug Chem. 13:47-58

Hammond SM, Boettcher S, Caudy AA, Kobayashi R, Hannon GJ. (2001) Argonaute2, a link between genetic and biochemical analyses of RNAi. Science, 293:1146-50

Hannon GJ. (2002) RNA interference. Nature, 418:244-51

Hansen CB, Kao GY, Moase EH, Zalipsky S, Allen TM. (1995) Attachment of antibodies to sterically stabilized liposomes: evaluation, comparison and optimization of coupling procedures. Biochim Biophys Acta. 1239:133-44

Harding JA, Engbers CM, Newman MS, Goldstein NI, Zalipsky S (1997) Immunogenicity and pharmacokinetic attributes of poly(ethylene glycol)-grafted immunoliposomes. Biochim Biophys Acta. 1327:181-92

Hashida H, Takabayashi A, Kanai M, Adachi M, Kondo K, Kohno N, Yamaoka Y, Miyake M. (2002) Aminopeptidase N is involved in cell motility and angiogenesis: its clinical significance in human colon cancer. Gastroenterology. 122:376-86

Hashida M, Nishikawa M, Yamashita F, Takakura Y. (2001) Cell-specific delivery of genes with glycosylated carriers. Adv Drug Deliv Rev. 52:187-96

Hatefi A, Megeed Z, Ghandehari H (2006) Recombinant polymer-protein fusion: a promising approach towards efficient and targeted gene delivery. J Gene Med. 8:468-76

Hauswirth AW, Florian S, Printz D, Sotlar K, Krauth MT, Fritsch G, Schernthaner GH, Wacheck V, Selzer E, Sperr WR, Valent P. (2007) Expression of the target receptor CD33 in CD34+/CD38-/CD123+ AML stem cells. Eur J Clin Invest. 37:73-82.

Heath TD, Fraley RT, Papahdjopoulos D. (1980) Antibody targeting of liposomes: cell specificity obtained by conjugation of F(ab')2 to vesicle surface. Science,210:539-41

Heidenreich O, Krauter J, Riehle H, Hadwiger P, John M, Heil G, Vornlocher HP, Nordheim A. (2003) AML1/MTG8 oncogene suppression by small interfering RNAs supports myeloid differentiation of t(8;21)-positive leukemic cells. Blood. 101:3157-63

Hemmi H, Takeuchi O, Kawai T, Kaisho T, Sato S, Sanjo H, Matsumoto M, Hoshino K, Wagner H, Takeda K, Akira S. (2000) A Toll-like receptor recognizes bacterial DNA. Nature. 408:740-5

Hermanson GT (1996) Bioconjugate Techniques, Academic Press, San Diego

Hirsch M, Ziroli V, Helm M, Massing U. (2008) Preparation of small amounts of sterile siRNA-liposomes with high entrapping efficiency by dual asymmetric centrifugation (DAC). J Control Release. 135:80-8

't **Hoen PA**, de Kort F, van Ommen GJ, den Dunnen JT (2003) Fluorescent labelling of cRNA for microarray applications. Nucleic Acids Res. 31:20

Hogrefe RI, Lebedev AV, Zon G, Pirollo KF, Rait A, Zhou Q, Yu W, Chang EH (2006) Chemically modified short interfering hybrids (siHYBRIDS): nanoimmunoliposome delivery in vitro and in vivo for RNAi of HER-2. Nucleosides Nucleotides Nucleic Acids. 25:889-907

Honoré I, Grosse S, Frison N, Favatier F, Monsigny M, Fajac I (2005) Transcription of plasmid DNA: influence of plasmid DNA/polyethylenimine complex formation. J Control Release. 107:537-46

Hoogenboom HR. (2005) Selecting and screening recombinant antibody libraries. Nat Biotechnol. 23:1105-16

Hope KJ, Jin L, Dick JE. (2003) Human acute myeloid leukemia stem cells. Arch Med Res. 34:507-14

Hornung V, Guenthner-Biller M, Bourquin C, Ablasser A, Schlee M, Uematsu S, Noronha A, Manoharan M, Akira S, de Fougerolles A, Endres S, Hartmann G. (2005) Sequence-specific potent induction of IFN-alpha by short interfering RNA in plasmacytoid dendritic cells through TLR7. Nat Med. 11:263-70

Howard KA, Rahbek UL, Liu X, Damgaard CK, Glud SZ, Andersen MØ, Hovgaard MB, Schmitz A, Nyengaard JR, Besenbacher F, Kjems J. (2006) RNA interference in vitro and in vivo using a novel chitosan/siRNA nanoparticle system. Mol Ther. 14:476-84

Huang RT, Wahn K, Klenk HD, Rott R. (1979) Association of the envelope glycoproteins of influenza virus with liposomes--a model study on viral envelope assembly. Virology, 97:212-7

Hu-Lieskovan S, Heidel JD, Bartlett DW, Davis ME, Triche TJ. (2005) Sequence-specific knockdown of EWS-FLI1 by targeted, nonviral delivery of small interfering RNA inhibits tumor growth in a murine model of metastatic Ewing's sarcoma. Cancer Res. 65:8984-92

Hust M, Dübel S. (2005) Phage display vectors for the in vitro generation of human antibody fragments. Methods Mol Biol. 295:71-96

Iden DL, Allen TM. (2001) In vitro and in vivo comparison of immunoliposomes made by conventional coupling techniques with those made by a new post-insertion approach. Biochim Biophys Acta. 1513:207-16

Ikeda Y, Taira K. (2006) Ligand-targeted delivery of therapeutic siRNA. Pharm Res. 23:1631-40

Ishida T, Iden DL, Allen TM. (1999) A combinatorial approach to producing sterically stabilized (Stealth) immunoliposomal drugs. FEBS Lett. 460:129-33

Ishii K, Usui S, Sugimura Y, Yoshida S, Hioki T, Tatematsu M, Yamamoto H, Hirano K. (2001) Aminopeptidase N regulated by zinc in human prostate participates in tumor cell invasion. Int J Cancer. 92:49-54

Jackson AL, Burchard J, Schelter J, Chau BN, Cleary M, Lim L, Linsley PS. (2006a) Widespread siRNA "off-target" transcript silencing mediated by seed region sequence complementarity. RNA, 12:1179-87

Jackson AL, Burchard J, Leake D, Reynolds A, Schelter J, Guo J, Johnson JM, Lim L, Karpilow J, Nichols K, Marshall W, Khvorova A, Linsley PS. (2006b) Position-specific chemical modification of siRNAs reduces "off-target" transcript silencing. RNA, 12:1197-205.

Jakubowiak A, Pouponnot C, Berguido F, Frank R, Mao S, Massague J, Nimer SD. (2000) Inhibition of the transforming growth factor beta 1 signaling pathway by the AML1/ETO leukemia-associated fusion protein. J Biol Chem. 275:40282-7

Jin L, Hope KJ, Zhai Q, Smadja-Joffe F, Dick JE. (2006) Targeting of CD44 eradicates human acute myeloid leukemic stem cells.Nat Med.12:1167-74

Jordan CT, Upchurch D, Szilvassy SJ, Guzman ML, Howard DS, Pettigrew AL, Meyerrose T, Rossi R, Grimes B, Rizzieri DA, Luger SM, Phillips GL (2000) The interleukin-3 receptor alpha chain is a unique marker for human acute myelogenous leukemia stem cells. Leukemia. 14:1777-84

Jurcic J. (2007) Ab therapy of AML: native anti-CD33 Ab and drug conjugates. Cytotherapy, 4:1-6

Judge AD, Sood V, Shaw JR, Fang D, McClintock K, MacLachlan I. (2005) Sequence-dependent stimulation of the mammalian innate immune response by synthetic siRNA. Nat Biotechnol. 23:457-62

Kagoshima H, Shigesada K, Satake M, Ito Y, Miyoshi H, Ohki M, Pepling M, Gergen P. (1993) The Runt domain identifies a new family of heteromeric transcriptional regulators. Trends Genet. 9:338-41

Kell WJ, Burnett AK, Chopra R, Yin JA, Clark RE, Rohatiner A, Culligan D, Hunter A, Prentice AG, Milligan DW. (2003) A feasibility study of simultaneous administration of gemtuzumab ozogamicin with intensive chemotherapy in induction and consolidation in younger patients with acute myeloid leukemia. Blood 102:4277-83

Kelm S, Schauer R. (1997) Sialic acids in molecular and cellular interactions. Int Rev Cytol. 175:137-240

Khoury M, Louis-Plence P, Escriou V, Noel D, Largeau C, Cantos C, Scherman D, Jorgensen C, Apparailly F. (2006) Efficient new cationic liposome formulation for systemic delivery of small interfering RNA silencing tumor necrosis factor alpha in experimental arthritis. Arthritis Rheum. 54:1867-77

Kidane A, Lantz GC, Jo S, Park K. (1999) Surface modification with PEO-containing triblock copolymer for improved biocompatibility: in vitro and ex vivo studies. J Biomater Sci Polym Ed. 10:1089-105

Kim SH, Mok H, Jeong JH, Kim SW, Park TG. (2006) Comparative evaluation of target-specific GFP gene silencing efficiencies for antisense ODN, synthetic siRNA, and siRNA plasmid complexed with PEI-PEG-FOL conjugate. Bioconjug Chem. 17:241-4

Kim YJ, Neelamegam R, Heo MA, Edwardraja S, Paik HJ, Lee SG. (2008) Improving the productivity of single-chain Fv antibody against c-Met by rearranging the order of its variable domains. J Microbiol Biotechnol. 18:1186-90

Kipriyanov SM, Moldenhauer G, Strauss G, Little M. (1998) Bispecific CD3 x CD19 diabody for T cell-mediated lysis of malignant human B cells. Int J Cancer. 77:763-72

Kirpotin D, Park JW, Hong K, Zalipsky S, Li WL, Carter P, Benz CC, Papahadjopoulos D. (1997) Sterically stabilized anti-HER2 immunoliposomes: design and targeting to human breast cancer cells in vitro. Biochemistry, 36:66-75

Kircheis R, Kichler A, Wallner G, Kursa M, Ogris M, Felzmann T, Buchberger M, Wagner E. (1997) Coupling of cell-binding ligands to polyethylenimine for targeted gene delivery. Gene Ther. 4:409-18

Kleinman ME, Yamada K, Takeda A, Chandrasekaran V, Nozaki M, Baffi JZ, Albuquerque RJ, Yamasaki S, Itaya M, Pan Y, Appukuttan B, Gibbs D, Yang Z, Karikó K, Ambati BK, Wilgus TA, DiPietro LA, Sakurai E, Zhang K, Smith JR, Taylor EW, Ambati J. (2008) Sequence- and target-independent angiogenesis suppression by siRNA via TLR3. Nature. 452:591-7

Kolbe A (2007) Establishing the post-insertion method for the generation of immunoliposomes directed against FAP-expressing tumour stroma cells, Diploma thesis

Kong Y, Ruan L, Ma L, Cui Y, Wang JM, Le Y. (2007) RNA interference as a novel and powerful tool in immunopharmacological research. Int Immunopharmacol. 7:417-26

Koning GA, Morselt HW, Velinova MJ, Donga J, Gorter A, Allen TM, Zalipsky S, Kamps JA, Scherphof GL. (1999) Selective transfer of a lipophilic prodrug of 5-fluorodeoxyuridine from immunoliposomes to colon cancer cells. Biochim Biophys Acta. 1420:153-67

Koning GA, Morselt HW, Gorter A, Allen TM, Zalipsky S, Scherphof GL, Kamps JA. (2003) Interaction of differently designed immunoliposomes with colon cancer cells and Kupffer cells. An in vitro comparison. Pharm Res. 20:1249-57

Kontermann RE. (2006) Immunoliposomes for cancer therapy. Curr Opin Mol Ther. 8:39-45

Kügler M, Stein C, Schwenkert M, Saul D, Vockentanz L, Huber T, Wetzel SK, Scholz O, Plückthun A, Honegger A, Fey GH (2009) Stabilization and humanization of a single-chain Fv antibody fragment specific for human lymphocyte antigen CD19 by designed point mutations and CDR-grafting onto a human framework. Protein Eng Des Sel. 22:135-47

Kurreck J. (2003) Antisense technologies. Improvement through novel chemical modifications. Eur J Biochem. 270:1628-44

Kurreck J. (2009) RNA interference: from basic research to therapeutic applications. Angew Chem Int Ed 48:1378-98

Ladner RC, Sato AK, Gorzelany J, de Souza M. (2004) Phage display-derived peptides as therapeutic alternatives to antibodies. Drug Discov Today. 9:525-9

Lamberton JS, Christian AT (2003) Varying the nucleic acid composition of siRNA molecules dramatically varies the duration and degree of gene silencing. Mol Biotechnol. 24:111-20

Lapidot T, Sirard C, Vormoor J, Murdoch B, Hoang T, Caceres-Cortes J, Minden M, Paterson B, Caligiuri MA, Dick JE. (1994) A cell initiating human acute myeloid leukaemia after transplantation into SCID mice.Nature.367:645-8

Lee ES, Yoon CH, Kim YS, Bae YS. (2007) The double-strand RNA-dependent protein kinase PKR plays a significant role in a sustained ER stress-induced apoptosis. FEBS Lett. 581:4325-32

Lendeckel U, Arndt M, Frank K, Wex T, Ansorge S. (1999) Role of alanyl aminopeptidase in growth and function of human T cells. Int J Mol Med. 4:17-27

Leserman LD, Barbet J, Kourilsky F, Weinstein JN. (1980) Targeting to cells of fluorescent liposomes covalently coupled with monoclonal antibody or protein A. Nature, 288:602-4

Lewis DL, Wolff JA. (2005) Delivery of siRNA and siRNA expression constructs to adult mammals by hydrodynamic intravascular injection. Methods Enzymol. 392:336-50

Linggi B, Müller-Tidow C, van de Locht L, Hu M, Nip J, Serve H, Berdel WE, van der Reijden B, Quelle DE, Rowley JD, Cleveland J, Jansen JH, Pandolfi PP, Hiebert SW. (2002) The t(8;21) fusion protein, AML1 ETO, specifically represses the transcription of the p14(ARF) tumor suppressor in acute myeloid leukemia. Nat Med. 8:743-50

Li X, Stuckert P, Bosch I, Marks JD, Marasco WA. (2001) Single-chain antibody-mediated gene delivery into ErbB2-positive human breast cancer cells. Cancer Gene Ther. 8:555-65

Liu J, Carmell MA, Rivas FV, Marsden CG, Thomson JM, Song JJ, Hammond SM, Joshua-Tor L, Hannon GJ. (2004) Argonaute2 is the catalytic engine of mammalian RNAi. Science, 305:1437-41

Look AT, Ashmun RA, Shapiro LH, Peiper SC. (1989) Human myeloid plasma membrane glycoprotein CD13 (gp150) is identical to aminopeptidase N. J Clin Invest. 83:1299-307

Luan Y, Xu W. (2007) The structure and main functions of aminopeptidase N. Curr Med Chem. 14:639-47

Lutterbach B, Westendorf JJ, Linggi B, Patten A, Moniwa M, Davie JR, Huynh KD, Bardwell VJ, Lavinsky RM, Rosenfeld MG, Glass C, Seto E, Hiebert SW. (1998) ETO, a target of t(8;21) in acute leukemia, interacts with the N-CoR and mSin3 corepressors. Mol Cell Biol. 18:7176-84

Manil L, Couvreur P. (1986) Specificity of anticancer treatment:aims and limits of targeting. I. Targeting carriers. Rev Med Liege. 41:977-95

Mao S, Neu M, Germershaus O, Merkel O, Sitterberg J, Bakowsky U, Kissel T. (2006) Influence of polyethylene glycol chain length on the physicochemical and biological

properties of poly(ethylene imine)-graft-poly(ethylene glycol) block copolymer/SiRNA polyplexes. Bioconjug Chem. 17:1209-18

Martin FJ, Hubbell WL, Papahadjopoulos D. (1981) Immunospecific targeting of liposomes to cells: a novel and efficient method for covalent attachment of Fab' fragments via disulfide bonds. Biochemistry, 20:4229-38

Martinez N, Drescher B, Riehle H, Cullmann C, Vornlocher HP, Ganser A, Heil G, Nordheim A, Krauter J, Heidenreich O. (2004) The oncogenic fusion protein RUNX1-CBFA2T1 supports proliferation and inhibits senescence in t(8;21)-positive leukaemic cells. BMC Cancer. 4:44

Martinez Soria N, Tussiwand R, Ziegler P, Manz MG, Heidenreich O. (2009) Transient depletion of RUNX1/RUNX1T1 by RNA interference delays tumour formation in vivo. Leukemia. 23:188-90

Marty C, Scheidegger P, Ballmer-Hofer K, Klemenz R, Schwendener RA (2001) Production of functionalized single-chain Fv antibody fragments binding to the ED-B domain of the B-isoform of fibronectin in Pichia pastoris. Protein Expr Purif. 21:156-64

Maruyama K, Iwasaki F, Takizawa T, Yanagie H, Niidome T, Yamada E, Ito T, Koyama Y. (2004) Novel receptor-mediated gene delivery system comprising plasmid/protamine/sugar-containing polyanion ternary complex. Biomaterials 25:3267-3273

Mastrobattista E, Storm G, van Bloois L, Reszka R, Bloemen PG, Crommelin DJ, Henricks PA (1999) Cellular uptake of liposomes targeted to intercellular adhesion molecule-1 (ICAM-1) on bronchial epithelial cells. Biochim Biophys Acta. 1419:353-63

McCaffrey AP, Meuse L, Pham TT, Conklin DS, Hannon GJ, Kay MA. (2002) RNA interference in adult mice. Nature.418:38-9

McKenzie SB (1996) Textbook of Hematology, 2nd edition, Williams and Wilkins, Baltimore

Mechtersheimer G, Möller P. (1990) Expression of aminopeptidase N (CD13) in mesenchymal tumors. Am J Pathol. 137:1215-22

Merdan T, Kunath K, Fischer D, Kopecek J, Kissel T. (2002) Intracellular processing of poly(ethylene imine)/ribozyme complexes can be observed in living cells by using confocal laser scanning microscopy and inhibitor experiments. Pharm Res.19:140-6

Merdan T, Callahan J, Petersen H, Kunath K, Bakowsky U, Kopecková P, Kissel T, Kopecek J. (2003) Pegylated polyethylenimine-Fab' antibody fragment conjugates for targeted gene delivery to human ovarian carcinoma cells. Bioconjug Chem. 14:989-96

Messerschmidt SK, Kolbe A, Müller D, Knoll M, Pleiss J, Kontermann RE (2008) Novel single-chain Fv' formats for the generation of immunoliposomes by site-directed coupling. Bioconjug Chem. 19:362-9

Messerschmidt SK, Beuttler J, Rothdiener M, Kontermann RE (2009) Recombinant antibody molecules in nanobiotechnology: immunoliposomes. Springer protocols antibody engineering. Kontermann RE, Dübel S (Ed.), Springer-Verlag, Heidelberg

Mirick GR, Bradt BM, Denardo SJ, Denardo GL. (2004) A review of human anti-globulin antibody (HAGA, HAMA, HACA, HAHA) responses to monoclonal antibodies. Not four letter words.Q J Nucl Med Mol Imaging. 48:251-7.

Mitelman F, Heim S. (1992) Quantitative acute leukemia cytogenetics. Genes Chromosomes Cancer. 5:57-66

Miyawaki-Shimizu K, Predescu D, Shimizu J, Broman M, Predescu S, Malik AB. (2006) siRNA-induced caveolin-1 knockdown in mice increases lung vascular permeability via the junctional pathway. Am J Physiol Lung Cell Mol Physiol 290:405-13

Miyoshi H, Shimizu K, Kozu T, Maseki N, Kaneko Y, Ohki M. (1991) t(8;21) breakpoints on chromosome 21 in acute myeloid leukemia are clustered within a limited region of a single gene, AML1. Proc Natl Acad Sci U S A. 88:10431-4

Monfardini C, Veronese FM. (1998) Stabilization of substances in circulation. Bioconjug Chem. 9:418-50

Morrissey DV, Lockridge JA, Shaw L, Blanchard K, Jensen K, Breen W, Hartsough K, Machemer L, Radka S, Jadhav V, Vaish N, Zinnen S, Vargeese C, Bowman K, Shaffer CS, Jeffs LB, Judge A, MacLachlan I, Polisky B. (2005) Potent and persistent in vivo anti-HBV activity of chemically modified siRNAs. Nat Biotechnol. 23:1002-7

Moschetta A, vanBerge-Henegouwen GP, Portincasa P, Palasciano G, van Erpecum KJ. (2001) Cholesterol crystallization in model biles: effects of bile salt and phospholipid species composition. J Lipid Res. 42:1273-81

Mukherjee S, Ghosh RN, Maxfield FR. (1997) Endocytosis. Physiol Rev. 77:759-803

Mulloy JC, Cammenga J, MacKenzie KL, Berguido FJ, Moore MA, Nimer SD. (2002) The AML1-ETO fusion protein promotes the expansion of human hematopoietic stem cells. Blood. 99:15-23

Nadler LA, Anderson KC, Schlossman SF. (1983) Human T and B cell derived malignancies. Rinsho Ketsueki. 24:987-95

Nellis DF, Ekstrom DL, Kirpotin DB, Zhu J, Andersson R. (2005) Preclinical manufacture of an anti-HER2 scFv-PEG-DSPE, liposome-inserting conjugate. 1. Gram-scale production and purification. Biotechnol Prog 21:205-20

New RRC. (1990). Liposomes: a practical approach: IRL Press, Michigan

Nielsen UB, Kirpotin DB, Pickering EM, Hong K, Park JW, Refaat Shalaby M, Shao Y, Benz CC, Marks JD. (2002) Therapeutic efficacy of anti-ErbB2 immunoliposomes targeted by a phage antibody selected for cellular endocytosis. Biochim Biophys Acta. 1591:109-118

Nishida K, Mihara K, Takino T, Nakane S, Takakura Y, Hashida M, Sezaki H. (1991) Hepatic disposition characteristics of electrically charged macromolecules in rat in vivo and in the perfused liver. Pharm Res. 8:437-44

Niwa R, Hatanaka S, Shoji-Hosaka E, Sakurada M, Kobayashi Y, Uehara A, Yokoi H, Nakamura K, Shitara K. (2004) Enhancement of the antibody-dependent cellular cytotoxicity of low-fucose IgG1 Is independent of FcgammaRIIIa functional polymorphism. Clin Cancer Res. 10:6248-55

Nobs L, Buchegger F, Gurny R, Allémann E. (2004) Current methods for attaching targeting ligands to liposomes and nanoparticles. J Pharm Sci. 93:1980-92

Nusser AK (2009) Immunoliposomes targeting EGFR and HER2 receptor – an approach for HER2 receptor silencing in an adherent cell model, Diploma thesis

O'Connell PJ, Gerkis V, d'Apice AJ. (1991) Variable O-glycosylation of CD13 (aminopeptidase N). J Biol Chem. 266:4593-7

Okuda T, van Deursen J, Hiebert SW, Grosveld G, Downing JR. (1996) AML1, the target of multiple chromosomal translocations in human leukemia, is essential for normal fetal liver hematopoiesis. Cell, 84:321-30

Okuda T, Cai Z, Yang S, Lenny N, Lyu CJ, van Deursen JM, Harada H, Downing JR (1998) Expression of a knocked-in AML1-ETO leukemia gene inhibits the establishment of normal definitive hematopoiesis and directly generates dysplastic hematopoietic progenitors. Blood. 91:3134-43

Orr SJ, Morgan NM, Elliott J, Burrows JF, Scott CJ, McVicar DW, Johnston JA. (2007) CD33 responses are blocked by SOCS3 through accelerated proteasomal-mediated turnover. Blood, 109:1061-8

Pabst T, Mueller BU, Harakawa N, Schoch C, Haferlach T, Behre G, Hiddemann W, Zhang DE, Tenen DG. (2001) AML1-ETO downregulates the granulocytic differentiation factor C/EBPalpha in t(8;21) myeloid leukemia. Nat Med. 7:444-51

Palliser D, Chowdhury D, Wang QY, Lee SJ, Bronson RT, Knipe DM, Lieberman J (2006) An siRNA-based microbicide protects mice from lethal herpes simplex virus 2 infection. Nature. 439:89-94

Parisi E, Draznin J, Stoopler E, Schuster SJ, Porter D, Sollecito TP.(2002) Acute myelogenous leukemia: advances and limitations of treatment. Oral Surg Oral Med Oral Pathol Oral Radiol Endod. 93:257-63

Park JW, Hong K, Kirpotin DB, Papahadjopoulos D, Benz CC. (1997) Immunoliposomes for cancer treatment. Adv Pharmacol. 40:399-435.

Park JW, Hong K, Kirpotin DB, Colbern G, Shalaby R, Baselga J, Shao Y, Nielsen UB, Marks JD, Moore D, Papahadjopoulos D, Benz CC. (2002) Anti-HER2 immunoliposomes: enhanced efficacy attributable to targeted delivery. Clin Cancer Res. 8:1172-81

Paschka P, Marcucci G, Ruppert AS, Mrózek K, Chen H, Kittles RA, Vukosavljevic T, Perrotti D, Vardiman JW, Carroll AJ, Kolitz JE, Larson RA, Bloomfield CD; Cancer and Leukemia Group B. (2006) Adverse prognostic significance of KIT mutations in adult acute myeloid leukemia with inv(16) and t(8;21): a Cancer and Leukemia Group B Study. J Clin Oncol. 24:3904-11

Pasqualini R, Koivunen E, Kain R, Lahdenranta J, Sakamoto M, Stryhn A, Ashmun RA, Shapiro LH, Arap W, Ruoslahti E. (2000) Aminopeptidase N is a receptor for tumor-homing peptides and a target for inhibiting angiogenesis. Cancer Res. 60:722-7

Pastorino F, Brignole C, Marimpietri D, Sapra P, Moase EH, Allen TM, Ponzoni M. (2003) Doxorubicin-loaded Fab' fragments of anti-disialoganglioside immunoliposomes selectively inhibit the growth and dissemination of human neuroblastoma in nude mice. Cancer Res. 63:86-92

Patil Y, Panyam J. (2009) Polymeric nanoparticles for siRNA delivery and gene silencing Int J Pharm. 367:195-203

Paul SP, Taylor LS, Stansbury EK, McVicar DW. (2000) Myeloid specific human CD33 is an inhibitory receptor with differential ITIM function in recruiting the phosphatases SHP-1 and SHP-2. Blood. 96:483-90

Peer D, Zhu P, Carman CV, Lieberman J, Shimaoka M. (2007) Selective gene silencing in activated leukocytes by targeting siRNAs to the integrin lymphocyte function-associated antigen-1. Proc Natl Acad Sci U S A. 104:4095-100

Peer D, Park EJ, Morishita Y, Carman CV, Shimaoka M. (2008) Systemic leukocyte-directed siRNA delivery revealing cyclin D1 as an anti-inflammatory target. Science, 319:627-30

Peipp M, Simon N, Loichinger A, Baum W, Mahr K, Zunino SJ, Fey GH (2001) An improved procedure for the generation of recombinant single-chain Fv antibody fragments reacting with human CD13 on intact cells. J Immunol Methods. 251:161-76

Pelicci PG. (2004) Do tumor-suppressive mechanisms contribute to organism aging by inducing stem cell senescence? J Clin Invest. 113:4-7

Petersen H, Fechner PM, Martin AL, Kunath K, Stolnik S, Roberts CJ, Fischer D, Davies MC, Kissel T. (2002) Polyethylenimine-graft-poly(ethylene glycol) copolymers: influence of copolymer block structure on DNA complexation and biological activities as gene delivery system. Bioconjug Chem. 13:845-54

Pillé JY, Li H, Blot E, Bertrand JR, Pritchard LL, Opolon P, Maksimenko A, Lu H, Vannier JP, Soria J, Malvy C, Soria C (2006) Intravenous delivery of anti-RhoA small interfering RNA loaded in nanoparticles of chitosan in mice: safety and efficacy in xenografted aggressive breast cancer. Hum Gene Ther. 17:1019-26

Prakash TP, Allerson CR, Dande P, Vickers TA, Sioufi N, Jarres R, Baker BF, Swayze EE, Griffey RH, Bhat B. (2005) Positional effect of chemical modifications on short interference RNA activity in mammalian cells. J Med Chem. 48:4247-53

Press OW, Farr AG, Borroz KI, Anderson SK, Martin PJ (1989) Endocytosis and degradation of monoclonal antibodies targeting human B-cell malignancies. Cancer Res. 49:4906-12

Puri A, Kramer-Marek G, Campbell-Massa R, Yavlovich A, Tele SC, Lee SB, Clogston JD, Patri AK, Blumenthal R, Capala J. (2008) HER2-specific affibody-conjugated thermosensitive liposomes (Affisomes) for improved delivery of anticancer agents. J Liposome Res. 18:293-307

Ravetch JV, Lanier LL (2000) Immune inhibitory receptors. Science.290:84-9

Razak K, Newland AC. (1992) The significance of aminopeptidases and haematopoietic cell differentiation. Blood Rev. 6:243-50

Read ML, Singh S, Ahmed Z, Stevenson M, Briggs SS, Oupicky D, Barrett LB, Spice R, Kendall M, Berry M, Preece JA, Logan A, Seymour LW. (2005) A versatile reducible polycation-based system for efficient delivery of a broad range of nucleic acids. Nucleic Acids Res. 33:e86

Rejman J, Oberle V, Zuhorn IS, Hoekstra D (2004) Size-dependent internalization of particles via the pathways of clathrin- and caveolae-mediated endocytosis. Biochem J. 377:159–169

Rhoades KL, Hetherington CJ, Harakawa N, Yergeau DA, Zhou L, Liu LQ, Little MT, Tenen DG, Zhang DE. (2000) Analysis of the role of AML1-ETO in leukemogenesis, using an inducible transgenic mouse model. Blood.96:2108-15

Rivest V, Phivilay A, Julien C, Bélanger S, Tremblay C, Emond V, Calon F (2007) Novel liposomal formulation for targeted gene delivery. Pharm Res. 24:981-90

Rozema DB, Lewis DL, Wakefield DH, Wong SC, Klein JJ, Roesch PL, Bertin SL, Reppen TW, Chu Q, Blokhin AV, Hagstrom JE, Wolff JA (2007) Dynamic PolyConjugates for targeted in vivo delivery of siRNA to hepatocytes. Proc Natl Acad Sci U S A. 104:12982-7

Rüger R, Müller D, Fahr A, Kontermann RE. (2005) Generation of immunoliposomes using recombinant single-chain Fv fragments bound to Ni-NTA-liposomes. J Drug Target. 13:399-406

Sabbath KD, Ball ED, Larcom P, Davis RB, Griffin JD. (1985) Heterogeneity of clonogenic cells in acute myeloblastic leukemia. J Clin Invest. 75:746-53

Santos AN, Langner J, Herrmann M, Riemann D. (2000) Aminopeptidase N/CD13 is directly linked to signal transduction pathways in monocytes. Cell Immunol. 201:22-32

Sapra P, Allen TM. (2002) Internalizing antibodies are necessary for improved therapeutic efficacy of antibody-targeted liposomal drugs. Cancer Res. 62:7190-4

Sapra P, Allen TM. (2003) Ligand-targeted liposomal anticancer drugs. Prog Lipid Res. 42:439-62

Sapra P, Allen TM. (2004) Improved outcome when B-cell lymphoma is treated with combinations of immunoliposomal anticancer drugs targeted to both the CD19 and CD20 epitopes. Cancer Res. 10:2530-7

Sapra P, Moase EH, Ma J, Allen TM. (2004) Improved therapeutic responses in a xenograft model of human B lymphoma (Namalwa) for liposomal vincristine versus liposomal doxorubicin targeted via anti-CD19 IgG2a or Fab' fragments. Clin Cancer Res. 10:1100-1

Sasaki K, Kogure K, Chaki S, Nakamura Y, Moriguchi R, Hamada H, Danev R, Nagayama K, Futaki S, Harashima H. (2008) An artificial virus-like nano carrier system: enhanced endosomal escape of nanoparticles via synergistic action of pH-sensitive fusogenic peptide derivatives. Anal Bioanal Chem. 391:2717-27

Sato Y, Murase K, Kato J, Kobune M, Sato T, Kawano Y, Takimoto R, Takada K, Miyanishi K, Matsunaga T, Takayama T, Niitsu Y. (2008) Resolution of liver cirrhosis using vitamin A-coupled liposomes to deliver siRNA against a collagen-specific chaperone. Nat Biotechnol. 26:431-42

Schauer R. (1982) Chemistry, metabolism, and biological functions of sialic acids. Adv Carbohydr Chem Biochem. 40:131-234

Scherer LJ, Rossi JJ. (2003) Approaches for the sequence-specific knockdown of mRNA. Nat Biotechnol. 21:1457-65

Schiffelers RM, Ansari A, Xu J, Zhou Q, Tang Q, Storm G, Molema G, Lu PY, Scaria PV, Woodle MC. (2004) Cancer siRNA therapy by tumor selective delivery with ligand-targeted sterically stabilized nanoparticle. Nucleic Acids Res. 32:e149

Schmiedl A, Breitling F, Winter CH, Queitsch I, Dübel S (2000) Effects of unpaired cysteines on yield, solubility and activity of different recombinant antibody constructs expressed in E. coli. J Immunol Methods. 242:101-14

Schwemmlein M, Peipp M, Barbin K, Saul D, Stockmeyer B, Repp R, Birkmann J, Oduncu F, Emmerich B, Fey GH. (2006) A CD33-specific single-chain immunotoxin mediates potent apoptosis of cultured human myeloid leukaemia cells. Br J Haematol. 133:141-51

Schwemmlein M, Stieglmaier J, Kellner C, Peipp M, Saul D, Oduncu F, Emmerich B, Stockmeyer B, Lang P, Beck JD, Fey GH. (2007a) A CD19-specific single-chain immunotoxin mediates potent apoptosis of B-lineage leukemic cells. Leukemia, 21:1405-12

Schwemmlein M (2007b) Entwicklung und Charakterisierung rekombinanter Exotoxin A-Fusionsproteine zur Therapy von Leukämien, Dissertation

Shan G, Li Y, Zhang J, Li W, Szulwach KE, Duan R, Faghihi MA, Khalil AM, Lu L, Paroo Z, Chan AW, Shi Z, Liu Q, Wahlestedt C, He C, Jin P. (2008) A small molecule enhances RNA interference and promotes microRNA processing. Nat Biotechnol. 26:933-40.

Shim MS, Kwon YJ. (2009) Acid-Responsive Linear Polyethylenimine for Efficient, Specific, and Biocompatible siRNA Delivery. Bioconjug Chem.

Shoemaker SG, Hromas R, Kaushansky K. (1990) Transcriptional regulation of interleukin 3 gene expression in T lymphocytes. Proc Natl Acad Sci U S A.87:9650-4

Sievers EL, Appelbaum FR, Spielberger RT, Forman SJ, Flowers D, Smith FO, Shannon-Dorcy K, Berger MS, Bernstein ID (1999) Selective ablation of acute myeloid leukemia using antibody-targeted chemotherapy: a phase I study of an anti-CD33 calicheamicin immunoconjugate. Blood, 93:3678-84

Sievers EL. (2004) Native antibody and antibody-targeted chemotherapy for acute myeloid leukemia. Adv Pharmacol. 51:169-83

Simard P, Leroux JC. (2009) pH-sensitive immunoliposomes specific to the CD33 cell surface antigen of leukemic cells. Int J Pharm

Sioud M. (2005) On the delivery of small interfering RNAs into mammalian cells. Expert Opin Drug Deliv. 2:639-51

Song E, Zhu P, Lee SK, Chowdhury D, Kussman S, Dykxhoorn DM, Feng Y, Palliser D, Weiner DB, Shankar P, Marasco WA, Lieberman J. (2005) Antibody mediated in vivo delivery of small interfering RNAs via cell-surface receptors. Nat Biotechnol. 23:709-17

Soutschek J, Akinc A, Bramlage B, Charisse K, Constien R, Donoghue M, Elbashir S, Geick A, Hadwiger P, Harborth J, John M, Kesavan V, Lavine G, Pandey RK, Racie T, Rajeev KG, Röhl I, Toudjarska I, Wang G, Wuschko S, Bumcrot D, Koteliansky V, Limmer S, Manoharan M, Vornlocher HP. (2004) Therapeutic silencing of an endogenous gene by systemic administration of modified siRNAs. Nature, 432:173-8

Stuart DD, Allen TM. (2000) A new liposomal formulation for antisense oligodeoxynucleotides with small size, high incorporation efficiency and good stability. Biochim Biophys Acta. 1463:219-29

Szoka F Jr, Papahadjopoulos D. (1980) Comparative properties and methods of preparation of lipid vesicles (liposomes). Annu Rev Biophys Bioeng. 9:467-508

Takahashi A, Satake M, Yamaguchi-Iwai Y, Bae SC, Lu J, Maruyama M, Zhang YW, Oka H, Arai N, Arai K. (1995) Positive and negative regulation of granulocyte-macrophage colony-stimulating factor promoter activity by AML1-related transcription factor, PEBP2. Blood. 86:607-16

Takei Y, Kadomatsu K, Yuzawa Y, Matsuo S, Muramatsu T. (2004) A small interfering RNA targeting vascular endothelial growth factor as cancer therapeutics. Cancer Res. 64:3365-70

Takeshita F, Minakuchi Y, Nagahara S, Honma K, Sasaki H, Hirai K, Teratani T, Namatame N, Yamamoto Y, Hanai K, Kato T, Sano A, Ochiya T. (2005) Efficient delivery of small interfering RNA to bone-metastatic tumors by using atelocollagen in vivo. Proc Natl Acad Sci U S A. 102:12177-82

Taussig DC, Pearce DJ, Simpson C, Rohatiner AZ, Lister TA, Kelly G, Luongo JL, Danet-Desnoyers GA, Bonnet D. (2005) Hematopoietic stem cells express multiple myeloid markers: implications for the origin and targeted therapy of acute myeloid leukemia. Blood. 106:4086-92

Taylor AM, Zhu Q, Casey JR. (2001) Cysteine-directed cross-linking localizes regions of the human erythrocyte anion-exchange protein (AE1) relative to the dimeric interface. Biochem J. 359:661-8

Taylor VC, Buckley CD, Douglas M, Cody AJ, Simmons DL, Freeman SD. (1999) The myeloid-specific sialic acid-binding receptor, CD33, associates with the protein-tyrosine phosphatases, SHP-1 and SHP-2. J Biol Chem.274:11505-12

Tedder TF, Isaacs CM (1989) Isolation of cDNAs encoding the CD19 antigen of human and mouse B lymphocytes. A new member of the immunoglobulin superfamily. J Immunol. 143:712-7

Thomas M, Gessner A, Vornlocher HP, Hadwiger P, Greil J, Heidenreich O (2005) Targeting MLL-AF4 with short interfering RNAs inhibits clonogenicity and engraftment of t(4;11)-positive human leukemic cells. Blood. 106:3559-66

Thomas M, Greil J, Heidenreich O. (2006) Targeting leukemic fusion proteins with small interfering RNAs: recent advances and therapeutic potentials. Acta Pharmacol Sin. 27:273-81

Tijsterman M, Ketting RF, Plasterk RH. (2002) The genetics of RNA silencing. Annu Rev Genet. 36:489-519

Tokuhara T, Hattori N, Ishida H, Hirai T, Higashiyama M, Kodama K, Miyake M. (2006) Clinical significance of aminopeptidase N in non-small cell lung cancer. Clin Cancer Res. 12:3971-8

Tomlinson I, Holliger P. (2000) Methods for generating multivalent and bispecific antibody fragments. Methods Enzymol. 326:461-79.

Torchilin VP, Goldmacher VS, Smirnov VN. (1978) Comparative studies on covalent and noncovalent immobilization of protein molecules on the surface of liposomes. Biochem Biophys Res Commun. 85:983-90

Torchilin VP. (2005) Fluorescence microscopy to follow the targeting of liposomes and micelles to cells and their intracellular fate. Adv Drug Deliv Rev. 57:95-109.

Ulyanova T, Blasioli J, Woodford-Thomas TA, Thomas ML. (1999) The sialoadhesin CD33 is a myeloid-specific inhibitory receptor. Eur J Immunol. 29:3440-9

Ungaro F, De Rosa G, Miro A, Quaglia F. (2003) Spectrophotometric determination of polyethylenimine in the presence of an oligonucleotide for the characterization of controlled release formulations. J Pharm Biomed Anal. 31:143-9

Urban-Klein B, Werth S, Abuharbeid S, Czubayko F, Aigner A. (2005) RNAi-mediated gene-targeting through systemic application of polyethylenimine (PEI)-complexed siRNA in vivo. Gene Ther. 12:461-6

Vitale C, Romagnani C, Falco M, Ponte M, Vitale M, Moretta A, Bacigalupo A, Moretta L, Mingari MC. (1999) Engagement of p75/AIRM1 or CD33 inhibits the proliferation of normal or leukemic myeloid cells. Proc Natl Acad Sci U S A. 96:15091-6

Vitale C, Romagnani C, Puccetti A, Olive D, Costello R, Chiossone L, Pitto A, Bacigalupo A, Moretta L, Mingari MC. (2001) Surface expression and function of p75/AIRM-1 or CD33 in acute myeloid leukemias: engagement of CD33 induces apoptosis of leukemic cells Proc Natl Acad Sci U S A. 98:5764-9

Völkel T, Hölig P, Merdan T, Müller R, Kontermann RE. (2004) Targeting of immunoliposomes to endothelial cells using a single-chain Fv fragment directed against human endoglin (CD105). Biochim Biophys Acta. 1663:158-66

Wagner E, Zenke M, Cotten M, Beug H, Birnstiel ML. (1990) Transferrin-polycation conjugates as carriers for DNA uptake into cells. Proc Natl Acad Sci U S A. 87:3410-4.

Walter RB, Raden BW, Kamikura DM, Cooper JA, Bernstein ID. (2005) Influence of CD33 expression levels and ITIM-dependent internalization on gemtuzumab ozogamicin-induced cytotoxicity. Blood.105:1295-302

Wang S, Wang Q, Crute BE, Melnikova IN, Keller SR, Speck NA. (1993) Cloning and characterization of subunits of the T-cell receptor and murine leukemia virus enhancer core-binding factor. Mol Cell Biol. 13:3324-39

Wang J, Hoshino T, Redner RL, Kajigaya S, Liu JM. (1998) ETO, fusion partner in t(8;21) acute myeloid leukemia, represses transcription by interaction with the human N-CoR/mSin3/HDAC1 complex. Proc Natl Acad Sci U S A. 95:10860-5

Wang GP, Qi ZH, Chen FP (2008) Treatment of acute myeloid leukemia by directly targeting both leukemia stem cells and oncogenic molecule with specific scFv-immunolipoplexes as a deliverer. Med Hypotheses. 70:122-7

Weiner LM, Carter P. (2003) The rollercoaster ride to anti-cancer antibodies. Nat Biotechnol. 21:510-1

Weissig V, Lasch J, Klibanov AL, Torchilin VP (1986) A new hydrophobic anchor for the attachment of proteins to liposomal membranes. FEBS Lett. 202:86-90

Wels W, Beerli R, Hellmann P, Schmidt M, Marte BM, Kornilova ES, Hekele A, Mendelsohn J, Groner B, Hynes NE. (1995) EGF receptor and p185erbB-2-specific single-chain antibody toxins differ in their cell-killing activity on tumor cells expressing both receptor proteins. Int J Cancer. 60:137-44

Westendorf JJ, Yamamoto CM, Lenny N, Downing JR, Selsted ME, Hiebert SW. (1998) The t(8;21) fusion product, AML-1-ETO, associates with C/EBP-alpha, inhibits C/EBP-alpha-dependent transcription, and blocks granulocytic differentiation. Mol Cell Biol. 18:322-33

Whitehead KA, Langer R, Anderson DG. (2009) Knocking down barriers: advances in siRNA delivery. Nat Rev Drug Discov.8:129-38.

Wilms B, Hauck A, Reuss M, Syldatk C, Mattes R, Siemann M, and Altenbuchner J. (2001) High-cell-density fermentation of L-N-Carbamoylase using an expression system based on the Escherichia coli rhaBAD promoter. Biotechnol Bioeng 73:95-103

Wolfrum C, Shi S, Jayaprakash KN, Jayaraman M, Wang G, Pandey RK, Rajeev KG, Nakayama T, Charrise K, Ndungo EM, Zimmermann T, Koteliansky V, Manoharan M, Stoffel M. (2007) Mechanisms and optimization of in vivo delivery of lipophilic siRNAs. Nat Biotechnol. 25:1149-57

Wright M, Grim J, Deshane J, Kim M, Strong TV, Siegal GP, Curiel DT. (1997) An intracellular anti-erbB-2 single-chain antibody is specifically cytotoxic to human breast carcinoma cells overexpressing erbB-2. Gene Ther. 4:317-22

Wu-Scharf D, Jeong B, Zhang C, Cerutti H. (2000) Transgene and transposon silencing in Chlamydomonas reinhardtii by a DEAH-box RNA helicase. Science, 290:1159-62

Xu L, Huang CC, Huang W, Tang WH, Rait A, Yin YZ, Cruz I, Xiang LM, Pirollo KF, Chang EH. (2002) Systemic tumor-targeted gene delivery by anti-transferrin receptor scFv-immunoliposomes. Mol Cancer Ther. 1:337-46

Xu Y, Wellner D, Scheinberg DA. (1997) Cryptic and regulatory epitopes in CD13/aminopeptidase N. Exp Hematol. 25:521-9

Yergeau DA, Hetherington CJ, Wang Q, Zhang P, Sharpe AH, Binder M, Marín-Padilla M, Tenen DG, Speck NA, Zhang DE. (1997) Embryonic lethality and impairment of haematopoiesis in mice heterozygous for an AML1-ETO fusion gene. Nat Genet. 15:303-6

Yuan C, O'Connell RJ, Jacob RF, Mason PR, Treistman SN (2007) Regulation of the Gating of BKCa Channel by Lipid Bilayer Thickness. J biol chemistry. 282:7276–7286

Yuan Y, Zhou L, Miyamoto T, Iwasaki H, Harakawa N, Hetherington CJ, Burel SA, Lagasse E, Weissman IL, Akashi K, Zhang DE. (2001) AML1-ETO expression is directly involved in the development of acute myeloid leukemia in the presence of additional mutations. Proc Natl Acad Sci U S A. 98:10398-403

Zein N, Sinha AM, McGahren WJ, Ellestad GA. (1988) Calicheamicin gamma 1I: an antitumor antibiotic that cleaves double-stranded DNA site specifically. Science. 240:1198-201

Zhang S, Xu Y, Wang B, Qiao W, Liu D, Li Z. (2004) Cationic compounds used in lipoplexes and polyplexes for gene delivery. J Control Release. 100:165-80

Zheng X, Vladau C, Zhang X, Suzuki M, Ichim TE, Zhang ZX, Li M, Carrier E, Garcia B, Jevnikar AM, Min WP. (2009) A novel in vivo siRNA delivery system specifically targeting dendritic cells and silencing CD40 genes for immunomodulation. Blood. 113:2646-54

Zimmermann TS, Lee AC, Akinc A, Bramlage B, Bumcrot D, Fedoruk MN, Harborth J, Heyes JA, Jeffs LB, John M, Judge AD, Lam K, McClintock K, Nechev LV, Palmer LR, Racie T, Röhl I, Seiffert S, Shanmugam S, Sood V, Soutschek J, Toudjarska I, Wheat AJ, Yaworski E, Zedalis W, Koteliansky V, Manoharan M, Vornlocher HP, MacLachlan I. (2006) RNAi-mediated gene silencing in non-human primates. Nature. 441:111-4

Homepages

Alnylam Pharmaceuticals (2008) www.alnylam.com

American Cancer Society (2009) www.cancer.org

Creative PEGworks (2009) www.creativepegworks.com

Nanocs (2009) www.nanocs.com

Nature Publishing Group (2005) www.nature.com

6 Sequences

scFv' CD13

```
                                                                    NcoI
                                                                   -+-----
                                                          SfiI
                                                         ---------+----
  1  atgaaatacc tattgcctac ggcagccgct ggattgttat tactcgcggc ccagccggcc atggcggact acaaagacgt
     >>.....................pelB-leader'.....................>>
       m  k  y   l  l  p   t  a  a  a   g  l  l   l  l  a   a  q  p
                                                                        >>scFv CD13-1.>
                                                                          d   y  k  d

 81  tgtgatgacc caaactccac tctccctgcc tgtcagtctt ggagatcaag cctccatctc ttgcagatct agtcagagca
     >.....................................scFv CD13-1.....................................>
     v  v  m  t   q  t  p   l  s  l   p  v  s  l   g  d  q   a  s  i   s  c  r  s   s  q  s

161  ttgtacatag taatggaaac acctatttag aatggtacct gcagaaacca ggccagtctc caaagctcct gatctacaaa
     >.....................................scFv CD13-1.....................................>
      i  v  h   s  n  g  n   t  y  l   e  w  y   l  q  k  p   g  q  s   p  k  l   l  i  y  k

241  gtttccaacc gattttctgg ggtcccagac aggttcagtg gcagtggatc agggacagat ttcacactca agatcagcag
     >.....................................scFv CD13-1.....................................>
       v  s  n   r  f  s   g  v  p  d   r  f  s   g  s  g   s  g  t  d   f  t  l   k  i  s

321  agtggaggct gaggatctgg gagtttatta ctgttttcaa ggttcacatg ttccgtggac gttcggtgga ggcaccaagc
     >.....................................scFv CD13-1.....................................>
     r  v  e  a   e  d  l   g  v  y   y  c  f  q   g  s  h   v  p  w   t  f  g  g   g  t  k

401  tggaaatcaa acgtggtggt ggtggttctg gtggtggtgg ttctggcggc ggcggctccg gtggtggtgg atcccaggtt
     >.....................................scFv CD13-1.....................................>
      l  e  i   k  r  g  g   g  g  s   g  g  g   g  s  g  g   g  g  s   g  g  g   g  s  q  v

481  cagctgcagc agtctggagc tgagctgatg aagcctgggg cctcagtgaa gatttcctgc aaggctactg gctacacatt
     >.....................................scFv CD13-1.....................................>
       q  l  q   q  s  g   a  e  l  m   k  p  g   a  s  v   k  i  s  c   k  a  t   g  y  t

561  caatagctac tggatcgagt gggtaaagca gaggcctgga catggccttg agtggattgg agagatttta cctggaagtg
     >.....................................scFv CD13-1.....................................>
     f  n  s  y   w  i  e   w  v  k   q  r  p  g   h  g  l   e  w  i   g  e  i  l   p  g  s

641  gtagtactaa ctacaatgag aagttcaacg gcaaggccac attcactgca gatgcatcct ccaacacagc ctacatgcaa
     >.....................................scFv CD13-1.....................................>
      g  s  t   n  y  n  e   k  f  n   g  k  a   t  f  t  a   d  a  s   s  n  t   a  y  m  q

721  ctcagcagcc tgacatctga ggactctgcc gtctattact gtgccagggt ctactatggt acctacggga gggtctactg
     >.....................................scFv CD13-1.....................................>
       l  s  s   l  t  s   e  d  s  a   v  y  y   c  a  r   v  y  y  g   t  y  g   r  v  y

                                    NotI                                                EcoRI
                                   --+-----                                             -+--
801  gggccaaggc accactctca ccgtctcctc ggcggccgca catcatcacc atcaccacgg cggagcatgc taataagaat
     >..........scFv CD13-1..........>>
     w  g  q  g   t  t  l   t  v  s   s
                                              >>....His-Tag....>>
                                               h  h  h   h  h  h
     --
881  tc
```

scFv' CD19

```
                                                                    NcoI
                                                                   -+-----
                                                          SfiI
                                                         ---------+----
  1  atgaaatacc tattgcctac ggcagccgct ggattgttat tactcgcggc ccagccggcc atggcggact acaaagatat
     >>.....................pelB-leader'.....................>>
       m  k  y   l  l  p   t  a  a  a   g  l  l   l  l  a   a  q  p
                                                          scFv CD19 (4G7) >>...........>
```

```
                                                                    d   y   k   d

 81  tgtgatgacc caggctgcac cctctatacc tgtcactcct ggagagtcag tatccatctc ctgcaggtct agtaagagtc
     >.................................scFv CD19 (4G7).................................>
     i  v  m  t   q  a  a   p  s  i   p  v  t  p   g  e  s   v  s  i   s  c  r  s   s  k  s

161  tcctgaatag taatggcaac acttacttgt attggttcct gcagaggcca ggccagtctc ctcagctcct gatatatcgg
     >.................................scFv CD19 (4G7).................................>
      l  l  n   s  n  g  n   t  y  l   y  w  f   l  q  r  p   g  q  s   p  q  l   l  i  y  r

241  atgtccaacc ttgcctcagg agtcccagac aggttcagtg gcagtgggtc aggaactgct ttcacactga gaatcagtag
     >.................................scFv CD19 (4G7).................................>
        m  s  n   l  a  s   g  v  p  d   r  f  s   g  s  g   s  g  t  a   f  t  l   r  i  s

321  agtggaggct gaggatgtgg gtgtttatta ctgtatgcaa catctagaat atccgctcac gttcggtgct gggaccaagc
     >.................................scFv CD19 (4G7).................................>
     r  v  e  a   e  d  v   g  v  y   y  c  m  q   h  l  e   y  p  l   t  f  g  a   g  t  k

401  tggaaatcaa acgtggtggt ggtggttctg gtggtggtgg ttctggcggc ggcggctccg gtggtggtgg atcccaggtt
     >.................................scFv CD19 (4G7).................................>
      l  e  i   k  r  g  g   g  g  s   g  g  g   g  s  g  g   g  g  s   g  g  g   g  s  q  v

481  cagcttcagc agtctggacc tgagctgata aagcctgggg cttcagtgaa gatgtcctgc aaggcttctg gatacacatt
     >.................................scFv CD19 (4G7).................................>
        q  l  q   q  s  g   p  e  l  i   k  p  g   a  s  v   k  m  s  c   k  a  s   g  y  t

561  cactagctat gttatgcact gggtgaagca gaagcctggg cagggccttg agtggattgg atatattaat ccttacamtg
     >.................................scFv CD19 (4G7).................................>
     f  t  s  y   v  m  h   w  v  k   q  k  p  g   q  g  l   e  w  i   g  y  i  n   p  y  ?

641  atggtactaa gtacaatgag aagttcaaag gcaaggccac actgacttca gacaaatcct ccagcacagc ctacatggag
     >.................................scFv CD19 (4G7).................................>
      d  g  t   k  y  n  e   k  f  k   g  k  a   t  l  t  s   d  k  s   s  s  t   a  y  m  e

721  ctcagcagcc tgacctctga ggactctgcg gtctattact gtgcaagagg gacttattac tacggtagta gggtatttga
     >.................................scFv CD19 (4G7).................................>
        l  s  s   l  t  s   e  d  s  a   v  y  y   c  a  r   g  t  y  y   y  g  s   r  v  f

                                                  NotI
                                               --+------
801  ctactggggc caaggcacca ctctcacagt caccgtctcc tcggcggccg cacatcatca ccatcaccac ggcggagcat
     >..............scFv CD19 (4G7).............>>
     d  y  w  g   q  g  t   t  l  t   v  t  v  s   s
                                                           >>....His-Tag....>>
                                                             h  h   h  h  h  h

             EcoRI
            -+-----
881  gctaataaga attc
```

scFv' CD33

```
                                                                  NcoI
                                                                -+-----
                                                          SfiI
                                                       ---------+----
  1  atgaaatacc tattgcctac ggcagccgct ggattgttat tactcgcggc ccagccggcc atggcggact acaaagacat
     >>.....................pelB-leader'.....................>>
       m  k  y   l  l  p   t  a  a  a   g  l  l   l  l  a   a  q  p
                                                                     >>...........>
                                                                        d   y  k  d


 81  tgtgatgacc cagtctcaca aattcctgct tgtatcagta ggagacaggg tcagcatcac ctgcaaggcc agtcaggatg
     >.................................scFv CD33 (K132).................................>
     i  v  m  t   q  s  h   k  f  l   l  v  s  v   g  d  r   v  s  i   t  c  k  a   s  q  d

161  tgagtactgc tgtagcctgg tatcaacaga aaccaggaca atctcctaaa ctactgattt actcggcatc ctaccggtac
     >.................................scFv CD33 (K132).................................>
      v  s  t   a  v  a  w   y  q  q   k  p  g   q  s  p  k   l  l  i   y  s  a   s  y  r  y

241  actggagtcc ctgatcgctt cataggcagt ggatctggga cagatttcac tcttaccatc agcagtgtgc aggctgaaga
```

```
     >................................scFv CD33 (K132).................................>
       t  g  v   p  d  r   f  i  g  s   g  s  g   t  d  f   t  l  t  i   s  s  v   q  a  e

321  cctggcagat tacttctgtc agcaacatta tagcactccg ctcacgttcg gtgctgggac caagctggaa ataaaacgtg
     >................................scFv CD33 (K132).................................>
     d  l  a  d   y  f  c   q  q  h   y  s  t  p   l  t  f   g  a  g   t  k  l  e   i  k  r

401  gtggtggtgg ttctggtggt ggtggttctg gcggcggcgg ctccagtggt ggtggatccg aggtgcagct gaaggagtca
     >................................scFv CD33 (K132).................................>
      g  g  g   g  s  g  g   g  g  s   g  g  g   g  s  s  g   g  g  s   e  v  q   l  k  e  s

481  ggacctggcc tggtggcgcc ctcacagagc ctgtccatca catgcactgt ctcagggttc ccattaacca gctatggtgt
     >................................scFv CD33 (K132).................................>
       g  p  g   l  v  a   p  s  q  s   l  s  i   t  c  t   v  s  g  f   p  l  t   s  y  g

561  aagctgggtt cgccagcctc caggaaaggg tctggagtgg ctgggagtaa tatggggtga cgggagcaca aattatcatt
     >................................scFv CD33 (K132).................................>
     v  s  w  v   r  q  p   p  g  k   g  l  e  w   l  g  v   i  w  g   d  g  s  t   n  y  h

641  cagctctcat atccagactg agcatcagca aggataactc caagagccaa gttttcttaa aactgaacaa tctgcaaact
     >................................scFv CD33 (K132).................................>
      s  a  l   i  s  r  l   s  i  s   k  d  n   s  k  s  q   v  f  l   k  l  n   n  l  q  t

721  gatgacacag ccacgtacta ctgtgcccgt gatacttact acccctacta tgctatggac tattggggtc aaggaacctc
     >................................scFv CD33 (K132).................................>
       d  d  t   a  t  y   y  c  a  r   d  t  y   y  p  y   y  a  m  d   y  w  g   q  g  t

                       NotI                                              EcoRI
                    --+------                                          -+----
801  agtcaccgtc tcctcggcgg ccgcacatca tcaccatcac cacggcggag catgctaata agaattc
     >..............>> scFv CD33 (K132)
     s  v  t  v   s  s
                              >>....His-Tag.....>>
                                h   h  h  h  h   h
```

scFv' CD33 V_HV_L HC2

```
                                                                      NcoI
                                                                    -+-----
  1  atgaaatacc tattgcctac ggcagccgct ggattgttat tactcgcggc ccagccggcc atggcggagg tgcagctgaa
     >>.....................pelB-leader'.....................>>
       m  k  y   l  l  p   t  a  a  a   g  l  l   l  l  a   a  q  p
                                                                        >>...........>
                                                                          e  v  q  l

 81  ggagtcagga cctggcctgg tggcgccctc acagagcctg tccatcacat gcactgtctc agggttccca ttaaccagct
     >.............................scFv' CD33 VHVL HC2.............................>
     k  e  s  g   p  g  l   v  a  p   s  q  s  l   s  i  t   c  t  v   s  g  f  p   l  t  s

161  atggtgtaag ctgggttcgc cagcctccag gaaagggtct ggagtggctg ggagtaatat ggggtgacgg gagcacaaat
     >.............................scFv' CD33 VHVL HC2.............................>
      y  g  v   s  w  v  r   q  p  p   g  k  g   l  e  w  l   g  v  i   w  g  d   g  s  t  n

241  tatcattcag ctctcatatc cagactgagc atcagcaagg ataactccaa gagccaagtt ttcttaaaac tgaacaatct
     >.............................scFv' CD33 VHVL HC2.............................>
       y  h  s   a  l  i   s  r  l  s   i  s  k   d  n  s   k  s  q  v   f  l  k   l  n  n

321  gcaaactgat gacacagcca cgtactactg tgcccgtgat acttactacc cctactatgc tatggactat tggggtcaag
     >.............................scFv' CD33 VHVL HC2.............................>
     l  q  t  d   d  t  a   t  y  y   c  a  r  d   t  y  y   p  y  y   a  m  d  y   w  g  q

401  gaacctcagt caccgtctcg agtggtggag gcggttcagg cggaggtggc tctggcggtg gagggagtgg tggaggcagt
     >.............................scFv' CD33 VHVL HC2.............................>
      g  t  s   v  t  v  s   s  g  g   g  g  s   g  g  g  g   s  g  g   g  g  s   g  g  g  s

481  gcacaggaca ttgtgatgac ccagtctcac aaattcctgc ttgtatcagt aggagacagg gtcagcatca cctgcaaggc
     >.............................scFv' CD33 VHVL HC2.............................>
       a  q  d   i  v  m   t  q  s  h   k  f  l   l  v  s   v  g  d  r   v  s  i   t  c  k

561  cagtcaggat gtgagtactg ctgtagcctg gtatcaacag aaaccaggac aatctcctaa actactgatt tactcggcat
     >.............................scFv' CD33 VHVL HC2.............................>
     a  s  q  d   v  s  t   a  v  a   w  y  q  q   k  p  g   q  s  p   k  l  l  i   y  s  a
```

```
641  cctaccggta cactggagtc cctgatcgct tcataggcag tggatctggg acagatttca ctcttaccat cagcagtgtg
     >.............................scFv' CD33 VHVL HC2.............................>
      s  y  r   y  t  g  v   p  d  r   f  i  g   s  g  s  g   t  d  f   t  l  t   i  s  s  v

721  caggctgaag acctggcaga ttacttctgt cagcaacatt atagcactcc gctcacgttc ggtgctggga ccaagctgga
     >.............................scFv' CD33 VHVL HC2.............................>
       q  a  e   d  l  a   d  y  f  c   q  q  h   y  s  t   p  l  t  f   g  a  g   t  k  l

                                                                          EcoRI
                                                                         -+----
801  aataaaacgt gcggccgcac atcatcacca tcaccacggc ggatccagcg gctccggatg ctaagaattc
     >....................scFv' CD33 VHVL HC2.....................>>
     e  i  k  r   a  a  a   h  h  h   h  h  h  g   g  s  s   g  s  g   c
```

scFv' CD33 V_HV_L HC4

```
                                                                    NcoI
                                                                  -+-----
  1  atgaaatacc tattgcctac ggcagccgct ggattgttat tactcgcggc ccagccggcc atggcggagg tgcagctgaa
     >>....................pelB-leader'.....................>>
       m  k  y   l  l  p   t  a  a  a   g  l  l   l  l  a   a  q  p
                                                                  >>...........>
                                                                    e   v  q  l

 81  ggagtcagga cctggcctgg tggcgccctc acagagcctg tccatcacat gcactgtctc agggttccca ttaaccagct
     >.............................scFv' CD33 VHVL HC4.............................>
     k  e  s  g   p  g  l   v  a  p   s  q  s  l   s  i  t   c  t  v   s  g  f  p   l  t  s

161  atggtgtaag ctgggttcgc cagcctccag gaaagggtct ggagtggctg ggagtaatat ggggtgacgg gagcacaaat
     >.............................scFv' CD33 VHVL HC4.............................>
      y  g  v   s  w  v  r   q  p  p   g  k  g   l  e  w  l   g  v  i   w  g  d   g  s  t  n

241  tatcattcag ctctcatatc cagactgagc atcagcaagg ataactccaa gagccaagtt ttcttaaaac tgaacaatct
     >.............................scFv' CD33 VHVL HC4.............................>
       y  h  s   a  l  i   s  r  l  s   i  s  k   d  n  s   k  s  q  v   f  l  k   l  n  n

321  gcaaactgat gacacagcca cgtactactg tgcccgtgat acttactacc cctactatgc tatggactat tggggtcaag
     >.............................scFv' CD33 VHVL HC4.............................>
     l  q  t  d   d  t  a   t  y  y   c  a  r  d   t  y  y   p  y  y   a  m  d  y   w  g  q

401  gaacctcagt caccgtctcg agtggtggag gcggttcagg cggaggtggc tctggcggtg gagggagtgg tggaggcagt
     >.............................scFv' CD33 VHVL HC4.............................>
      g  t  s   v  t  v  s   s  g  g   g  g  s   g  g  g  g   s  g  g   g  g  s   g  g  g  s

481  gcacaggaca ttgtgatgac ccagtctcac aaattcctgc ttgtatcagt aggagacagg gtcagcatca cctgcaaggc
     >.............................scFv' CD33 VHVL HC4.............................>
       a  q  d   i  v  m   t  q  s  h   k  f  l   l  v  s   v  g  d  r   v  s  i   t  c  k

561  cagtcaggat gtgagtactg ctgtagcctg gtatcaacag aaaccaggac aatctcctaa actactgatt tactcggcat
     >.............................scFv' CD33 VHVL HC4.............................>
     a  s  q  d   v  s  t   a  v  a   w  y  q  q   k  p  g   q  s  p   k  l  l  i   y  s  a

641  cctaccggta cactggagtc cctgatcgct tcataggcag tggatctggg acagatttca ctcttaccat cagcagtgtg
     >.............................scFv' CD33 VHVL HC4.............................>
      s  y  r   y  t  g  v   p  d  r   f  i  g   s  g  s  g   t  d  f   t  l  t   i  s  s  v

721  caggctgaag acctggcaga ttacttctgt cagcaacatt atagcactcc gctcacgttc ggtgctggga ccaagctgga
     >.............................scFv' CD33 VHVL HC4.............................>
       q  a  e   d  l  a   d  y  f  c   q  q  h   y  s  t   p  l  t  f   g  a  g   t  k  l

                                                                                  EcoRI
                                                                                 -+--
801  aataaaacgt gcggccgcac atcatcacca tcaccacggc ggatccagcg gcggatccag cggctccgga tgctaagaat
     >...........................scFv' CD33 VHVL HC4...........................>>
     e  i  k  r   a  a  a   h  h  h   h  h  h  g   g  s  s   g  g  s   s  g  s  g   c

    --
881  tc
```

scFv' CD33 $V_L V_H$ HC2

```
                                                                    NcoI
                                                                  -+-----
  1 atgaaatacc tattgcctac ggcagccgct ggattgttat tactcgcggc ccagccggcc atggcggact acaaagacat
    >>.....................pelB-leader'.....................>>
      m  k  y  l  l  p  t  a  a  a  g  l  l  l  l  a  a  q  p
                                                                                >>..........>
                                                                                  d  y  k  d

 81 tgtgatgacc cagtctcaca aattcctgct tgtatcagta ggagacaggg tcagcatcac ctgcaaggcc agtcaggatg
    >..............................scFv' CD33 VLVH HC2.............................>
    i  v  m  t  q  s  h  k  f  l  l  v  s  v  g  d  r  v  s  i  t  c  k  a  s  q  d

161 tgagtactgc tgtagcctgg tatcaacaga aaccaggaca atctcctaaa ctactgattt actcggcatc ctaccggtac
    >..............................scFv' CD33 VLVH HC2.............................>
     v  s  t  a  v  a  w  y  q  q  k  p  g  q  s  p  k  l  l  i  y  s  a  s  y  r  y

241 actggagtcc ctgatcgctt cataggcagt ggatctggga cagatttcac tcttaccatc agcagtgtgc aggctgaaga
    >..............................scFv' CD33 VLVH HC2.............................>
      t  g  v  p  d  r  f  i  g  s  g  s  g  t  d  f  t  l  t  i  s  s  v  q  a  e

321 cctggcagat tacttctgtc agcaacatta tagcactccg ctcacgttcg gtgctgggac caagctggaa ataaaacgtg
    >..............................scFv' CD33 VLVH HC2.............................>
    d  l  a  d  y  f  c  q  q  h  y  s  t  p  l  t  f  g  a  g  t  k  l  e  i  k  r

401 gtggtggtgg ttctggtggt ggtggttctg gcggcggcgg ctccagtggt ggtggatccg aggtgcagct gaaggagtca
    >..............................scFv' CD33 VLVH HC2.............................>
     g  g  g  g  s  g  g  g  g  s  g  g  g  g  s  s  g  g  g  s  e  v  q  l  k  e  s

481 ggacctggcc tggtggcgcc ctcacagagc ctgtccatca catgcactgt ctcagggttc ccattaacca gctatggtgt
    >..............................scFv' CD33 VLVH HC2.............................>
      g  p  g  l  v  a  p  s  q  s  l  s  i  t  c  t  v  s  g  f  p  l  t  s  y  g

561 aagctgggtt cgccagcctc caggaaaggg tctggagtgg ctgggagtaa tatggggtga cgggagcaca aattatcatt
    >..............................scFv' CD33 VLVH HC2.............................>
    v  s  w  v  r  q  p  p  g  k  g  l  e  w  l  g  v  i  w  g  d  g  s  t  n  y  h

641 cagctctcat atccagactg agcatcagca aggataactc caagagccaa gttttcttaa aactgaacaa tctgcaaact
    >..............................scFv' CD33 VLVH HC2.............................>
     s  a  l  i  s  r  l  s  i  s  k  d  n  s  k  s  q  v  f  l  k  l  n  n  l  q  t

721 gatgacacag ccacgtacta ctgtgcccgt gatacttact acccctacta tgctatggac tattggggtc aaggaacctc
    >..............................scFv' CD33 VLVH HC2.............................>
      d  d  t  a  t  y  y  c  a  r  d  t  y  y  p  y  y  a  m  d  y  w  g  q  g  t

                                                                              EcoRI
                                                                            -+----
801 agtcaccgtc tcctcggcgg ccgcacatca tcaccatcac cacggcggat ccagcggctc cggatgctaa gaattc
    >.......................scFv' CD33 VLVH HC2.....................>>
    s  v  t  v  s  s  a  a  a  h  h  h  h  h  g  g  s  s  g  s  g  c
```

scFv' CD33 $V_L V_H$ HC4

```
                                                                    NcoI
                                                                  -+-----
  1 atgaaatacc tattgcctac ggcagccgct ggattgttat tactcgcggc ccagccggcc atggcggact acaaagacat
    >>.....................pelB-leader'.....................>>
      m  k  y  l  l  p  t  a  a  a  g  l  l  l  l  a  a  q  p
                                                                                >>..........>
                                                                                  d  y  k  d

 81 tgtgatgacc cagtctcaca aattcctgct tgtatcagta ggagacaggg tcagcatcac ctgcaaggcc agtcaggatg
    >..............................scFv' CD33 VLVH HC4.............................>
    i  v  m  t  q  s  h  k  f  l  l  v  s  v  g  d  r  v  s  i  t  c  k  a  s  q  d

161 tgagtactgc tgtagcctgg tatcaacaga aaccaggaca atctcctaaa ctactgattt actcggcatc ctaccggtac
    >..............................scFv' CD33 VLVH HC4.............................>
     v  s  t  a  v  a  w  y  q  q  k  p  g  q  s  p  k  l  l  i  y  s  a  s  y  r  y

241 actggagtcc ctgatcgctt cataggcagt ggatctggga cagatttcac tcttaccatc agcagtgtgc aggctgaaga
    >..............................scFv' CD33 VLVH HC4.............................>
      t  g  v  p  d  r  f  i  g  s  g  s  g  t  d  f  t  l  t  i  s  s  v  q  a  e
```

```
321  cctggcagat tacttctgtc agcaacatta tagcactccg ctcacgttcg gtgctgggac caagctggaa ataaaacgtg
     >..............................scFv' CD33 VLVH HC4.............................>
     d  l  a  d   y  f  c   q  q  h   y  s  t  p   l  t  f   g  a  g   t  k  l  e   i  k  r

401  gtggtggtgg ttctggtggt ggtggttctg gcggcggcgg ctccagtggt ggtggatccg aggtgcagct gaaggagtca
     >..............................scFv' CD33 VLVH HC4.............................>
      g  g  g   g  s  g  g   g  g  s   g  g  g   g  s  s  g   g  g  s   e  v  q   l  k  e  s

481  ggacctggcc tggtggcgcc ctcacagagc ctgtccatca catgcactgt ctcagggttc ccattaacca gctatggtgt
     >..............................scFv' CD33 VLVH HC4.............................>
       g  p  g   l  v  a   p  s  q  s   l  s  i   t  c  t   v  s  g  f   p  l  t   s  y  g

561  aagctgggtt cgccagcctc caggaaaggg tctggagtgg ctgggagtaa tatggggtga cgggagcaca aattatcatt
     >..............................scFv' CD33 VLVH HC4.............................>
     v  s  w  v   r  q  p   p  g  k   g  l  e  w   l  g  v   i  w  g   d  g  s  t   n  y  h

641  cagctctcat atccagactg agcatcagca aggataactc caagagccaa gttttcttaa aactgaacaa tctgcaaact
     >..............................scFv' CD33 VLVH HC4.............................>
      s  a  l   i  s  r  l   s  i  s   k  d  n   s  k  s  q   v  f  l   k  l  n   n  l  q  t

721  gatgacacag ccacgtacta ctgtgcccgt gatacttact acccctacta tgctatggac tattggggtc aaggaacctc
     >..............................scFv' CD33 VLVH HC4.............................>
       d  d  t   a  t  y   y  c  a  r   d  t  y   y  p  y   y  a  m  d   y  w  g   q  g  t

801  agtcaccgtc tcctcggcgg ccgcacatca tcaccatcac cacggcggat ccagcggcgg atccagcggc tccggatgct
     >..............................scFv' CD33 VLVH HC4.............................>>
     s  v  t  v   s  s  a   a  a  h   h  h  h  h   h  g  g   s  s  g   g  s  s  g   s  g  c

        EcoRI
       -+----
881  aagaattc
```

Acknowledgements

First I want to thank Prof. Dr. Roland Kontermann for giving me the opportunity to do my PhD under his excellent supervision and for all the helpful advice and suggestions during the experimental and theoretical part and all concerns of this study.

I would like to thank Dr. Olaf Heidenreich from Newcastle University for close collaboration, practical and theoretical advice in all RNAi questions and beyond.

Special thanks to Dr. Dafne Müller and all the members of the laboratory, Julia Beuttler, Kirstin Zettlitz, Sylvia Messerschmidt, Roland Stork, Anja Nusser, Jan Körner, Philipp Diebolder, Volker Baum, Martin Altvater and Nadine Fuß for helpful discussions, encouragement and an excellent working atmosphere. Special thanks go to Julia Beuttler who rendered every assistence in the fermentation process, Nadine Fuß for relieving me of particular experiments, Sabine Münkel for performing size exclusion chromatography and to my graduant Anja Nusser for her help and shared ambition in the field of siRNA delivery.

Thanks to Prof. Dr. Georg Fey from the University of Erlangen-Nuremberg for providing the scFv molecules and for helpful conversations and to Prof. Dr. Thomas Kissel from the Universtity of Marburg for collaboration. Special thanks to Dr. Anja Scholz and Patricia Garrido Castro from Newcastle University for performing real-time PCR and to Olivia Merkel from the University of Marburg for the synthesis of immunopolyplexes and her friendly support.

I would like to thank my husband Marco Rothdiener and my familiy for their love and patience and their support during my studies and during my work on this thesis.

The project was funded by Deutsche Krebshilfe e. V., support code 107026.

Declaration

I hereby assure that I performed the present study independently without further help or other materials than stated.

Miriam Rothdiener

Stuttgart, 27th of August 2009

Curriculum vitae

Persönliche Angaben

Miriam Rothdiener, geb. Rether
geboren am 10.03.1979 in Landstuhl
verheiratet

Schulausbildung

1985-1989 Grundschule Linden
1989-1998 Sickingen Gymnasium Landstuhl

Berufsausbildung

1998-2001 staatl. Lehranstalt für medizinisch-technische Laboratoriumsassistenten an den Universitätskliniken des Saarlandes, Homburg/Saar

Hochschulausbildung

2001-2006 Studium der Dipl. Biologie an der technischen Universität Kaiserslautern mit dem Hauptfach Humanbiologie und -genetik und den Nebenfächern Neurophysiologie und Biochemie
Diplomarbeit im Fachbereich Physik, Abteilung Laser in der Medizin mit dem Thema „Photodynamische Therapie“

Promotion

2006-2009 Universität Stuttgart
Institut für Zellbiologie und Immunologie
Thema der Arbeit: „Zielgerichtete siRNATrägersysteme für die Behandlung der akuten myeloischen Leukämie (AML)“

Beruflicher Werdegang

seit 2009 Universitätsklinikum Tübingen
Zentrum für Regenerationsbiologie und Regenerative Medizin

Publikationen

Stork, R., Zettlitz, K.A., Müller, D., **Rether, M**., Hanisch, F.G. & Kontermann, R.E. (2008) N-glycosylation as novel strategy to improve pharmacokinetic properties of bispecific single-chain antibodies. J Biol Chem. 283, 7804-12

Beuttler, J., **Rothdiener, M**., Müller, D., Nilsson, F.Y. & Kontermann, R.E. (2009) Targeting of epidermal growth factor receptor (EGFR)-expressing tumor cells with sterically-stabilized affibody liposomes (SAL)

Rothdiener, M., Beuttler, J., Messerschmidt, S.K.E. & Kontermann, R.E. (2009) Antibody targeting of nanoparticles to tumor specific receptors: immunoliposomes In: Cancer nanotechnology in Methods in molecular biology series. Grobmyer, S. & Moudgil, B. (Ed.) Humana Press Inc.

Messerschmidt, S.K.E., Beuttler, J., **Rothdiener, M.** & Kontermann, R.E. (2009) Recombinant antibody molecules in nanobiotechnology: immunoliposomes In: Springer protocols antibody engineering. Kontermann R.E. & Dübel, S. (Ed.) Springer-Verlag Heidelberg

In Vorbereitung:

Rothdiener, M., Müller, D., Schwemmlein, M., Fey, G.H., Heidenreich, O. & Kontermann, R.E. (2009) Targeted delivery of siRNA to CD33-positive tumor cells

Preise

2008 Gewinn des Poster Awards anlässlich der Jahreskonferenz der Controlled Release Society in Braunschweig

Stuttgart, im August 2009